EFFECT OF PYROLIGNEOUS ACID APPLICATION ON TOMATO GROWTH AND ALLEVIATION OF ALUMINUM STRESS

by

Raphael Ofoe

Submitted in partial fulfilment of the requirements
for the degree of Doctor of Philosophy

at

Dalhousie University
Halifax, Nova Scotia
August 2023

Dalhousie University is located in Mi'kma'ki, the
ancestral and unceded territory of the Mi'kmaq.
We are all Treaty people.

DEDICATION

I dedicate this PhD thesis to God-the Father Almighty, my mother, Christiana Kwakunanka and my lovely wife and daughter, Henrietta Adobea Ofoe and Blandina Adansie Ofoe.

TABLE OF CONTENT

LIST OF TABLES

LIST OF FIGURES

ABSTRACT

Aluminum (Al) toxicity is a major constraint to global crop production in acidic soils. Pyroligneous acid (PA), a reddish-brown smoky liquid produced during the pyrolysis of biomass, can enhance crop growth and tolerance to diverse environmental stresses. However, its use in enhancing crop productivity and resilience to Al stress is unknown. This thesis investigated the biostimulatory effect of PA on productivity and its regulatory mechanism in promoting Al tolerance in tomato (*Solanum lycopersicum* 'Scotia'). Soil application of 0.25% PA increased plant morpho-physiological parameters while 0.5% PA increased fruit yield. However, soil application of 2% PA reduced plant growth and yield, but considerably increased fruit phytochemical contents. Foliar application of 0.25% and 0.5% PA combined with full NPK (0.63, 0.28, 1.03 g/L) rate increased chlorophyll fluorescence indices, while 2% PA increased leaf chlorophyll content. The 2% PA combined with full NPK rate increased fruit yield, number of marketable fruits and fruit phytochemicals. Seed priming with 2% PA for 24 h enhanced seed germination and seedling growth parameters under Al stress. Treatments of four-week-old tomato seedlings with 0.25% and 0.5% PA enhanced root growth, leaf gas exchange parameters and chlorophyll content under Al stress, while 1% PA exacerbated Al phytotoxicity on plant morphology. Seed priming and seedling treatment with PA reduced hydrogen peroxide and malonaldehyde contents, and increased osmolyte content. Seedlings of PA-primed seeds exhibited enhanced antioxidant activity and relatively high expression of auxin response factor and antioxidant genes. Seedling treatment with PA under Al stress increased antioxidant enzymes and reactive oxygen species-scavenging activities, restricted Al uptake and facilitated the availability and translocation of boron, manganese, sodium and phosphorus in tomato plants. Analysis of central carbon metabolism (CCM) revealed increased glycolysis, tricarboxylic acid cycle and electron transport chain metabolites in PA-treated plants. However, the Calvin-Benson cycle and pentose phosphate pathway metabolites were reduced. The CCM pathway metabolites exhibited a strong coordinated association in PA-treated plants. The findings of this thesis indicate that PA application in mainstream agriculture represents an eco-friendly strategy that can be used to: (1) increase crop productivity and nutritional qualities; (2) improve early crop establishment, detoxify Al and enhance Al tolerance in agricultural production systems.

LIST OF ABBREVIATIONS AND SYMBOLS USED

ddH_2O: sterile distilled water
µg: Microgram
µL: Microliter
µM: Micromolar
AAFC: Agriculture and agri-food Canada
ABA: Abscisic acid
ABC: Adenosine triphosphate binding cassette
ACC: 1-aminocyclopropane-1-carboxylic acid
ADP: Adenosine diphosphate
$AlCl_3$: Aluminum chloride
ALMT: Al-activated malate transporter
ALS1: Aluminum sensitive 1
ALT2: Aluminum Tolerant 2
ANOVA: Analysis of Variance
APX: Ascorbate peroxidase
ARF: Auxin response factors
ART1: Aluminum resistance transcription factor 1
ATP: Adenosine triphosphate
B: Boron
BHA: Butylated hydroxyanisole
BHT: Butylated hydroxytoluene
BSA: Bovine serum albumin
Ca: Calcium
CAT: Catalase
CBC: Calvin-Benson cycle
CCM: Central carbon metabolism
Cd: Cadmium
cDNA: Complementary DNA
CDT3: Cadmium transporter 3
CFIA: Canadian food inspection agency
cm: Centimeter
CO_2: Carbon dioxide
Cu: Copper
CV: Coefficient of variation
DAG: Diacylglycerol
DAT: Days after transplanting
DBS: DNA double-strand breaks
DDR: DNA damage response
DHAP: Dihydroxyacetone phosphate
DHAR: Dehydroascorbate reductase
DI/LC-MS/MS: Direct injection mass spectrometry with a reverse-phase liquid chromatography-mass spectrometry
DNCB: 2,4-dinitrochlorobenzene
DPPH: 1,1-diphenyl-2-picrylhydrazyl
DTT: Dithiothreitol
EC: Electric conductivity
EDTA: Ethylene diamine tetra acetic acid
ERF: Ethylene response factor
ETC: Electron transport chain
EU: European union
FAD: Flavin adenine dinucleotide
FAOSTAT: Food and agriculture organization corporate statistical database
Fe: Iron

$FeCl_3$: Ferric chloride
Fm: Maximum chlorophyll fluorescence
FMN: Flavin mononucleotides
Fo: Initial chlorophyll fluorescence
Fv: Variable chlorophyll fluorescence
FW: Fresh weight
g: gram
g: gravity
GAE: Gallic acid equivalent
GI: Germination index
GPX: Guaiacol peroxidase
GR: Glutathione reductase
GRI: Germination rate index
GV: Germination velocity
H_2O_2: Hydrogen peroxide
HCl: Hydrochloric acid
ICP-MS: Inductively coupled plasma-mass-spectrometry
IFP: Initial seed germination percentage
JA: Jasmonic acid
L: Liter
LC: Liquid chromatography
LOD: Limit of detection
LysoPC: Lysophosphatidylcholine
m: Meter
M: Molar
MATE: Multidrug and toxic compound extrusion
MDA: Malondialdehyde
MDHAR: Monodehydroascorbate reductase
Mg: Magnesium
mg: Milligram
MGR: Mean germination rate
MGT: Mean germination time
MGT1: Magnesium transporter 1
min: Minutes
mm: Millimeter
mM: Millimolar
Mn: Manganese
Mt: Million tonnes
Na: Sodium
NaClO: Sodium hypochlorite
NAD: Nicotinamide adenine dinucleotide
NADPH: Nicotinamide adenine dinucleotide phosphate
NaOH: Sodium hydroxide
ND: Not determined
Ni: Nickel
NIP: Nodulin 26-like intrinsic protein
nm: Nanometers
NPK: Nitrogen (N), phosphorus (P), potassium (K)
NRAMP: Natural resistance-associated macrophage protein
OA: Organic acid
ºC: Degrees Celsius
PA: Pyroligneous acid
PALT1: Plasma membrane Al transporter 1
PC: Phosphatidylcholine
PC: Phosphatidylcholine
PCR: Polymerase chain reaction
PM: Plasma membrane

PME: Pectin methylesterases
POD: Peroxidase
PP: Pyrophosphate
PPP: Pentophosphate pathway
PSII: Photosystem II
RBC: Root border cells
ROS: Reactive oxygen species
s: Second
SOD: Superoxide dismutase
SOG1: Suppressor of gamma response 1
STAR1/2: Sensitive to aluminum rhizotoxicity 1 / 2
STOP: Sensitive to protein rhizotoxicity
SUV2: sensitive to UV 2
TA: Titratable acidity
TCA: Tricarboxylic acid
TDS: Total dissolved solids
TPC: Total phenolics content
TSS: Total soluble solids
UDP: Uridine diphosphate
UPLC-MRM/MS: Ultrahigh LC-multiple reaction monitoring/mass spectroscopy
UV: Ultraviolet
VALT: Vacuolar Al transporter
wt: Weight
XET: Xyloglucan endotransglucosylase
XTH: Xyloglucan endotransglucosylase-hydrolase
Zn: Zinc

ACKNOWLEDGMENTS

I would like to, first of all, thank the Almighty God for the knowledge and protection during my study. A special thanks to my supervisor Dr Lord Abbey for his tremendous support and guidance. I am very grateful for the invaluable insights at every stage of this PhD and for grooming me to become a good researcher without forgetting your help in times of critical family challenges. You and your family were always there for me in difficult times, and you expressed profound love, care and support in every way you can. I strongly believe words are not enough to accommodate how awesome you have been to me and my family. I say thank you very much.

I would like to also thank my co-supervisor, Dr Raymond Thomas and supervisory committee members, Dr Gefu Wang-Pruski and Dr Bourlaye Fofana, for their immense contributions which have been the core of this PhD. You all provide me with irreplaceable insights in formulating strong research questions and constructive feedback that has shaped my view of science and my PhD at large.

I would like to extend my deepest thanks to my lovely wife, Henrietta Ofoe and mother, Christiana Kwakunanka for their unending love and prayers throughout my PhD. Also, I would like to thank Dr Samuel Asiedu and Dr Emmanuel Yiridoe for their support, guidance and encouragement. My profound gratitude to all my wonderful lab mates especially Dr Lokandha Gunupuru, Efoo Bawa Nutsukpo, Dengge Qin, Sparsha Chada and Anagha Kumar, who contributed in diverse ways to make this work a success. I would like to thank Taylor Main of Charlottetown Research and Development Center for his assistance in the mineral element analysis of the various plant tissues. Finally, I would like to thank the Natural Sciences and Engineering Research Council of Canada for funding my PhD and Proton Plant for supplying the biostimulant for the work.

CHAPTER 1: INTRODUCTION

1. Thesis background

An increase in crop production and resilience against environmental stresses are the fundamental principles to the adoption of sustainable practices to help feed the growing human population, which is expected to reach 9.8 billion by 2050 (United Nations, 2019) and to help slow global climate change. This increase in population has a consequence on the demand for nutrient-dense food, which must be doubled by 2050 (Henchion et al., 2017). However, current crop production is significantly constrained by several environmental stresses. Among these stresses, acidic soils (pH < 5) contribute to significant decline in crop yield globally (Kochian et al., 2004). Acidic soils constitute approximately 60% of tropical and subtropical soils and 50% of the worlds agricultural land, which support up to 80% of vegetable production (Kochian et al., 2004; Sade et al., 2016; Slessarev et al., 2016).

A remarkable characteristic of acidic soils is the presence of trivalent aluminum ions (Al^{3+}) that instigate an array of Al-induced toxicity syndrome in plants. The danger posed by this stress is further exacerbated by climate change and intensive use of synthetic chemical fertilizers, which is estimated to affect over 50% of global agricultural lands by 2050 (Jamil et al., 2011; Daliakopoulos et al., 2016). Most major crops are sensitive to micromolar concentration of Al, which results in root growth inhibition and perturbs numerous metabolic and molecular processes that results in considerable crop loss. Al interacts with root membrane components and destroys root cell integrity and limit water and nutrient acquisition (Kochian et al., 2015). Such disruption of root cell integrity facilitates Al-induced reactive oxygen species (ROS) accumulation, which instigate oxidative damage of numerous cellular biomolecules including nucleic acids, proteins and

membrane lipids (Boscolo et al., 2003; Valadez-González et al., 2007; Yi et al., 2010). Additionally, Al reduces photosynthetic activities, electron transfer rates and destabilizes and/or delays microtubule cytoskeleton organization (Amenós et al., 2009; Ribeiro et al., 2013; Baranova et al., 2016; Cárcamo et al., 2019).

Furthermore, the intensive use of synthetic chemical fertilizers for boosting crop yields has stimulated greater public concern of its side effects on the environment, ecological systems and life forms (Bindraban et al., 2020). As a result, current trends in agriculture require reduced synthetic chemical fertilizer useage while placing more emphasis on alternative strategies that stimulate plant productivity and resilience to environmental stresses as well as ensure environmental sustainability (Pretty & Bharucha, 2014; Pareek et al., 2020). One such strategy is the use of pyroligneous acid (PA), which is considered as a sustainable byproduct in agriculture for enhancing crop growth and productivity (Mmojieje, 2016; Grewal et al., 2018; Lu et al., 2020). PA, also known as wood vinegar, is a translucent reddish-brown liquid produced by carbonization of plant biomass in the presence of limited oxygen supply during pyrolysis (Mathew & Zakaria, 2015; Grewal et al., 2018). As an organic material, it is rich in bioactive compounds including phenolics, sugar derivatives, alcohols, alkanes and organic acids with acetic acid accounting for approximately 50% of the solution composition (Mathew & Zakaria, 2015; Crepier et al., 2018; Grewal et al., 2018). These chemical properties mainly depend on the feedstock, temperature, heating rate, residence time and particle sizes. Most PA obtained from different plant biomasses are produced at pyrolysis temperature range of 200–550 °C (Wei et al., 2010; Theapparat et al., 2014). Besides, PA produced from different plant species may present varying quantities of bioactive constituents and different levels of bioactivity (Mu et al., 2004; Wei et al., 2010;

Theapparat et al., 2014; Mathew et al., 2015) . However, no studies have investigated the metabolic and mineral element profile of PA produced at high pyrolytic temperature (i.e., > 1000 °C).

Moreover, nutrient-rich properties of PA have attracted the interest of farmers and researchers and its widely used as a biostimulant in agriculture (Dissatian et al., 2018; Pimenta et al., 2018; Wang et al., 2019b). Notably, PA application has been demonstrated to act as an insect repellent (Chalermsan et al., 2009; Mmojieje & Hornung, 2015), antimicrobial agents (Jung, 2007; Mourant et al., 2007), foliar fertilizer (Polthanee et al., 2015; Zhai et al., 2015) and soil enhancer (Lashari et al., 2013). Recent studies have reported that PA enhances seed germination rate, vegetative and reproductive growth of several plants species (Mungkunkamchao et al., 2013; Grewal et al., 2018; Lei et al., 2018; Shan et al., 2018; Wang et al., 2019b). However, the rate of PA applied for promoting plant growth varies between studies. For instance, foliar application of 1:800 (v/v) dilution enhanced growth and yield of tomato (*Solanum lycopersicum*) (Mungkunkamchao et al., 2013) whereas soil application of 20% PA increased the growth and yield of rockmelon (*Cucumis melo* var. Cantalupensis) (Zulkarami et al., 2011) suggesting that the applied concentration depends on the type of crop and the nature of the application. Generally, the high acidity of PA necessitates its use at low concentrations for plant growth and productivity (Grewal et al., 2018). Despite the significant effect of PA on plant growth, the underlying biostimulatory mechanisms remain elusive. Additionally, PA use in crop production in Canada is relatively new due to limited studies on its efficacy for growth promotion and recommended rates of application in Canadian production systems.

Moreover, studies on the antioxidant properties of phenolic compounds present in PA revealed that PA exhibit high ROS-scavenging activities, reducing power and anti-lipid peroxidation capacity (Loo et al., 2007; Wei et al., 2010). These activities are influenced by the pyrolytic temperature as high temperature of 550ºC showed strongest antioxidant activity compared to those of 311 ºC (Wei et al., 2010). This suggests that PA application does not only have the potential in enhancing crop growth and productivity, but also, can contribute significantly to abiotic stress mitigation although not yet investigated. Also, studies focusing on the effect of PA application in Al stress mitigation in plants are limited. In a recent drought study using proteomics, Wang et al. (2019b) revealed that priming seeds with 1:900 PA dilution triggered drought defence mechanisms in the root of 14-day old wheat seedlings. This mechanism was characterized by increased antioxidants and other stress-related proteins including glutathione, glyceraldehyde-3-phosphate and dehydrogenase. They therefore suggested that PA can promote normal cellular balance and metabolic response under stress condition. Regardless of the effect of PA, it is imperative to investigate the impact of such properties on plants under aluminum stress and the potential mitigation effect. Besides, PA mitigation of abiotic stress is not fully understood. Therefore, it can be hypothesized that PA application can promote plant growth and induce antioxidant accumulation through modulation of antioxidant pathway and other stress-response related genes under aluminum stress conditions. The understanding of the efficacy of PA on plants will not only be important in enhancing crop productivity and resilience, but will also reduce the cost of production through reduced fertilizer application, while improving environmental sustainability during crop cultivation.

1.1 Research aims and objectives

This research project aims at advancing our knowledge on the biostimulatory effect of PA on plant growth and development under greenhouse condition by examining the physiological and molecular mechanisms. It will also elucidate the regulatory mechanism of PA in promoting aluminum stress tolerance in plants. The understanding of these effects will aid in making an appropriate recommendation in terms of the right concentration for enhancing crop productivity under greenhouse condition in Nova Scotia and Canada. Furthermore, the establishment of wood vinegar as a novel biostimulant in Canada will not only reduce the cost of production but also promote environmental sustainability.

1.2.1 Specific objectives

1. Examine the metabolites and complete mineral element composition of PA derived from white pine (*Pinus strobus*) at 1100 °C
2. Investigate the effect of priming of tomato 'Scotia' seeds with PA on germination and seedling growth under Al stress
3. Assess the effect of soil application of PA on plant growth and productivity of tomato 'Scotia' under greenhouse condition
4. Evaluate the effect of foliar PA application and NPK fertilizer on physiological parameters and yield of tomato 'Scotia' under greenhouse condition
5. Examine the effect PA application on tomato 'Scotia' growth under Al stress
    - *Morpho-physiological and biochemical responses of tomato to PA treatments under Aluminum stress condition*

- *Central carbon metabolic profile of tomato leaves induced by PA treatment under Aluminum stress condition*

1.3 Thesis organization

This thesis is organized into manuscript format and comprised of a total of nine chapters. Chapter 1 is the introduction and objectives of this thesis. Chapter 2 provides a comprehensive literature review on Al stress toxicity, plant mechanisms of Al tolerance and the potential of PA in mitigating environmental stresses. The study objectives 1 to 5 are presented under Chapters 3, 4, 5, 6, 7 and 8 respectively. Chapter 9 is the overall thesis conclusions with contribution to knowledge, thesis limitations and recommendations for future studies. It is important to note that Chapter 2, 3, 4 and 7 have been published while Chapter 5 and 6 have been submitted for publication.

CHAPTER 2: LITERATURE REVIEW

A version of this chapter has been published in **Frontiers in Plant Science Journal**. The citation is:

Ofoe, R., Thomas, R. H., Asiedu, S. K., Wang-Pruski, G., Fofana, B., & Abbey, L. (2022). Aluminum in plant: Benefits, toxicity and tolerance mechanisms. *Frontiers in Plant Science*, *13*. https://doi.org/10.3389/fpls.2022.1085998. (Impact factor = 7.1)

2.1 Overview of tomato plant biology

Tomato (*Solanum lycopersicum*) belongs to the Solanaceae family with over 3000 species which occupy diverse range of habitat (Knapp & Peralta, 2016; Gatahi, 2020). The Solanaceae consists of several economic important crop plants, which are used as food [e.g. potato (*Solanum tuberosum*), eggplant (*Solanum melongena*), tamarillo (*Solanum betaceum*), tomatillo (*Physalis ixocarpa*), pepper (*Capsicum spp*) and tomato], ornamentals (e.g. *petunia spp*) and medicines [tobacco (*Nicotiana tabacum*), henbane (*Hyoscyamus niger*), deadly nightshade (*Atropa belladonna*), *Datura spp*] (Knapp & Peralta, 2016; Heuvelink, 2018). Tomato is thought to have originated and domesticated in America. Although the time and location for its domestication remains unclear, two locations have been proposed - Peru-Ecuador area and Mexico (Sims, 1980; Heuvelink, 2005; Peralta et al., 2005). Today, cultivated tomato have been well improved after several years of domestication due to the selection of vast morphological, agronomic and nutritional traits from wild species *via* plant breeding (Heuvelink, 2005). The plant is a perennial in its natural habitat but often grown as an annual (Gatahi, 2020). It grows to a height of about 1 –

3 m with an angular weaker stem that is covered by hairy trichomes and secretes volatile compounds (Gatahi, 2020). Its leaves are arranged in alternate form on the stem and the average fruit weight of a common tomato is *ca*. 100 g (OECD, 2017; Gatahi, 2020).

Botanically, tomato fruit is developed from a fertilized ovary and classified as a fruit but commercially treated as a vegetable due to its use (Peralta et al., 2005). It produces ovoid or globular fleshy fruits with confined seeds in the pulp (OECD, 2017). The outer tissue (pericarp) is coated with a cuticular layer and the inside consist of the placenta, which holds the seeds (OECD, 2017). Fruit development and ripening usually takes seven to nine weeks from anthesis to the end of maturation and the colour of the fruit is obtained from the pericarp (Heuvelink, 2005; OECD, 2017; Gatahi, 2020). Tomato is a diploid model species for studying cultivated dicotyledonous plants and fleshy climacteric fruit ripening and physiology, biochemistry, genetics, hormone function and molecular biology (Sato et al., 2012; Heuvelink, 2018; Gatahi, 2020). Also, it has numerous traits of agronomic importance including fleshly fruits, compound leaves and sympodial shoots that cannot be investigated in other model plants such as *Arabidopsis thaliana* and *Oryza sativa* (Sato et al., 2012; Heuvelink, 2018). Moreover, its comparatively short life cycle and fully sequenced genome act as a good genomic reserve to better understand the molecular, biochemical, metabolic and cellular processes related to fruit development and plant stress tolerance mechanisms (Sato et al., 2012; Suresh et al., 2014).

2.2 Tomato production and benefits

Tomato is one of the highest valued and most consumed vegetable crop globally (Heuvelink, 2018). It is cultivated in both open fields and under greenhouse conditions for the fresh and/or processed food markets. Greenhouses are often used for large scale production. Total world

production is estimated at 189 million tonnes (Mt) with a harvested area of 5.2 million hectares in 2021 (FAOSTAT, 2023). China is the leading tomato producer (67.5 Mt) which account for 36% of the world's production followed by India (21.2 Mt), Turkey (13.1 Mt) and United States (10.7 Mt) (FAOSTAT, 2023). Canada is ranked 42nd globally and second in North America tomato production, with a total production of 515,013 t in 2021 (AAFC, 2022a; FAOSTAT, 2023). In 2021, Canada produced 279,627 t of fresh market tomato under greenhouse condition from a cultivated area of about 685 ha with a farm gate value of CAD$ 714.8 million (AAFC, 2022b). Although huge volumes of tomato are produced, over 75 t of greenhouse and 125,371 t of field-grown tomato are imported yearly to meet the increasing demand (AAFC, 2022b, a). Moreover, the popularity of tomato fruits relates to its phytochemical and nutritional qualities as well as its use in diverse forms: either fresh or processed (Chaudhary et al., 2018; Heuvelink, 2018). The fresh or processed tomato is utilized in various parts of the world as dried tomatoes (dried fruits, powder, flakes), tomato preserves (tomato paste, tomato puree, tomato juice or whole peeled tomatoes) and several tomato-based foods including salads, ketchups, soups, sauces and curries (Heuvelink, 2018).

Nutritionally, tomato fruits are known to contain high levels of phytochemicals of human health importance (Quinet et al., 2019). It is an excellent source of fiber, phenolics, flavonoids, vitamin (A, B complex, C and E), carotenoids and minerals (phosphorus, potassium, magnesium, iron, copper and manganese) (Beecher, 1998). Phenolics and carotenoids are the most abundant phytochemicals with lycopene being the most common followed by β-carotene, gamma-carotene, lutein and phytoene (Beecher, 1998; Chaudhary et al., 2018). Additionally, these bioactive compounds have been demonstrated to exhibit high antioxidant capacity which protect cells

against oxidative stress by scavenging reactive oxygen species (Chaudhary et al., 2018). These antioxidant properties have been reported through *in vitro* and *in vivo* studies to induce anti-inflammatory, anti-proliferative, anti-tumorigenic, anti-atherogenic, anti-cancer, anti-mutagenic and anti-carcinogenic effects (Gloria et al., 2014; Lin et al., 2014; Chaudhary et al., 2018). Such effects contribute largely to the prevention of chronic diseases including cardiovascular, cancer, atherosclerosis, and neurodegenerative disorders (Chaudhary et al., 2018; Nowak et al., 2018).

2.3 Soil acidity and aluminum concern

Increasing crop productivity and quality are fundamental for achieving global food and nutritional security. The attainment of such goals is significantly constrained by several environmental factors including soil acidity and its associated Al phytotoxicity. Globally, acidic soils have been a concern and the major theme for scientific research. Acidic soils include oxisols or ultisols which have a pH value of below 5 and are widely distributed in many regions of the world (Kochian et al., 2015). Acidic soils are more prevalent in tropical and subtropical regions and account for 60% of their soils, and 50% of the world's agricultural lands, which hold up to 80% of global vegetable cultivation (Sade et al., 2016; Slessarev et al., 2016). While most soil acidity in tropical and subtropical regions occurs naturally, anthropogenic factors have recently become a major contributor to soil acidity in those regions and other parts of the world (Parth et al., 2011; Pavlů et al., 2021). Such factors include long-term and indiscriminate use of synthetic fertilizers, imbalance of soil nutrient cycle, organic matter build-up, excessive uptake and leaching of basic cations (Parth et al., 2011; Sade et al., 2016). The impact of soil acidity on crops is compounded by metal toxicity with Al^{3+} being the major limiting factor (Kochian et al., 2015). Moreover, the destructive impact of soil acidity is further aggravated by climate change and the endless heightened use of synthetic chemicals for crop production (Bojórquez-Quintal et al., 2017; Bungau et al., 2021).

Al is the third most ubiquitous metal in the earth's crust after oxygen and silicon. However, Al is neither required in biological systems and to date, no scientific evidence has proven its use in any biological processes in living organisms, which remains a biochemical enigma. The chemistry of Al interactions in soils is remarkably complex and still not fully understood by researchers, possibly due to the wide array of organometallic and multinucleated complexes and co-occurring ions in soils (Buchanan et al., 2015; Chauhan et al., 2021). In most soils, Al exists as non-toxic aluminum silicates and oxides to which plant roots are exposed and exhibit no deleterious effects (Buchanan et al., 2015). However, a decrease in soil pH below 5 facilitates Al solubility into monomeric forms [Al $(OH)^{2+}$, Al^{3+}, Al $(OH)_2^{+}$ and Al $(OH)_4^{-}$]. Among these, the trivalent form (Al^{3+}) is the most deleterious to plant growth and productivity because it stimulates a range of Al-related toxicity in most plants (Kochian et al., 2015; Silva et al., 2020).

Over the past decades, several studies have demonstrated the effect of Al on growth and productivity in several plant species (Kochian et al., 2015; Sade et al., 2016; Bojórquez-Quintal et al., 2017; Singh et al., 2017). Generally, most of these studies reported the toxic effects of Al and the tolerance mechanisms of plants (Awasthi et al., 2019; Borges et al., 2020; Fang et al., 2020), while a few reported beneficial effects on plant growth (Muhammad et al., 2019; Sun et al., 2020b). In recent years, significant genetic diversities in Al tolerance and novel sustainable strategies have been identified in several crop species due to the agronomic importance of crop cultivation on acid soils (Kochian et al., 2015). Such studies are crucial in advancing our knowledge and identifying Al-induced tolerant genes and their associated mechanism for better crop improvement, thus contributing to global food security.

2.4 Aluminum benefits and toxicity in plants

Generally, Al effects on plant growth and productivity have been viewed as a major threat to the attainment of global food security. Such effects have been demonstrated by earlier and more recent studies with root growth inhibition being the most obvious symptom of Al toxicity (Wang et al., 2016; Jaskowiak et al., 2018). On the other hand, stimulation of root and whole plant growth has been recognized as a beneficial effect of Al in several plant species (Arasimowicz-Jelonek et al., 2014; Muhammad et al., 2019; Liu et al., 2020). However, the levels of Al used in most of these studies are not clearly defined. While the levels of Al are expressed in its compound forms in some studies (Wang et al., 2016; Li et al., 2018b), others expressed it in a trivalent form which gives a better representation of the amount of Al plant roots are exposed to (Awasthi et al., 2017; Jaskowiak et al., 2018; Sun et al., 2020b). Moreover, the toxic or beneficial effect of Al on plant growth depends largely on the growing conditions, Al concentration and duration of exposure, plant species and physiological age (Huang et al., 1992; Bojórquez-Quintal et al., 2017; Aguilera et al., 2019; Ofoe et al., 2022b). For example, low Al concentration of 0.25 and 0.5 mM did not affect *Trifolium* and tomato seedling root growth whereas high concentrations of 1.25 mM remarkably restricted root growth (Bortolin et al., 2020; Ofoe et al., 2022b). In barley (*Hordeum vulgare*), low concentrations between 5-20 μM had no significant effect on root grow while concentrations of 40 and 60 μM reduced root growth. Similarly, exposure of plants to low Al doses for a short period inhibited root growth whereas no inhibitory effect was noticed with higher Al concentrations for long exposures time (Zhou et al., 2011). These suggest that different plant species have varied response mechanisms to Al toxicity.

2.4.1 Benefits of aluminum to plant

Over the past decades, there has been overwhelming published evidence on the beneficial effects of Al on plants (Arasimowicz-Jelonek et al., 2014; Muhammad et al., 2019; Liu et al., 2020; Sun et al., 2020b). However, to date, no research has proven the biological significance of Al at the cellular level.

2.4.1.1 Promotion of plant growth and metabolism

Al-induced plant growth promotion is often noticed in plants adapted to acidic soils, native species and Al hyperaccumulators (Arasimowicz-Jelonek et al., 2014; Bojórquez-Quintal et al., 2017; Sun et al., 2020b). Hyperaccumulators are indifferent to the concentration and duration of Al exposure and exhibit no toxic effect even at higher Al doses. For example, Rehmus et al. (2014) showed that a low Al dose of 300 µM enhanced the root biomass of *Tabebuia chrysantha* tree seedlings while a high concentration of 2400 µM induced an inhibitory effect. According to Pollard et al. (2014), two types of hyperaccumulators can be observed in plants: obligate and facultative. Obligate hyperaccumulators are plants that can only grow on metalliferous soils and are unable to survive once a particular metal is absent. In contrast, facultative hyperaccumulators can grow and survive regardless of the presence or absence of a given metal in soils. Applying these two types to Al hyperaccumulators might not be conclusive since Al growth studies have only been performed for fewer plant species (Schmitt et al., 2016).

Tree species such as *Camellia* spp (tea), *Symplocos paniculate, Quercus Serrata*, *Coffea arabica, Vochysia tucanorum* and *Melastoma malabathricum* are known to be Al-hyperaccumulators and can grow on acidic soils (Hajiboland et al., 2013a; Bojórquez-Quintal et al., 2014; Schmitt et al., 2016; Liu et al., 2020; Sun et al., 2020b; Bressan et al., 2021). In tea (*Camellia japonica*), Liu et

al. (2020) demonstrated that treatment of 2-year-old plants with 0.5-1 mM Al enhanced root biomass *via* elongation and proliferation of lateral roots, chlorophyll content, net photosynthetic capacity and accumulation of nitrogen (N), phosphorus (P), iron (Fe), manganese (Mn), zinc (Zn), and copper (Cu) in the fine roots. Although the mechanism of Al-induced growth stimulation in *camellia* species remains elusive, it was suggested that the increased accumulation of nutrient elements could be an Al-induced mechanism (Liu et al., 2020). However, it is unclear how Al could facilitate the uptake of some macronutrients such as P and N which are known to be relatively unavailable under low soil pH. Similarly, Sun et al. (2020b) using five *C. sinensis* varieties showed that Al treatment enhanced new root growth in a dose-dependent manner while tea plants deprived of Al treatment exhibited damaged root tips and no new root formation. Root tip ultrastructural analysis revealed that Al is crucial for meristematic cell development and activities as root cells of Al-treated tea plants were dense with a large and noticeable nucleus compared to Al-deprived plants. Interestingly, Al localization examination indicated that Al is contained in the nuclei of root meristems and translocated to the cytosol upon removal which worsens DNA damage and suggests that Al could primarily function in tea plants root growth via DNA integrity maintenance (Sun et al., 2020b). Also, Bressan et al. (2021) showed that exposure of *Vochysia tucanorum* seedling to 1110 μM Al exhibited increased root growth, root, stem and leaf biomass and conserved high photochemical performance and leaf gas exchange rates. Additionally, seedlings with no Al exposure showed no new root formation after 7 days and stopped growing with increased pre-existing roots necrosis and leaf chlorosis. Exposure of *M. malabathricum* seedlings to 0.5 mM Al considerably improved root and shoot growth, and relative dry weight via secretion of root mucilage which facilitates Al accumulation and improves nutrient (P, K, Ca and Mg) and water uptake (Watanabe et al., 2005; Watanabe et al., 2008b, a). In *Q. serrata,* Al stimulates root

elongation and activities and decreased root starch and sucrose content but increased glucose and ABA content in Al-treated roots (Moriyama et al., 2016). In the case of deciduous *S. paniculate,* it was reported that Al stimulates root growth and elongation in seedlings while saplings developed new twigs, leaves and roots thereby considerably enhancing the overall biomass (Schmitt et al., 2016).

Although most of the growth stimulation effects of Al in plants were reported in tree species that are adapted to acid soils, fewer studies have demonstrated such benefits in some economically important crops. For example, in maize (*Zea mays*) plants, low Al dose treatment inhibited root growth but significantly increased leaf growth rate in an Al exposure duration-dependent manner (Wang et al., 2015b). In rice (*Oryza sativa*) plants, Al enhanced root elongation (Famoso et al., 2011), chlorophyll and carotenoid contents as well as shoot height (Nhan & Hai, 2013). Similarly, Moreno-Alvarado et al. (2017) demonstrated using four rice cultivars exposed to 200 µM Al that Al considerably increased plant height, chlorophyll and sugar contents, root length and root fresh and dry biomass but did not affect amino acid and proline contents. In Al-tolerant soybean (*Glycine max*), 25 µM Al for 24, 36 or 48 h markedly increased callus and root growth (Du et al., 2010). Recently, it was reported in tomato that 500 µM Al stimulated total root length, hypocotyl and root surface areas as well as the overall total seedling fresh weight (Ofoe et al., 2022b). Poschenrieder et al. (2015) suggested that two modes of Al-induce growth stimulation can be noticed in plant species; (1) immutable boost (long-term) in growth stimulated by Al in hyper-tolerant plants; and (2) momentary increase (short-term) in growth as observed in most laboratory studies. Despite the plant growth stimulation effects reported by several authors, it remains elusive the exact mechanisms underpinning such effects. Nevertheless, a few possible mechanisms have been proposed by some studies (Figure 2.1A). Evidence from Al-hyperaccumulators studies indicates

that Al-mediated growth stimulations are closely related to increase nutrient uptake (Watanabe et al., 2005; Liu et al., 2020), activation of antioxidants and metabolic enzymes pathways (Hajiboland et al., 2013a; Xu et al., 2016a), elevated secretion of mucilage and organic acids that bind other heavy metals (Watanabe et al., 2008b, a; Xu et al., 2016a), maintenance of DNA integrity (Sun et al., 2020b), decreased toxicity of other heavy metals (Hajiboland et al., 2013b) and increased accumulation of carbohydrate and phenolic compounds (Moriyama et al., 2016; Xu et al., 2016a; Maejima et al., 2017).

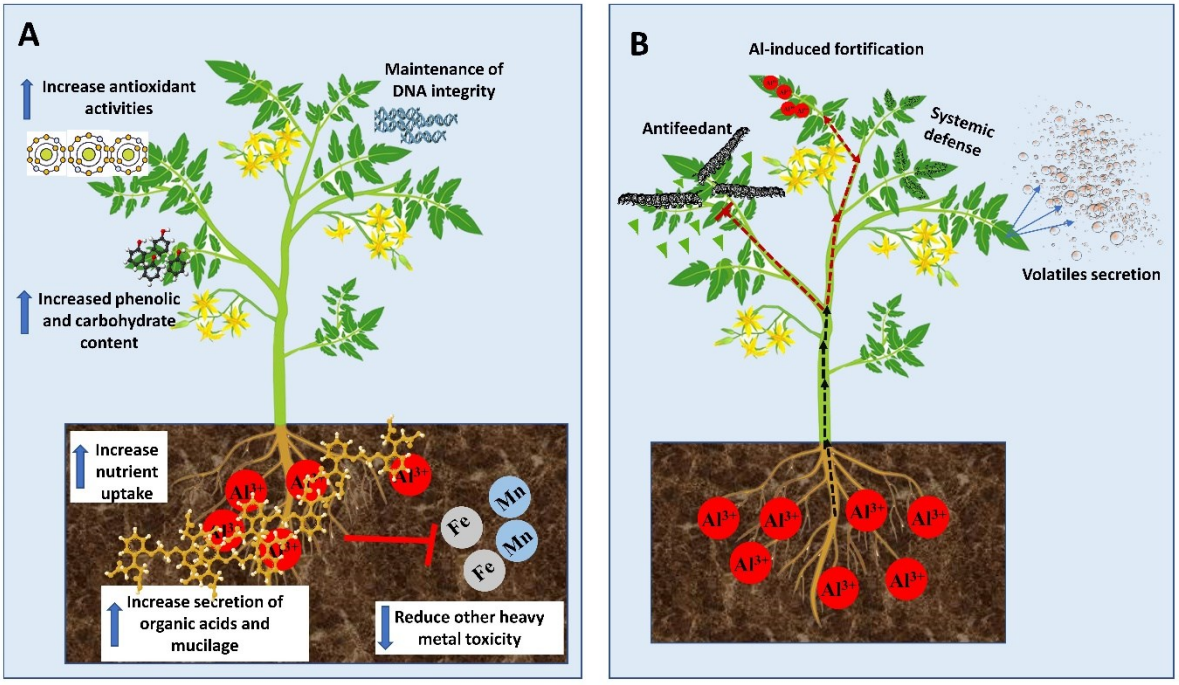

Figure 2.1. Benefits of Aluminum to plant growth and development. (A) Mechanisms of Al-mediated growth simulation. (B) Mechanism of Al-mediated protection against biotic stress.

2.4.1.2 Mitigation of abiotic and biotic stresses

Studies on the beneficial effect of Al have focused on plant growth stimulation and enhancement of nutrient uptake while its positive effects on biotic and abiotic stresses have not been widely

explored in the literature. Al has been reported to promote plant resistance to biotic (pathogens and herbivores) and abiotic stresses including nutrient deficiency and ion toxicity (Kaur et al., 2016; Bojórquez-Quintal et al., 2017). In tall fescue (*Festuca arundinacea*), Al enhanced plant growth and reduced the biomass and severity of white grubs (Coleoptera: Scarabaeidae) (Potter et al., 1996). Although the mechanism of such a defense response is unknown, it was suggested that Al accumulation in leaf tissues forms a sensory barrier that inhibits female insects from oviposition and thereby, reducing grubs population. In plant pathological studies, Al inhibits blast rot pathogen (*Thielaviopsis basicola Ferraris*) spores' germination and vegetative growth (Meyer et al., 1994). Similarly, Al enhanced resistance to potato late blight pathogen (*Phytophthora infestans*) by restricting mycelia and sporangial germination (Andrivon, 1995) and inducing defence responses in susceptible potato plants (Arasimowicz-Jelonek et al., 2014). Such a protective mechanism was characterized by localized accretion of ROS (e.g. H_2O_2) in roots and systemic induction of nitric oxide and salicylic acid-dependent pathways in leaves. These correlated with pathogen-related gene expressions and protein activities (Arasimowicz-Jelonek et al., 2014). Although it remains unclear how Al mediates such responses, various ways have been presented (Figure 2.1B), which suggests that Al could be deployed as an effective strategy for devastating disease control.

Despite the increased solubility and availability of Al in acidic soils, the presence of other metals such as Mn and Fe are high and can induce a toxic effect in plants (Bojórquez-Quintal et al., 2017; Muhammad et al., 2019). Rice plants treated with 200 µM Mn alone affected shoot and root growth whereas the addition of 200 µM Al alleviated Mn toxicity (i.e., leaf chlorosis and necrosis) in rice seedlings (Wang et al., 2015d). Such Al-induced mitigation of Mn toxicity was enhanced by reduced Mn uptake in roots and subsequent accumulation in shoots due to changed membrane

potential and modified cell membrane binding properties in rice roots (Wang et al., 2015d). Likewise, Muhammad et al. (2016) demonstrated that Al-induced antagonistic interaction with Mn and ameliorates Mn toxicity in three genotypes of barley (*Hordeum vulgare*). Moreover, toxic levels of Fe induce oxidative stress via excess production of ROS in plants which facilitate cellular damage and loss of functions (Zahra et al., 2021). Al-induced alleviation of Fe toxicity has been reported in tea (Hajiboland et al., 2013b), *M. malabathricum* (Watanabe et al., 2006) and rice plants (Alia et al., 2015). In these species, Al decreased root cell surface charges to restrict Fe uptake and translocation and hindered bronzing of leaves of treated plants. In hydroponic studies, Yang et al. (2016c) showed that exposure of tea plants to fluoride (F) inhibited the growth of shoots and roots while the addition of Al neutralized F toxicity by forming an Al-F complex to stimulate the growth of tea plants. Also, P deficiency is a major concern in acidic soils and Al has been reported to promote P uptake in plants (Li et al., 2016a). In maize, Al application induces the expression of genes that prevents inorganic P starvation (Maron et al., 2008), while Al up-regulated low P-responsive protein accumulation in citrus (*Citrus sinensis*) leaves. Such proteins include purple acid phosphatases, pyrophosphatases, phosphoenolpyruvate carboxylase, glycerophosphodiester phosphodiesterase and ribonucleases, which are known to play critical roles in plant adaptation to Pi-limitation by hydrolyzing organic P and/or (pyrophosphate) PPi to Pi, enhancing Pi acquisition and utilization, inducing Pi release from macromolecules and remobilizing Pi availability (Li et al., 2016a).

2.5 Aluminum phytotoxicity

Al toxicity to plants is one of the major threats to crop productivity under acidic soils (Kochian et al., 2015). Al triggers a series of Al-induced phytotoxic syndrome which includes disruption of

root growth and development, reduction in photosynthesis and plant growth, accumulation of reactive oxygen species (ROS) and damage of cellular and biochemical components.

2.5.1 Inhibition of root growth and development

The primary symptoms of Al toxicity in plants are rapid inhibition of root growth and disruption of root morphology (Buchanan et al., 2015; Zhang et al., 2019a). Such reduction in root growth has been widely used as a marker in evaluating Al toxicity or Al tolerance plants (Awasthi et al., 2017). Root tips are the most sensitive part of the root system and respond to micromolar concentrations of Al (Huang et al., 2014b). It has been established that the root tip is the most prominent plant organ and the distal transition zone between the apical meristem and elongation zone of roots plays a critical role in sensing Al toxicity (Yang & Horst, 2015; Zhu et al., 2017; Zhang et al., 2019b; Zhu et al., 2019; Wu et al., 2022). This suggests that Al toxicity or tolerance mechanism should predominantly focus on root studies. Al-induced inhibition of root growth and disruption of root structure has been reported in several plant species and the timing of symptoms development varies from plant to plant (Yanık & Vardar, 2015; Balzergue et al., 2017; Amaral et al., 2018; Furlan et al., 2018; Agarwal et al., 2019; Chen et al., 2020; Ofoe et al., 2022b). For instance, while inhibition of Al-sensitive maize root elongation was observed after 30 min of Al exposure (Llugany et al., 1995), root growth inhibition of soybean occurred after 5 min of Al exposure (Kopittke et al., 2015). Al affects root tip cell division and elongation which results in abnormal cell organization and thickening of the root cell wall (Yan et al., 2018; Zhu et al., 2019). Al-induced root growth inhibition results from several interactions between Al^{3+} and cellular components of plant roots (Buchanan et al., 2015; Silva et al., 2020). Root cell walls are composed of pectin, cellulose and hemicellulose, which serve as a protective barrier against harmful

environmental cues and are crucial for plant defence (Geng et al., 2017; Wu et al., 2022). These structural materials are rich in negatively charged phosphate and carboxylic groups, which can interact with Al ions (Geng et al., 2017). Increasing evidence revealed that Al initially targets the root epidermis and cortex and instantly binds to root cell walls which jeopardises cell wall integrity and functions including cell expansion and whole root growth(Yang & Horst, 2015; Geng et al., 2017; Zhu et al., 2017; Wu et al., 2022). However, the exact mechanism of Al-induced root growth inhibition remains elusive.

2.5.2 Reduction of water and nutrient uptake

Exposure of plants to Al toxicity instigates water stress, particularly physiological drought that restricts plant capacity to acquire water and nutrients (Buchanan et al., 2015; Kochian et al., 2015). Such impedance in nutrient uptake is facilitated by Al-induced disruption of root cells, inhibition of root growth and reduction in root volume. Previous studies have provided compelling evidence that Al affects plasma membrane functions and thereby, regulating the flow of ions to important parts of the plant for physiological processes (Guo et al., 2007; Gupta et al., 2013). Moreover, the active transport of nutrients is triggered by hydrogen ion gradients which are mediated by proton antiporters located at the plasma membrane (Zhang et al., 2019a). Al binds to the negatively charged phospholipid bilayers of the plasma membrane which destabilizes membrane potential and inhibits H^+-adenosine triphosphatase (H^+-ATPase) proton exclusion activities. Consequently, this affects transport of nutrient ions including K^+, NH_4^+, Mg^{2+} and Ca^{2+} (Gupta et al., 2013; Zhang et al., 2017a). In maize, Mariano et al. (2015) used a divided-root-chamber technique to reveal that Al altered nutrient uptake in the roots and considerably reduced the net uptake of Ca and Mg but not K content. Moustaka et al. (2016) reported that exposure of Al-sensitive wheat (*Triticum*

aestivum) plant to increasing Al concentration (0–148 μM) resulted in decreased Ca and Mg content in leaf tissue. In pea (*Pisum sativum*), Kichigina et al. (2017) indicated that Al reduced K, Mg, Zn, Mn and S content in the root and shoots of Al-treated plants. Guo et al. (2018) showed that Al treatment did not only reduce N, P, K, Ca, Mg and S uptake but also decreased the relative water content of citrus root and leaves. In sugarcane, Al significantly reduced nutrient use efficiency of macro and micronutrients (Borges et al., 2020). Additionally, P deficiency is a major concern in acidic soils as Al has a high affinity to P and forms insoluble Al-P compounds in soils (Magalhaes et al., 2018). Numerous studies have reported that Al reduces P uptake and utilization in several plant species such as Eucalyptus (Teng et al., 2018), oat (*Avena sativa*) (Djuric et al., 2011), *Citrus grandis* (Guo et al., 2017) and soybean (Chen et al., 2019b). These studies indicate that Al toxicity results in plant nutritional imbalance, which can affect the growth and productivity of crops.

2.5.3 Reduction of photosynthetic capacity

The impact of Al toxicity on plant photosynthesis has been studied extensively in several plant species (Yang et al., 2015; Yusuf et al., 2016; Guo et al., 2018; Cheng et al., 2020). In Al-sensitive barley, Al treatment markedly reduced chlorophyll content and fluorescence as well as gas exchange parameters including net photosynthetic rate, intercellular CO_2 concentration, stomatal conductance and transpiration rate (Ali et al., 2011). In *Citrus*, Al-induced a decrease in chlorophyll pigment and altered chlorophyll a (Chla) fluorescence transient and fluorescence parameter which resulted in the overall reduction of leaf photosynthesis (Jiang et al., 2008; Guo et al., 2018). Similar effects of Al-induced reduction in total chlorophyll content, chlorophyll fluorescence and leaf photosynthesis rate were reported in maize (Zhao et al., 2017), rye (*Secale*

cereale) (Silva et al., 2012), *Eucalyptus* (Yang et al., 2015), peanut (*Arachis hypogaea*) (Shen et al., 2014), cocoa (*Theobroma cacao*) (Ribeiro et al., 2013), alfalfa (*Medicago sativa*) (Cheng et al., 2020), rice (Phukunkamkaew et al., 2021) and highbush blueberry (*Vaccinium corymbosum*) (Cárcamo et al., 2019). Evidence revealed that the decrease in leaf photosynthesis under Al stress is indicative of the performance of photosystem II (PSII) (Jiang et al., 2008; Guo et al., 2018). Chlorophyll a fluorescence induction analysis of Al treated citrus leaves showed a significant reduction of the maximum quantum yield of primary photochemistry (Fv/Fm), maximum chlorophyll fluorescence (Fm), total PSII performance index, the quantum yield of electron transport and oxygen-evolving complex (Jiang et al., 2008). Moreover, such Al-induced impairment in the overall photosynthetic electron transport network from PSII was proposed as the major cause of reduction in leaf CO_2 assimilation (Jiang et al., 2008). It was also suggested that Al toxicity could block electron transport and diminish PSII photochemistry thereby impeding leaf photosynthesis (Li et al., 2012).

2.5.4 Oxidative stress and cellular damage

Rapid production and accumulation of ROS including superoxide ($O_2^{\cdot -}$), hydrogen peroxide (H_2O_2), singlet oxygen ($^1O_2$) and hydroxyl (OH^{-}) radicals are one of the most important alterations in cell metabolism of plants under Al stress (Huang et al., 2014b; Furlan et al., 2018). Imbalance ROS production occurs a few minutes after Al exposure, which induces oxidative stress in plants and facilitates the damage of cellular components such as nucleic acids, membrane lipids and proteins (Huang et al., 2014b; Guo et al., 2018; Yamamoto, 2019). Such ROS are generated in either the mitochondria, peroxisome or chloroplast in response to Al treatment (Shavrukov & Hirai, 2016; Turkan, 2018). Al-induced ROS accumulation has been reported in several plant

species such as tomato (Borgo et al., 2020; Ofoe et al., 2022b), rice (Awasthi et al., 2017; Awasthi et al., 2019; Bera et al., 2019), black gram (*Vigna mungo*) (Chowra et al., 2017), tea (Devi et al., 2020), soybean (Chen et al., 2019b), highbush blueberry (Cárcamo et al., 2019), *Trifolium* (Bortolin et al., 2020) and peanut (Huang et al., 2014a; Huang et al., 2014b). Despite its deleterious effect, ROS can perform a dual function in plants; acting as important signal molecules to regulate metabolic and physiological processes and activating the expression of antioxidant machinery for Al-stress mitigation (Turkan, 2018).

Moreover, it was previously established that Al induces excessive ROS production *via* two main mechanisms, (1) rapid activation of NADPH oxidase in the plasma membrane (Kawano et al., 2003) and (2) distortion of mitochondrial electron transfer pathways (Yamamoto et al., 2002). NADPH oxidase-mediated ROS production occurs immediately and halts within the first 20 s after Al exposure. However, mitochondrial dysfunction-mediated ROS production occurs several hours after Al exposure suggesting that Al could enter the cell and perturb the normal function of these organelles. These indicate that as Al binds to the plasma membrane it activates the initial ROS signal *via* NADPH oxidase-mediated pathways, which could possibly activate antioxidant pathways for initial ROS detoxification. Besides, Al enters the cell and distorts membrane organelles including the mitochondrion which results in cellular damage. Interestingly, several studies have shown that Al-induced-ROS generation facilitates lipid peroxidation, the most remarkable symptom of oxidative stress, which accelerates membrane loss and protein degradation, and ultimately results in programmed cell death (Singh et al., 2017; Yamamoto, 2019; Ofoe et al., 2022b). Lipid peroxidation follows a chain of free radical reactions which results in the production of malondialdehyde (MDA), a highly reactive end product. In tomato plants, Al treatment enhances the production and accumulation of MDA and destabilizes membrane

functions (Borgo et al., 2020; Ofoe et al., 2022b). In tea plants, Devi et al. (2020) demonstrated that increasing Al doses increases ROS production which elicits lipid peroxidation and oxidation of macromolecules in roots and leaves of treated plants while in black gram, protein carbonylation was also observed (Chowra et al., 2017). Similarly, Al-induced ROS-mediated MDA accumulation was reported in rice (Ma et al., 2012), soybean (Chen et al., 2019b), tobacco (Yamamoto et al., 2002) and pea (Huang et al., 2014b).

2.5.5 Nucleus and DNA damage

The maintenance of nuclear materials is crucial for plant survival under environmental stress. It has been reported that upon Al attachment with the cell wall and further penetration into the cell *via* the disruption of the plasma membrane, it interacts with nuclear structures which subsequently affect the integrity of DNA and chromosomes (Eekhout et al., 2017; Jaskowiak et al., 2018; Szurman-Zubrzycka et al., 2019). It is suggested that the DNA is the major cellular target of Al where it binds to the negatively charged phosphodiester backbone and leads to changes in DNA conformation from B-form to Z-form. This reduces DNA replication by increasing DNA firmness which results in difficulty in unwinding DNA (Gupta et al., 2013; Eekhout et al., 2017; Wei et al., 2021a). In pea plants, Huang et al. (2014a) used DAPI-staining of root tip cells to reveal that increasing Al exposure time from 4-12 h disorganized root cells, compromised membrane integrity and the affected nuclei appeared squished, lobed and abnormal in shape. These resulted in DNA fragmentation and shortening, and degradation of nuclear chromatin after 4 h exposure to 100 µM $AlCl_3$. Similarly, a cytological study of *Pinus massoniana* roots indicated that Al toxicity disrupts cell division, which was characterized by physiological alteration of nucleoproteins and induction of four types of chromosomal aberrations including chromosomal adhesion, chromosomal

fragmentation, c-mitosis, and chromosomal bridges (Zhang et al., 2014a). Such Al-induced chromosomal aberration might be irreversible and could result in programmed cell death.

Moreover, in a study of Al-induced cell death in six cereal roots, Vardar et al. (2016) demonstrated that DNA fragmentation which is indicative of cell death was induced at 30 mins after 100 μM $AlCl_3$ treatment. The Al-induced cell death was noticed in barley, triticale (×*Triticosecale*), oat and rye roots, but not in wheat and maize. These data suggest that wheat and maize might be comparatively more tolerant than the other plant species. Likewise, Jaskowiak et al. (2018) showed that Al significantly reduced cell mitotic activity, and stimulated micronuclei formation and disintegrated nuclei in barely root cells in a time-dependent manner. Also, the TUNEL test and flow cytometry analysis indicates that Al toxicity damages DNA, alters cell cycle and delays cell division in barley meristematic root cells. Although it is obvious that Al instigates disruption of cell cycles, it remains elusive whether such disruptions occur throughout the cell cycle and if it is species and region dependent as most studies focus on root tips. Additionally, monitoring cytotoxic changes in time and whether these changes could be reversed after Al withdrawal will help elucidate the Al-induced cell cycle effects.

Although the mechanism of how Al damages DNA remains unknown, loss-and-gain of function mutational analyses have provided insight into understanding the effect of Al on DNA double-strand breaks (DSBs) (Nezames et al., 2012; Sjogren et al., 2015; Eekhout et al., 2017; Sjogren & Larsen, 2017). Mutants in key DNA damage response (DDR) genes such as *suppressor of gamma response 1* (*SOG1*), *ataxia telangiectasia* and *RAD3 related* (*ATR*), *sensitive to UV 2* (*SUV2*) and *aluminum Tolerant 2* (*ALT2*) have been shown to partially reverse growth inhibition in mutants

defective in ABC transporter required for normal growth (Al-sensitive 3 (ALS3) under Al toxicity (Nezames et al., 2012; Sjogren et al., 2015; Eekhout et al., 2017; Sjogren & Larsen, 2017). ATR is an important DNA checkpoint regulator enlisted by SUV2 to strengthen single-stranded DNA because of a delay in replication fork movement, whereas ATM associates with ATR and functions in detecting DNA double-strand breaks (Hu et al., 2016b; Szurman-Zubrzycka et al., 2019). SOG1 is a central DDR transcription factor that is phosphorylated by both ATR and ATM to modulate genes involved in DNA damage response (Yoshiyama et al., 2013). ALT2 is a WD-40 protein that is crucial for assessing DNA integrity (Nezames et al., 2012). Further studies in *Arabidopsis* and barley revealed that *atr* mutants exhibited improved root growth even at high Al concentrations (Chen et al., 2019a; Szurman-Zubrzycka et al., 2019). On the other hand, Sjogren et al. (2015) demonstrated that *atm* suppressed Al-hypersensitivity and increased DNA synthesis-dependent endoreplication levels in *als3* mutants. Similarly, Chen et al. (2019a) revealed that *atm* mutants compromised their recovery after exposure to high Al treatment. These suggest that Al does not interfere with DNA replication and that high Al dose may predominantly cause DSBs but not single strand breaks since ATM is important for sensing DSBs.

2.5.6 Cytoskeleton disruption

Cytoskeleton primarily functions in various cellular processes including cell growth, cell differentiation, cell division and internal arrangement which contribute to root growth (Gardiner et al., 2012; Quezada et al., 2022). It consists of a network of microtubules, actin filaments and other related proteins which are potential targets for cytosolic Al toxicity (Gardiner et al., 2012; Sade et al., 2016). It has been well documented that Al destabilizes and/or delays microtubule cytoskeleton arrangements and alters tubules polymerization resulting in restriction of root growth

(Amenós et al., 2009; Baranova et al., 2016). In *P. massoniana* root cells, Al exposure induces an aberrant formation of microtubule arrangement which was characterized by short microtubule fragments (Zhang et al., 2014a). Moreover, increasing Al concentration for a longer duration severely perturbed the microtubule organization and performance of phragmoplast and mitotic spindle fibres which were attributed to extensive depolymerization of microtubules and actin filaments (Zhang et al., 2014a). Fang et al. (2020) showed that the effect of Al toxicity on actin filaments organizations is Al concentration-dependent as 100 μM $AlCl_3$ had no distinct effect on actin filaments, whereas treatment of *Malus domestica* pollen tubes with 600 μM $AlCl_3$ triggers an abnormal adjustment of the actin filaments. Interestingly, transcriptomic analyses revealed that Al toxicity downregulated numerous genes involved in cytoskeleton metabolism in two citrus species roots (Guo et al., 2017) and leaves (Li et al., 2016a), and tea roots (Fan et al., 2019a). These studies suggested that cytoskeletal components in roots, leaves and pollen tube cells could be a primary target for Al toxicity and thereby, inhibiting cell growth and division. Nevertheless, it remains unclear how Al might interact with cytoskeletal elements. Furthermore, it was suggested that Al can perturb the total cytoskeleton dynamics by directly associating with cytoskeletal elements and/or indirectly altering cytosolic Ca^{2+} signalling networks that are critical in cytoskeletal stabilization (Amenós et al., 2009; Gupta et al., 2013; Sade et al., 2016).

2.6 Mechanisms of aluminum tolerance in plants

Plants are sessile and exposed to varying degrees of Al stress. However, most plants have evolved diverse mechanisms including physiological, biochemical and molecular mechanisms to cope and survive under Al toxicity. Such mechanisms are broadly grouped into two types: Al external exclusion mechanism which is aimed at avoiding Al from entering root cells; and symplastic or

internal tolerance mechanism which allows entry of Al into root cells, detoxification and compartmentalization into subcellular compartments (Kochian et al., 2015; Kopittke et al., 2015; Sade et al., 2016; Bojórquez-Quintal et al., 2017; Furlan et al., 2020).

2.6.1 Aluminum exclusion mechanism

2.6.1.1 Exudation of organic compounds

Organic acids (OA) efflux is the most characterised and well-documented mechanism in Al tolerance in plants. In response to the rhizotoxic effect of Al, most plant roots release deprotonated anions that bind Al at the rhizosphere to form non-toxic complexes and impede root entry (Kochian et al., 2015). The commonly identified OAs secreted by plants in response to Al exposure are citrate, malate and oxalic acids (Figure 2.2A) (Kichigina et al., 2017). Root exudation of OA is Al^{3+}-dependent, and the type of OA secreted differs from plant to plant (Table 2.1), but large differences occur mainly in cereals (Schroeder et al., 2013; Bojórquez-Quintal et al., 2017). Citrate and malate are the most common OA efflux by several plant species, whereas oxalate secretion has only been identified in buckwheat (*Fagopyrum esculentum*) and Taro (*Colocasia esculenta*) (Buchanan et al., 2015). These OAs are components of the tricarboxylic acid cycle localised in the mitochondria, ubiquitous in all plant cells and exhibit different chelating abilities with Al ions (Brunner & Sperisen, 2013). Moreover, plant cells are rich in OAs but secretes specific ones in response to Al which suggest the involvement of specific transport mechanisms. Some plant species including wheat, *Arabidopsis*, common bean (*Phaseolus vulgaris*) and soybean have been identified to exude more than one OA in response to Al exposure (Table 2.1). Although the mechanism of simultaneous release of OA in response to Al remains unknown, this indicates that multi-transport response and co-expression may function in these plants. Several studies have

revealed that the time for Al-induced OA secretion varies from plant to plant (Kichigina et al., 2017; Silva et al., 2018; Ma et al., 2020b). Based on the duration and rate of OA released after Al exposure, two patterns of Al-induced secretion of OA have been proposed (Figure 2.2B). In pattern I, no obvious delay in time and rate of OA secretion was observed upon Al exposure (Figure 2.2B). Such a pattern occurs within minutes of Al exposure and has been observed in buckwheat, wheat, barley and beets (Zheng et al., 2005; Gruber et al., 2010; Li et al., 2017; Silva et al., 2018). The rapid OA secretion could suggest that Al interacts with a pre-existing anion channel and require no induction of transporter genes. However, in pattern II, there is a notable delay in time and rate of OA secretion after Al exposure (Figure 2.2B).

Table 2.1. Different plants secrete distinct organic acids.

Plant species	OA type Release	Transporter Gene(s)	Reference
Amaranthus hypochondriacus	Citrate and Oxalate	Unknown	(Fan et al., 2016)
Arabidopsis thaliana	Malate and Citrate	*AtALMT1* and *AtMATE1*	(Liu et al., 2009)
Brassica napus	Malate	*BnALMT1/2*	(Ligaba et al., 2006)
Brassica Oleracea	Malate	*BoALMT1*	(Zhang et al., 2018)
Cajanus cajan	Citrate	*CcMATE4*	(Dong et al., 2019)
Callisthene fasciculata	Citrate and Oxalate	Unknown	(de Souza et al., 2020)
Camelia sinensis	Oxalate	Unknown	(Devi et al., 2020)
Camelina sativa	Malate	*CsALMT1*	(Park et al., 2017)
Citrus sinensis	Citrate	Unknown	(Yang et al., 2012)
Eucalyptus camaldulensis	Citrate	*EcMATE1*	(Sawaki et al., 2013)
Fagopyrum esculentum	citrate	*FeMATE1; FeMATE2*	(Lei et al., 2017b)
Fagopyrum esculentum	Oxalate	Unknown	(Wang et al., 2015a)
Glycine max	Citrate and Malate	*GmMATE and GmALMT1*	(Liang et al., 2013; Liu et al., 2016b)
Glycine soja	Citrate	*GsMATE*	(Ma et al., 2018)
Gossypium hirsutum	Citrate	*GhMATE1*	(Kundu & Ganesan, 2020)

Hevea brasiliensis	Malate	*HbALMT1, HbALMT2, HbALMT13, and HbALMT1*	(Ma et al., 2020b)
Hordeum vulgare	Mate and Citrate	*HvAACT* and *HvALMT1*	(Furukawa et al., 2007; Gruber et al., 2010)
Lupinus albus	Malate	*LaALMT1*	(Zhou et al., 2020)
Medicago sativa	Malate	*MsALMT1*	(Chen et al., 2013)
Oryza sativa	Citrate	*OsFRDL2, OsFRDL4*	(Yokosho et al., 2016a; Li et al., 2018a; Huang et al., 2019)
Phaseolus vulgaris	Citrate	*PvALMT* and *PvMATE*	(Njobvu et al., 2020)
Pisum sativum	Citrate	Unknown	(Kichigina et al., 2017)
Populus trichocarpa	Citrate and Malate	*PoptrMATE54 and PoptrALMT10*	(Cardoso et al., 2020)
Populus trichocarpa	Citrate	*PtrMATE1; PtrMATE2*	(Li et al., 2017)
Secale cereale	Malate and Citrate	*ScALMT1; ScFRDL2*	(Collins et al., 2008; Liu et al., 2009; Santos et al., 2018)
Secale cereale	Oxalate	Unknown	(de Sousa et al., 2016)
Solanum lycopersicum	Malate	*SlALMT3, SlALMT9*	(Ye et al., 2017; Wang et al., 2020b)
Sorghum bicolor	Malate	*SbMATE1*	(Sivaguru et al., 2013; Melo et al., 2019)
Triticum aestivum	Malate and citrate	*TaALMT1 and TaMATE1, TaMATE1B*	(Garcia-Oliveira et al., 2014; Silva et al., 2018; Liu et al., 2021a)
Vigna umbellate	Citrate	*VuMATE1*	(Liu et al., 2016c)
Zea mays	Citrate	*ZmMATE1*	(Maron et al., 2013; Du et al., 2021)

OA secretion may delay by several hours to days and the rate of secretion may increase with the time of Al exposure. For example, in poplar, citrate secretion was induced 12−24 hours after Al treatment (Li et al., 2017) while malate secretion in *Hevea brasiliensis* occurred 2−5 days after Al treatment (Ma et al., 2020b). A similar Al-induced OA secretion pattern has been observed in

maize (Du et al., 2021), rice (Yokosho et al., 2016a), sorghum (Sivaguru et al., 2013), rye (Silva et al., 2013) and *Arabidopsis* (Liu et al., 2009).

Comparative studies of Al tolerant varieties were used to identify genes encoding malate and citrate transporter (Kochian et al., 2015). Previous studies have identified Al-activated malate transporter (ALMT) in wheat (*TaALMT1*) (Sasaki et al., 2004) which encodes an Al^{3+}-activated anion channel on the plasma membrane for malate efflux and the multidrug and toxic compound extrusion (MATE) family of genes comprising of sorghum (*Sorghum bicolour*) (*SbMATE*) (Magalhaes et al., 2007) and barley aluminium-activated citrate transporter 1 (*HvAACT1*) (Furukawa et al., 2007) that encode plasma membrane citrate transporters at the root apex. These transporters release specific OA from plant roots into the rhizosphere in response to Al exposure. Silva et al. (2018) indicated that the *ALMT1* gene is made up of five intron and six exons and is not related to the *MATE* gene (Upadhyay et al., 2019; Wang et al., 2020a), suggesting that Al-tolerance in sorghum and wheat evolved independently and that distinctly different genes encode the same physiological response to Al-tolerance. The homolog of these genes has recently been cloned in other crops (Table 2.1) which indicates that the primary determinant for the type of OA to be secreted depends on the plant species and the family of transporter genes expressed.

Moreover, accumulating evidence indicates that not all *ALMT* and *MATE* genes are involved in Al-tolerance but perform other physiological functions (Sasaki et al., 2016; Sharma et al., 2016; dos Santos et al., 2017). For instance, in Arabidopsis, four members of ALMT (*AtALMT4, AtALMT6, AtALMT9* and *AtALMT12*) (Liu & Zhou, 2018) mediate guard cell regulation while in tomato, two members (*SIALMT4* and *SIALMT5*) are involved in fruit development and seed OA

content (Sasaki et al., 2016). Likewise, *VvMATE1* and *VvMATE2* are involved in proanthocyanin transport in *Vitis vinifera* fruit development (Pérez-Díaz et al., 2014), while in rice, *OsMATE2* regulate Arsenic uptake (Das et al., 2018). Similar physiological and developmental function of ALMT and MATE other than Al-tolerance has been reported in *Vitis vinifera* (De Angeli et al., 2013), barley (Xu et al., 2015), strawberry (Chen et al., 2018b), blueberry (Chen et al., 2015) and *Lotus japonicus* (Takanashi et al., 2016). Nonetheless, transporters for oxalate efflux are still elusive even though it was shown to be involved in Al-tolerance (Wang et al., 2015a). Although the mechanism of how Al-induced anion channels remain unclear and is still a major debate among researchers, three possibilities have been proposed to describe the patterns of Al-induced OA secretion (Ma et al., 2001): (1) Al directly interacts with anions channels and opens it for OA efflux; (2) Al is sensed by a specific plasma membrane receptor (unknown) and through cytoplasmic transduction pathways activate the anion channels for OA efflux. (3) Al enters the cell by unknown means and interacts directly or indirectly with anions efflux channels. However, Wang et al. (2022) used cryo-electron microscopy and electrophysiological measurements to reveal that AtALMT1 is composed of six transmembrane helix (TM) and six cytosolic α-helices. Al binds to the external structure on AtALMT1 which triggers changes in the TM1-2 loop and TM5-6 loop conformational resulting in the opening of the anion gate for malate efflux (Wang et al., 2022). This suggests that Al indeed interacts with anion channels to secrete OA for external Al detoxification (Pattern I, Figure 2.2B). Nevertheless, it is relatively unknown whether this mechanism is the same for other plant species.

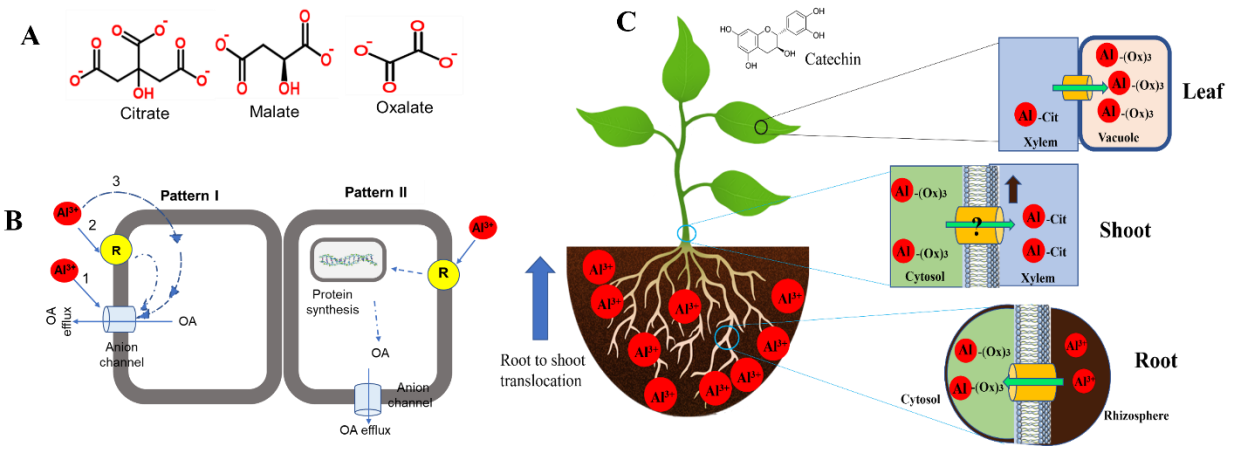

Figure 2.2. Al-induced modes of organic acid (OA) released and internal tolerance in plant roots. (A) Structure of the types of OA exudes by different plant species in response to Al exposure. (B) Proposed mode of Al-induced OA secretion (Modified from Ma et al. (2001)). (C) Internal detoxification and compartmentalization of Al in plants.

2.6.1.2 Release of other organic compounds

Some plants do not only exude organic acids to chelate Al ions but other secondary metabolites including benzoxazinoids and phenolics compounds have been reported (Morita et al., 2011; Maejima et al., 2017; Zhao et al., 2019). In *C. sinensis*, Morita et al. (2011) indicated that caffeine, a phenolic compound, was released by the roots in response to Al exposure. In Al tolerant species, Maejima et al. (2017) showed that *Melastoma malabathricum* and *Melaleuca cajuputi* roots produced higher phenolic content in their roots which could chelate Al ions. Similarly, *Eucalyptus camaldulensis* produces oenothein B in its roots in response to Al exposure which detoxifies external Al and thereby, promoting Al tolerance (Tahara et al., 2014). Intriguingly, recent studies demonstrated that Al-tolerant maize roots secrets two benzoxazinoids such as DIMBOA (2,4-dihydroxy-7-methoxy-1,4-benzoxazin- 3-one) and MBOA (6-methoxy-benzoxazolin-2-one) to prevent Al entry into the root cells (Guimaraes et al., 2014; Zhao et al., 2019). *In vitro* study indicated that both DIMBOA and MBOA chelates Al and form a non-toxic DMBOA-Al and

MBOA-Al complexes in the rhizosphere (Zhao et al., 2019). Although secondary compounds are known to be less effective chelators compared to OAs, it remains unknown how phenolics and benzoxazinoids are secreted in response to Al exposure. Additionally, regulatory and transporter genes involved in their release have not yet been identified and still unclear whether other plant species may utilize this mechanism.

2.6.1.3 Secretion of root mucilage and formation of border cells

Exudation of mucilage and formation of border cells around the root apex is an important exclusion mechanism employed by some plant species to thrive in Al toxic environment (Cai et al., 2013; Okamoto & Yano, 2017; Feng et al., 2019). In several plant species, the root border cells (RBCs) serve as a protective shield between the root apex and Al toxicity by enhancing the packing of mucilage (Cai et al., 2013). Mucilage is a gel-like polysaccharide material that is secreted from the root cap and border cells (Cai et al., 2013). It is rich in negatively charged carboxyl compounds including uronic acids, that immobilize toxic metal cations and render them non-toxic to plants (Watanabe et al., 2008b, a). Roots of *M. malabathricum* exude mucilage which facilitates Al accumulation and its removal reduced Al binding (Watanabe et al., 2008b, a). Similarly, Okamoto and Yano (2017) found that maize seedlings secret mucilage in their root tips and its removal enhances rapid recovery which lowered Al accumulation. Interestingly, Yang et al. (2016a) showed that Al accumulates in the akali-soluble pectin of RBC due to an increase in uronic acid content which chelates Al and inhibits its entry into the root apiece of pea. A similar Al exclusion effect of RBC has been observed in rice (Cai et al., 2012b; Nagayama et al., 2019), *castor (Ricinus communis)* (Alves Silva et al., 2014), and soybean (Cai et al., 2012b). However, the removal of RBCs from root apex increased Al sensitivity and accumulation in rice (Cai et al., 2012b), soybean

(Cai et al., 2013) and pea (Yang et al., 2016a). These suggested that RBCs are a vital Al exclusion mechanism in these plant species. Recently, Feng et al. (2019) reported that the RBCs surface of pea roots possess a layer of silica nanoparticles, which serves as an external Al-resistant covering that chelate Al in the apoplastic space and restrict its buildup in the cytoplasm. Nevertheless, it remains unknown how this mucilage is secreted and whether its secretion and RBC formation are conserved in plants.

2.6.1.4 Increase in rhizosphere pH

Rhizosphere pH is crucial for the solubility and the toxic effects of Al on plants and it is viewed as an Al exclusion mechanism (Yang et al., 2011d). In response to Al toxicity, some plants have evolved strategies to increase their rhizosphere pH, which was shown to decrease Al solubility and activity(Bose et al., 2010; Yang et al., 2011d; Wang et al., 2015a). Thus, restricting Al entry into the root cell and promoting Al tolerance (Kochian et al., 2015). Al-tolerant wheat varieties and other plant species elevate rhizosphere pH (from 4.5 to 4.8 in wheat treated plants *via* increased influx of H^+ ions (Bose et al., 2010; Yang et al., 2011d; Wang et al., 2015a). Moreover, exudation of OA to the rhizosphere in response to Al toxicity can alter rhizosphere pH (Javed et al., 2013). Although this is not well investigated, secretion of OA has been reported to stimulate the influx of H^+ ions that can increase rhizosphere pH (Yang et al., 2011b; Wang et al., 2015a). The involvement of PM H^+-ATPase has been demonstrated to play a vital role in modulating rhizosphere pH (Bose et al., 2010; Yang et al., 2011d). In Al-tolerant wheat, PM H^+-ATPase activity was considerably higher and correlated with an increase in rhizosphere pH compared to the Al-sensitive variety (Yang et al., 2011d). Furthermore, Li et al. (2018b) revealed that the root surface pH of a pea plant

was increased by regulation of PM H^+-ATPase activity and polar auxin transport which reduced Al-accumulation in the root.

2.6.2 Internal tolerance mechanism

2.6.2.1 Cell wall modification

Root cell wall is the principal barrier against harmful environmental cues and is considered a major target of Al (Yang & Horst, 2015; Geng et al., 2017; Zhu et al., 2017; Wu et al., 2022). Root cell walls are rich in carboxylic material including pectin, cellulose and hemicellulose, which possess a high affinity for Al ions (Geng et al., 2017; Wu et al., 2022). Adsorption capacity study in *Arabidopsis* revealed that hemicellulose in root cell wall exhibits the highest affinity compared to pectin and was suggested as the core target of Al (Yang et al., 2011a). Several studies have shown that alteration in cell wall composition is crucial for enhancing Al tolerance (Wang et al., 2015c; Xu et al., 2018; Yan et al., 2018; Riaz et al., 2019; Xu et al., 2019; Zhu et al., 2019). Such modifications in cell wall structures are promoted by a complex network of cell wall enzymes including xyloglucan endotransglucosylase (XET), xyloglucan endotransglucosylase-hydrolase (XTHs), pectin methylesterases (PME) and expansin (Zhu et al., 2012; Yang et al., 2013b; Kochian et al., 2015). *XTH* genes encode xyloglucan endohydrolase (XEH) and XET that catalyse the formation of cellulose-hemicellulose (xyloglucan) matrix and contribute to cell wall expansion (Zhu et al., 2012). In *Arabidopsis*, Al reduced the expression and activity of XTH17 and XTH31 in root cells whereas mutants of *XTH17* and *XTH31* exhibited improved Al tolerance by lowering hemicellulose content and retaining less Al in their cell wall (Zhu et al., 2014). Similarly, in *Phaseolus vulgaris*, expression of *XTH genes* and XET activities significantly reduced Al binding by changing cell wall porosity in root tips and enhancing Al tolerance (Zhang et al., 2016). Such

alteration in the cell wall porosity act as physical barrier to Al entry and restricts Al penetration to the root cell.

Cell wall pectin content and methylation influence the degree of Al tolerance (Yang et al., 2013b). Yang et al. (2011c) reported in buckwheat (*Fagopyrum tataricum*) that higher Al accumulation in Al-sensitive cultivar is facilitated by pectin content rather than the degree of methylation. The Al-sensitive cultivar exhibited a greater sensitivity of *pectin* methylesterases activity to Al which resulted in a significant increase in low-methyl-ester pectins and decrease of high-methyl-ester pectins (Yang et al., 2011c). Furthermore, Li et al. (2016b) observed that pectin content increased in Al-sensitive than Al-tolerant *pea cultivar and Al* PME activity was enhanced in the sensitive cultivar resulting in higher demethylesterified pectin content thereby enhancing Al accumulation in the root cell wall. Moreover, higher demethylated pectin mediated by PME results in the formation of negatively charged demethylesterified pectin and leads to an increase in Al ion binding (Li et al., 2016b). These suggest that Al-tolerant cultivars exhibit low PME activity and increase methylated pectin content. Furthermore, pectin methylesterase genes have been revealed to contribute to Al tolerance in several plant species. In *Arabidopsis*, *PME46* was reported to enhance Al tolerance by reducing PME activities and decreasing Al binding to cell walls (Geng et al., 2017). Unlike other PMEs, *PME46* has an PME inhibitor domain (N-terminal pro region) which promotes unprocessed PMEs retention and represses PME enzyme activity suggesting that PME46 activity could activate transcriptional repression of other *PMEs* thereby facilitating the accumulation of methylated pectin in the cell wall (Geng et al., 2017). Methylated pectin exhibits lower negative charge which will bind less Al and promote Al tolerance. Also, in alfalfa (*Medicago sativa*), polygalacturonase genes, *MsPG1* and *MsPG4,* were reported to increase Al tolerance by

enhancing cell wall plasticity and porosity and reducing Al accumulation in the cell wall (Li et al., 2020; Fan et al., 2022).

Molecular evidence revealed that in rice, *OsSTAR1* (Sensitive to Aluminum Rhizotoxicity 1) and *OsSTAR2* (Sensitive to Aluminum Rhizotoxicity 2) genes encode a bacterial-type ATP binding cassette (ABC) transporter protein for cell wall modification during Al toxicity. OsSTAR1 and OsSTAR2 interact to form a vesicle membrane-localized complex in root cells that export UDP-glucose from the cytoplasm into the cell wall perhaps through vesicular exocytosis (Huang et al., 2009). These compounds could bind to Al in the apoplast or utilize as substrates by cell wall modifying enzymes and thereby, reducing Al binding and damage to the cell wall (Buchanan et al., 2015). Recently, STAR1 and STAR2 were functionally characterised in buckwheat to regulate Al tolerance (Che et al., 2018b; Xu et al., 2018; Xu et al., 2019) and SbSTAR1 in sorghum (Gao et al., 2021). Similar to OsSTAR1/OsSTAR2 complex, FeSTAR1 and FeSTAR2 form an ABC transport protein that export UDP-glucose which influence hemicellulose metabolism by modulating XET activities (Xu et al., 2018; Xu et al., 2019). Additionally, SbSTAR1 enhanced Al tolerance when expressed in *Arabidopsis* lines (Gao et al., 2021). Although the counterpart of SbSTAR1 had not been characterised, it was suggested that it could mediate Al resistance *via* modulation of hemicellulose content in the root cell wall. These suggest that STAR1 and STAR2-mediated Al tolerance could be a conserved mechanism in plants although not yet identified in other plant species. Nevertheless, it remains unclear how the UDP-glucose exactly mediates Al tolerance and how it influences XET activity.

2.6.2.2 Internal detoxification and compartmentalization

Studies on Al tolerance mechanisms in Al-resistant plants and/or Al-hyperaccumulators have increased our understanding of how these plants detoxify Al within their roots (Kochian et al., 2015). Al-resistant plant species including hydrangea, *melastoma malabatbricum,* buckwheat and black tea (*Camellia sinensis*) can take up, detoxify and accumulate relatively high content of Al in their leaf tissues without displaying Al toxicity effects (Wang et al., 2015b; Bojórquez-Quintal et al., 2017). Evidence revealed that internal detoxification of Al is mediated by intracellular Al chelation and compartmentalization of Al-OA complexes into vacuoles (Figure 2.2C). In buckwheat, Al is taken up into the root cell and forms a non-toxic complex with oxalate at a 1:3 (Al-oxalate) ratio (Klug & Horst, 2010). During Al transport from root to shoot, the Al-oxalate is loaded into the xylem sap where Al-oxalate is exchanged for Al-citrate (1:1). In the leaves, Al-citrate is converted to Al-oxalate and sequestered into the vacuoles (Wang et al., 2015b). Although the mechanism of ligand exchange during xylem loading and unloading is unknown, a similar Al-detoxification mechanism was observed in *melastoma malabatbricum* and *C. fasciculata* (de Souza et al., 2020). Moreover, Al forms a no-toxic complex with catechin in the leaves of tea plants (Fu et al., 2020), whereas, in hydrangea, Al is complexed with 3-caffeoylquinic and delphinidin 3-glucoside in the sepals and citrate in the leaves (Ma et al., 1997). In *Andropogon virginicus*, a wild species of Poaceae, Al is accumulated in the leaf's trichomes and spikes of which some Al portions are secreted as viscous sap from the trichome apex (Ezaki et al., 2013).

2.6.2.2.1 Transporters for internal Al tolerance

Several studies have identified and functionally characterized transporter genes that mediate internal Al detoxification and sequestration. In rice, natural resistance-associated macrophage

protein (Nramp) Al transporter 1 (OsNrat1) encodes a unique plasma membrane transporter that mediates the influx of Al ions and contributes to Al tolerance in rice (Xia et al., 2010; Li et al., 2014). This high influx of Al ions mediated by OsNrat1 could reduce Al levels in the root cell wall by transporting Al into the root cells and subsequently sequestered into the vacuole thus promoting Al tolerance (Huang et al., 2012). Similarly, ALS1 (Aluminum sensitive 1) is an ABC transporter that is localized on the tonoplast and crucial for vacuolar Al sequestration and internal detoxification of Al in rice (Huang et al., 2012), *Arabidopsi*s (Larsen et al., 2007; Kochian et al., 2015), and buckwheat (Lei et al., 2017a). *AtALS1* is constitutively expressed in the roots and vasculature of Arabidopsis (Larsen et al., 2007) while in rice while *OsALS1* is expressed in the roots and induced by Al exposure (Huang et al., 2012). However, in buckwheat, *FeALS1.1* expression is upregulated by Al in both roots and leaves whereas *FeALS1.2* is not affected by Al (Lei et al., 2017a). Although *Nrat1* has not yet been characterized in other plant species, the similarities in localization and expression pattern of *OsALS1* and *OsNrat1* (Xia et al., 2010; Huang et al., 2012) could suggest that these transporters act collectively to mediate the internal detoxification of Al in rice. In buckwheat, FeIREG1 which belongs to the IRON REGULATED/ferroportin (IREG) transporters, is located in the tonoplast and sequesters Al into root vacuoles to enhance internal Al tolerance (Yokosho et al., 2016b). Similarly, FeIREG1 homolog has been characterized in soybean (GmIREG3) and overexpression of *FeIREG1* and *GmIREG3* in Arabidopsis promotes Al tolerance (Yokosho et al., 2016b; Cai et al., 2020). Moreover, Negishi et al. (2012) demonstrated in hydrangea (*Hydrangea macrophylla*) roots that two members of the aquaporin family, plasma membrane Al transporter 1 (*PALT1*) and vacuolar Al transporter *(VALT*), mediate cytosolic Al influx and subsequent sequestration into the vacuoles, respectively. Nevertheless, it remains unknown which Al form is transported by these two

aquaporins. Similarly, Wang et al. (2017) revealed that a plasma membrane-localized member of the nodulin 26-like intrinsic protein (NIP) plays a critical role in Al uptake and internal tolerance mechanism in Arabidopsis. NIP1;2 is an Al-malate transporter which mediates the removal of Al from root cell walls into the cytosol and facilitates xylem loading and root-to-shoot translocation of Al-malate (Wang et al., 2017). Additionally, the function of NIP1;2 depends on an operational Al-induced malate transporter, which is mediated by AtALMT1 in *Arabidopsis* roots. Besides, NIP1;2 and ALMT1 exhibit an epistatic association, which suggests a coordinated expression and that both NIP1;2 and ALMT1 act in the same pathway to mediate Al tolerance in *Arabidopsis* (Wang et al., 2020a). Therefore, effective coordination between Al exclusion and the internal tolerance mechanism is paramount to attaining Al tolerance in *Arabidopsis*.

2.6.2.2.2 Transcriptional regulation of Al tolerance in Plants

Mutational and molecular analyses have provided compelling evidence that Al activates coordinate expression of Al-tolerant genes (Figure 2.3). Several transcription factors have been reported to regulate the expression of downstream genes required to enhance Al tolerance. In *Arabidopsis*, a C2H2 zinc finger transcription factor, *sensitive to protein rhizotoxicity 1* (*STOP1*) localised in the nucleus was reported to play a critical role in Al tolerance (Iuchi et al., 2007). AtSTOP1 modulate the expression of *AtALMT1via* direct binding to consensus sequences in its promoter region (Tokizawa et al., 2015). Additionally, AtSTOP1 was reported to control the expression of *AtMATE* and *ALS3* to mediate Al tolerance (Kochian et al., 2015). Nevertheless, it remains unknown whether AtSTOP1 directly interact with these genes. Moreover, Al exposure was showed not to affect the expression of AtSTOP1 but stimulate the expression of several AtSTOP1 regulated downstream genes (Iuchi et al., 2007; Sawaki et al., 2009) suggesting that Al post-transcriptionally

modulates AtSTOP1. Intriguingly, it was revealed that Al stress stimulates the build-up of AtSTOP1 proteins and F-box proteins, REGULATION OF ATALMT1 EXPRESSION 1 (RAE1) and RAE1 homolog 1 (RAH1) which can interact with STOP1 proteins to mediate its degradation via the ubiquitin– 26S proteasome pathway (Zhang et al., 2019c; Fang et al., 2021b). Similarly, Guo et al. (2020) reported that HPR1, which encodes a constituent of the THO/TREX complex reduces AtSTOP1 protein accumulation by regulating nucleocytoplasmic export of AtSTOP1 mRNA. Furthermore, Fang et al. (2021a) demonstrated that SUMO E3 ligase SIZI partially modifies AtSTOP1 proteins *via* SUMOylation to modulate AtSTOP1 functions. These studies suggest that both post-transcriptional and post-translational mechanisms could regulate AtSTOP1 stability and function.

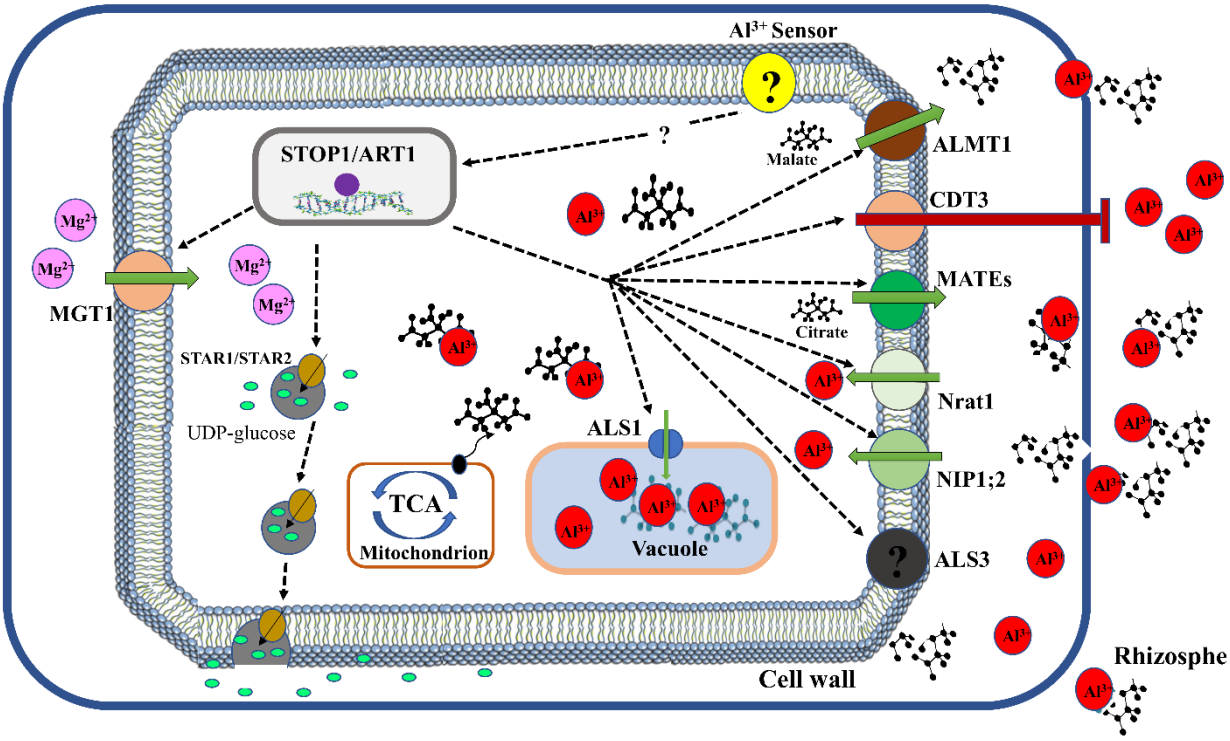

Figure 2.3. Transcriptional regulation of Al tolerance in plants. Al-stress is sensed by an unknown sensor and triggers activation of a C2H2-type zinc finger transcription factor (STOP1 or ART1) to initiate downstream signalling of Al tolerance genes. ALMT1, aluminum-activated malate transporter 1 for malate transport; CDT3, cadmium transport 3 block Al entry; MATEs, multidrug and toxic compound extrusion

for citrate transport (e.g. OsFRDL4 and OsFRDL2 in rice, AtMATE1 in Arabidopsis); Nrat1, natural resistance-associated macrophage protein (Nramp) Al transporter 1 facilitate Al influx; NIP1;2, plasma membrane-localized nodulin 26-like intrinsic protein transport Al-malate transporter in their cell; ALS3, Aluminum sensitive 3 promote Al influx; ALS1, aluminum sensitive 1 enhance sequestration of Al-OA complex into the vacuole; TCA, tricarboxylic acid cycle mediate OA production; STAR1/STAR2, sensitive to aluminum rhizotoxicity 1/2 facilitate UDP-glucose transport; MGT1, magnesium transporter 1 for magnesium influx.

In rice, a homolog of AtSTOP1, OsART1 (Al Resistance Transcription factor 1) is localized in the nucleus and performs a comparable role in Al tolerance (Yamaji et al., 2009). Like AtSTOP1, OsART1 regulate numerous Al-responsive genes involved in exclusion and internal Al tolerance mechanisms. These genes include *OsFRDL2*, *OsFRDL4*, *OsNrat1*, *OsSTAR1*/*OsSTAR2* complex, *OsALS1*, *OsART2*, *OsMGT1*, *OsEXPA10* and *OsCDT3* (Huang et al., 2009; Chen et al., 2012; Xia et al., 2013; Che et al., 2016; Yokosho et al., 2016a; Che et al., 2018a; Lu et al., 2018). Moreover, OsCDT3 encodes a predicted cysteine-rich peptide protein located at the plasma membrane of rice root cells which directly binds Al and restricts Al entry into root cell, thus contributing to Al tolerance in rice (Xia et al., 2013). *OsEXPA10* is an expansin gene whose expression is induced by Al and required for root cell expansion during Al stress (Che et al., 2016). However, its role in rice high Al tolerance is minimal. Recently, a homolog of OsART1, OsART2 was shown to be up-regulated by Al and regulate Al tolerance in rice as *osart2* knockout lines exhibit hypersensitivity to Al (Che et al., 2018a). Transcriptomic analysis indicated that OsART2 regulation of genes does not overlap with ART1 genes but modulates four genes which are implicated in Al tolerance. This suggests that OsART1 and OsART2 regulate different Al tolerance pathways and the latter could play an additional role in rice Al tolerance. Unlike AtSTOP1, the regulation mechanism of OsART1 stability and function remains unknown.

Furthermore, AtSTOP1/OsART1 homologs have been identified in several plant species including pigeon pea (CcSTOP1) (Daspute et al., 2018), sorghum (SbSTOP1) (Gao et al., 2019), tobacco (NtSTOP1) (Ito et al., 2019), cotton (GhSTOP1) (Kundu et al., 2019), rye (ScSTOP1) (Silva-Navas et al., 2021), soybean (GmSTOP1) (Wu et al., 2018; Zhou et al., 2018), tea (CsSTOP1) (Zhao et al., 2018), rice bean (VuSTOP1) (Fan et al., 2015), tomato (SlSTOP1) (Zhang et al., 2022), barley (HvATF1) (Wu et al., 2020) and wheat (TaSTOP1) (Garcia-Oliveira et al., 2013). Nevertheless, it remains unknown how Al stress transduces the signal to activate and stabilize STOP1/ART1.

2.6.2.3 Osmolytes accumulation

Production and build of osmolytes or compatible solutes are biochemical mechanisms employed by several plants under Al stress to promote retention of water status, transfer of cellular energy, macromolecules and membrane stabilization and ROS scavenging and thereby, contributing to the maintenance of cellular homeostasis (Pandey et al., 2016; Ejaz et al., 2020). Osmolytes are water-soluble uncharged molecules, which include amino acids (e.g. proline, γ-aminobutyric acid), sugars (trehalose, sucrose, glucose) and ammonium compounds (glycine betaine, choline, proline betaine) and whose accumulation do not interfere with cellular functions (Ejaz et al., 2020). In buckwheat, proline and total sugar content increased proportionally to Al concentration and was implicated in Al tolerance (Pirzadah et al., 2019). In two rye plants with different Al tolerance, de Sousa et al. (2020) demonstrated that proline content increased by threefold and 20% in Al-tolerant and Al-sensitive lines respectively due to the regulation of proline biosynthetic pathways which include enhanced glutamate and ornithine pathways for proline biosynthesis and re-oxidation to 1-pyrroline-5-carboxylate. Moreover, Bera et al. (2019) revealed that rice plants accumulated high

levels of glycine betaine in response to Al exposure. However, the activity of betaine aldehyde dehydrogenase, an important enzyme that mediates glycine betaine biosynthesis was considerably reduced which suggests that an unknown alternative pathway for glycine betaine production may function in rice to alleviate Al-induce osmotic stress. Similarly, the involvement of elevated osmolyte levels in response to Al exposure has been reported in alfalfa (Ma et al., 2020a), lettuce (Silva & Matos, 2016), rice (Awasthi et al., 2019) and sugarcane (Mantovanini et al., 2019). Furthermore, as Al toxicity induce water stress, these osmolyte function as osmoprotectants by reducing intracellular water potential, regulating turgor dynamics and stabilizing proteins and membrane integrity, thereby promoting Al tolerance (Ejaz et al., 2020).

2.6.2.4 Production and activation of antioxidants

The alleviation of Al-induced excessive ROS accumulation *via* antioxidant production and associated enzyme activities in plant cells is one of the most characterized defense mechanisms reported in several plant species (Gill & Tuteja, 2010; Awasthi et al., 2019). This antioxidant defense pathway is categorized into the enzyme-mediated and non-enzymatic antioxidant systems. The enzyme-mediated defense system involves an increase in activities and accumulations of antioxidant enzymes including ascorbate peroxidase (APX), monodehydroascorbate reductase (MDHAR), dehydroascorbate reductase (DHAR), guaiacol peroxidase (GPX), peroxidases (POD), superoxide dismutase (SOD), catalase (CAT), and glutathione reductase (GR) and/or upregulation of antioxidant enzyme genes expression which is induced by Al stress in several plants and levels correlate to Al tolerance (Sharma et al., 2012; Yusuf et al., 2016; Liu et al., 2018b; Awasthi et al., 2019; Devi et al., 2020; Du et al., 2020; Salazar-Chavarria et al., 2020). SOD is the first line of defence against oxidative stress, which catalyses the dismutation of $O_2^{\cdot-}$ radicles into oxygen and

H_2O_2. The H_2O_2 is subsequently reduced into water by APX, GPX, CAT and POD (Sharma et al., 2012). Reduction of H_2O_2 by APX is mediated by using ascorbic acid as an electron donor which is the first step of the ascorbate-glutathione cycle (Sharma et al., 2012). However, the non-enzymatic antioxidants which include ascorbate, carotenoid, phenolics, flavonoids and glutathione act together with the enzymatic antioxidants to detoxify ROS and promote Al tolerance (de Sousa et al., 2016; Maejima et al., 2017; Du et al., 2020; Ejaz et al., 2020). In two rye genotypes, ROS scavenging was mediated by GPX and POD in Al-sensitive lines while CAT catalyzed this function in Al-tolerant lines suggesting the role of different enzymes in ROS mitigation. In buckwheat cultivars, antioxidant activities were enhanced in an Al dose-dependent manner which correlated to significant Al tolerance (Pirzadah et al., 2019; Salazar-Chavarria et al., 2020). Similarly, antioxidant enzyme activities and antioxidant metabolites (glutathione disulfide, ascorbic acid, dehydroascorbate and reduced glutathione) contents were significantly increased in wheat roots exposed to Al stress (Yusuf et al., 2016; Liu et al., 2018b). A similar conclusion was reported in rice (Awasthi et al., 2019; Ribeiro et al., 2022), watermelon (Malangisha et al., 2020), citrus (Yan et al., 2019), sorghum (Zhou et al., 2017), soybean (Zeng et al., 2020), maize (Du et al., 2021) and tomato (Ofoe et al., 2022b) where Al stimulated the activities of antioxidant enzymes and promoted Al tolerance in these plants. These indicate that both enzymatic and non-enzymatic antioxidants detoxify Al-induce excessive ROS production and promote Al tolerance in plants.

2.6.2.5 Hormonal regulation of aluminum stress

Phytohormones have been reported as key regulators of Al-induced root growth inhibition (Guo et al., 2014; Yang et al., 2017a; Yang et al., 2017b). In *Arabidopsis* roots, Yang et al. (2014) demonstrated that Al stress increases localized auxin biosynthesis in the root apex transition zone

via the Trp aminotransferase 1 (TAA1)-dependent pathway. *TAA1* was upregulated in the root apex and mediated inhibition of root growth in response to Al treatment. Similarly, Liu et al. (2016a) recently reported that YUCCA (YUC), a flavin monooxygenase-like protein, also modulates Al-induced localized auxin biosynthesis in *Arabidopsis* root apex transition and contributes considerably to root-growth inhibition under Al stress. This suggests that there could be other components of the Al-induced root growth inhibition pathway, which are yet to be identified. Moreover, an Al-induced increase in auxin accumulation in the root apex is regulated by auxin response factors (ARFs) (Yang et al., 2014; Liu et al., 2016a). In response to Al stress, ARFs control Al-induced root growth inhibition by modulating the expression of auxin signalling genes, IPT-dependent cytokinin biosynthetic genes and cell wall modification associated genes (Yang et al., 2014; Bai et al., 2017; Li et al., 2021). Besides, auxin act synergistically with ethylene to stimulate inhibition of root growth under Al stress (Yang et al., 2014; Liu et al., 2016a). Al induces the expression of 1-aminocyclopropane-1-carboxylic acid (ACC) oxidase (ACO) and ACC synthase (ACS) genes and enhances ethylene biosynthesis (Yu et al., 2016). Tian et al. (2014) demonstrated that ethylene negatively regulates Al-induced malate exudation by aiming at TaALMT1 activities through an unknown mechanism. Heterologous expression of soybean ethylene response factor (*GsERF1*) in *Arabidopsis* enhanced ethylene and ABA-mediated Al tolerance by upregulating ACS genes and ABA-response genes (Li et al., 2022). Similarly, Chen et al. (2018a) revealed that the expression of soybean glycine-rich protein-like gene (*GmGRPL*) can promote Al tolerance by controlling auxin and ethylene levels in *Arabidopsis* roots. Interestingly, exogenous application of 6-benzylaminopurine and the use of cytokinin mutant lines showed that cytokinin work in synergy with auxin and act downstream of ethylene to promote Al-

induced inhibition of root growth (Yang et al., 2017b). However, the understanding of cytokinin-mediated Al stress tolerance is limited.

ABA has been shown to regulate Al tolerance in plants. In buckwheat, Reyna-Llorens et al. (2015) reported that Al stress-induced endogenous accumulation of ABA, which triggered the expression of *FeALS3*, contributes to Al tolerance. Similarly, ABA enhanced APX and CAT antioxidant activities in buckwheat seedlings to alleviate Al stress (Salazar-Chavarria et al., 2020). Promoter region analysis of VuMATE1 transport in rice revealed the presence of an ABA-responsive element, which suggest that ABA could trigger citrate secretion under Al stress (Liu et al., 2016c). However, Fan et al. (2019b) recently indicated that Al stress triggers the endogenous accumulation of ABA in rice beans and that ABA-mediated Al stress tolerance is regulated by ABI5 which enhances cell wall modification and osmoregulation but not citrate efflux. In rice, an ABA stress and ripening genes (ASR) were reported to heighten Al stress tolerance by modulating the expression of *OsSTAR1*, *OsNrat1* and *OsFRDL4* (Arenhart et al., 2016). Also, Gavassi et al. (2021) found that Al stress induces 9-cis- epoxy carotenoid dioxygenase (NCED) gene expression which enhanced ABA biosynthesis in *Citrus limonia* roots and controlled leaf stomatal conductance.

Recently, Yang et al. (2017a) established that exogenous application of jasmonic acid (JA) promotes Al-induced root growth inhibition and that expression of CORONATINE INSENSITIVE1 (COI1) and MYC2, a JA receptor and a JA signalling regulator, respectively, were up-regulated in response to Al stress. Additionally, melatonin has been reported to play a vital role in Al tolerance. In soybean, Zhang et al. (2017b) showed that melatonin content in roots increased with Al treatment which enhanced citrate and malate secretion as well as increased

antioxidant activities. Similarly, exogenous application of melatonin enhanced Al tolerance in *Brassica napus* by increasing photosynthetic capacities and antioxidant activities (Sami et al., 2020). Moreover, Zhang et al. (2019b) showed that melatonin ameliorates Al-induced root growth reduction by interrupting nitric reductase- and nitric oxide synthase-dependent nitric oxide production which contributes to cell cycle progression and quiescent centre cellular activity. Furthermore, Sun et al. (2020a) established that exogenous application of melatonin considerably decreased cell wall polysaccharide content and pectin methylesterase activity and promote antioxidant enzyme activities to facilitate ROS scavenging and Al exclusion from root tips of wheat seedlings. However, it remains unclear how these phytohormones crosstalk with each other and other understudied plant hormones to induce root growth inhibition under Al stress. These studies indicate that plants respond to Al stress by regulating the biosynthesis, accumulation and distribution of various phytohormones which are involved in Al tolerance.

2.7 Biostimulants

Global crop production is faced with the challenge to double crop yield in order to feed the increasing population while enhancing efficient resource use and ensuring environmental sustainability. In fact, the use of synthetic chemicals in agriculture is completely inevitable and known to guarantee a continuous increase in crop productivity. However, the intensive use of these chemicals have resulted in numerous environmental and health concerns. As a result, crop production in recent years has begun to shift toward sustainable practices that emphasize alternative strategies to stimulate plant productivity and resilience to environmental stresses with a significant reduction in synthetic chemical use (Dudaš et al., 2016). One such eco-friendly innovation is the use of biostimulants to improve plant growth, yield, nutrient use efficiency and

quality of edible plant parts as well as promote plant tolerance to several biotic and abiotic stresses (Colla & Rouphael, 2015; Francesca et al., 2021; Maach et al., 2021). According to the EU Regulation on fertilizing products on the EU market, a plant biostimulant is a product that stimulates plant nutrition processes independent of the product's nutrient content with the purpose of enhancing one or more of the following plant characteristics: efficient nutrient use, quality trait, tolerance to environmental stress or nutrient availability in soil (EU, 2019). Such biostimulants include humic acids, seaweeds extract, protein hydrolysates, silicon and plant growth-promoting rhizobacteria. Additionally, pyroligneous acids (PA) have been reported to induce biostimulatory effects on plant productivity and promote tolerance to biotic and abiotic stress (Mungkunkamchao et al., 2013; Grewal et al., 2018; Lei et al., 2018; Wang et al., 2019a; Zhu et al., 2021b).

2.7.1 Pyrolysis and pyroligneous acid production

Pyroligneous acid (PA) is a natural and environmentally friendly by-product obtained from the pyrolysis of plant biomass (Grewal et al., 2018). Pyrolysis is the thermal degradation of organic biomass in the presence of limited oxygen to produce biochar (Grewal et al., 2018; Pereira et al., 2022). Moreover, organic biomasses are reservoirs for numerous chemical nutrients which can be converted to more valuable products during this process (Pereira et al., 2022). Pyrolysis of organic biomass for charcoal production has been utilized for thousands of years but has recently become of interest to researchers. Pyrolysis is an environmentally controlled thermal process which takes place in a kiln or a pyrolysis reactor to produce a carbon-rich fraction (biochar), volatile condensable materials and non-condensable gases (Figure 2.4) (Grewal et al., 2018; Pereira et al., 2022). The condensable materials are formed primarily by water, soluble organic compounds and insoluble tar, while the non-condensable gases are constituted by a blend of inert gases (CO_2 and N_2) with combustible gases (H_2, CH_4, C_3H_8, CO and C_2H_6) (Mathew & Zakaria, 2015; Pereira et

al., 2017). Pyrolysis technology has been continuously evolving to enhance various manufacturing goals such as graphene production.

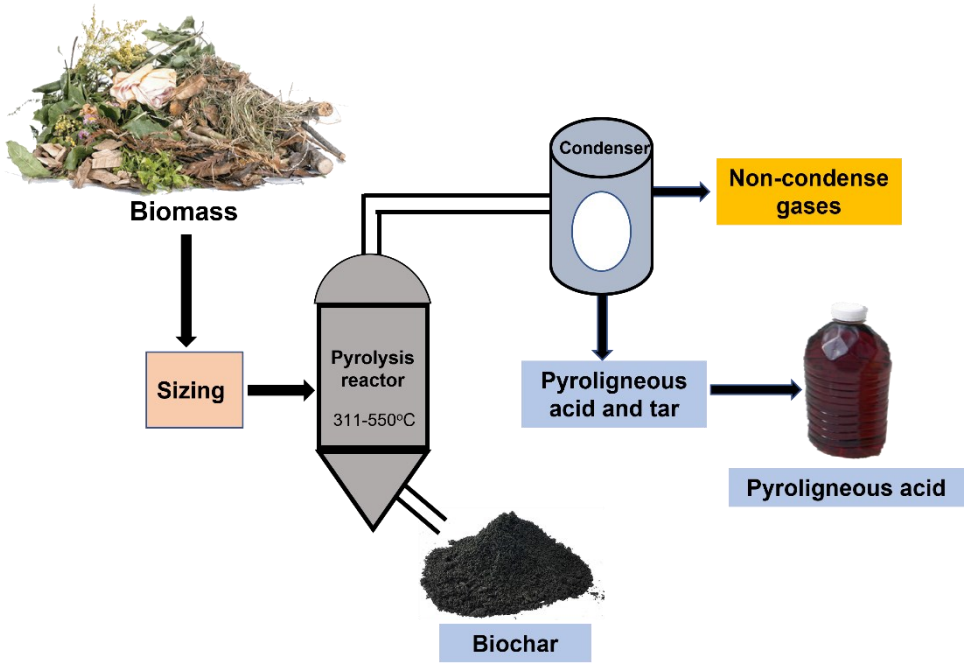

Figure 2.4. Production of pyrolytic products

Generally, the type of pyrolysis used is classified as slow and fast pyrolysis depending on the temperature, heating rate, and resident time. Slow pyrolysis is an energy-efficient process which produces large amounts of biochar compared to gaseous and liquid products. It is widely utilized for small-scale and farm-based biochar production. Slow pyrolysis results in 35 wt% biochar, 30 wt% liquid and 35 wt% gas (Grewal et al., 2018). The temperature for this type of pyrolysis ranges from 250 – 400 °C depending on the nature of the feedstock with a residence time of 5 – 30 min and a low heating rate of 0.1 – 10 °C/min (Mathew & Zakaria, 2015; Grewal et al., 2018; Pecha & Garcia-Perez, 2020). Contrarily, in fast pyrolysis, the biomass is rapidly heated at a rate of 10 – 10000 °C/min and a temperature of above 500 °C for a very short residence time (< 5 s) (Pecha & Garcia-Perez, 2020). This results in increased liquid production of 60 – 75 wt% together with

biochar and gases of 15 – 25 wt% and 10 – 20 wt% respectively (Bridgwater et al., 1999). Since biomass has low thermal conductivity, sizing the biomass to 1 – 2 mm is needed before fast pyrolysis to ensure high heat transfer from the reactor to the biomass (Tan et al., 2021). At such high temperatures and heating rates, the biomass generates high pyrolysis vapour which has a short residence time and could decrease carbon deposition amount (Pecha & Garcia-Perez, 2020; Tan et al., 2021). In both pyrolysis, the gaseous phase (smoke) including water vapour, tar, and volatiles is channelled through a long tube, condensed and collected using filter and cold traps (Mathew & Zakaria, 2015). The condensed smoke forms a crude reddish-brown liquid called bio-oil or liquid smoke. The crude liquid is stabilized by allowing it to stand for six months in a closed container at ambient temperature (Fagernäs et al., 2012; Theapparat et al., 2014). This results in the formation of three phases according to their weight with wood tar at the bottom, condensed aqueous translucent PA in the middle and light oil on the top. This aqueous translucent PA is also known as wood vinegar, wood distillate or liquid smoke which has a smoky odour and the colour may vary from light yellow to reddish-brown depending on the feedstock (Grewal et al., 2018; Theapparat et al., 2018).

2.7.2 Chemical properties of pyroligneous acid

Pyroligneous acid has a complex chemistry and contains mixtures of both polar and non-polar compounds of varying molecular weight (Theapparat et al., 2018). Moreover, the chemical constituent of PA depends on the feedstock, heating rate, resident time, and pyrolysis temperature (Wei et al., 2010; Mathew et al., 2015; Grewal et al., 2018). Plant biomasses are the major feedstock which consists of polymers of the cell wall. Generally, cellulose and hemicellulose (65%−75%) and lignin (18%−35%) are the major components of these biomasses and principal constituents on wood while water-soluble inorganic minerals and organic extracts (usually

4%−10%) include components such as lipids, essential oils, alkaloid and resins as minor components (Mohan et al., 2006; Balat, 2008; Grewal et al., 2018; Theapparat et al., 2018). Typically, the percentage weight of these components is not only dependent on the plant species but also on other factors including age, location and soil characteristics. This suggests the feedstock used will result in different PA compositions. Several feedstocks of wood and agricultural biomass have been utilized in PA production (Grewal et al., 2018). These include bamboo (*Dendrocalamus asper*) (Mu et al., 2003, 2004; Theapparat et al., 2014), *Eucalyptus grandis* (Theapparat et al., 2014; Pimenta et al., 2018), *Rhizophora apiculate* (Loo et al., 2007, 2008), oak (*Quercus* sp.) (Guillén & Manzanos, 2002; Velmurugan et al., 2009; Choi et al., 2014), *Leucaena leucocephala*, *Azadirachta indica*, *Eucalyptus camaldulensis*, and *Hevea brasilie*nsis (Theapparat et al., 2014), *Litchi chinensis* (Yang et al., 2016b), cotton (*Gossypium hirsutum*) stalk (Pütün et al., 2005), pineapple (*Ananas comosus*) waste (Mathew et al., 2015), shells of coconut (*Cocos nucifera*), walnut (*Juglans regia*) (Wei et al., 2010; Zhai et al., 2015) and almond (*Prunus dulcis*) (Gonzalez et al., 2005) and sugarcane (*Saccharum officinarum*) waste and bagasse (Garcìa-Pèrez et al., 2002).

Moreover, PA contains 80–90% water as a major component and over 200 water-soluble chemical compounds including mineral elements, aldehydes, nitrogenous compounds, alkyl aryl ethers**,** esters, alcohols, ketones and diketones, organic acids, phenols derivatives, sugar, syringol and guaiacol derivatives (Wei et al., 2010; Grewal et al., 2018). The complex organic chemical properties of PA have been extensively reviewed by several authors (Mohan et al., 2006; Theapparat et al., 2014; Mathew et al., 2015; Grewal et al., 2018; Theapparat et al., 2018). Due to the presence of high organic acids including propanoic acid, formic acid and acetic acid in PA, a

pH range of 2.1 – 4.4 have been reported for different PAs that correlates with the pyrolysis temperature. For example, Zhai et al. (2015) and Wei et al. (2010) reported a pH range of 2.51 - 3.92 from walnut shell PA as pyrolysis temperature was increased, whereas Mathew et al. (2015) reported a pH of 4.4 for PA derived from pineapple waste at varying pyrolytic temperature between 200 and 500 °C. Likewise, the pH of eight PAs produced from five different wood species ranged between 2.9 and 3.50 (Theapparat et al., 2014). According to Guillén and Manzanos (2002), the nitrogenous, phenolic, ketones, esters, furan and pyran derivatives contribute to PA's smoky aroma. Besides, the PAs from which these chemical properties were identified were produced at a pyrolysis temperature range of 200 – 550 °C (Wei et al., 2010; Mathew et al., 2015; Grewal et al., 2018). Nevertheless, little is known about the chemical and metabolic properties of PA produced at temperatures above 1000°C.

Interestingly, several studies have shown that PA contains butenolide (3-methyl-2H-furo[2,3-*c*]pyran-2-one) which is a bioactive compound found in smoke (Flematti et al., 2004; Van Staden et al., 2004; Dixon et al., 2009; Flematti et al., 2009). Butenolide has been categorized into a novel class of phytohormones known as karrikins or karrikinolide (Chiwocha et al., 2009; Dixon et al., 2009). Its mode of action and signalling mechanisms have been demonstrated to mimic that of known plant hormones (Van Staden et al., 2006; Gomez-Roldan et al., 2008). Additionally, karrikins are thermally stable, long-lasting, aqueous soluble and can remain highly potent at a broad range of concentrations which suggests that appropriate PA application can regulate plant growth and development (Van Staden et al., 2004; Flematti et al., 2009).

2.7.3 Use of pyroligneous acid in diverse field

The recognition of PA as an environmentally friendly product has attracted the interest of both researchers and key stakeholders in diverse fields. As a result, the global PA market is valued at USD 5.15 million in 2021 and is expected to reach 9.71 million by the end of 2030 with a compound annual growth rate of 7.3% (Straits Research, 2023). PA has been used extensively in food, medicine and agriculture. In medicine, PA has been reported to stimulate anti-inflammatory effects against 2,4-dinitrochlorobenzene-induced dermatitis by inhibiting the proliferation of epithelial cells in mice (Lee et al., 2011). Similarly, PA has been shown to reduce the expression of inflammatory mediator and pyrin domain-containing 3 inflammasome activation in mice by preventing ROS production thereby alleviating the progression of chronic diseases including Alzheimer's, cancer, atherosclerosis, and kidney disorders (Ho et al., 2013). In the food industry, PA is used to render smoke flavour and aroma to foods and preservatives for specific foods due to its high antioxidant and antimicrobial activities (Imamura & Watanabe, 2007; Mathew & Zakaria, 2015; Wang et al., 2021). Besides, PA has been approved by several regulatory bodies in the USA (FDA, 2018) and the European Union (EC, 2021) for smoke flavouring and preservation of foods which suggests that PA is safe for human consumption and for animals by extension. Moreover, the agricultural sector is the largest potential user of PA due to the increasing concern about sustainable agricultural practices, high cost of production and its multiplex uses in crop production (Pereira et al., 2022). It has been used to improve seed germination, crops productivity and nutritional qualities as well as mitigation of diverse abiotic stresses.

2.7.3.1 Germination and seedling growth characteristics

The biostimulatory effects of PA on seed germination and seedling growth characteristics have been reported by several authors (Mu et al., 2004; Kulkarni et al., 2006; Pereira et al., 2022).

Although the concentrations of PA used in these studies vary and depend on the feedstock and the tested crop, similar germination and growth improvement were reported. For instance, a significant increase in germination and growth components of wheat was observed with 1:900 (*v/v*) PA (Wang et al., 2019b), while rice seedling vigour, shoot and root lengths, and fresh weight were improved by 1:500 (*v/v*) PA (Kulkarni et al., 2006). Similarly, seed priming with varying rates of PA promotes rapid and uniform seed emergence, seeding vigour and growth characteristics of rice (Dissatian et al., 2018), maize (Sparg et al., 2006), *Acacia sp* (Kulkarni et al., 2007), papaya (*Carica papaya*) (Chumpookam et al., 2012), cucumber (*Cucumis sativus*) (Lei et al., 2018), rape (*Brassica napus*) (Shan et al., 2018), lettuce (*Lactuca sativa*), watercress (*Rorippa nasturtium-aquaticum*) and chrysanthemum (*Chrysanthemum coronarium*) (Mu et al., 2003, 2004). PA treatments resulted in a significant increase of N and Mg content in the roots and shoots as well as chlorophyll contents of Papaya seedlings (Chumpookam et al., 2012). It is worth noting that most of the seed germination effects of PA have been observed at concentrations below 2% while higher have been noticed to induce phytotoxic effects (Chumpookam et al., 2012; Grewal et al., 2018). Despite the seed germination and seedling growth effects of PA reported by numerous authors, the exact mechanism remains unclear. However, it has been proposed that the presence of karrikins in PA plays an active role in promoting seed gemination and growth characteristics by increasing nuclei percentage at the 4C stage in primed seeds (Flematti et al., 2004; Van Staden et al., 2004; Dixon et al., 2009). Dissatian et al. (2018) showed that PA priming suppresses MDA production and increases antioxidant enzymes and amylase activities for germination and growth improvement. Also, It has been postulated that the presence of organic acids and alcohol derivatives in PA could activate glycolysis and TCA cycle for energy production during seed germination (Miyoshi & Sato, 1997; Grewal et al., 2018). These suggest that the complex chemical

composition of PA could make it more challenging to fully understand its biostimulatory mechanisms in plants.

2.7.3.2 Crop productivity and nutritional qualities of edible parts

The improvement of crop vegetative, reproductive and yield have been reported extensively (Grewal et al., 2018). For example, foliar application of PA at 1:500 increased tomato yield but had no effect on fruit nutritional quality (Kulkarni et al., 2008). Mungkunkamchao et al. (2013) reported that foliar PA application at 1:800 enhanced tomato aboveground weight, fruit number, fresh and dry fruit weight, and Brix content of tomato fruit. Soil application of 20% PA increased the growth and yield of rockmelon (*Cucumis melo* var. *cantalupensis*) (Zulkarami et al., 2011). Similarly, Travero and Mihara (2016) showed that PA application at 30% considerably increased soybean yield with no effect on plant growth. Besides, PA application increased the chlorophyll contents which improved photosynthetic abilities and result in increased growth of rice (Berahim et al., 2014; Ahadiyat et al., 2018), sweet pepper (Jeong et al., 2006), tobacco (Ye et al., 2022), and lettuce (Vannini et al., 2021; Fedeli et al., 2022b). Mu et al. (2006) indicated that PA application increased the yield of cucumber, lettuce, and cole (*Brassica oleracea* var. *capitata* f. *rubra*) while a significant increase in tiller number, filled grains per panicle and 1000 grain weight were noted in rice following PA treatment (Masum et al., 2013; Berahim et al., 2014). These indicate that the effectiveness of PA in improving crop productivity depends on the type of crop, mode of application and the PA concentration used. Typically, the low pH of PA necessitates its use in crop production at low concentrations (Grewal et al., 2018). This implies that a suitable concentration can supply the right quantity of bioactive compounds to promote beneficial effects on crop growth and quality (Nelson et al., 2012).

Interestingly, few studies have demonstrated that crop nutritional qualities are influenced by PA application. In chickpeas, foliar PA application increased the starch, total polyphenol, essential free amino acids, soluble protein and antioxidant capacity of the edible seeds (Fedeli et al., 2022a). Additionally, PA treatment increased all mineral elements in chickpea seeds except for Mg and K contents. In tomato, PA treatment had no effect on total phenolic content and 2-diphenyl-1-picrylhydrazyl (DPPH) radical scavenging activities but increased total fruit number and weight (Benzon & Lee, 2017). On the other hand, treatment of strawberry (*Fragaria* × *ananassa*) plants with PA strongly increased the total phenolic content in the leaves (Kårlund et al., 2014) while foliar PA application increased starch, glucose and fructose content with no effect on mineral element content of lettuce leaves (Fedeli et al., 2022b).

Similar to other crop biostimulants, PA cannot be deemed as a fertilizer since it might not directly furnish adequate nutrients to plants. However, numerous studies have indicated that the co-application of PA with other fertilizing amendments enhances its efficiency in improving crop growth and productivity. For instance, Mungkunkamchao et al. (2013) reported that the co-application of PA with bio-extracts obtained from fermented plant residues increased tomato growth, yield and soluble contents in fruits. Zulkarami et al. (2011) indicated that 10% PA application with local formulation enhanced the fruit weight and Brix content of rockmelon. Also, Ahadiyat et al. (2018) reported that PA application in combination with NPK fertilizer increased the grain yield of upland rice and suppressed the intensity of pests and diseases. Zhu et al. (2021b) showed that PA combined with other plant growth regulatory substances increased the growth and seed yield of rapeseeds. Also, Fedeli et al. (2022b) reported that PA combined with 3% soy lecithin and 5% flavonoid-rich wood garlic extract increased the biomass, chlorophyll, sugar and starch content of lettuce. Additionally, co-application of PA with soil amendments including compost

(Lashari et al., 2013; Liu et al., 2018a), manure (Chen et al., 2010; Lashari et al., 2013) and biochar (Lashari et al., 2013; Shen et al., 2020) have demonstrated to increase the productivity of crops. This suggests that PA can be treated as a fertilizer additive which acts synergistically with other amendments to increase the growth and yield of crops. Such effect is associated with PA's ability to improve the chemical and biological properties of soils which promote nutrient uptake through the stimulation of metabolic and biochemical processes in plants (Lashari et al., 2013; Mungkunkamchao et al., 2013; Rui et al., 2014).

2.7.3.3 Mitigation of abiotic stresses heavy metal remediation

The use of PA in alleviating abiotic stresses has recently gained attention in the scientific literature. Although such studies are limited, PA has been reported to promote plant growth and development, and tolerance against cold, drought, salinity and heavy metal stresses (Theerakulpisut et al., 2016; Wang et al., 2019a; Wang et al., 2019b; Ma et al., 2022). This stress tolerance effect of PA has been attributed to its high phenolic contents, which are crucial in scavenging ROS and mediating cellular homeostasis (Wang et al., 2019b). It has been established that PA induces high ROS-scavenging activities, reducing power, and anti-lipid peroxidation capacity (Loo et al., 2007, 2008; Wei et al., 2010) suggesting that these properties can promote plant growth and tolerance to stresses.

Under cold stress, PA enhanced the growth of rice (Wang et al., 2019a) and rapeseed (Zhu et al., 2022) seedlings by increasing osmolyte accumulation and antioxidant activities. Specifically, PA treatment increased proline, soluble sugar, protein contents and SOD activity of rapeseed leaves

(Zhu et al., 2022). However, MDA content and stomatal conductance were significantly reduced while enhancing water use efficiency under cold stress.

In wheat, Wang et al. (2019b) revealed that seed priming with PA enhanced root and shoot growth under drought-stress conditions. Physiological and root proteomics analysis showed that PA alters ABA production, regulates stomatal aperture to decrease water loss and facilitates the activation of antioxidants and other stress-related proteins. Such drought defence activation was related to reduced ROS and MDA increased glycolytic and TCA metabolic pathway proteins which suggests that PA promote sufficient ATP production to accommodate the energy demand of plants under drought stress (Wang et al., 2019b). Moreover, a recent study indicates that PA application at 3-day intervals increased *Pandanus amaryllifolius* tolerance to drought stress (Mohd Amnan et al., 2023). The PA-treated plants exhibited increased leaf-relative water content, chlorophyll content, root-to-shoot ratio and antioxidant activities (Mohd Amnan et al., 2023).

Under salinity stress, seed priming with PA enhanced rice seedling growth and membrane stability by increasing K^+ and reducing Na^+ ions in the shoot (Theerakulpisut et al., 2016). The PA-primed rice seedlings displayed reduced osmotic stress by lessening Na^+ uptake and promoting more water absorption. Additionally, PA priming boosted osmolytes and antioxidant activities to mitigate salinity-induced oxidative stress (Theerakulpisut et al., 2016). Similarly, Ma et al. (2022) revealed that pre-treatment of rapeseeds with PA under salinity stress increased chlorophyll, leaf gas exchange parameter, biomass production, and reduced Na^+ uptake and salt transporter expression. Biochemical examination of PA-treated plants revealed that PA reduced lipid peroxidation, ROS-induced oxidative stress and enhanced proline and antioxidant activities thereby promoting salt

tolerance (Ma et al., 2022). Despite these effect of PA in alleviating salt stress, the exact mechanism remains elusive.

Moreover, the use of PA in heavy metal stress mitigation has been widely reported by several authors. Benzon and Lee (2017) revealed that PA treatment of heavy metal-contaminated soils improved mustard growth, reduced metal concentrations in soil and restricted plant uptake via phytostabilization. Also, PA application enhanced the growth and phytoextraction of Cd and Zn in *Sedum alfredii* plant (Zhou et al., 2022). Although the exact mechanism remains unknown, it was revealed that PA increased soil C, N and P availability, enhanced the activities of soil enzymes such as protease, phosphatase, invertase and urease and increased soil bacterial diversity (Steiner et al., 2008; Rui et al., 2014; Zhou et al., 2022). Such changes in soil microbial diversity promote plant growth and metal stress tolerance (Zhou et al., 2022). In lead (Pb) contaminated fields, the application of PA with humic acid reduced Pb availability in the soil by over 50% through absorption and electrostatic interaction between Pb and oxygen-rich functional compounds in PA (Zhu et al., 2021a). Interestingly, PA has been shown to immobilize heavy metals when added to compost (Liu et al., 2018a) and manure (Chen et al., 2010). The addition of PA to municipal soil waste compost exhibited higher adsorption of Zn, Cd, Ni and Cu metals (Liu et al., 2018a). Similarly, the co-application of PA and charcoal reduced total N loss and the mobility of Zn and Cu metals in pig manure compost (Chen et al., 2010). Moreover, PA is rich in organic substances with adsorption sites which can chelate metals and render them immobile (Benzon & Lee, 2017; Grewal et al., 2018). Functional groups of organic compounds including carboxyl, phenoxyl and hydroxyl can easily form complexes with metals present in soil (Benzon & Lee, 2017; Zhu et al., 2021a) thereby restricting their uptake and toxic effect on plant growth and development. These

studies suggest that PA application can be used to detoxify metal stress in agricultural soils. However, more studies are required to elucidate the PA mechanism in enhancing plant growth and productivity under these environmental stresses.

CHAPTER 3: METABOLITES, ELEMENTAL PROFILE AND CHEMICAL ACTIVITIES OF *PINUS STROBUS* HIGH TEMPERATURE DERIVED PYROLIGNEOUS ACID

A version of this chapter has been published in **Chemical and Biological Technologies in Agriculture Journal**. The citation is:

Ofoe, R., Gunupuru, L.R. & Abbey, L. (2022). Metabolites, elemental profile and chemical activities of *Pinus strobus* high temperature-derived pyroligneous acid. *Chemical and Biological Technologies in Agriculture*, 9, 85. https://doi.org/10.1186/s40538-022-00357-5. (Impact factor = 6.6)

3. ABSTRACT

Pyroligneous acid (PA) is an aqueous smoky fraction produced during pyrolysis of plant biomass. The chemical composition of PA from different plant biomass have been studied but reports on PA metabolites and elemental profiles are rare. In this study, we examined the metabolites, elemental profiles and the associated chemical activities of PA derived from white pine (*Pinus strobus*) at 1100^{o}C compared to similar work done elsewhere using different biomass at lower temperatures. PA from *P. strobus* biomass exhibited a lower electrical conductivity (2.05 mS/cm), salinity (1.03 g/L) and total dissolved solids (1.42 g/L) but higher ^{o}Brix content (9.35 ± 0.06) compared to PA from other feedstock. The *P. strobus* PA showed a higher antioxidant activity characterized by enhanced radical scavenging activity against 1,1-diphenyl-2-picrylhydrazyl free

radicle (78.52%) and accumulation of higher total phenolic (95.81 ± 1.45 gallic acid equivalents (GAE)/mL) and flavonoid content (49.46 µg quercetin/mL). Metabolite profiling by direct injection mass spectrometry with a reverse-phase liquid chromatography-mass spectrometry (DI/LC-MS/MS) identified a total of 156 metabolites. Four main groups including organic acids (90.87%), hexose (8.60%), carnitine (0.3%) and phospholipids (0.24%) were found in the PA. Mineral element analysis revealed that the *P. strobus* PA contained high concentrations of nitrogen (N), potassium (K), calcium (Ca) and zinc (Zn), while the content of sodium (Na) and trace/heavy metals were present at levels below the reported limit. This study indicates that *P. strobus* PA is a valuable product that can be used in agriculture to improve plant growth and productivity under normal and environmentally stressful conditions.

Keywords: wood vinegar; white pine; pyrolysis; biostimulant; plant growth promoter

3.1 INTRODUCTION

Pyroligneous acid (PA) is a yellow or reddish-brown translucent aqueous fraction produced by the pyrolysis of organic biomass in the presence of limited oxygen (Grewal et al., 2018). It is also known as wood vinegar, smoke water or liquid smoke; and comprised of a complex mixture of over 200 different aqueous organic compounds. Water, phenolic compounds, and organic acids are typically, the major constituents of PA but also contains nitrogen, sugar derivates, alcohols, and esters (Wei et al., 2010; Grewal et al., 2018; Zheng et al., 2018). However, the chemical composition of PA depends on the feedstock, temperature, heating rate, and residence time .

Pyroligneous acid has been recognized as a safe natural product and used extensively in diverse areas including agriculture, medicine and food (Cai et al., 2012a; Grewal et al., 2018). In

agriculture, it is used as a biostimulant to enhance seed germination, crop yield and productivity (Mu et al., 2004; Mungkunkamchao et al., 2013; Wang et al., 2019b; Zhu et al., 2021b). Additionally, it is used as a herbicide (Liu et al., 2021b), insect repellent (Mmojieje & Hornung, 2015), soil conditioners (Lashari et al., 2013) and antimicrobial agent for controlling several plant diseases (Jung, 2007; Mourant et al., 2007). In medicine, PA has been reported to exhibit anti-inflammatory effects against 2,4-dinitrochlorobenzene (DNCB) induced dermatitis by inhibiting the proliferation of epithelial cells in mice (Lee et al., 2011). Other biological activities such as antifungal, termiticidal, antitermitic and strong antioxidant effects have also been reported (Wei et al., 2010; Oramahi & Yoshimura, 2013; Onoda et al., 2016; Yang et al., 2016b).

These beneficial effects of PA have been attributed to its numerous bioactive compounds. For instance, the antioxidant and anti-lipid peroxidation capacity of PA is due to its phenolic compounds, which induce high ROS-scavenging and reducing power activities (Loo et al., 2007; Wei et al., 2010). The antimicrobial and anti-inflammatory activities of PA was positively correlated to its high organic acid and phenolic compounds (Wei et al., 2010; Marumoto et al., 2012; Oramahi & Yoshimura, 2013; Onoda et al., 2016). All these properties indicate that PA possesses a great potential to be used as a sustainable product. However, these biological activities can be influenced by the pyrolytic temperature as high pyrolytic temperatures between 311°-550°C was demonstrated to have the strongest antioxidant activity (Wei et al., 2010).

Moreover, various PA have been produced from different plant materials including pineapple (*Ananas comosus*) waste (Mathew et al., 2015), bamboo (*Dendrocalamus asper*) (Mu et al., 2004; Theapparat et al., 2014), oak (*Quercus sp*) (Guillén & Manzanos, 2002), *Eucalyptus grandis*

(Guillén & Manzanos, 2002; Theapparat et al., 2014), *Rhizophora apiculate* (Loo et al., 2007, 2008), *Litchi chinensis* (Yang et al., 2016b), walnut (*Juglans regia*) shell (Wei et al., 2010; Zhai et al., 2015), coconut (*Cocos nucifera*) shell (Wititsiri, 2011), *Leucaena leucocephala*, *Azadirachta indica*, *Eucalyptus camaldulensis*, and *Hevea brasilie*nsis (Theapparat et al., 2014). Generally, most PAs are produced at a pyrolysis temperature range of 200° to 550°C (Wei et al., 2010; Theapparat et al., 2018). However, little is known about the chemical composition of PA produced from temperatures above 1000°C. Many studies have reported that PA produced from different plant species might present varying quantities of bioactive constituents and levels of bioactivity. However, no study has investigated the metabolic and mineral element profile of PA produced at high pyrolytic temperature (>1000^{o}C). In this paper, we examined the metabolic and mineral element profile, and the antioxidant activity of PA produced from *P. strobus* at 1100^{o}C.

3.2 MATERIALS AND METHODS

3.2.1 Study location and materials

This study was performed in the Department of Plant, Food, and Environmental Sciences, Faculty of Agriculture, Dalhousie University, Truro. PA was prepared from white pine (*P. strobus*) biomass using fast pyrolysis. The front portion of the 22 ft long tube through which the biomass traverses receives a maximum heat flux of 22.6 W/sq inches. The average heat flux imposed on the tube was 15 W/sq. inches. The PA was produced at a pyrolysis temperature of 1100°C and prepared by Proton Power Inc (Lenoir City, USA). The PA was stored in the dark at room temperature for stability until further analysis. Chemicals used for this study were of analytical grade. The chemical reagents were 1,1-diphenyl-2-picrylhydrazyl (DPPH), trichloroacetic acid (TCA), ferric chloride ($FeCl_3$), gallic acid, quercetin, Folin-Ciocalteau reagent and aluminum

chloride ($AlCl_3$) obtained from Thermo Fisher Scientific Co. (Canada); and potassium ferricyanide [$K_3Fe(CN)_6$], butylated hydroxyanisole (BHA), dithiothreitol (DTT), ethylene diamine tetra acetic acid (EDTA), L-Ascorbic acid and sodium carbonate purchased from BioShop Canada Inc. (Canada).

3.2.2 Mineral nutrient and chemical analysis

Complete elemental composition of PA was determined at the Research and Productivity Council (RPC) Science and Engineering facility in Fredericton, New Brunswick using inductively coupled plasma-mass-spectrometry (ICP-MS) (Donohue et al., 1992). For the chemical analysis, PA samples were poured into a 100 mL beaker and 500 µL was used for ^{o}Brix content determination using a handheld refractometer (Atago, Japan). The pH, salinity, total dissolved solids (TDS) and electric conductivity (EC) were measured using a 3-in-1 multimeter (EC 500 ExStik II S/N 252957, EXTECH Instrument, Taiwan).

3.2.3 Total phenolics

Total phenolics content (TPC) of PA was determined using the Folin-Ciocalteu method described by Dudonne et al. (2009) with little modification. Briefly, 200 µL of PA was added to 400 µL of 10% (v/v) Folin-Ciocalteau reagent and mixed thoroughly for 5 min. A solution of 1.6 µL of 700 mM Na_2CO_3 was then added to the mixture. After incubation in the dark at room temperature for 30 mins, the absorbance was measured at 765 nm against a blank. TPC was calculated using a gallic acid standard curve and expressed as mg gallic acid equivalent.

3.2.4 Total flavonoid

Total flavonoid of PA was estimated following the colorimetric method described by (Yang et al., 2016b) with little modification. One mL of PA was added to equal volume of 95% methanol and 1 mL of the resultant mixture was mixed with 0.1 mL of 10% $AlCl_3$, 0.1 mL of 1 M potassium acetate, and 2.8 mL distilled water. The reaction was incubated at room temperature for 40 min and absorbance was read at 415 nm against a blank without $AlCl_3$. Total flavonoid content was estimated using the quercetin standard curve (0 – 250 µg/mL quercetin).

3.2.5 DPPH free radical scavenging capacity

The DPPH free radical scavenging capacity of PA was determined using the method described by (Dudonne et al., 2009) with slight modification. Aliquots of 100 µL of PA in methanol (1:1, v/v) was added to 2.9 mL of 60 µM fresh DPPH methanolic solution. The mixture was vortexed and incubated in the dark at room temperature for 30 min. The absorbance of the reaction mixture was measured at 515 nm against a methanol blank and the radical scavenging activity calculated using the formula: Inhibition (%) = $[(A_B – A_S)/ A_B] \times 100\%$; where A_B is the absorbance of the blank sample and A_S is the absorbance of the PA sample.

3.2.6 DI/LC-MS/MS Method

Targeted metabolic analysis was performed at the metabolic core facility, The Metabolomics Innovation Centre (TMIC), Alberta, Canada. A targeted quantitative metabolomics approach was applied to analyze the PA samples using a combination of the direct injection mass spectrometry (DI-MS/MS) along with reverse-phase chromatography tandem mass spectrometry (RPLC-MS/MS) custom methods (Zheng et al., 2021). This method involved using multiple reaction

monitoring (MRM) pairs to merge analytes extraction and derivation, and selective mass spectrometric detection. This identifies and quantifies up to 207 endogenous metabolites including amino acids, biogenic amines and derivatives, acylcarnitines, glycerophospholipids, sphingolipids, uremic toxins and sugars. The samples were analysed in a 96 deep-well plate with an attached filter plate using sealing tape to hold the solvents and reagents included in the plate assay. To prepare all metabolites except organic acids, the PA sample was vortexed followed by centrifugation at 13000 × *g*. Afterwards, 10 µL of the sample was loaded onto the middle of the filter on the upper 96-well plate and dried through a stream of nitrogen. Phenyl-isothiocyanate was subsequently added for derivatization and incubated at room temperature for 20 mins. The filter spots were further dried using an evaporator. The targeted metabolites were extracted by adding 300 µL of extraction solvent (5 mM ammonium acetate in methanol) to each well. The extracts were obtained by centrifugation from the 96-well filter plate to a Nunc® 96 DeepWell™ plate. Finally, the extracts were further diluted with MS running solvent and metabolites quantification were based on isotope-tagged internal standards and other endogenous standards. The first 14 wells were used for one blank, three zero samples, seven standards and three quality control samples. For absolute qualification of organic acid, 150 µL of ice-cold methanol and 10 µL of the isotope-labelled internal standard mixture was added to 50 µL of a serum sample for overnight protein precipitation followed by 20 min centrifugation at 13000 × *g*. Aliquots of 50 µL of supernatant was pipetted directly into the centre of each well of a Nunc® 96 DeepWell™ plate. 3-nitrophenylhydrazine (NPH) reagent was added to each well and the plate incubated at room temperature for 2 h. The reaction mixture was further diluted with water and stabilized with butylated hydroxytoluene (BHT) for RPLC-MS/MS analysis. The mass spectrometric analysis was carried out on an ABSciex 4000 Qtrap® tandem mass spectrometry instrument (Applied

Biosystems/MDS Analytical Technologies, Foster City, CA) equipped with an Agilent 1260 series RPLC system (Agilent Technologies, Palo Alto, CA). The samples were delivered to the mass spectrometer by RPLC method followed by a direct injection (DI) method.

3.2.7 Statistical analysis

The experimental results for the chemical analyses were expressed as mean and standard deviation (SD) of quadruplicate measurements. Metabolic profile data analysis was done using Analyst 1.6.2 and MultiQuant 3.0.3 software and reported as is.

3.3 RESULTS AND DISCUSSION

3.3.1 Chemical qualities and antioxidant activities

Table 3.1 shows the chemical qualities of PA, which represent important summation of its chemical constituents. The PA from pine had an acidic pH of 2.3, which was lower than those of other PAs reported in the literature (Table 3.1). For instance, Wei et al. (2010) reported a pH range from 2.98 to 3.32 for walnut shell PA produced at varying pyrolytic temperatures between 90° and 550°C; while a pH of 4.4 was reported for pineapple waste at varying pyrolytic temperature between 200° and 500ºC (Mathew et al., 2015). Similarly, the pH of eight PAs produced from five different wood species ranged between 2.9 to 3.50 (Theapparat et al., 2014). Zhai et al. (2015) reported that the pH of walnut shell PA increased from 2.51 to 3.92 as pyrolysis temperature was increased. The differences in pH (2.3) of the white pine PA in the present study compared to those of previous studies can be attributed to differences in feedstock and the pyrolytic temperature used (Wei et al., 2010; Grewal et al., 2018). Moreover, wood biomass is composed of cellulose, hemicellulose and lignin which forms a major constituent of plant cell wall (Theapparat et al.,

2018). During pyrolysis, these structures are disintegrated to produce a wide range of organic compounds with organic acid being the major component of the derived PA (Wei et al., 2010; Grewal et al., 2018). Also, increased pyrolysis temperature could result in a significant reduction in moisture content, thereby concentrating the amount of organic constituents (Lu et al., 2019). Thus, the low pH of the PAs can be explained by the increase in the production of organic acids from structural compounds subjected to high temperature during pyrolysis.

Table 3.1. Chemical characteristics of wood vinegar obtained from *Pinus strobus*.

Chemical Indices	**Content**
pH	2.30 ± 0.03
Salinity (g/L)	1.03 ± 0.01
TDS (g/L)	1.42 ± 0.01
EC (mS/cm)	2.05 ± 0.01
°Brix	9.35 ± 0.06

Values are means ± SD of four individual replicates. TDS, total dissolved solids; EC, Electrical conductivity.

Pyroligneous acid contains water-soluble salts consisting of sodium and potassium salts (Theapparat et al., 2018). We found that the salt content of pine PA was 1.03 g/L (Table 3.1). Generally, the salt content of PA is strongly influenced by the chemical composition of the plant biomass (Theapparat et al., 2018). Salt content typically constitutes 15% of herbaceous plant biomass whereas woods contains lower salt content (i.e., 0.3-0.4%) (Hon & Minemura, 2001). Hence, the high salt content of the pine wood PA could be attributed to reduction in moisture content of wood biomass, thereby concentrating the amount of salt ions (Lu et al., 2019). A recent study revealed that the salinity of a solution exhibits a strong association with its total dissolve solids (TDS) and electrical conductivity (EC) (Vehniwal et al., 2020). TDS content represents the

amount of inorganic salt and little organic substances dissolved in a solution. In this study, the TDS content of PA was 1.42 g/L, which was considerably lower than that reported by Shen et al. (2020). They showed that carbonation of corn (*Zea mays*) straw at 600ºC yielded a PA with TDS of 35.0 g/L with a EC value of 2.05 mS cm^{-1}, which was slightly lower than the ECs of other PA e.gs, 3.54 $mScm^{-1}$ (Najafi-Ghiri et al., 2022)). The lower TDS and EC values could be attributed to the low inorganic salt content in woody plants compared to herbaceous plants (Hon & Minemura, 2001). Furthermore, the analysis of ºBrix content of the white pine PA (Table 3.1) showed a higher value than PA produced from other wood species. For examples *D. asper*, 5.60; *H. brasiliensis,* 6.00; *L. leucocephala*, 3.80 - 4.60; *A. indica,* 3.00 - 3.40; and *E. camaldulensis,* 3.40 - 4.60 (Theapparat et al., 2014), bamboo, 6.6; Oak, 1.70; and pine, 2.00 (Mun et al., 2007).

Generally, total phenolic and flavonoid are common compounds found in plant extracts. These compounds have been reported to induce multiple biological effects such as antioxidant activity and are used to categorize products considered as a source for natural antioxidants (Mathew et al., 2015; Yang et al., 2016b). The total phenolic and flavonoid contents in the PA were estimated to be 95.81 mg GAE/mL and 49.46 µg quercetin/mL, respectively (Figure 3.1). The total phenolic and flavonoid content of the PA is relatively higher than those reported from other plant sources (Mathew et al., 2015; Yang et al., 2016b). DPPH radical scavenging assay has been widely used to assess the antioxidant capacity of PA from diverse plant sources (Loo et al., 2007, 2008; Wei et al., 2010; Zhai et al., 2015; Yang et al., 2016b). It involves reducing organic nitrogen free radicals with hydrogen-donating antioxidants leading to the generation of a non-radical form. In the present study, the PA exhibited a stronger DPPH radical scavenging activity of 78.5% (Figure 3.1). The results of the DPPH scavenging activity is comparable to earlier reports (Wei et al., 2010; Mathew

et al., 2015). Previous studies have demonstrated that the significant ROS-scavenging activity of PA is due to its rich phenolic compounds that cause a strong antioxidant activity (Loo et al., 2007; Wei et al., 2010). Moreover, the search for natural antioxidants has increased significantly due to the adverse effect of synthetic antioxidants such as butylated hydroxyanisole (BHA) and butylated hydroxytoluene (BHT) (Lourenço et al., 2019). The present results suggest that PA produced from pine at high temperature (1100 ^{o}C) could be a significant source of natural antioxidant that can be used in food, medicine, and agriculture.

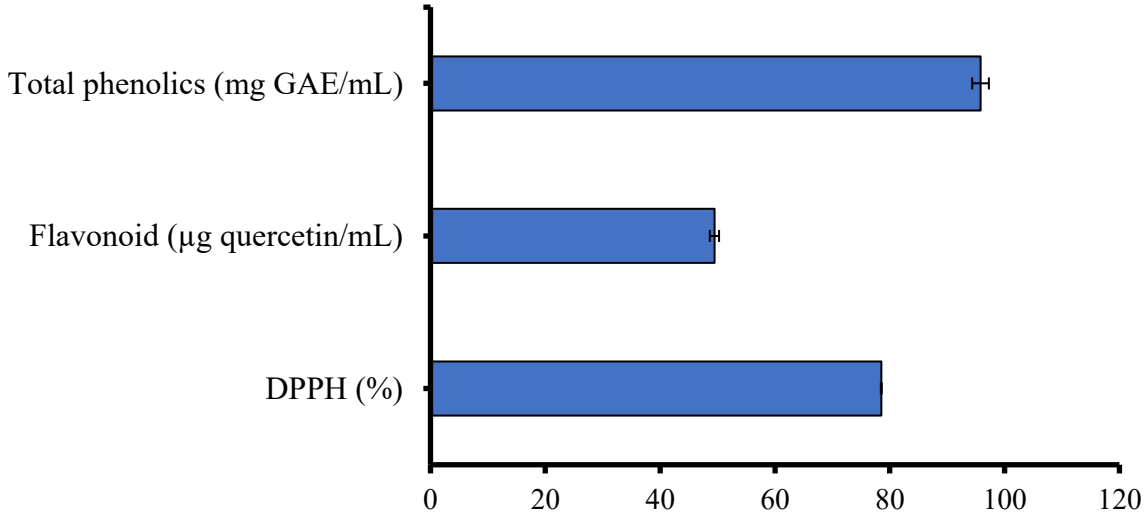

Figure 3.1. Antioxidant activity of wood vinegar obtained from *Pinus strobus*. DPPH, DPPH free radical scavenging ability. Values are mean ± S.D of four individual measurements.

3.3.2 Metabolites profile of pyroligneous acid

The metabolites profile analyses of PA produced from white pine at higher pyrolysis temperature revealed a total of 156 metabolites. These metabolites can be categorized into organic acids, hexose, carnitine and acylcarnitine, and phospholipids (Figure 3.2).

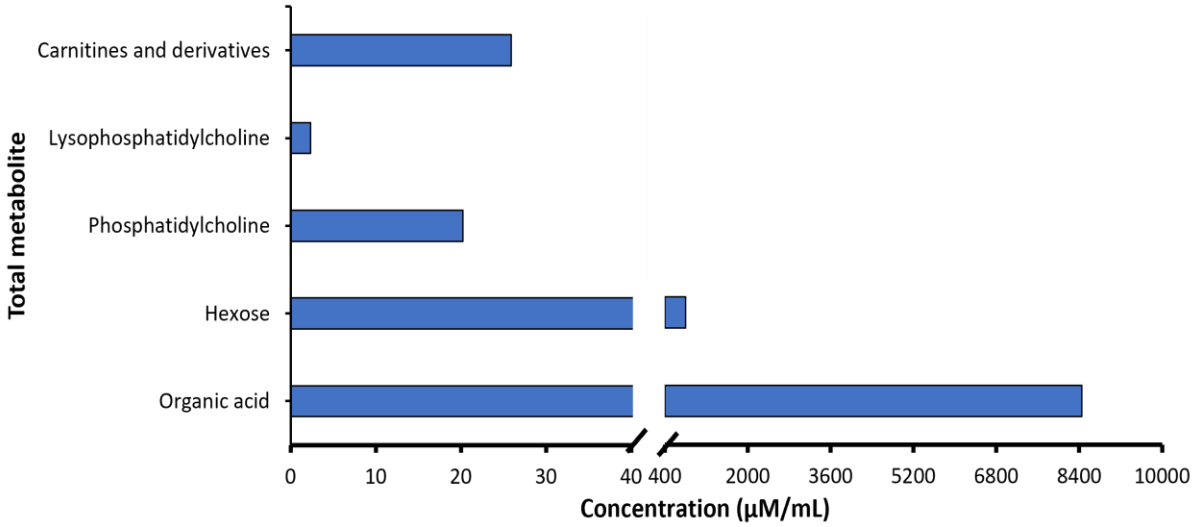

Figure 3.2. Total metabolite composition of PA obtained from *Pinus strobus*. Values are based on pooled samples with no replication.

3.3.2.1 Organic acids and hexose

Organic acids are the major class of metabolites in the white pine PA and comprised approximately, 90.9% (i.e., 8446.12 µM/mL) of the total metabolites identified (Figure 3.2; Table 3.2). The total organic acids are made up of 25 individual organic acids with varying levels. Notably, propanoic acid was the highest organic acid accounting for approximately, 48.8% of the total organic acids whereas methylmalonic acid, indole acetic acid, oxaloacetic acid, abscisic acid, aconitic acid and jasmonic acid were minor components (Table 3.2). Apart from propanoic acid, other organic acids influenced the high total organic acid content of the PA and include malic acid, butyric acid, succinic acid, glutaric acid, glyceric acid, β-Hydroxybutyric acid, lactic acid, Benzoic acid, oxalic acid, salicylic acid, citric acid, pyruvic acid and α-ketoglutaric acid. Similar high composition of organic acid has been reported previously as the major component of PA by several authors (Theapparat et al., 2014; Zhai et al., 2015; Zheng et al., 2021). Total organic acids constituted 60.6% in walnut shell PA (Zhai et al., 2015), 30.8% in walnut tree branches PA (Wei

et al., 2010) and 2.7% in pineapple waste PA. Specifically, the high propanoic acid content in the white pine PA in the present study is consistent with the results of previous studies (Wei et al., 2010; Stefanidis et al., 2014; Zhai et al., 2015). During pyrolysis, the integral component of wood (i.e., cellulose, hemicellulose and lignin) undergoes pyrolytic chemical reactions resulting in the formation of different compounds (Grewal et al., 2018). Degradation of hemicellulose presents the main origin to produce organic acids including propanoic acid as monomers (Choi et al., 2014; Stefanidis et al., 2014; Hu et al., 2017). Although the chemical properties of the feedstock were not investigated, it can be surmised that the high organic acid composition of PA could be due to a high hemicellulose content of the feedstock. Furthermore, the presence of phytohormones (i.e., salicylic acid, indole acetic acid, abscisic acid and jasmonic acid) in PA could explain its biostimulatory properties in regulating physiological and cellular responses of plants when applied (Wang et al., 2019b; Zhu et al., 2021b). Intriguingly, the rich organic acids in PA were demonstrated to possess numerous adsorption sites, which can chelate heavy metals and render them less toxic in soils and unavailable for plant uptake (Chen et al., 2010; Liu et al., 2018a; Zhu et al., 2021a). Thus, this study suggests that PA can be used appropriately to remediate heavy metal pollutants in degraded soils (Benzon & Lee, 2017; Shuang et al., 2020).

Thermal degradation of cellulose has been reported to yield the production of sugars (Stefanidis et al., 2014). In this study, hexose, a simple sugar with six carbon atoms accounted for 8.6% (800 μM) of the total metabolites (Table 3.2). Similar reports have indicated that PA contains sugar and its derivatives, and their concentration is dependent on the feedstock and pyrolysis temperature (Wei et al., 2010; Mathew et al., 2015; Zhai et al., 2015; Grewal et al., 2018).

Table 3.2. Metabolic profile of organic acids in PA obtained from *Pinus strobus*.

Metabolite name	**LOD (µM/mL)**	**Content (µM/mL)**
Propionic acid	0.03	4120.00
Succinic acid	0.02	1022.00
Lactic acid	0.87	809.00
Butyric acid	0.08	568.00
Benzoic acid	0.01	494.00
Glutaric acid	0.03	436.00
Pyruvic acid	0.06	434.00
Glyceric acid	0.04	238.00
β-Hydroxybutyric acid	0.04	97.60
Malic acid	0.06	70.30
Valeric acid	0.05	64.80
Oxalic acid	0.10	47.80
para-Hydroxyphenylacetic acid	0.07	11.30
α-Ketoglutaric acid	0.02	10.30
Citric acid	0.18	9.83
Salicylic acid	0.06	8.33
Fumaric acid	0.03	1.99
Shikimic acid	0.32	1.87
HPHPA	0.01	0.99
Methylmalonic acid	0.01	0.01
Oxaloacetic acid	0.08	< 0.09
Jasmonic acid	0.09	< 0.09
Abscisic acid	0.04	< 0.04
Aconitic acid	0.03	< 0.03
Indole acetic acid	0.02	< 0.02
Total		**8446.12**
Hexose	18.50	800.00

Values are based on pooled samples with no replication. LOD, Limit of detection; HPHPA,3-(3-hydroxyphenyl)-3-hydroxypropionic acids.

The white pine PA sugar content as confirmed by the °Brix (Table 3.1) were considerably higher than those reported in the literature because of the higher pyrolytic temperature. Cellulose is composed of a linear homopolysaccharide of glucose moieties that are connected to a beta-glycosidic bond. It has been demonstrated that at a higher pyrolytic temperature above 300°C, cellulose depolymerizes to glucose monomers with the subsequent removal of water. This results in levoglucosan formation (Balat, 2008) thereby reducing the simple sugar levels in PA. Besides, Hu et al. (2019) reported that pyrolysis of pine biomass at 500°C yields the highest levoglucosan content. Nevertheless, the level of levoglucosan was not examined and will require further investigation in this study.

3.3.2.2 Carnitine and Acylcarnitine

Carnitine and acylcarnitine are ubiquitous compounds identified in all living organisms including plants, which are known to play numerous critical biological, physiological and metabolic functions specifically related to beta oxidation and energetics in the mitochondria (Jacques et al., 2018). In this study, our result revealed the presence of a significant amount of carnitine and acylcarnitines in PA obtained from white pine (Figure 3.2; Table 3.3). Carnitine and acylcarnitine accounted for 0.3% of the total identified metabolites and consisted of one free carnitine and 38 acylcarnitines which comprised of 4 short-chain acylcarnitines (C2-C4), 4 medium-chain acylcarnitines (C6-C12), 3 long-chain acylcarnitines (C14-C18), 15 hydroxyl-/dicarboxyl-chain acylcarnitines, 8 monounsaturated acylcarnitines and 4 polyunsaturated acylcarnitines (Table 3.3).The presence of carnitines in PA could be due to the feedstock used. Moreover, previous studies have reported the presence of carnitines and acylcarnitine in several plant species including avocado (*Persea americana*) and cauliflower (*Brassica oleracea var. botrytis*) (Panter & Mudd,

1969), barley (*Hordeum vulgare*) (Ariffin et al., 1982), pea (*Pisum sativum*) (Wood et al., 1983; Masterson & Wood, 2000; Masterson & Wood, 2009), tobacco (*Nicotiana tabacum*), *Arabidopsis thaliana*, flax (*Linum usitatissimum*) and rape (*Brassica napus*) seeds (Bourdin et al., 2007). Although no studies have reported the presence of carnitine in woody plants, it is plausible that our finding of carnitine in PA can be attributed to its presence in the pine feedstock. Interestingly, carnitines are heat stable when exposed to a temperature range of 80°-130°C (Goula et al., 2018). Furthermore, its presence in PA produced at 1100°C could suggest that carnitines are stable even at higher temperatures and could implicate a critical role in plants.

Functionally, carnitines are known to be involved in fatty acid metabolism by shuttling activated fatty acids into the mitochondrion as acylcarnitine for β-oxidation reaction (Jacques et al., 2018). Additionally, environmental stress studies revealed that carnitine and its subclasses can accumulate at high concentrations and act as osmolytes to protect cells against salt and chilling-induced osmotic stress (Angelidis & Smith, 2003; Canovas et al., 2007; Charrier et al., 2012). It has been suggested that carnitines could facilitate fatty acid intercellular transport as an important part of membrane lipids adjustment process during chilling stress response (Angelidis & Smith, 2003). In maize (*Zea mays*), exogenous carnitine effectively enhanced seedling growth under both normal and cold stress conditions *via* modulation of photosynthesis, nitrogen assimilation and antioxidant enzyme activities (Turk et al., 2020). Interestingly, carnitine modified saturated and unsaturated fatty acids ratio in maize cell membranes in support of more unsaturated fatty acid production to safeguard cellular membranes from cold stress damage (Turk et al., 2020). Evidence revealed that exogenous application of 5 μM carnitine stimulated significant internal carnitine accumulation in 7-day-old Arabidopsis seedling without causing developmental defects leading to

induced antioxidant properties and increased seedling growth and salt stress tolerance (Charrier et al., 2012). Therefore, the utilization of PA in crop production could provide a sustainable avenue for environmental stress mitigation.

Table 3.3. Metabolic profile of total Carnitine and Acylcarnitine in PA obtained from *Pinus strobus*.

Metabolite name	**Formula**	**LOD (µM)**	**Content (µM/mL)**
Carnitine	C0	0.22	6.73
Short-chain acylcarnitines			
Acetylcarnitine	C2	0.13	1.37
Propionylcarnitine	C3	0.08	0.68
Butyrylcarnitine	C4	0.05	0.50
Valerylcarnitine	C5	0.03	0.25
Medium-chain acylcarnitines			
Octanoylcarnitine	C8	0.03	0.32
Nonaylcarnitine	C9	0.01	0.25
Decanoylcarnitine	C10	0.06	0.31
Dodecanoylcarnitine	C12	0.04	0.52
Long-chain acylcarnitines			
Tetradecanoylcarnitine	C14	0.03	0.22
Hexadecanoylcarnitine	C16	0.03	0.30
Octadecanoylcarnitine	C18	0.02	0.21
Hydroxyl-/dicarboxyl-chain acylcarnitines			
Hydroxypropionylcarnitine	C3OH	0.03	0.84
Hydroxybutyrylcarnitine	C4OH	0.02	0.44
Hydroxyvalerylcarnitine	C5OH	0.03	0.47
Hydroxytetradecenoylcarnitine	C14:1OH	0.06	0.25
Hydroxytetradecadienylcarnitine	C14:2OH	0.05	0.60
Hydroxyhexadecanoylcarnitine	C16OH	0.04	0.12
Hydroxyhexadecenoylcarnitine	C16:1OH	0.05	0.23
Hydroxyhexadecadienylcarnitine	C16:2OH	0.04	0.27
Hydroxyoctadecenoylcarnitine	C18:1OH	0.06	0.20

Glutarylcarnitine	C5DC	0.02	0.62
Methylglutarylcarnitine	C5MDC	0.02	0.39
Glutaconylcarnitine	C5:1DC	0.03	0.37
Pimelylcarnitine	C7DC	0.02	0.30
Butenylcarnitine	C4:1	0.02	0.23
Dodecanedioylcarnitine	C12DC	0.01	0.11
Monounsaturated acylcarnitines			
Propenoylcarnitine	C3:1	0.03	0.28
Tiglylcarnitine	C5:1	0.03	0.14
Hexenoylcarnitine	C6:1	0.02	0.15
Decenoylcarnitine	C10:1	0.12	0.12
Dodecenoylcarnitine	C12:1	0.08	5.91
Tetradecenoylcarnitine	C14:1	0.07	0.25
Hexadecenoylcarnitine	C16:1	0.02	0.31
Octadecenoylcarnitine	C18:1	0.04	0.29
Polyunsaturated acylcarnitines			
Decadienylcarnitine	C10:2	0.05	0.45
Tetradecadienylcarnitine	C14:2	0.05	0.37
Hexadecadienylcarnitine	C16:2	0.05	0.27
Octadecadienylcarnitine	C18:2	0.06	0.26
Total			**25.92**

Values are based on pooled samples with no replication. LOD, Limit of detection.

3.3.2.3 Phospholipids

Total phospholipids represented 0.24% of the total identified metabolites and are comprised of 76 phosphatidylcholines (PC, Table 3.4A) and 14 lysophosphatidylcholines (LysoPC, Table 3.4B). Both PC and LysoPC accounted for about 0.22% and 0.03%, respectively, of the composition (Figure 3.2). Moreover, lignocellulosic-derived feedstocks are composed of phospholipids found in the plasma membrane of cells (Garcia-Montoto et al., 2021). A previous study revealed that PCs are the main phospholipids in the outermost sapwood of pine, and vital for plasma membrane

formation (Piispanen & Saranpaa, 2002). Similarly, characterization of pyrolysis tar obtained from different wood species showed that pine tar contains significantly higher hydrophobic extractives including phospholipids compared with that of oak and bamboo (Ku & Mun, 2006). Additionally, high phospholipid accumulation was noted to increase in twig bark and wood of poplar plants and functions to harden plants during frost stress (Watanabe et al., 2018). The transformation of these phospholipids during pyrolysis is unknown and requires further investigation. However, the presence of phospholipids in PA from the white pine biomass can further confirm their ubiquitous nature in plant extracts.

Intriguingly, PCs are the most abundant phospholipids and function in maintaining cell membrane integrity even under stressful environmental conditions (Cowan, 2006). PCs are known to play critical roles in mediating physiological and cellular metabolisms including cell elongation and signalling and defence *via* association with other membrane proteins (Cui & Houweling, 2002). Also, PCs act as precursors for the biosynthesis of diverse signalling molecules including LysoPC, diacylglycerol (DAG), phosphatidic acids and arachidonic acid (Cowan, 2006). LysoPC serves as a secondary messenger that mobilises vacuolar proton pool and stress-activating enzymes for defence response (Viehweger et al., 2002). A recent study demonstrated that exogenous PC treatment of peach (*Prunus persica*) seedlings expanded guard cells to maintain sufficient gas exchange, promote proline accumulation, lowered lipid peroxidation and increase cell membrane integrity, which enhanced tolerance to drought stress (Sun et al., 2020c). Similarly, LysoPC has been reported to stimulate the immune response of solanaceous plants against potato (*Solanum tuberosum*) virus Y and *Phytophthora infestans* by restricting pathogen proliferation (Spivak et al., 2003). All these results imply that the white pine PA can be highly efficacious for use to

enhance plant growth by protecting membrane integrity and activating biological processes and components against both biotic and abiotic stresses.

Table 3.4. Metabolic profile of phospholipids [(A) Phosphatidylcholine (B) Lysophosphatidylcholine] in pyroligneous acid (PA) obtained from *Pinus strobus*.

(A) Phosphatidylcholine

Metabolite name	Formula	LOD (µM)	Content (µM/mL)
Phosphatidylcholine diacyl	PC aa C24:0	0.02	0.10
Phosphatidylcholine diacyl	PC aa C26:0	0.27	0.51
Phosphatidylcholine diacyl	PC aa C28:1	0.05	0.06
Phosphatidylcholine diacyl	PC aa C30:2	0.02	0.08
Phosphatidylcholine diacyl	PC aa C30:0	0.02	0.14
Phosphatidylcholine diacyl	PC aa C32:3	0.03	0.34
Phosphatidylcholine diacyl	PC aa C32:2	0.04	6.68
Phosphatidylcholine diacyl	PC aa C32:1	0.06	1.10
Phosphatidylcholine diacyl	PC aa C32:0	0.01	0.13
Phosphatidylcholine diacyl	PC aa C34:4	0.02	0.03
Phosphatidylcholine diacyl	PC aa C34:3	0.01	0.07
Phosphatidylcholine diacyl	PC aa C34:2	0.07	0.23
Phosphatidylcholine diacyl	PC aa C34:1	0.11	0.23
Phosphatidylcholine diacyl	PC aa C36:6	0.13	0.08
Phosphatidylcholine diacyl	PC aa C36:5	0.05	0.13
Phosphatidylcholine diacyl	PC aa C36:4	0.05	0.13
Phosphatidylcholine diacyl	PC aa C36:3	0.08	0.11
Phosphatidylcholine diacyl	PC aa C36:2	0.02	0.27
Phosphatidylcholine diacyl	PC aa C36:1	0.01	0.19
Phosphatidylcholine diacyl	PC aa C36:0	0.08	0.15
Phosphatidylcholine diacyl	PC aa C38:6	0.81	0.13
Phosphatidylcholine diacyl	PC aa C38:5	0.55	0.08
Phosphatidylcholine diacyl	PC aa C38:4	0.08	0.08
Phosphatidylcholine diacyl	PC aa C38:3	0.08	0.06
Phosphatidylcholine diacyl	PC aa C38:1	0.05	0.07

Phosphatidylcholine diacyl	PC aa C38:0	0.11	0.09
Phosphatidylcholine diacyl	PC aa C40:6	0.11	0.12
Phosphatidylcholine diacyl	PC aa C40:5	0.02	0.12
Phosphatidylcholine diacyl	PC aa C40:4	0.16	0.12
Phosphatidylcholine diacyl	PC aa C40:3	0.09	0.07
Phosphatidylcholine diacyl	PC aa C40:2	0.81	0.06
Phosphatidylcholine diacyl	PC aa C40:1	0.58	0.05
Phosphatidylcholine diacyl	PC aa C42:6	1.18	0.07
Phosphatidylcholine diacyl	PC aa C42:5	0.47	0.14
Phosphatidylcholine diacyl	PC aa C42:4	0.09	0.35
Phosphatidylcholine diacyl	PC aa C42:2	0.06	0.09
Phosphatidylcholine diacyl	PC aa C42:1	0.18	0.08
Phosphatidylcholine diacyl	PC aa C42:0	0.11	0.05
Phosphatidylcholine acly-alkyl	PC ae C30:2	0.07	0.05
Phosphatidylcholine acly-alkyl	PC ae C30:1	0.07	0.05
Phosphatidylcholine acly-alkyl	PC ae C30:0	0.08	0.11
Phosphatidylcholine acly-alkyl	PC ae C32:2	0.02	3.42
Phosphatidylcholine acly-alkyl	PC ae C32:1	0.04	0.18
Phosphatidylcholine acly-alkyl	PC ae C34:3	0.29	0.07
Phosphatidylcholine acly-alkyl	PC ae C34:2	0.36	0.32
Phosphatidylcholine acly-alkyl	PC ae C34:1	0.35	0.46
Phosphatidylcholine acly-alkyl	PC ae C34:0	0.07	0.29
Phosphatidylcholine acly-alkyl	PC ae C36:5	0.05	0.11
Phosphatidylcholine acly-alkyl	PC ae C36:4	0.07	0.07
Phosphatidylcholine acly-alkyl	PC ae C36:3	0.04	0.03
Phosphatidylcholine acly-alkyl	PC ae C36:2	0.01	0.11
Phosphatidylcholine acly-alkyl	PC ae C36:1	0.02	0.13
Phosphatidylcholine acly-alkyl	PC ae C36:0	0.02	0.12
Phosphatidylcholine acly-alkyl	PC ae C38:6	0.04	0.10
Phosphatidylcholine acly-alkyl	PC ae C38:5	0.06	0.07
Phosphatidylcholine acly-alkyl	PC ae C38:4	0.06	0.04
Phosphatidylcholine acly-alkyl	PC ae C38:3	0.03	0.05
Phosphatidylcholine acly-alkyl	PC ae C38:2	0.02	0.07
Phosphatidylcholine acly-alkyl	PC ae C38:1	0.01	0.10

Phosphatidylcholine acly-alkyl	PC ae C38:0	0.12	0.12
Phosphatidylcholine acly-alkyl	PC ae C40:6	0.08	0.11
Phosphatidylcholine acly-alkyl	PC ae C40:5	0.01	0.07
Phosphatidylcholine acly-alkyl	PC ae C40:4	0.01	0.06
Phosphatidylcholine acly-alkyl	PC ae C40:3	0.01	0.06
Phosphatidylcholine acly-alkyl	PC ae C40:2	0.01	0.06
Phosphatidylcholine acly-alkyl	PC ae C40:1	0.07	0.07
Phosphatidylcholine acly-alkyl	PC ae C42:5	0.03	0.23
Phosphatidylcholine acly-alkyl	PC ae C42:4	0.01	0.18
Phosphatidylcholine acly-alkyl	PC ae C42:3	0.01	0.09
Phosphatidylcholine acly-alkyl	PC ae C42:2	0.01	0.06
Phosphatidylcholine acly-alkyl	PC ae C42:1	0.01	0.06
Phosphatidylcholine acly-alkyl	PC ae C42:0	0.02	0.06
Phosphatidylcholine acly-alkyl	PC ae C44:6	0.02	0.07
Phosphatidylcholine acly-alkyl	PC ae C44:5	0.02	0.12
Phosphatidylcholine acly-alkyl	PC ae C44:4	0.01	0.11
Phosphatidylcholine acly-alkyl	PC ae C44:3	0.00	0.16
Total			**20.21**
(B) Lysophosphatidylcholine			
lysophosphatidylcholine acyl C14:0	LysoPC a C14:0	0.19	0.35
lysophosphatidylcholine acyl C16:0	LysoPC a C16:0	0.02	0.30
lysophosphatidylcholine acyl C16:1	LysoPC a C16:1	0.05	0.22
lysophosphatidylcholine acyl C17:0	LysoPC a C17:0	0.15	0.26
lysophosphatidylcholine acyl C18:0	LysoPC a C18:0	0.03	0.17
lysophosphatidylcholine acyl C18:1	LysoPC a C18:1	0.05	0.17
lysophosphatidylcholine acyl C18:2	LysoPC a C18:2	0.27	0.17
lysophosphatidylcholine acyl C20:3	LysoPC a C20:3	0.02	0.02
lysophosphatidylcholine acyl C20:4	LysoPC a C20:4	0.03	0.20
lysophosphatidylcholine acyl C24:0	LysoPC a C24:0	0.13	0.12
lysophosphatidylcholine acyl C26:0	LysoPC a C26:0	0.03	0.10
lysophosphatidylcholine acyl C26:1	LysoPC a C26:1	0.03	0.09
lysophosphatidylcholine acyl C28:0	LysoPC a C28:0	0.02	0.09
lysophosphatidylcholine acyl C28:1	LysoPC a C28:1	0.08	0.06
Total			**2.34**

Values are based on pooled samples with no replication. LOD, Limit of detection.

3.3.3 Mineral element content

The mineral nutrient analysis showed 33 mineral elements in PA. Several elements were detected, which includes macroelements (nitrogen (N), phosphorus (P), potassium (K), calcium (Ca), and magnesium (Mg)), microelements (Iron (Fe), zinc (Zn), copper (Cu), boron (B), manganese (Mn), molybdenum (Mo)), trace and/or heavy metals (aluminum, antimony, arsenic, barium, beryllium, bismuth, cadmium, chromium, cobalt, lead, lithium, nickel, rubidium, selenium, silver, strontium, tellurium, thallium, tin, uranium, vanadium) and sodium (Na) (Table 3.5). The highest elemental content was noted for Kjeldah N followed by K, nitrate and nitrite, Ca, and Zn (Table 3.5). In this study, the total Kjeldah N which includes organic N, ammonia and ammonium was 460 mg/L whereas other inorganic N such as nitrate and nitrite recorded 100 mg/L. Potassium content was 180 mg/L which was higher than values previous studies. For instance, PA derived from oak contained 13.23 mg/L of K (Rui et al., 2014), mangrove wood PA contained moderate levels of K (Zulkarami et al., 2011), fruitwood PA contained 0.01 mg/L (Najafi-Ghiri et al., 2022) while 3.63-11.79 mg/L of K was recorded in Durian (*Durio zibethinus*) PA produced between 350° - 550°C (Setiawati et al., 2019). Also, Ca content in the white pine PA was 100 mg/L which was higher than Durian PA (14.72 mg/L) produced at 550°C (Setiawati et al., 2019) and mangrove wood (8.82 mg/L) (Zulkarami et al., 2011). Conversely, the Ca content was lower when compared to other PAs produced from corn straw (276 mg/L) (Shen et al., 2020) and oak (375.88 mg/L) (Rui et al., 2014). Zn content in this study was 10 mg/L which was higher than PA derived from fruitwood (5.5 mg/L)(Najafi-Ghiri et al., 2022) and mangrove wood PA (Zulkarami et al., 2011), but lower than PA obtained from oak PA (16.71 mg/L) (Rui et al., 2014) and Durian PA (36.52-42.71 mg/L) produced at pyrolysis temperature between 350° - 550°C (Setiawati et al., 2019). Additionally,

Mg, Fe, Cu, B, Mn, Mo, Na and all the trace and heavy metals were present at levels below the reported limits (Table 3.5). In contrast, Setiawati et al. (2019) and Rui et al. (2014) reported high levels of Mg (5.92-10.42 mg/L and 133.43 mg/L), Fe (233.02-282.02 mg/L and 578.62 mg/L) and Na (14.03-14.72 mg/L and 146.15 mg/L) in Durian and oak PA, respectively compared to the PA values for the white pine in the present study. Furthermore, these differences in PA elemental compositions can be attributed to the different feedstock, plant growth conditions and the pyrolysis temperature.

Table 3.5. Mineral nutrient composition of pyroligneous acid (PA) obtained from *Pinus strobus*..

Mineral element	Unit	RL	Content
Kjeldahl Nitrogen	mg/L	50.00	460.00
Nitrate & Nitrite	mg/L	50.00	100.00
Aluminum	mg/L	1.00	2.00
Antimony	mg/L	0.10	< 0.10
Arsenic	mg/L	1.00	< 1.00
Barium	mg/L	1.00	< 1.00
Beryllium	mg/L	0.10	< 0.10
Bismuth	mg/L	1.00	< 1.00
Boron	mg/L	1.00	< 1.00
Cadmium	mg/L	0.01	0.20
Calcium	mg/L	50.00	100.00
Chromium	mg/L	1.00	< 1.00
Cobalt	mg/L	0.10	< 0.10
Copper	mg/L	1.00	< 1.00
Iron	mg/L	20.00	< 20.00
Lead	mg/L	0.10	0.60
Lithium	mg/L	0.10	< 0.10
Magnesium	mg/L	10.00	< 10.00
Manganese	mg/L	1.00	1.00
Molybdenum	mg/L	0.10	< 0.10

Nickel	mg/L	1.00	< 1.00
Potassium	mg/L	20.00	180.00
Rubidium	mg/L	0.10	0.10
Selenium	mg/L	1.00	< 1.00
Silver	mg/L	0.10	< 0.10
Sodium	mg/L	50.00	< 50.00
Strontium	mg/L	1.00	< 1.00
Tellurium	mg/L	0.10	< 0.1.00
Thallium	mg/L	0.10	< 0.10
Tin	mg/L	1.00	< 1.00
Uranium	mg/L	0.10	< 0.10
Vanadium	mg/L	1.00	< 1.00
Zinc	mg/L	1.00	10.00

Results are based on pooled samples with no replication. RL; reporting limit

Generally, plant growth and development are influenced extensively by mineral nutrient availability. While N is a key factor that modulate vegetative growth through its involvement in proteins, enzymes and chlorophyll synthesis, K function in enzyme activation, photosynthesis and water relation improvement, and assimilate transportation (Tripathi et al., 2014; Gul et al., 2019; Kumar et al., 2021). Also, Ca is critical for cell elongation and division, facilitate soil nutrient uptake and ameliorate plant tissue resistance against biotic and abiotic stresses by acting as a signalling messenger for downstream activation of defensive genes and pathways (Hirschi, 2004; Morgan et al., 2013; Yang et al., 2013a; Hu et al., 2016a). Thus, the presence of high N, K and Ca contents suggest that PA can be used as an alternative nutrient source in crop production for promoting plant growth and yield. Additionally, the presence of very low contents of Na and heavy metals in PA derived from the white pine could imply that using PA for crop production may not increase soil salinity and heavy metal.

3.4 CONCLUSION

Pyroligneous acid obtained from *Pinus* (white pine) was analyzed for its chemical qualities, antioxidant activities and complete metabolite and mineral nutrient profile following pyrolysis of over 1000°C. The results revealed that white pine PA had a lower electrical conductivity, salinity, and total dissolved solids but higher in °Brix. Moreover, the antioxidant activity assay showed a higher radical scavenging activity against DPPH which could be ascribed to the high total phenolic and flavonoid contents. Metabolic profiling indicates that white pine PA contains 156 metabolites of which organic acids represent 90.9% followed by hexose, carnitines and acylcarnitines, and phospholipids. Mineral elements analysis showed higher contents of N, K, Ca and Zn with lower content of trace elements or heavy metals. Therefore, the presence of these bioactive compounds and elements in white pine PA offers a potential use of PA as an alternative source of plant growth promoter for enhancing plant productivity and inducing resilience to environmental stresses.

CHAPTER 4: SEED PRIMING WITH PYROLIGNEOUS ACID ENHANCES TOMATO SEED GERMINATION AND PLANT GROWTH UNDER ALUMINUM STRESS

A version of this chapter has been published in **Plant Stress Journal**. The citation is:

Ofoe, R., Gunupuru, L. R., Wang-Pruski, G., Fofana, B., Thomas, R. H., & Abbey, L. (2022). Seed priming with pyroligneous acid mitigates aluminum stress, and promotes tomato seed germination and seedling growth. *Plant Stress*, *4*, 100083. https://doi.org/10.1016/j.stress.2022.100083. (Impact factor = 5.2)

4. ABSTRACT

Aluminum (Al) toxicity in acidic soils is a major constraint for seed germination and crop growth. Pyroligneous acid (PA) is rich in bioactive compounds that can enhance crop growth and tolerance to environmental stresses including toxic trace elements, but under studied. In this study, we investigated the effect of tomato (*Solanum lycopersicum* L. 'Scotia') seed priming with different rates of PA (i.e., 0, 0.5:100, 1:100, 1:300, 1:600, 1:900, 1:1200, and 2:100 PA/ddH_2O (*v*/*v*)) on germination and seedling growth under different growing medium Al concentrations (i.e., 0, 0.5, and 1.25 mM aluminum chloride termed Al). The results showed that priming tomato seed with 2:100 PA for 24 hr significantly ($p < 0.01$) enhanced seed germination indices and seedling growth. PA significantly ($p < 0.05$) improved seed germination index and seedling vigour irrespective of the imposed Al stress compared to the control, but not seed germination percentage. Priming with PA also increased the total lengths and surface areas of seedling hypocotyls and roots, root volume, and seedling fresh weight. In most cases, seedling growth of both the control and the PA primed

groups were not affected by the 0.5 mM Al. Additionally, hydrogen peroxide and malonaldehyde contents of seedlings were reduced while proline and soluble protein contents were significantly ($p < 0.001$) increased in PA primed seedlings compared to the control. Furthermore, PA-primed seedlings exhibited enhanced peroxidase (POD) activities, and relatively high expression of *auxin response factor* (*ARF2A*) and antioxidant genes (i.e., *glutathione reductase* (*GR)*, *POD, superoxide dismutase* (*SOD*)*, catalase* (*CAT*), and *ascorbate peroxidase 1* (*APX1*)). These findings suggest that seed priming with PA can mitigates Al stress, and improve tomato seed germination and seedling growth *via* improving antioxidant defence system against Al-induced oxidative stress. Future studies will be required to investigate molecular mechanisms.

Keywords: Solanaceae; wood vinegar; pyrolysis; heavy metal; crop stress; osmopriming

4.1 INTRODUCTION

Acidic soils with pH < 5.0 are widespread in many regions, which contribute significantly to crop loss (Kochian et al., 2004). Globally, acidic soils constitute approximately 50% of the global agricultural land (Kochian et al., 2004; Sade et al., 2016; Slessarev et al., 2016). An increase in soil acidity is caused by either natural and/or anthropogenic factors that leads to excessive use of synthetic chemical fertilizers, imbalance in soil nutrient cycle, and extreme uptake or leaching of basic cations (Bojórquez-Quintal et al., 2017). A notable characteristic of acidic soils is the presence of trivalent aluminum ions (Al^{3+}) that instigate an array of Al-induced toxicity syndrome in plants. Al is the third most abundant metal after oxygen and silicon, and exists in soils as non-toxic oxides and aluminum silicate, which interact with crop roots. At a pH below 5.0, Al dissociates into toxic trivalent forms (Kochian et al., 2015), and soil Al content between 2-5 ppm

is deleterious to sensitive plants whereas Al above 5 ppm is toxic to tolerant species (Gazey, 2018). However, the danger posed by this stress is further exacerbated by climate change and the intensive use of synthetic chemical fertilizers (Bojórquez-Quintal et al., 2017).

Seed germination is a complex cellular and physiological processes that involve water imbibition, depletion of storage nutrients, seed respiration, nucleic acid synthesis, and mitochondrial repair and proliferation resulting in root and hypocotyl elongation (Bewley et al., 2012). However, most major crops including tomato (*Solanum lycopersicum*) are sensitive to micromolar concentration of trace elements toxicity including Al, with the root tip being the primary target (Kochian et al., 2015; Singh et al., 2017; Yamamoto, 2019). Numerous studies have revealed that tomato seedlings are highly sensitive to lower concentration of Al ranging from 5 to 500 µM (Zhou et al., 2009; Surapu et al., 2014; Jin et al., 2021). Al toxicity distorts root system through inhibition of root cell elongation and cell division, perturbs several metabolic processes, induces programmed cell death leading to significant crop growth reduction, yield loss or total crop failure (Kochian et al., 2015; Bojórquez-Quintal et al., 2017). Al binds root membrane surfaces, disrupts cell integrity by crystallizing cell walls, and restricts water and nutrient flow (Kochian et al., 2015). Consequently, Al exposure triggers the accumulation of reactive oxygen species (ROS) that causes oxidative damage of cellular components including membrane lipids, proteins, and nucleic acids that lead to several metabolic alterations (Valadez-González et al., 2007; Yi et al., 2010; Yamamoto, 2019). ROS accumulation promotes membrane lipid peroxidation, which causes loss of plasma membrane integrity and electrolyte leakage that ultimately, leads to cell death (Singh et al., 2017; Yamamoto, 2019). Most plants have evolved cellular and molecular mechanisms to mitigate the phytotoxic effect of Al. Plant response to Al stress is characterized by: (1) an activation of antioxidant defence

machinery involving upregulation of genes in metabolic pathways and/or accumulation of antioxidant enzymes including peroxidases (POD), superoxide dismutase (SOD), catalase (CAT), and glutathione reductase (GR); and (2) the accumulation of osmolytes such as proline and sugar (Kochian et al., 2015; Singh et al., 2017; Pirzadah et al., 2019).

Current trend in agriculture focuses on sustainable practices and use of less synthetic chemicals. It also places more emphasis on alternative strategies that stimulate plant productivity and resilience to environmental stresses, and ensure environmental sustainability (Pretty & Bharucha, 2014; Pareek et al., 2020). Seed priming for many crops has been demonstrated as a unique pre-emergence technique to improve seed viability, germination rate, seedling vigour, and plant growth under varying environmental conditions (Theerakulpisut et al., 2016; Cao et al., 2019; Wang et al., 2019b; Bortolin et al., 2020). Pyroligneous acid (PA), also known as wood vinegar, is a translucent reddish-brown liquid produced by carbonization of crop biomass in the presence of limited oxygen supply (Mathew & Zakaria, 2015; Grewal et al., 2018). PA has a complex chemistry, and it is notably rich in bioactive compounds such as phenolics, sugar derivatives, alcohols, alkanes, and organic acids with acetic acid accounting for 50% of the solution (Mathew & Zakaria, 2015; Crepier et al., 2018; Grewal et al., 2018). These chemical properties mainly depend on the feedstock, pyrolysis temperature, heating rate, residence time, and particle sizes. Due to its chemical properties, PA has gained prominence as clean technology, and is widely used as a biostimulant in agriculture (Pimenta et al., 2018; Wang et al., 2019b). Furthermore, PA contains a biologically active compound called butenolide (3-methyl-2H-furo[2,3-c]pyran-2-one), which belongs to a novel group of growth regulators recently known as karrikinolide or karrikins (Van Staden et al., 2004; Chiwocha et al., 2009; Dixon et al., 2009; Flematti et al., 2009). Karrikins are

water-soluble, heat stable and long-lasting and can remain highly effective at a wide range of concentrations (Van Staden et al., 2004; Flematti et al., 2009). These karrikins as found in PA was reported to stimulate seed germination, seedling growth and development, and its signalling mechanism strongly mimic that of most recently identified plant hormones (Flematti et al., 2004; Van Staden et al., 2006; Gomez-Roldan et al., 2008; Umehara et al., 2008; Dixon et al., 2009). As such, the use of PA to improve plant growth and development has attracted more attention lately as an environmentally sustainable by-product from pyrolysis for improving plant productivity and alleviating environmental stresses (Mmojieje, 2016; Grewal et al., 2018; Wang et al., 2019b; Lu et al., 2020). It has also been demonstrated that PA can be used as an insect repellent (Chalermsan et al., 2009; Mmojieje & Hornung, 2015), antimicrobial agent (Jung, 2007; Mourant et al., 2007), foliar fertilizer (Polthanee et al., 2015; Zhai et al., 2015) and soil enhancer (Lashari et al., 2013).

Recent studies showed that PA enhances seed germination rate, vegetative and reproductive growth of several plants species (Mu et al., 2003; Mungkunkamchao et al., 2013; Grewal et al., 2018; Lei et al., 2018; Shan et al., 2018; Wang et al., 2019b). However, the recommended PA application rate varies between studies, and depends on the feedstock and the tested crop. For instance, a significant increase in germination and growth components of wheat (*Triticum aestivum*) were observed with 1:900 (*v*/*v*) PA (Wang et al., 2019b); while rice (*Oryza sativa*) seedling vigour, shoot and root lengths, and fresh weight were improved by 1:500 (*v*/*v*) PA (Kulkarni et al., 2006). Other studies revealed high ROS-scavenging activities, reducing power, and anti-lipid peroxidation capacity in PA (Loo et al., 2007; Wei et al., 2010). These suggest that PA has the potential to enhance plant growth and productivity, and can contribute significantly to plant tolerance to abiotic stress. A recent proteomics study by Wang et al. (2019b) showed that

priming seeds with 1:900 (*v/v*) PA triggered drought defence mechanisms in the root of wheat seedlings. This mechanism was associated with increased antioxidative and other stress-related proteins such as glutathione, glyceraldehyde-3-phosphate and dehydrogenase. It is also suggested that PA can promote normal cellular balance and metabolic processes under stress conditions, which requires further investigation. Although studies focusing on the use of PA in mitigating environmental stresses in plants are limited, to date, no study has investigated its importance in alleviating Al stress in plants. Therefore, we hypothesized that PA can promote plant growth and induce antioxidants accumulation through modulation of antioxidant pathway genes and other stress-responsive genes under Al stress. Accordingly, the objective of the present study was to determine the effect of seed priming with different concentrations of PA on tomato 'Scotia' seed germination and seedlings growth. We also examined the possible regulatory mechanisms involved in PA-promoting Al stress tolerance in tomato seedlings.

4.2 MATERIALS AND METHODS

4.2.1 PA concentration and seed priming time on Germination and seedling growth

Tomato (*Solanum lycopersicum* L.'Scotia') seeds were purchased from Halifax Seeds (NS, Canada). Pyroligneous acid made from white pine biomass was obtained from Proton Power Inc. (TN, USA). The tomato seeds were sterilized with 10% sodium hypochlorite (NaClO) for 10 min and washed thoroughly three times with sterile distilled water (ddH_2O). Subsequently, the seeds were sterilized in 70% ethanol for 5 min and then washed five times. The cleaned seeds were primed by soaking in different concentrations of PA diluted in ddH_2O i.e., 2:100, 1:100, 0.5:100, 1:300, 1:600, 1:900, 1:1200 PA/ddH_2O (*v/v*) at different soaking times (1, 2, 4, 6, 12 and 24 hr). The treated seeds were air-dried under a laminar flow unit for 15 min, and incubated at 4ºC in a

refrigerator for 7 days to normalize metabolic activities. Ten seeds per treatment were placed in a 16.5 × 18 cm CYG germination pouch (Mega International, USA) and saturated with 25 mL sterile ddH_2O. Seeds were incubated in the dark for 2 days at 25°C, and subsequently grown in a growth chamber under a day/night temperature regime of 25/20°C, 16/8 h day/night illumination, light intensity of 300 µmol $m^{-2} \cdot s^{-1}$ and relative humidity of 70%. The experiment was arranged in a completely randomized design (CRD) with three replications (n=30) and repeated twice. Every three days, 3-5 mL of sterile distilled water was added to maintain regular moisture for the germinating seeds until data collection.

4.2.2 Seed germination and seedling characteristics

Initial seed germination percentage (IFP) was recorded 3 days after treatment. Seeds were considered germinated when the radicle emerged at approximately 3-mm length (Hayat et al., 2020). Final seed germination was recorded at 7 days post-treatment. Other germination indices including mean germination time (MGT), mean germination rate (MGR), germination velocity (GV), germination rate index (GRI), germination index (GI) were determined using the following formulas (Kader, 2005; Ranal et al., 2009). MGT = $\sum N.x / \sum N$; MGR = $1/\mathrm{MGT}$; GV = $(N_1 + N_2 + N_3 + \cdots + N_x)/100 \times (N_1T_1 + N_2T_2 + \cdots + N_xT_x)$; GRI = $\mathrm{G1}/1 + \mathrm{G2}/2 + \mathrm{G3}/3 + \ldots + \mathrm{Gx}/\mathrm{x}$; GI = $(10 \times N_1) + (9 \times N_2) + (8 \times N_3) + \cdots + (1 \times N_x)$, where N = number of seeds germinated on day x, T = number of days from seeding corresponding to N, G1 = germination percentage at the first day after sowing, G2 = germination percentage at the second day after sowing. At 7 days post-treatment, root and hypocotyl morphological parameters were analysed for five seedlings using a root scanning apparatus (STD4800 Scanner, Epson Perfection V850 Pro) equipped with WinRHIZO^{TM}2000 software (Regent Instruments, QC, Canada). The

WinRHIZO^{TM}2000 software recognizes scanned digital root and hypocotyl images, and analyses morphological traits such as total lengths of root and hypocotyl, root surface area and root volume (Himmelbauer, 2004). Mean fresh weight of the seedlings was also recorded from the weight of five seedlings.

4.2.3 PA priming effect on aluminum tolerance

To further delineate the effect of PA in promoting Al tolerance in tomato 'Scotia' plants, sterilized seeds were primed in sterile ddH_2O and 2:100 PA for 24 h. Treated seeds were air-dried and kept at 4^oC for 7 days. Twelve seeds were distributed in each CYG germination pouch containing 25 mL of 25% strength Hoagland nutrient solution. The pH of the nutrient solution was adjusted with sodium hydroxide and hydrochloric acid to 5.0 and supplemented with three aluminum chloride ($AlCl_3$) doses: 0.0 (control), 0.50 (moderate), and 1.25 mM (high) corresponding to 0, 0.1 and 0.25 mM Al^{3+} activity, respectively. These doses were based on previous studies where tomato seedlings were reported to be hypersensitive at concentrations between 5 to 500 µM (Zhou et al., 2009; Surapu et al., 2014; Jin et al., 2021). In order to assess PA effects on higher Al dose, 1.25 mM was also examined. The nutrient solution was renewed every 3 days to maintain adequate moisture content. Seeds were incubated in the dark for 2 days and germination indices were taken consecutively for 7 days. The study was arranged in a CRD with four replications (n=48) and repeated twice. Growth, root and hypocotyl morphological traits were determined for five seedlings for each treatment on the 10th day. Whole plants were collected and immediately frozen in liquid nitrogen and stored at -80^oC for biochemical and gene expression analyses.

4.2.3.1 Lipid peroxidation and H_2O_2 production determination

Lipid peroxidation was determined based on malondialdehyde (MDA) concentration according to the method described by Hodges et al. (1999) with slight modifications. Briefly, a 0.1 g ground sample of seedling was homogenized in 1 mL of 0.1% (*w/v*) trichloroacetic acid (TCA). The homogenate was centrifuged at 16,000 *g* for 10 min at 4°C. A 500 µL of the supernatant was added to an equal amount of 0.5% thiobarbituric acid (TBA) in 20% TCA. The mixture was incubated at 95°C for 30 min, cooled on ice, and centrifuged at 12,000 *g* for 5 min. The absorbance of the supernatant was read at 532 nm and non-specific absorption at 600 nm. The concentration of MDA was calculated from the extinction coefficient 155 m/M cm using the equation C = [Abs (535–600) ÷155,000]x10^6. MDA concentration was expressed as nmol MDA g^{-1} FW. Hydrogen peroxide levels were determined according to the method described by Alexieva et al. (2001). 0.1 g of ground samples of seedlings were homogenized in 1 mL 0.1% (*w/v*) TCA. The mixture was centrifuged at 16,000 *g* for 10 min at 4°C. A 200 µL of the supernatant was mixed with 200 µL of 100 mM potassium phosphate buffer (pH 7.0) and 800 µL of 1 M KI. The reaction was developed for 1 h in the dark and the absorbance was read at 390 nm against a blank that consisted of 0·1% TCA in the absence of leaf extract. The level of H_2O_2 was calculated using a H_2O_2 standard curve.

4.2.3.2 Protein content and peroxidase enzyme activity

Approximately 0.2 g of ground plant sample was homogenized in 1.5 mL ice-cold extraction buffer (50 mM potassium phosphate buffer, with pH 7.0) and 1% polyvinylpyrrolidone and 0.1 mM EDTA). The homogenate was centrifuged at 15,000 g for 20 min at 4°C. The supernatant (crude enzyme extract) was put in a new microfuge tube on ice and the protein content was measured at 595 nm after 5 min of mixing with Bradford's reagent (Bradford, 1976). The protein content was

estimated from a standard curve of bovine serum albumin (200-900 µg mL^{-1}). Peroxidase (POD, EC 1.11.1.7) activity was determined using pyrogallol as substrate according to Chance and Maehly (1955) with slight modification. The reaction mixture was 100 mM potassium-phosphate buffer (pH 6.0), 5% pyrogallol, 0.5 % H_2O_2 and 100 µL of crude enzyme extract. Following reaction mixture incubation at 25°C for 5 min, 1 mL of 2.5 N H_2SO_4 was added to stop the reaction, and the absorbance was read at 420 nm against a blank (Milli-Q water). One unit of POD forms 1 mg of purpurogallin from pyrogallol in 20 s at pH 6.0 and 20°C.

4.2.3.3 Proline content

Proline content was determined as described by Bates et al. (1973). A 0.1 g ground sample of normal seedling was homogenized in 3 mL of 3% sulfosalicylic acid and centrifuged at 16,000 g for 5 min. 400 µL of the supernatant was added to a reaction mixture containing 400 µL of 3% sulfosalicylic acid, 800 µL glacial acetic acid, and 800 µL acidic ninhydrin, and incubated at 96°C for 1 hr. After the termination of the reaction on ice, 3 mL of toluene was added and vortexed for 30 s to extract red chromophore. The absorbance of the upper phase (chromophore containing toluene) was measured at 520 nm using toluene as blank. The free proline content was determined using L-proline standard curve and expressed as mg/g FW.

4.2.3.4 RNA extraction and cDNA synthesis

Root and shoot samples from the control and PA treated seedlings were ground in liquid nitrogen. Total RNA was extracted and purified from approximately 200 mg of ground tissue using GeneJET Plant RNA purification kit (Thermo Scientific, USA) according to the manufacturer's instruction. The total RNA was quantified using Nano-UV/Vis spectrophotometer and the intergity was

analysed on a 1% agarose gel stained with GelRed. The total RNA was treated with DNase I to remove DNA contamination. The first-strand of cDNA was synthesized from 200 ng of total RNA using iScript™ gDNA Clear cDNA Synthesis kit (Bio-Rad Laboratories, USA) according to the manufacturer's instruction. The cDNA was amplified using a conventional PCR in a 20 µL reaction mixture containing 2 µL 10× Taq Buffer, 0.25 µL Taq DNA polymerase, 0.2 µL 10 mM dNTPs, 0.4 µL each of 100 µM forward and reverse primers (Table S4.1) and 2.5 µL 100 ng cDNA. The PCR was performed with the following conditions: initial denaturation at 94ºC for 3 min, followed by 35 cycles with 94ºC for 30 s, 57ºC for 30 s, 72ºC for 1 min, and a final extension of 72ºC for 3 min.

4.2.3.5 Quantitative real-time PCR (qRT-PCR) analysis

The qRT-PCR assays were carried out in a QuantStudio 5 Real-Time PCR System (Thermo Fisher Scientific, USA) with an optical 96-well plate of 15 µL reaction mixture containing 10 µL 2 × SYBR Green qPCR mix, 0.2 µL of each specific primer (10 µM, Table S4.1) and 1 µL of 8 ng cDNA template. The qPCR condition consisted of an initial denaturation at 95ºC for 10 min, followed by 40 cycles of 95ºC for 15 s, 60ºC for 30 s, and 72ºC for 30 s, and a final extension of 72ºC for 5 min. Each reaction was replicated three times, and the EF1α reference gene was used as an internal expression control for normalization. A dissociation curve was generated for each amplicon and analysed by heating at 95ºC for 15 s followed by 60ºC for 1 min, and 95ºC for 10 min to ensure amplification specificity. Relative expression levels of the different genes were quantified using the comparative CT ($2^{-\Delta\Delta CT}$) method (Livak & Schmittgen, 2001).

4.2.4 Statistical analysis

All statistical analyses were performed using Minitab software version 20 (Minitab, Inc., State College, Pennsylvania, USA). Data obtained with different priming concentrations and times were subjected to a two-way analysis of variance (ANOVA). A Kruskal-Wallis test was carried out for initial seed germination percentage while all data for the Al study were analysed with one-way ANOVA. Post hoc means were compared using Tukey's Honestly Significant Difference (HSD) at $\alpha = 0.05$.

4.3 RESULTS

4.3.1 Seed germination and physiological responses to PA primed tomato 'Scotia' seed

4.3.1.1 PA enhanced seed germination indices

PA significantly ($p < 0.001$) increased the initial germination of tomato 'Scotia' seeds compared with the control, irrespective of the priming time (Table 4.1). Treatments 2:100 PA and 1:1200 PA increased the initial germination percentage by *ca*. 150% and *ca*. 128% respectively, compared with the control. Although priming time had no significant ($p > 0.05$) effect on the initial germination rate, seed priming for 24 hr recorded the highest initial germination percentage (Table 4.1). Moreover, germination velocity and mean germination rate were significantly ($p < 0.001$) improved with PA priming (Table 4.1). Notably, higher germination velocity and mean germination rate were ascribed to the 2:100 PA and 1:1200 PA treatments, but were lowered by the control and 1:300 PA. When tomato seeds were primed for 24 h the germination velocity and mean germination rate were not significantly ($p > 0.05$) different from those of the 2-, 4-, 6- and 12-hr primed seeds, but significantly ($p < 0.001$) higher than that of the 1 hr primed seeds.

Similarly, tomato seed germination index and germination rate index were significantly ($p < 0.001$) enhanced by PA priming compared with the control (Table 4.1). Among all the PA treatments, 2:100 PA had the highest germination index and germination rate i.e., *ca*. 12% and 30% respectively, compared to the control. On the other hand, these improvements in germination indices were independent of priming time.

Table 4.1. Germination effect of seed priming with pyroligneous acid (PA) on tomato seeding germination characteristics on the 7th day after germination with different priming time (1, 2, 4, 6, 12 and 24 h).

Treatment	Initial Germination (%) *	Germination Velocity	Mean Germination Rate	Germination Index	Germination Rate Index	Mean Germination time (days)	Final Germination (%)
Control	42.4±0.24 e	19.96±0.37 d	0.199±0.00 d	47.67±3.29 bc	32.59±2.93 c	5.02±0.09 a	97.06±6.16 a
0.5:100	67.4±0.96 cd	19.99±1.00 cd	0.200±0.01 cd	48.00±4.75 bc	33.50±4.69 bc	5.01±0.24 ab	97.37±7.05 a
1:100	63.3±0.86 cd	20.43±0.77 cd	0.204±0.01 cd	49.17±3.63 bc	34.54±3.70 bc	4.90±0.17 abc	97.52±6.08 a
1:300	49.6±0.55 de	19.92±0.64 d	0.199±0.01 d	46.56±4.15 c	31.93±3.44 c	5.02±0.16 a	95.73±7.67 a
1:600	68.6±1.34 cd	20.40±1.81 cd	0.204±0.02 cd	47.33±3.76 bc	33.55±4.43 bc	4.91±0.365 ab	94.59±7.32 a
1:900	85.5±1.49 bc	20.73±1.65 bc	0.207±0.02 bc	51.00±3.98 ab	36.86±5.51 b	4.83±0.33 bc	98.51±4.28 a
1:1200	96.8±1.83 ab	21.38±2.28 ab	0.214±0.02 ab	49.94±5.36 bc	37.14±6.58 b	4.69±0.43 cd	95.55±8.26 a
2:100	106.5±1.92 a	22.41±2.73 a	0.224±0.02 a	54.44±5.05 a	42.04±6.98 a	4.49±0.617 d	97.67±7.84 a
p-value	0.000	0.000	0.000	0.000	0.000	0.00	0.205
Time (h)	Initial Germination (%) *	Germination Velocity	Mean Germination rate	Germination Index	Germination Rate Index	Mean Germination time (days)	Final Germination (%)
1	58.3±1.60 a	20.25±2.09 b	0.203±0.02 b	48.29±4.75 a	33.77±5.76 a	4.95±0.40 a	96.87±7.79 a
2	77.3±1.20 a	20.61±1.22 ab	0.206±0.01 ab	49.17±4.05 a	35.19±4.80 a	4.86±0.27 ab	96.50±5.90 a
4	71.6±2.51 a	20.53±2.22 ab	0.205±0.03 ab	49.46±5.45 a	34.95±9.76 a	4.89±0.53 ab	96.87±7.79 a
6	68.8±1.50 a	20.51±1.61 ab	0.205±0.02 ab	49.08±4.85 a	34.74±5.96 a	4.88±0.33 ab	96.50±5.90 a
12	70.0±1.68 a	20.44±2.01 ab	0.204±0.02 ab	49.00±4.91 a	34.78±6.17 a	4.90±0.40 ab	96.99±7.22 a
24	88.9±1.96 a	21.10±2.32 a	0.211±0.02 a	50.58±5.39 a	37.17±6.84 a	4.75±0.44 b	97.22±7.80 a
p-value	0.131	0.024	0.024	0.541	0.097	0.022	0.994
Interaction							
PA*Time		***	***	***	***	***	ns

Values are means ± SD of three replicates (n=30) and different letters are significantly different by Tukey's honestly significant difference (HSD) ($p < 0.05$). The *** and ns indicate a significant difference at 0.001 and no significant difference respectively.

Maximum germination index and germination rate index were recorded for the 24-hr priming, which was not significantly ($p > 0.05$) different from the other priming duration. Furthermore, priming with PA significantly ($p < 0.001$) reduced the mean germination time of tomato seed, but had no significant ($p > 0.05$) effect on final germination percentage (Table 4.1). It was obvious that the 2:100 PA-primed seeds exhibited the least mean germination time which was similar to that of the 1:1200 PA primed seeds. Likewise, increasing priming time from 1 to 24 hr significantly ($p < 0.05$) reduced mean germination time, but had no significant ($p > 0.05$) effect on the final germination percentage (Table 4.1). The interactive effect of PA concentration and time revealed a highly significant ($p < 0.001$) effect on germination velocity, mean germination rate, germination index, germination rate index, and mean germination time but not ($p > 0.05$) final germination percentage (Table 4.1, Table S4.2).

4.3.1.2 PA enhances seedling growth parameters

Total root length, root surface area, and root volume were significantly ($p < 0.01$) increased by by *ca*. 29% and 23%, *ca.* 23 and 23%, and *ca.* 9% and 7% when seeds were primed with 2:100 PA and 1:100 PA respectively, compared to the control (Table 4.2). Additionally, priming time of 6 hr had a significantly higher total root length ($p < 0.001$), root surface area ($p < 0.01$), and root volume ($p < 0.005$) compared to the other priming times (Table 4.2). In most cases, priming time did not affect seedling growth parameters. For instance, higher total root length was noticed in 6 hr-primed seeds but was not significantly ($p > 0.05$) different from that of 2, 4, 6, 12, and 24 h primed seeds except for 1 hr exposure time. A similar trend was observed in total root surface area and root volume.

Table 4.2. Morphological effect of seed priming with pyroligneous acid (PA) on tomato seeding growth characteristics on the 7th day germination with different priming time (1, 2, 4, 6, 12 and 24 h).

Treatment	Total root length (cm)	Total surface area (cm^2)	Root volume (cm^3)	Hypocotyl length (cm)	Total hypocotyl surface (cm^2)	Fresh weight (g)
Control	12.27±3.54 de	8.06±2.64 d	0.0081±0.001 ab	3.33±1.07 b	2.49±0.66 c	0.114±0.02 c
0.5:100	11.76±3.99 e	8.21±2.88 cd	0.0076±0.002 bc	3.40±1.32 b	2.44±0.68 c	0.115±0.02 bc
1:100	15.04±3.66 ab	9.92±1.60 a	0.0087±0.001 a	3.93±1.07 a	2.83±0.46 a	0.126±0.01 ab
1:300	12.26±4.15 de	9.01±2.10 bc	0.0073±0.002 c	3.28±1.40 b	2.59±0.71 bc	0.114±0.02 c
1:600	12.82±4.03 cde	8.99±2.18 bcd	0.0076±0.002 bc	3.92±1.00 a	2.79±0.54 ab	0.116±0.01 bc
1:900	13.76±3.93 bc	9.19±2.37 ab	0.0080±0.002 ab	3.89±1.13 a	2.75±0.51 ab	0.124±0.01 abc
1:1200	14.40±4.89 abc	8.49±3.00 bcd	0.0082±0.001 ab	4.03±1.12 a	2.78±0.65 ab	0.124± 0.02 abc
2:100	15.80±4.80 a	9.95±2.31 a	0.0088±0.002 a	4.01±1.12 a	2.68±0.66 abc	0.128±0.01 a
p-value	0.000	0.000	0.008	0.000	0.000	0.000
Time (h)	Total root length (cm)	Total root surface area (cm^2)	Root volume (cm^3)	Hypocotyl length (cm)	Total hypocotyl surface (cm^2)	Fresh weight (g)
1	12.14±4.10 b	9.02±2.13 ab	0.0076±0.002 c	3.54±1.18 b	2.64±0.65 a	0.119±0.02 b
2	13.80±4.53 a	8.52±3.09 b	0.0083±0.002 ab	3.76±1.23 b	2.64±0.67 a	0.120±0.01 b
4	13.74±4.61 a	9.19±201 ab	0.0077±0.002 bc	3.56±1.05 b	2.62±0.59 a	0.115±0.01 b
6	14.42±5.19 a	9.48±2.43 a	0.0084±0.002 a	3.44±1.25 b	2.67±0.55 a	0.116±0.01 b
12	13.23±4.34 ab	8.86±2.81 ab	0.0080±0.002 abc	3.79±1.12 b	2.69±0.65 a	0.119±0.01 b
24	13.53±3.96 a	8.84±3.11 ab	0.0081±0.002 abc	4.24±1.16 a	2.74±0.65 a	0.130±0.01 a
p-value	0.000	0.008	0.003	0.000	0.516	0.000
Interaction						
PA*Time	***	***	***	***	***	***

Values are means ± SD of three replicates (n=30) and different letters are significantly different by Tukey's honestly significant difference (HSD) ($p < 0.05$). The *** indicates a significant difference at 0.001.

Moreover, hypocotyl length and total hypocotyl surface area were significantly ($p < 0.001$) improved in PA primed seeds compared to the control (Table 4.2). Maximum hypocotyl length was observed when seeds were primed with 1:1200 PA followed by 2:100 PA, and were increased but an average of 21% more than that of the control. Similarly, 1:100 PA primed seeds exhibited the highest hypocotyl surface area although not significantly ($p > 0.05$) different from the other PA treatments except for the 0.5:100 and 1:300 PA treatments. Also, 24 hr-primed seeds recorded a significantly ($p < 0.001$) higher hypocotyl length compared to all the other treatments. total hypocotyl surface area was increased in the seedlings of the 24 hr-primed seeds, this effect was not significantly ($p > 0.05$) different from the other treatments. Furthermore, seedling fresh weight was significantly ($p < 0.001$) increased with PA application (Table 4.2). A higher fresh weight was recorded when seeds were primed with 2:100 PA followed by 1:100 PA, but was not statistically significant ($p > 0.05$) (Table 4.2). In contrast, the control and 1:300 PA primed seeds both exhibited significantly ($p < 0.001$) lower fresh weights. Similarly, a priming time of 24 hr significantly ($p < 0.005$) increased seedling fresh weight compared to the other times. Interestingly, the interaction effect of PA concentration and time showed a significant ($p < 0.001$) and positive impact on all the examined growth parameters (Table 4.2, Table S4.3).

4.3.2 Seed priming with PA promotes Al tolerance in tomato seedlings

4.3.2.1 Seed germination indices and seedling growth

PA priming improved germination index of tomato seedlings under Al stress, but was not significantly ($p > 0.05$) different from that of the control and Al alone (Table 4.3). When seeds were PA primed without Al stress (i.e., 0 mM Al), the germination index was *ca.* 10% higher than the control. PA-primed seeds exhibited a slightly higher germination index compared to Al-treated

plants under both low and high Al exposure. Additionally, Al stress significantly ($p < 0.01$) increased mean germination time compared to the control; while PA priming exhibited a comparable effect to that of Al treatment alone. Similarly, the germination percentage of PA primed seeds was not different from that of the control without Al (Table 4.3).

Table 4.3. Germination indices of tomato seedling to aluminum stress.

Treatment	Germination Index	Mean Germination Time (days)	Germination percentage (%)	Seedling vigour
Control	57.04±2.31 ab	4.96±0.05 b	96.10±4.81 a	785.53±37.20 ab
0.5 mM Al	49.53±1.92 b	5.21±0.16 ab	79.49±4.81 b	841.81±94.40 a
1.25 mM Al	56.55±4.70 ab	5.47±0.33 a	86.22±6.98 ab	620.73±78.80 b
2% PA	62.82±3.30 a	5.58±0.15 a	93.96±4.17 a	753.48±175.50 ab
2% PA+0.5 mM Al	58.03±2.31 ab	5.39±0.22 a	89.79±4.17 ab	897.41±154.60 a
2%+1.25mM Al	57.05±4.70 ab	5.39±0.19 a	88.33±6.33 ab	708.31±74.00 ab
p-value	0.016	0.005	0.009	0.017

Tomato seeds were primed with 2% PA for 24 h and grown under ¼ strength Hoagland solution (pH=5.0) supplemented with 0.5 mM and 1.25 mM Al. Values are means ± SD of four replicates and different letters are significantly different by Tukey's honestly significant difference (HSD) ($p < 0.05$).

The germination percentage of PA-primed seeds was higher under both 0.5- and 1.25-mM Al but not significantly ($p > 0.05$) different from the control. Likewise, the seedling vigour of PA primed seeds was not different from the control under 0 mM Al (Table 4.3). Nevertheless, exposure of both control and PA primed seeds to 0.5 mM Al increased seedling vigour compared to 0 mM Al. Seedling vigour of PA primed seeds was *ca*. 14% higher for the 1.25 mM Al treatment compared to the control.

Growth of seedlings from PA primed seeds were promoted in media with added Al (Figures 4.1 & 4.2). In both control and PA primed seeds, hypocotyl length was significantly ($p < 0.01$) higher following treatment with 0.5 mM Al compared to 0 mM Al (Figure 4.1A). However, the adverse

effect of Al stress was more pronounced in the control seedlings that were treated with 1.25 mM Al without PA, while PA priming improved hypocotyl length by *ca.* 11% at the same higher Al concentration. Similarly, higher hypocotyl and root surface areas were recorded when both control and PA primed seeds were treated with 0.5 mM Al although not significantly ($p > 0.05$) different from that of 0 mM Al (Figures 4.1B-C and Figure 4.2). Seed priming with PA significantly ($p < 0.005$) increased hypocotyl and root surface areas by *ca*. 11% and *ca*. 54% respectively, upon exposure to 1.25 mM Al compared to control seedling with the same treatment. Furthermore, seed priming produced a staggering increase of *ca*. 19% in total root length compared with control (Figures 4.1D & 4.2).

Additionally, both the control and PA-primed seeds treated with 0.5 mM Al recorded the highest total root length compared to 0 mM Al. PA priming significantly ($p < 0.005$) mitigated Al stress and enhanced total root length by *ca.* 52% following treatment with 1.25 mM Al compared to control. Similarly, total root volume was not significantly ($p > 0.05$) affected by PA priming and 0.5 mM Al compared to control (Figure 4.1E). Nevertheless, PA primed seed significantly ($p < 0.001$) increased total root volume by *ca.* 52% following treatment with the 1.25 mM Al compared to control (Figure 4.2). Total seedling fresh weight was significantly ($p < 0.01$) enhanced with PA priming (Figure 4.1F). Total seedling fresh weight was increased in both control and PA primed seeds following treatment with 0.5 mM Al, which was not significantly ($p < 0.05$) different from seedlings that were treated with 0 mM Al. On the other hand, seedling fresh weight was significantly ($p < 0.01$) increased by *ca*. 22% in PA primed seeds compared to control (Figure 4.1F).

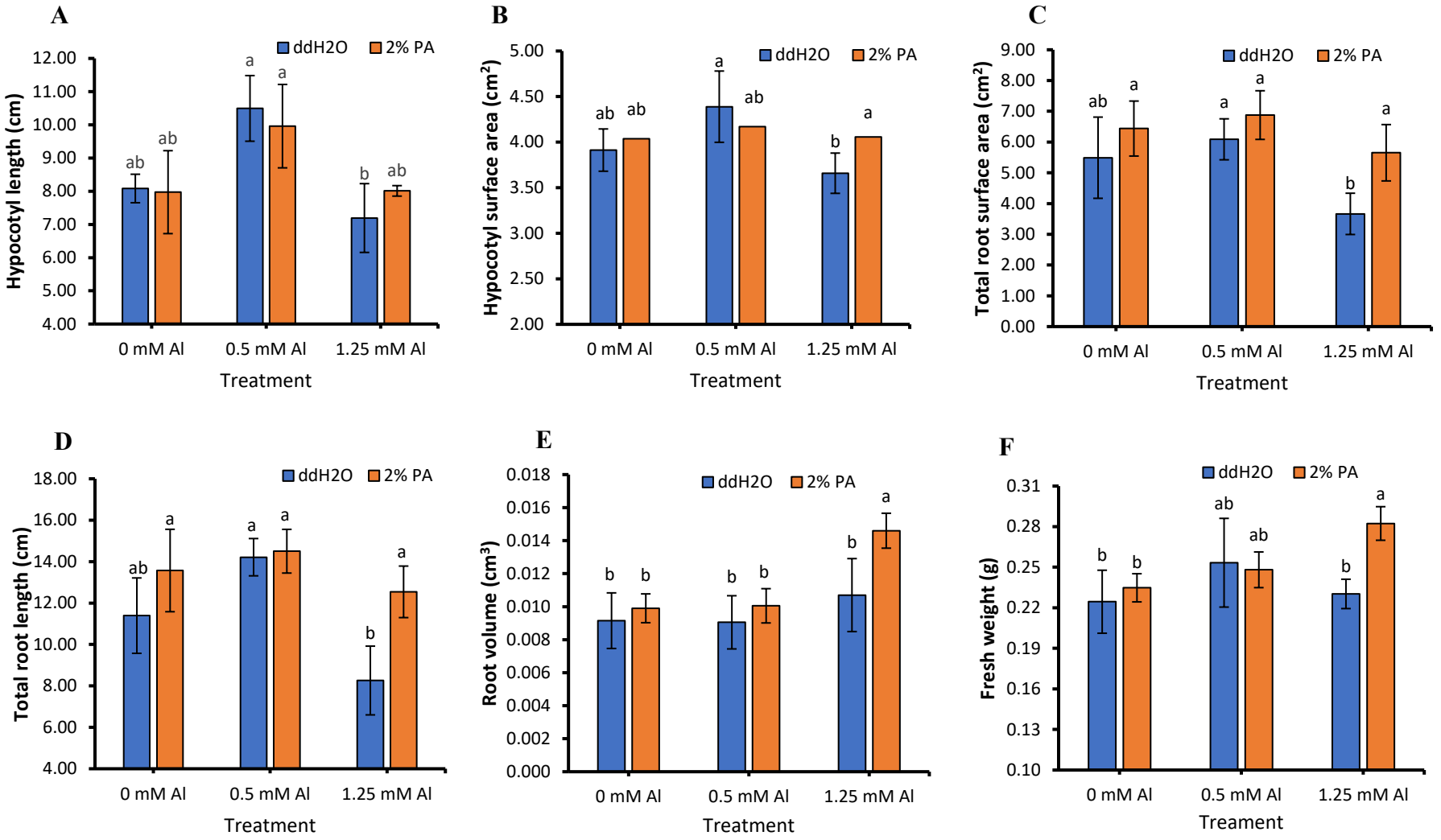

Figure 4.1. Growth response of tomato seedlings under aluminum stress. Tomato seeds were primed with 2% PA for 24 h and grown under ¼ strength Hoagland solution (pH=5.0) supplemented with 0.5 mM and 1.25 mM Al. Distilled water was taken as the control treatment. (a) Hypocotyl length (b) Hypocotyl surface area (c) Total root surface area (d) Total root length (e) Root volume (f) fresh weight of five seedlings. Values are means ± SD of four replicates (12 seedling per replicate) and different letters are significantly different by Tukey's honestly significant difference (HSD) ($p < 0.05$).

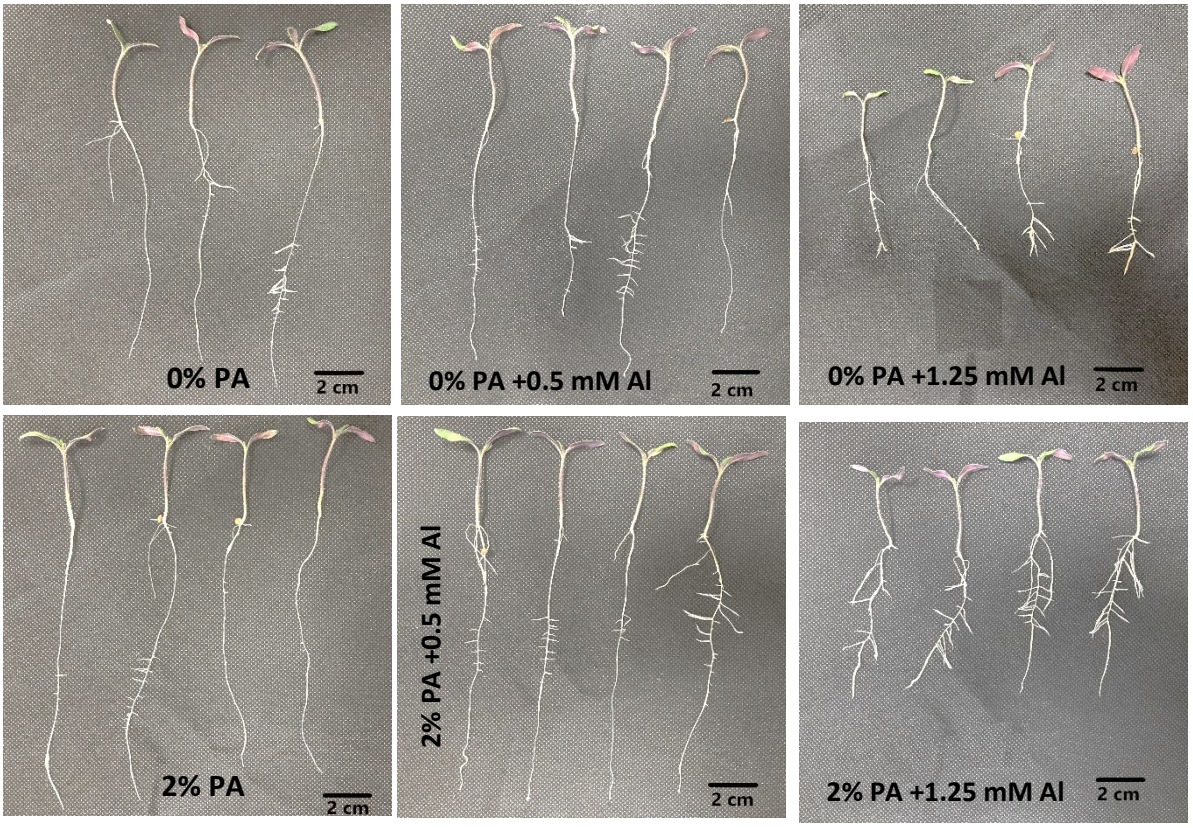

Figure 4.2. Growth comparison of tomato seedlings under aluminum stress. Tomato seeds were primed with 2% PA for 24 h and grown under ¼ strength Hoagland solution (pH=5.0) supplemented with 0.5 mM and 1.25 mM Al. Distilled water was taken as the control treatment**.**

4.3.2.2 ROS and lipid peroxidation

H_2O_2 content was determined to further assess the oxidative stress in both the control and PA primed seeds in response to Al stress. There was a considerably higher H_2O_2 abundance in control treatments compared to PA-primed seedlings, which exhibited low H_2O_2 content following 0 mM Al treatment (Figure 4.3A). H_2O_2 content was not significantly ($p > 0.05$) influenced by PA priming and 0.5 mM Al treatment.

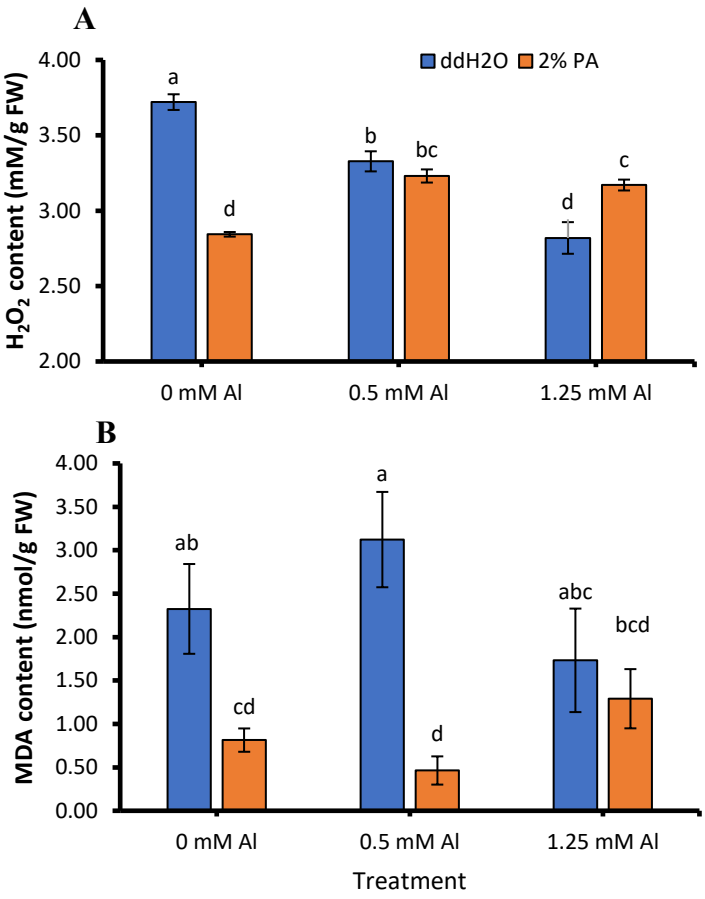

Figure 4.3. Oxidative stress of primed tomato seedlings in response to aluminum stress. (A) Generation of H_2O_2 in control and PA primed seedlings. (B) Malonaldehyde (MDA) content in the control wheat roots and PA treated seedlings. Tomato seeds were primed with 2% PA for 24 hr and grown under ¼ strength Hoagland solution (pH=5.0) supplemented with 0.5 mM and 1.25 mM Al. Values are means ± SD of four replicates and different letters are significantly different by Tukey's honestly significant difference (HSD) ($p < 0.05$).

However, H_2O_2 content was significantly ($p < 0.001$) lower in PA primed seedlings compared to control under 0 mM Al treatment. Furthermore, H_2O_2 content was significantly ($p < 0.001$) increased in PA primed seedlings under 1.25 mM Al treatment (Figure 4.3A). To further explore the extent of membrane lipid peroxidation damage elicited by ROS (H_2O_2), the production and accumulation of MDA was measured in both control and PA-primed seedlings under Al stress. MDA content was remarkably reduced by *ca.* 65% and *ca.* 85% in PA primed seedlings compared to the control under both 0 and 0.5 mM Al treatments, respectively. Although MDA content was

not altered by 1.25 mM Al, it was slightly lower in PA primed seedlings compared to the control (Figure 4.3B).

4.3.2.3 Antioxidant compounds accumulation and enzyme activity

Plant tissue proline content was not significantly ($p > 0.05$) affected by PA priming under 0 mM Al, but was reduced in both the control and the PA-primed seedlings under 0.5 mM Al compared to seedlings that were not treated with Al (Table 4.4).

Table 4.4. Antioxidant compounds accumulation and enzyme activity of tomato seedling in response to aluminum stress.

Treatment	Proline content (mg/g FW)	Protein (mg/g FW)	POD activities (U/g FW)
Control	0.96±0.03 b	9.25±0.02 f	0.90±0.02 d
0.5 mM Al	0.68±0.01 c	14.44±0.03 a	1.90±0.04 a
1.25 mM Al	0.63±0.01 d	10.69±0.01 d	0.82±0.02 e
2% PA	0.98±0.04 b	10.37±0.02 e	1.41±0.00 c
2% PA+0.5 mM Al	0.67±0.02 c	11.08±0.02 c	1.58±0.04 b
2%+1.25mM Al	1.37±0.01 a	11.32±0.02 b	1.91±0.04 a
P-value	0.000	0.000	0.000

Tomato seeds were primed with 2% PA for 24 h and grown under ¼ strength Hoagland solution (pH=5.0) supplemented with 0.5 mM and 1.25 mM Al. Values are means ± SD of four replicates and different letters are significantly different by Tukey's honestly significant difference (HSD) ($p < 0.05$).

Besides, seeds primed with PA had a considerably high proline content i.e., *ca.* 118% following treatment with 1.25 mM Al compared to the control seeds under the same condition. Moreover, it was revealed that PA-priming increased protein content by *ca*. 12% following 0 mM Al treatment compared to control (Table 4.4). Notably, high protein accumulation was recorded in control seedlings with 0.5 mM Al, which was *ca*. 23% higher than the average for the PA-primed

seedlings. PA primed seedlings accumulated higher protein content following 1.25 mM Al treatment compared to control. Similarly, POD activity was considerably increased by *ca.* 57% in PA primed seedlings following 0 mM Al treatment compared to control (Table 4.4). POD activity increased slightly in PA-primed seedlings treated with Al, but was significantly ($p < 0.001$) lower compared to control seedlings treated with 0.5 mM Al alone. However, POD activity increased significantly *(*$p < 0.001$) by *ca*. 133% in PA-primed seedlings following 1.25 mM Al treatment compared to control.

4.3.2.4 Relative expression of genes in tomato plants under Al stress

The results for gene expression revealed significant expression levels of antioxidant genes in seedlings from PA-primed seeds under Al stress (Figure 4.4). The expression of glutathione reductase (*GR*) gene in seedlings of PA primed seed was 4-fold higher than the control under 0 mM Al although this was not significantly ($p > 0.05$) different upon exposure to 0.5 mM Al (Figure 4.4A). Nevertheless, relative expression of *GR* was increased by 2.4-fold in seedlings of PA primed seeds compared to seedlings treated with 1.25 mM Al alone. Similarly, expression of catalase (*CAT*) gene increased substantially by 1.4-fold in seedlings of PA primed seeds with 0 mM Al treatment, but was not significantly ($p > 0.05$) affected by 0.5 mM or 1.25 mM Al (Figure 4.4B). Moreover, the expression of ascorbate peroxidase 1 (*APX1*) gene was not altered in both control and PA primed seedlings under 0 mM and 0.5 mM Al. A slightly higher *APX1* transcript abundance was noticed in seedlings of PA primed seeds under both 0 and 0.5 mM Al (Figure 4.4C). *APX1* transcript abundance was significantly ($p < 0.01$) increased by 1.9-fold in seedlings of PA primed seeds upon exposure to 1.25 mM Al.

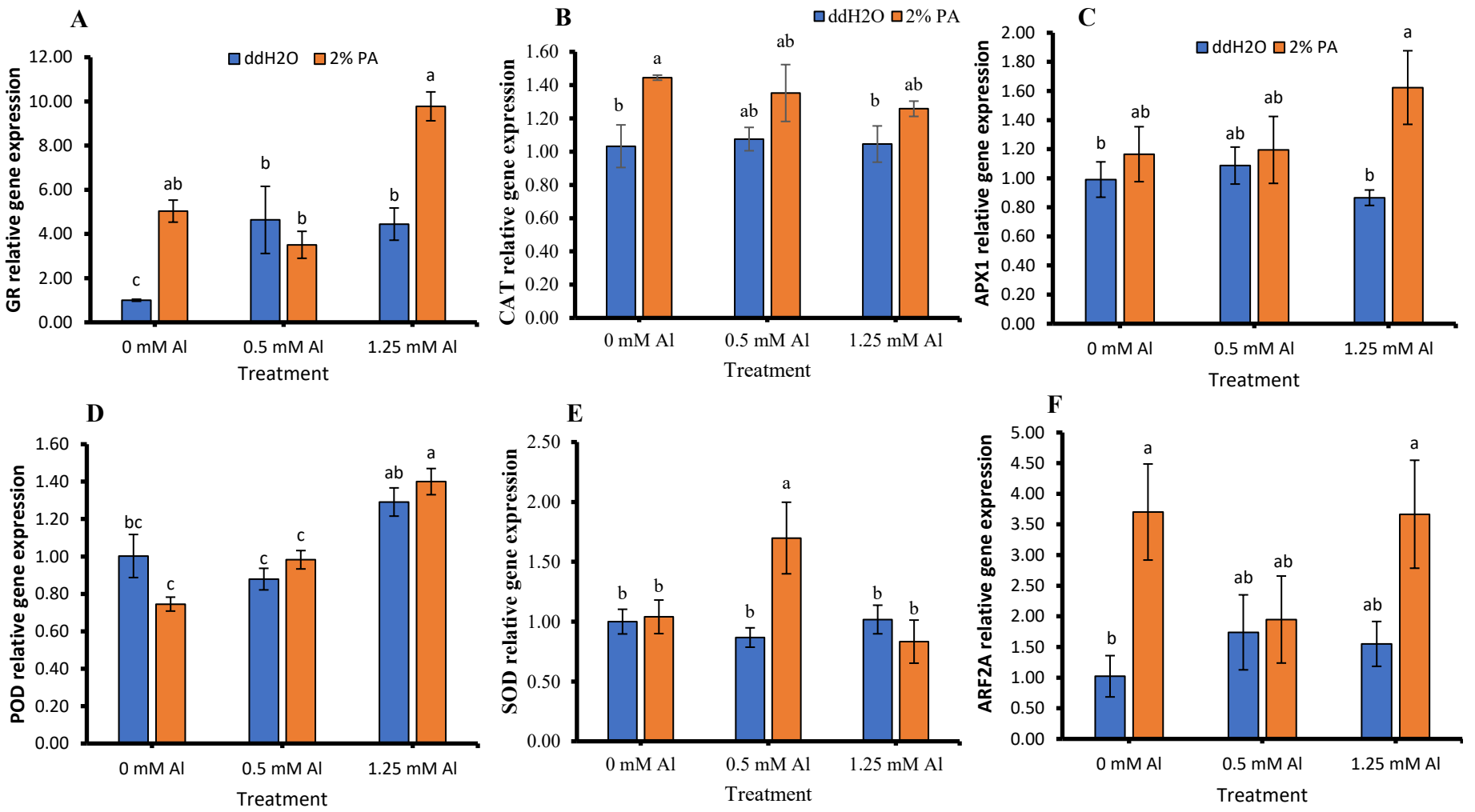

Figure 4.4. Gene expression pattern analysis of antioxidants and auxin transcription factor in both control and PA primed tomato seedlings under Al stress. (A) *SIGR* (B) *SICAT* (C) *APX1* (D) *SIPOD* (E) *SISOD* (F) *ARF2A*. Values are means ± SD of three independent experiments (biological replicates) and different letters are significantly different by Tukey's honestly significant difference (HSD) ($p < 0.05$).

Peroxidase (*POD*) gene expression analysis showed a gradual increase in control and PA primed seedlings with increasing Al concentration from 0 to 1.25 mM (Figure 4.4D). *POD* transcript abundance was not significantly ($p > 0.05$) affected by seed priming with PA and 0.5 mM Al treatment. However, *POD* expression increased markedly in seedlings of PA primed seeds following 1.25 mM Al treatment compared to 0.5 mM Al. Similarly, superoxide dismutase (*SOD*) gene expression was not affected by seed priming and 1.25 mM Al treatments (Figure 4.4E). However, *SOD* transcript abundance was significantly ($p < 0.005$) increased by approximately 2-fold in seedlings of PA primed seeds following 0.5 mM Al treatment compared to control seedlings under similar Al treatment. Results for *ARF2A* transcript levels revealed a markedly increase by 3.6-folds in seedlings of PA primed seeds without Al treatment, but was reduced following 0.5 mM Al treatment (Figure 4.4F). The reduction in *ARF2A* expression level with 0.5 mM Al treatment was comparable to the control. The relative expression of *ARF2A* was increased by 2.4-fold in seedlings of PA primed seeds following 1.25 mM Al treatment compared to control seedlings under similar Al treatment (Figure 4.4F).

4.4 DISCUSSION

Improvement in crop productivity and nutrient density in a sustainable way is touted as a major driver for meeting the increased global food demand. Re-purposing of waste such as PA from pyrolysis of plant biomass can be used as biostimulant for sustainable crop production (Gomez-Roldan et al., 2008). This is the first study which examine PA seed priming effect on Al stress mitigation in tomato seedlings. Seed germination begins with water imbibition, which strongly depends on growing media water potential (Bewley et al., 2012). In this study, exposure of tomato seeds to 2:100 PA for 24 h clearly showed an increase in seed germination parameters. This indicates that PA may actually facilitate water uptake and promotes the initiation of metabolic

activities that culminates in early seed germination and radicle emergence as explained by Bewley (1997). Several studies have consistently shown similar results for seed of different crop species treated with PA (Mu et al., 2003; Kulkarni et al., 2006; Van Staden et al., 2006; Grewal et al., 2018; Wang et al., 2019b). PA priming showed slightly improved germination percentage and germination index under Al stress although not significantly different from that of the control and Al alone (Table 4.3), which suggested PA mitigation of Al stress. Some studies have reported that Al had no significant effect on germination rates of tobacco (*Nicotiana tabacum*) (Burklew et al., 2012), lettuce (*Lactuca sativa*) (Silva & Matos, 2016), and *Trifolium* (Bortolin et al., 2020) seeds upon exposure to varying doses of Al.

Additionally, the presence of karrikins in PA plays a significant role in seed germination and seedling growth (Flematti et al., 2004; Van Staden et al., 2006; Gomez-Roldan et al., 2008; Umehara et al., 2008; Dixon et al., 2009). Therefore, this compound could possibly be the key driver for the rapid seed germination of the PA primed tomato 'Scotia' seeds. The chemical composition of PA is complex, which makes it more challenging to fully understand its biostimulatory mechanisms in plants. Apart from karrikins, PA is rich in other organic compounds including organic acids and several derivates of alcohol that could influence seed germination and seedling growth (Grewal et al., 2018). Alcohol has been reported to induce seed germination in several crop species (Miyoshi & Sato, 1997; Salehi et al., 2008). The presence of alcohol and its derivates could play a significant role in tomato seed germination although not investigated in this study. One postulated mechanism of alcohol stimulation of seed germination is its involvement in the activation of the Kreb's cycle and glycolysis for energy generation during seed germination and emergence (Miyoshi & Sato, 1997).

There were significant increases in total hypocotyl and root lengths, root volume, and overall fresh weight of tomato seedlings that were primed with PA compared to the control. This result agrees with previously reported studies by Ghebrehiwot et al. (2008). They reported that priming of *Eragrostis tef* (Zucc.) seeds with 1:500 smoke-water for 48 h increased percentage imbibition, and facilitated seed germination and seedling growth rate. Similarly, wheat seeds primed with 1:900 PA for 72 hr achieved high germination and seedling growth (Wang et al., 2019b). The differences in the reported best PA priming time and PA concentration by the different researchers could be ascribed to variations in crop type and possibly, different chemical compositions of the tested PA (Grewal et al., 2018). Additionally, exposure of the control (i.e., no PA) or PA primed seeds to 0.5 mM Al increased seedling vigour, hypocotyl and root lengths, and total fresh weight compared to growth under the 0 mM Al treatment (Figures 4.1 and 4.2). However, the vigour of PA primed seedlings was increased more than the control seedlings following 1.25 mM Al treatment (Table 4.3). These findings suggested that the 0.5 mM Al treatment stimulated growth of the tomato seedlings whereas the 1.25 mM Al treatment inhibited seedling growth. The finding of this study is similar to previous studies where low Al exposure enhanced crop growth and rice development (Famoso et al., 2011) and corn (*Zea mays*) (Wang et al., 2015d). The increase in seedling growth following 0.5 mM Al treatment with or without PA could also be partly due to the genotypic characteristics of the tomato cultivar. Those plants exhibiting satisfactory development under high Al concentration must have recruited mechanisms to tolerate Al stress, possibly *via* exudation of organic acids or activation of Al stress defence pathways including antioxidants accumulation (Bojórquez-Quintal et al., 2017; Singh et al., 2017). Furthermore, the increase in seedling growth under high Al with PA priming suggested alleviation of toxic effect of Al by the PA. Interestingly,

evidence suggests that smoke could activate enzymes involved in the activation of stored food reserves or alter membrane permeability for easy translocation of growth regulators (Van Staden et al., 1995). Karrikins have been demonstrated to increase nuclei percentage at the circularized chromosome conformation capture (4C) stage in primed tomato seeds (Jain & Van Staden, 2007). This could affect cell division and subsequently resulted in rapid radicle emergence with considerably higher seedling vigour indices and overall fresh weight.

Phytohormones are crucial regulators of plant root growth and development. In the present study, the increased root and hypocotyl growth could likely be due to enhanced auxin levels facilitated by PA priming of the tomato seeds (Figures 4.1D-E; Figure 4.2). Auxin pathway signalling and responses are mediated by numerous auxin response factors (ARF) family of transcription factor and auxin-induced proteins (Aux/IAAs) (Audran-Delalande et al., 2012; Zouine et al., 2014; Kirolinko et al., 2021). Gene expression analysis showed that PA significantly increased *SlARF2A* transcript abundance with or without Al stress (Figure 4.4E). In response to low auxin, Aux/IAA protein interacts with ARF to form heterodimers, thereby repressing auxin-responsive genes. However, at high auxin levels, Aux/IAA proteins are ubiquitinated by the SCF E3 ubiquitin ligase complex and degraded via the 26S proteasome. This releases the ARF repression and results in the activation of ARF-mediated auxin-responsive genes (Guilfoyle & Hagen, 2007; Mockaitis & Estelle, 2008). Interestingly, recent evidence indicates that in tomato seedlings, *SlARF2A* stimulates lateral root growth, and its transcripts abundance are positively modulated by auxin and gibberellic acid (GA), and negatively regulated by ethylene (Ren et al., 2017). Similarly, *SlARF2A* expression was reported in tomato roots, leaves, flowers, and fruits but strongly expressed in leaves, root tips, and lateral root formation sites, suggesting that it might play a critical role in

organ development (Xu et al., 2016b). Although the level of auxin in the seedlings was not examined, it is plausible that the increase in *SlARF2A* expression in seedlings from PA primed with or without Al stress can be ascribed to enhanced auxin levels, which promoted auxin-responsive genes and auxin-dependent phenotypes.

Generally, Al exposure triggers the accumulation of ROS including H_2O_2 in plant cells, which can cause oxidative damage of cellular components including membrane lipids, proteins, and nucleic acids leading to several metabolic alterations (Boscolo et al., 2003; Valadez-González et al., 2007; Yi et al., 2010; Yamamoto, 2019). PA priming decreased ROS content in plants that were not treated with Al, but the exposure of PA primed seeds to Al increased H_2O_2 levels (Figure 4.3A). The H_2O_2 levels of PA primed seeds under 0.5 mM Al were comparable to that of 1.25 mM Al (Figure 4.3), suggesting that PA priming could not reduce H_2O_2 induced by Al stress in tomato plants. During lettuce germination, an increase in H_2O_2 levels was reported to be associated with endosperm cap softening and radical elongation (Zhang et al., 2014b). To some extent, the increase in H_2O_2 could be attributed to the advanced repair of organelles and cell membranes. An increase in ROS accumulation instigates membrane lipids oxidation and production of MDA, which can exacerbate membrane structural damage *via* excessive MDA production (Sharma et al., 2012; Wei et al., 2021b). The result of the present study showed that in the absence of PA priming, MDA content was significantly increased under Al stress (Figure 4.3B). This finding is consistent with previously reported results where exposure of plants to Al stress elicits enhanced MDA accumulation (Surapu et al., 2014; Bortolin et al., 2020; Salazar-Chavarria et al., 2020). Moreover, MDA content was remarkably reduced in PA primed seedlings compared to the control under Al treatment (Figure 4.3B). This could be possibly due to suppression of Al uptake and activation of

antioxidants systems, which aided seedlings from the PA primed seeds to cope with Al-induced oxidative stress damage. This is highly expected as studies on antioxidant properties of phenolic compounds present in PA revealed high ROS-scavenging activities, reducing power, and anti-lipid peroxidation capacity (Loo et al., 2007; Wei et al., 2010). A similar effect of PA on membrane damage was reported in wheat seedlings under drought stress (Wang et al., 2019b). Other studies have reported similar results of membrane damage mitigation with salicylic acid seed priming under Al stress (Surapu et al., 2014; Bortolin et al., 2020).

In response to Al stress, plants have evolved numerous defensive mechanisms including antioxidants and osmolytes to scavenge and/or reduce ROS contents and maintain cellular homeostasis (Gill & Tuteja, 2010). In this study, PA priming had no effect on proline content under normal condition, but it was reduced with the application of 0.5 mM Al and increased upon exposure to 1.25 mM Al compared to the control (Table 4.4). Also, protein content was relatively increased in PA primed seeds under high Al stress and in control plants grown in 0.5 mM Al (Table 4.4). These indicate that 0.5 mM Al was not enough to elicit a stress response in tomato seedlings, and that PA contributes significantly to ameliorating the Al-induced cellular damage. A similar proline accumulation response was observed in tomato and *Trifolium* seedlings subjected to salicylic acid priming, which enhanced osmotic protection against Al stress (Surapu et al., 2014; Bortolin et al., 2020). Proline accumulation contributes to stress tolerance by cellular osmotic adjustment (i.e., maintenance of turgor pressure) and acts as molecular chaperones to protect and stabilize structures of macromolecules and organelles involved in maintaining membrane integrity (Verslues & Sharma, 2010; Silva & Matos, 2016; Pirzadah et al., 2019). It is plausible that the relatively high total protein and proline contents following PA priming may improve water-

holding capacity of cells, and provide protection to stabilize cell membranes from Al-induced damages.

The antioxidant defence system plays a vital role in stress-induced ROS scavenging and detoxification (Gill & Tuteja, 2010; Yang et al., 2016b; Waszczak et al., 2018; Wei et al., 2021b). This defence system constitutes diverse proteins super family including POD, SOD, CAT, GR, and APX1, which act together to improve plant stress tolerance and growth. In the present study, POD activity was significantly increased in PA primed seedlings with or without Al stress (Table 4.4). Increased POD activity in PA primed seedlings was expected as previous studies revealed that the phenolic compounds present in PA enhanced antioxidants activities by scavenging ROS radicals, reducing power and anti-lipid peroxidation capacity (Loo et al., 2007; Wei et al., 2010). Similarly, Wang et al. (2019b) indicated POD activity was enhanced in PA primed wheat seedlings under drought stress, which significantly improved crop growth. Functionally, POD counteracts the effect of stress through strengthening cell wall, mediating signal transduction, and scavenging harmful ROS by converting H_2O_2 accrued under oxidative stress into H_2O (Mittler et al., 2011; Herrero et al., 2013; Waszczak et al., 2018), This is likely the case in seedlings from PA primed seeds under Al stress in the present study. Numerous studies have indicated that POD abundance and activity increased considerably with seed priming in several plants under Al stress (Surapu et al., 2014; Alcantara et al., 2015; Silva & Matos, 2016; Bortolin et al., 2020).

Further gene expression analysis revealed that several genes that modulate antioxidant enzyme activities and are involved in detoxification and ROS scavenging during Al stress were up-regulated in seedlings from PA primed seeds (Figure 4.4). This suggests that PA triggers the

expression of antioxidants genes, which could promote the accumulation of antioxidant enzymes activities. These upregulated genes include *SIGR, SIPOD, SISOD, SICAT,* and *SIAPX1* (Figure 4.4). These genes amply revealed that oxidative stress can be triggered by Al stress, and that ROS scavenging and detoxifying enzymes are crucial for Al tolerance and metabolic adaptation in tomato seedlings. A similar observation showed that PA enhanced antioxidant transcript abundance in primed seedlings under drought stress (Wang et al., 2019b). Interestingly, significant up-regulation of antioxidant genes has also been observed in several seed-primed plants under different stresses including Al (Paul & Roychoudhury, 2017; Aghaee & Rahmani, 2019; Basit et al., 2021; Wiszniewska, 2021). SOD is extremely efficient in eradicating O^{2-} radicals in plants. SOD is converted to H_2O_2 and molecular oxygen. This H_2O_2 is further reduced to H_2O and O_2 by CAT, POD, and APX (Waszczak et al., 2018; Wei et al., 2021b). GR is crucial in maintaining the intracellular glutathione pool by reducing glutathione disulphide (GSSG) to sulphydryl from GSH, which further functions in scavenging ROS radicals (Yousuf et al., 2012). These results further confirmed that PA seed priming eventually ameliorated the general antioxidant defence system to alleviate internal oxidative stress damage under Al stress, and provided a conducive environment for enhanced plant growth and development (Figure 4.5). Besides, the result of this study demonstrates that PA priming has a potential in improving growth and performance of tomato plants under Al stress which could be extended to other major crops. Additionally, this study provides avenue for exploring PA effect on other environment stress that limits crop productions.

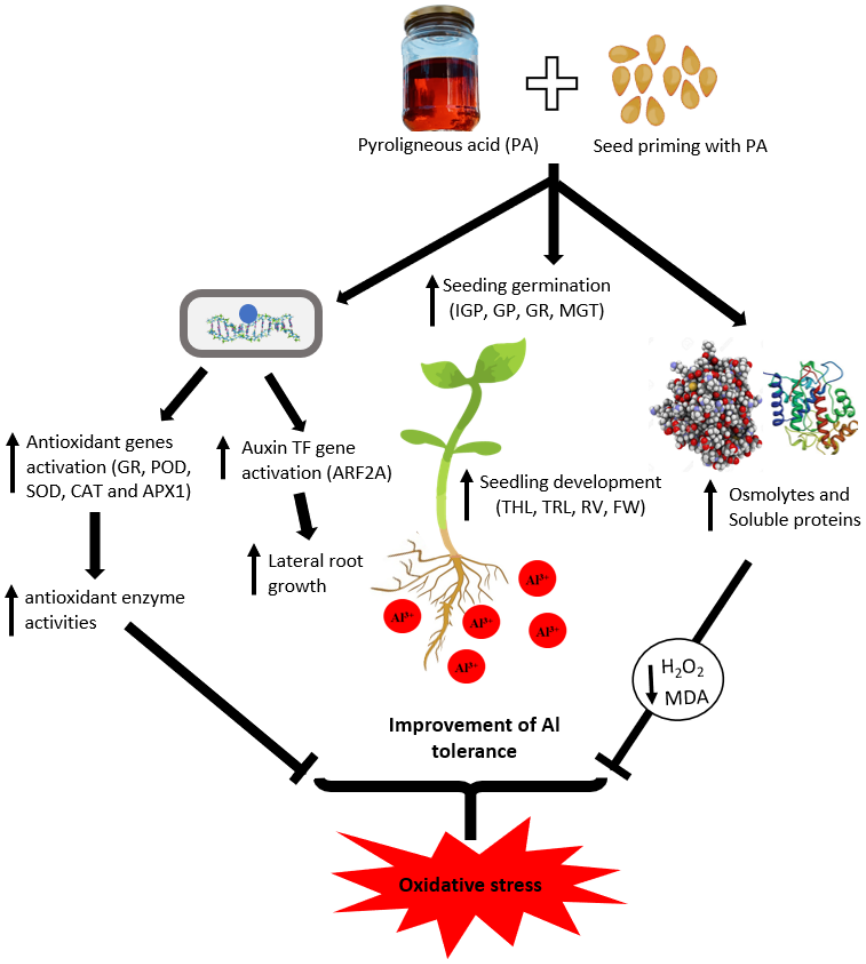

Figure 4.5. Proposed mechanism of seed priming with pyroligneous acid on tomato growth and aluminum (Al) stress mitigation. Priming seed with PA enhances seedling germination under both normal and Al stress condition by stimulating genes involved in antioxidants (*GR, POD, SOD, CAT, APX1*) and auxin response (*ARF2A*) pathways. This facilitates enhanced antioxidant enzyme activities coupled with increased accumulation of osmolytes and soluble proteins, thereby improving Al tolerance and resulting in increased seeding growth and development.

4.5 CONCLUSION

This is the first study examining the effect of PA on growth and Al stress mitigation in tomato seedlings. The result revealed that overall, tomato 'Scotia' seeds primed with 2:100 PA for 24 hr exhibited significant increase in germination indices and growth parameters. Exposure of PA primed seeds to varying Al stress revealed that PA improved germination index and seedling vigour but not germination percentage. Growth characteristics of seedlings from PA primed seeds

were significantly improved under Al stress and revealed better protection mechanisms. PA priming ameliorates the negative effect of Al stress by reducing H_2O_2 and MDA, and enhancing osmotic regulation *via* increased accumulation of proline and soluble proteins in the seedlings. Moreover, PA priming significantly increases antioxidants enzyme activities through induction of *GR*, *POD, SOD, CAT,* and *APX1* transcript abundance under Al stress. Thus, seed priming with PA could be a feasible approach to improve tomato seed germination and crop growth in the presence of Al stress particularly in acidic soils or growth media.

CHAPTER 5: EFFECT OF PYROLIGNEOUS ACID ON THE PRODUCTIVITY AND NUTRITIONAL QUALITY OF GREENHOUSE TOMATO

A version of this chapter has been published in **MDPI Plant Journal**. The citation is:

Ofoe, R., Qin, D., Gunupuru, L. R., Thomas, R. H., & Abbey, L. (2022). Effect of pyroligneous acid on the productivity and nutritional quality of greenhouse tomato. *Plants*, *11*(13), 1650. https://doi.org/10.3390/plants11131650. (Impact factor = 4.5)

5. ABSTRACT

Pyroligneous acid (PA) is a reddish-brown liquid obtained through the condensation of smoke formed during biochar production. PA contains bioactive compounds that can be utilized in agriculture to improve plant productivity and quality of edible parts. In this study, we investigated the biostimulatory effect of varying concentrations of PA (i.e., 0%, 0.25%, 0.5%, 1%, and 2% PA/ddH_2O (*v/v*)) application on tomato (*Solanum lycopersicum* 'Scotia') plant growth and fruit quality under greenhouse condition. Plants treated with 0.25% PA exhibited a significantly ($p < 0.001$) higher sub-stomatal CO_2 concentration and a comparable leaf transpiration rate and stomatal conductance. Total number of fruits was significantly ($p < 0.005$) increased by approximately, 65.6% and 34.4% following application of 0.5% and 0.25% PA, respectively compared to the control. The 0.5% PA enhanced total weight of fruits by approximately, 25.5%; while the 0.25% PA increased the elemental composition of the fruits. However, the highest PA concentration of 2% significantly ($p > 0.05$) reduced plant growth and yield, but significantly ($p <$

0.001) enhanced tomato fruit juice Brix, electrical conductivity, total dissolved solids, and titratable acidity. Additionally, total phenolic and flavonoid contents were significantly ($p < 0.001$) increased by the 2% PA. But the highest carotenoid content was obtained with the 0.5% and 1% PA treatments. Additionally, PA treatment of the tomato plants resulted in a significantly ($p < 0.001$) high total ascorbate content, but reduced fruit peroxidase activity compared to the control. These indicate that PA can potentially be used as a biostimulant for a higher yield and nutritional quality of tomato.

Keywords: *Solanum lycopersicum*; biostimulant; wood vinegar; soil drench; vegetable production; post-harvest quality

5.1 INTRODUCTION

Tomato (*Solanum lycopersicum*) is one of the most cultivated greenhouse vegetable crop worldwide (Gyimah et al., 2020), and is known to be a rich source of health-promoting phytochemicals including carotenoids, phenolics, flavonoids, and ascorbic acid (Chaudhary et al., 2018). These phytochemicals exhibit antioxidants properties, which protect cells against oxidative stress by scavenging reactive oxygen species. Its antioxidant properties are known to induce anticancer, anti-inflammatory, and chemo-preventive effects. Thus, contributing largely to the prevention of chronic diseases such as cardiovascular, cancer, atherosclerosis, and neurodegenerative disorders (Chaudhary et al., 2018; Nowak et al., 2018). The flavour and dietary qualities of food, which strongly influence consumers preference are usually associated with physical characteristics (e.gs, chewability and texture) and chemical composition (pH, ^{o}Brix, elements, carotenoids, phenolics, and flavonoid) (Rodrigues et al., 2020). These properties can be

influenced by growing conditions, environmental factors, and the genetic characteristics of the plant. As a result, current greenhouse producers seek alternative inputs which rely mostly on organic amendments to improve the yield and quality of tomato fruits. One such input is the use of pyroligneous acid (PA) which is a natural and environmentally friendly by-product of pyrolysis of plant biomass (Pan et al., 2015).

During pyrolysis, organic biomass is burnt at a high temperature under the presence of limited oxygen and the gaseous and smoke phase is condensed to produce a liquid smoke (Grewal et al., 2018). The condensed liquid smoke is stabilized by allowing it to stand for six months which results in the formation of wood tar at the bottom, light oil at the top and condensed aqueous translucent PA. This aqueous translucent PA is also known as wood vinegar, bio-oil or liquid smoke (Grewal et al., 2018). PA has a smoky odor and the colour may vary from light yellow to reddish-brown depending on the feedstock (Theapparat et al., 2014). It is a complex mixture containing 80-90% water as a major component and over 200 water-soluble chemical compounds including nitrogen, phenolics, organic acids, sugar derivates, alcohols, and esters (Wei et al., 2010; Grewal et al., 2018; Zheng et al., 2018). The chemical composition of PA mainly depends on the temperature, heating rate, feedstock, and residence time, and has been widely used in diverse areas including agriculture, food and medicine (Cai et al., 2012a; Grewal et al., 2018). Evidence revealed that PA also contains a butenolide, a biologically active compound, that belongs to a new family of phytohormones known as karrikinolide or karrikins (Chiwocha et al., 2009; Dixon et al., 2009). Interestingly, the signaling mechanism and mode of action of karrikins are analogous to that of known phytohormones (Van Staden et al., 2006; Gomez-Roldan et al., 2008; Dixon et al., 2009) suggesting that PA at an appropriate concentration can positively influence plant growth and

productivity. Furthermore, karrikins are thermal resistant, hydrophilic, and long-lasting and therefore, can remain highly potent at a wide range of concentrations. Several studies revealed that karrikins stimulates seed germination and regulate seedling photomorphogenesis by enhancing seedling sensitivity to light (Van Staden et al., 2004; Chiwocha et al., 2009; Dixon et al., 2009; Flematti et al., 2009; Kulkarni et al., 2010; Nelson et al., 2012).

PA is commonly used as a biostimulant to improve plant growth and productivity (Grewal et al., 2018). Depending on the concentration, PA can be used as an antimicrobial agent (Jung, 2007; Mourant et al., 2007), a herbicide (Liu et al., 2021b), a soil enhancer (Lashari et al., 2013), and an insect repellent (Mmojieje & Hornung, 2015) or promote root development (Wang et al., 2019b; Ofoe et al., 2022b) and microbial activities (Steiner et al., 2008) when diluted. Recent studies reported that PA enhances seed germination rate, vegetative and reproductive growth of several plants species (Mungkunkamchao et al., 2013; Grewal et al., 2018; Lei et al., 2018; Shan et al., 2018; Wang et al., 2019b; Ofoe et al., 2022b). However, the concentration of PA applied to promote plant growth varied between studies. For instance, it was reported that the application of 1:500 (v/v) increased tomato yield but did not affect fruit nutritional quality whereas according to Mungkunkamchao et al. (2013), 1:800 PA enhanced the growth and yield of tomato. Similarly, soil drench with 20% PA increased the growth and yield of rockmelon (*Cucumis melo* var. *cantalupensis*) (Zulkarami et al., 2011). These suggest that the effectiveness of PA is dependent on its concentration, type of crop, and mode of application. Generally, the high acidity of PA necessitates its use at low concentrations for plant growth and productivity (Grewal et al., 2018). As such appropriate concentration can contain the right proportions of several bioactive compounds which induce beneficial effects on crop growth and quality (Nelson et al., 2012).

Furthermore, phenolic compounds in PA induce high reactive oxygen species scavenging, reducing power activities and anti-lipid peroxidation capacity (Loo et al., 2007; Wei et al., 2010). However, the chemical composition and individual chemical activities can be influenced by the pyrolytic temperature, as high pyrolytic temperature between 311° - 550°C was demonstrated to exhibit the strongest antioxidant activity (Wei et al., 2010). It was amply demonstrated that high PA concentration increases the availability of phenolics and organic acids that could adversely affect plant growth performance (Loo et al., 2008). All these studies demonstrated the use of PA as a natural biostimulant with high efficacy for crop production but not extensively explored.

Accordingly, most studies on PA efficacy and use in crop production have focused on seed priming and foliar application. There is limited information on the efficacy of drench application on crop yield and especially, on crop quality (Grewal et al., 2018). Additionally, agricultural use of PA in Canada and globally is in its infant stage due to limited studies on its efficacy for growth promotion and that recommended application rate have not been clearly established. The understanding of how PA can regulate plant growth, yield and quality of tomato under greenhouse condition is a crucial necessity not only to growers but also to consumers and researchers. In this study, we investigated the biostimulatory effect of varying concentrations of PA for production and increase in nutritional quality of tomato 'Scotia' under greenhouse condition.

5.2 MATERIALS AND METHODS

5.2.1 Plant material and growing condition

The research was carried out in the greenhouse located in the Department of Plant, Food, and Environmental Sciences, Faculty of Agriculture, Dalhousie University between November 2020

and February 2021 and repeated in March (spring) and July (Summer) 2021. Tomato (*Solanum lycopersicum*) cultivar 'Scotia' seeds were purchased from Halifax Seeds (Halifax, Canada). Seeds were sterilized with 10% sodium hypochlorite (NaClO) for 10 min, and thoroughly washed three times with sterile distilled water (ddH_2O) followed by 70% ethanol sterilization for 5 min, and subsequently washed 5 times with sterile distilled water. The sterilized seeds were germinated in a 32-cell pack containing Pro-Mix® BX (Premier Tech Horticulture, Québec, Canada) and grown for 30 days in a growth chamber with a day/night temperature regime of 25°C, 16/8 h d^{-1} illumination, 300 µmol $m^{-2} \cdot s^{-1}$ light intensity and 70% relative humidity. The seedlings were transplanted at the third to fourth true-leaf stage into 11.35 l-plastic pots containing approximately, 1.5 kg of Pro-Mix® BX peat-based soilless medium. The plants were climate hardened for a week before the first treatment application under greenhouse conditions at 28°C/20°C (day/night cycle) temperature and 70% relative humidity with a 16 h photoperiod. Supplemental lighting was provided by a 600 W HS2000 high-pressure sodium lamp with NAH600.579 ballast (P.L. Light Systems, Beamsville, Canada) throughout the planting duration.

5.2.2 Experimental treatment and design

The five experimental treatments were arranged in a completely randomized design with four replications. The experimental treatments consisted of 0.25%, 0.5%, 1%, and 2% PA, and distilled water was used as a negative control. The PA derived from white pine biomass was obtained from Proton Power Inc (Lenoir City, USA). The company (Proton Power Inc.) produces and sells graphene and biochar and not PA. The PA is a by-product to them. So, this study, which was funded by the federal agency, was to test this by-product for potential commercialization in the future by which time it will be available to purchase. At present, PA samples may be obtained

from Proton Power for only research purposes before it can be available later for purchase. The chemical composition of the PA used in this study is listed in Table S5.1. All the treatments were applied biweekly as a soil drench to field capacity, and water-soluble compound fertilizer nitrogen-phosphorus-potassium (20:20:20) was applied at a 20-day interval. Pots were rearranged weekly on the bench to offset unpredictable occurrences due to variations in the environment. The entire study was repeated twice.

5.2.3 Plant growth and yield components

Plant growth parameters were measured at 50 days after transplanting (DAT). Plant height was measured from the stem collar to the highest leaf tip with a ruler and the stem girth (i.e., diameter of the main stem) was measured at 10 cm from the collar with Vernier calipers (Mastercraft®, Ontario, Canada). Total numbers of flowers and suckers (i.e., branching) were recorded for each treatment. Intracellular carbon dioxide concentration, net photosynthetic rate, and stomatal conductance were determined from the same four fully expanded leaves per plant using LC*i* portable photosynthesis system (ADC BioScientific Ltd., Hoddesdon, UK). Chlorophyll fluorescence indices including maximum quantum efficiency (F_v/F_m) and potential photosynthetic capacity (F_v/F_o) were measured on the same leaves using a Chlorophyll fluorometer (Optical Science, Hudson, NH, USA) (Maxwell & Johnson, 2000). Chlorophyll content was measured on the same leaves using a chlorophyll meter (SPAD 502-plus, Spectrum Technologies, Inc., Aurora, IL). The total fresh weight of the above-ground tissues (i.e., leaves and shoot) was measured with a portable balance (Ohaus navigator®, ITM Instruments Inc., Sainte-Anne-de-Bellevue, QC, Canada) and subsequently oven-dried at 65ºC for 72 h for dry weight determination. Tomato fruit yield, determined as the total fresh weight of ripe fruits per plant per treatment, was recorded using

the XT portable balance. The equatorial and polar diameters of the harvested fruits were measured with the digital Vernier caliper.

5.2.4 Fruit quality and phytochemical analysis

At harvest (75 DAT), seven representative ripe fruits based on size and colour were randomly selected and surface-sterilized with 70% ethanol. The pericarp (containing the epidermis) was excised from the longitudinal part of each fruit using a sterile scalpel blade. The pericarp was immediately frozen in liquid nitrogen and stored in a -80ºC freezer while the remaining fruits were frozen at -20ºC until further analysis. All frozen fruits were thawed at room temperature and fruit total soluble solids (TSS) were determined using a handheld refractometer (Atago, Japan). Briefly, ripe fruits were cut, placed in a clear Ziploc bag and hand squashed. The juice was poured into a 50 mL beaker and 500 µL was used for TSS determination expressed as degree Brix (ºBrix). Fruit juice qualities including pH, salinity, total dissolved solids (TDS), and electrical conductivity (EC) were determined with a multi-purpose pH meter (C 500 ExStik II S/N 252957, EXTECH Instrument, Nashua, New Hampshire, USA). For titratable acidity, 10 mL of juice from each treatment was diluted in 50 ml distilled water, and titratable acidity was determined at an endpoint of pH 8.1 with 0.1 N sodium hydroxide (NaOH). The mean titratable acidity was expressed in citric acid percentage (Gyimah et al., 2020). The elemental composition of the fruits was determined at the Nova Scotia Department of Agriculture Laboratory Services, Truro, using inductively coupled plasma mass spectrometry (PerkinElmer 2100DV, Wellesley, Massachusetts, USA) (Donohue et al., 1992).

5.2.4.1 Fruit carotenoid content

Fruit carotenoid content was determined as described by Lichtenthaler (1987). Briefly, 0.2 g of ground fruit pericarp was homogenized in 2 mL of 80% acetone. The homogenate was centrifuged at 15000 g for 15 min and the absorbance of the supernatant was measured at 646.8, 663.2, and 470 nm using a UV-Vis spectrophotometer with 80% acetone alone as the blank. Total carotenoid content was expressed as μg g^{-1} fresh weight (FW) of the sample.

5.2.4.2 Total ascorbate content

Total ascorbate was measured following the method described by Ma et al. (2008) with little modification. Approximately, 0.2 g of ground fruit pericarp was homogenized in 1.5 mL ice-cold freshly prepared 5% trichloroacetic acid (TCA). The mixture was vortexed for 2 min and centrifuged at 12000 *g* for 10 min at 4ºC. 100 μL of the supernatant was transferred into a new tube and 400 μL phosphate buffer (150 mM potassium dihydrogen phosphate (KH_2PO_4) (pH 7.4), 5 mM Ethylenediaminetetraacetic acid (EDTA)) was added. 100 μl of 10 mM Dithiothreitol (DTT) was added and vortexed for 30 s. A reaction mixture containing 400 μL of 10% (w/v) Trichloroacetic acid (TCA), 400 μL of 44% orthophosphoric acid, 400 μL of 4% (w/v) α- α 1 - dipyridyl in 70% ethanol and 200 μL of 30 g/L ferric chloride ($FeCl_3$) was added to obtain colour. The mixture was incubated at 40ºC for 60 min in a shaking incubator and the absorbance was measured at 525 nm. The total ascorbate content was determined using a standard L-ascorbic acid curve and expressed as μmol g^{-1} FW.

5.2.4.3. Soluble sugar content

Total sugar content of the tomato fruits was estimated following the phenol-sulphuric acid method described by Dubois et al. (1956). 0.2 g of ground fruit pericarp was homogenized in 10 mL of 90% ethanol and the mixture was incubated in a water bath at 60°C for 60 min. The final volume of the mixture was adjusted to 5 mL with 90% ethanol and centrifuged at 12000 rpm for 3 min. An aliquot of 1 mL was transferred into a thick-walled glass test tube containing 1 mL of 5% phenol and mixed thoroughly. 5 mL of concentrated sulphuric acid was added to the reaction mixture, vortexed for 20 s, and incubated in the dark for 15 min. The mixture was cooled to room temperature and the absorbance was measured at 490 nm against a blank. Total sugar was calculated using a standard sugar curve and expressed as µg of glucose g^{-1} FW.

5.2.4.4. Total phenolics content

Total phenolics content (TPC) was determined by the Folin-Ciocalteu assay described by Ainsworth and Gillespie (2007) with little modification. 0.2 g of ground fruit pericarp was homogenized in 1.5 mL of ice-cold 95% methanol and incubated in the dark at room temperature for 48 h. The mixture was centrifuged at 13000 *g* for 5 min before mixing 100 µL of the supernatant to 200 µL of 10% (v/v) Folin-Ciocalteau reagent. The mixture was vortexed for 5 min, mixed with 800 µL 700 mM Na_2CO_3, and incubated in the dark at room temperature for 2 h. The absorbance of the supernatant was measured at 765 nm against a blank. TPC was calculated using a gallic acid standard curve and expressed as mg gallic acid equivalents per g FW (mg GAE g^{-1} FW).

5.2.4.5. Total flavonoid content

Total flavonoid was estimated following the colorimetric method described by Chang et al. (2002). 0.2 g of ground fruit pericarp was homogenized in 1.5 mL of ice-cold 95% methanol followed by centrifugation at 15000 *g* for 10 min. 500 µL of supernatant was added to a reaction mixture containing 1.5 mL of 95% methanol, 0.1 mL of 10% aluminum chloride ($AlCl_3$), 0.1 mL of 1 M potassium acetate, and 2.8 mL distilled water. The mixture was incubated at room temperature for 30 min and the absorbance was measured at 415 nm against a blank lacking $AlCl_3$. Total flavonoid content was estimated using quercetin equivalents and expressed as percentage flavonoid using the formula:

$$\text{Total flavonoid} = \frac{([\text{flavonoids}](\mu g/mL) \times \text{total volume of methanolic extract } (mL))}{\text{mass of extract } (g)}$$

5.2.4.6. Protein content and peroxidase activity

For protein content and antioxidant enzyme activity**,** approximately 0.2 g of ground sample was homogenized in 3 mL ice-cold extraction buffer (50 mM potassium phosphate buffer (pH 7.0), 1% polyvinylpyrrolidone, and 0.1 mM EDTA). The homogenate was centrifuged at 15000 *g* for 20 min at 4ºC. The supernatant (crude enzyme extract) was transferred to a new microfuge tube on ice and the protein content was measured at 595 nm after 5 min of mixing with Bradford's reagent (Bradford, 1976). The protein content was estimated from a standard curve of bovine serum albumin (200-900 µg mL^{-1}). Peroxidase (POD, EC 1.11.1.7) activity was determined using Pyrogallol as substrate according to Chance and Maehly (1955) with little modification. The reaction mixture consisted of 100 mM potassium-phosphate buffer (pH 6.0), 5% pyrogallol, 0.5 % H_2O_2 and 100 µL of crude enzyme extract. Following reaction mixture incubation at 25ºC for 5 min, 1 mL of 2.5 N H_2SO_4 was added to stop the reaction and the absorbance was read at 420 nm

against a blank (ddH_2O). One unit of POD forms 1 mg of purpurogallin from pyrogallol in 20 s at pH 6.0 at 20°C.

5.2.5. Statistical analysis

All data obtained were subjected to one-way analysis of variance (ANOVA) with the averages of the two experiments (four replications in each experiment) using Minitab statistical software version 20 (Minitab Inc., State College, PA, USA). Treatment means were compared using Fisher's least significant difference (LSD) post hoc test at $p \leq 0.05$. Pearson correlation analysis was performed using XLSTAT version 19.1 (Addinsoft, New York, USA).

5.3 RESULTS

5.3.1 PA chemical composition

The chemical composition of PA is presented in supplementary Table S5.1. The most significant elements were nitrate and nitrite, calcium and potassium. Significant amounts of organic acids (i.e., salicylic acid, oxalic acid, propionic acid, and malic acid) and small amounts of shikimic acid and acylcarnithines were also present.

5.3.2 Morpho-physiological response

PA application had no significant ($p > 0.05$) effect on plant height, stem diameter, and number of branches and flowers (Table 5.1). Plant height non-significantly increased slightly with low PA concentrations i.e., 0.25% and 0.5% PA by *ca.* 5% compared to the control. The highest stem diameter was recorded with 0.25% PA followed by 2% PA but not statistically different from other treatments. Additionally, plants treated with 0.5% PA increased numbers of branches and flowers

by 13% and 8% respectively compared to that of the control although they were not statistically different ($p > 0.05$). Similarly, PA treatments had no significant ($p > 0.05$) effect on F_v/F_m, F_v/F_o, and chlorophyll content (Table 5.2). The effect of PA on F_v/F_m and F_v/F_o was comparable to the control. Likewise, PA had no significant ($p > 0.05$) effect on leaf intracellular CO_2 and photosynthetic rate (Table 5.2). However, leaf transpiration rate, sub-stomatal CO_2, and stomatal conductance were significantly ($p < 0.001$) reduced by PA compared to the control. Plants treated with 0.25% and 0.5% PA showed significant ($p < 0.001$) reductions of these physiological characteristics except for sub-stomatal CO_2, which was increased by 3% with 0.25% PA compared to the control. On the other hand, plants treated with the 1% and 2% PA exhibited significant ($p < 0.001$) reductions in leaf transpiration rate, sub-stomatal CO_2, and stomatal conductance compared to the other PA treatments. The application of 0.25% PA increased above-ground fresh weight but similar to the control (Figure 5.1A). However, tomato plants treated with 0.5% and 1% PA reduced the above-ground fresh weight by 13% compared to the control. The above-ground dry weight of the tomato plant treated with 0.25% PA was significantly ($p < 0.005$) increased by *ca*. 11% compared to the control (Figure 5.1B). In contrast, the 0.5% and 1% PA reduced the above-ground plant dry weight but was not statistically ($p > 0.05$) different from those of the control and the 2% PA treatment.

Table 5.1. Morphological response of tomato 'Scotia' plants treated with pyroligneous acid (PA).

Treatment	Plant height (cm)	Stem diameter (mm)	Branch number	Flower number
Control	57.82 ± 2.86a	9.60 ± 0.80a	6.52 ± 0.58a	33.50 ± 7.23a
0.25% PA	60.50 ± 5.79a	10.02 ± 0.61a	5.81 ± 0.96 a	27.25 ± 7.80a
0.5% PA	60.62 ± 5.23a	9.32 ± 0.77a	7.04 ± 0.82a	38.00 ± 8.41a
1% PA	57.71 ± 6.40a	9.51 ± 0.92a	5.70 ± 1.73a	31.00 ± 11.86a
2% PA	56.07 ± 2.97a	9.81 ± 0.49a	6.38 ± 1.50a	32.25 ± 11.41a
p-value	0.565	0.689	0.480	0.622

Values are means ± SD of four replicates and different letters indicates significant ($p < 0.05$) difference according to Fisher least significant difference (LSD).

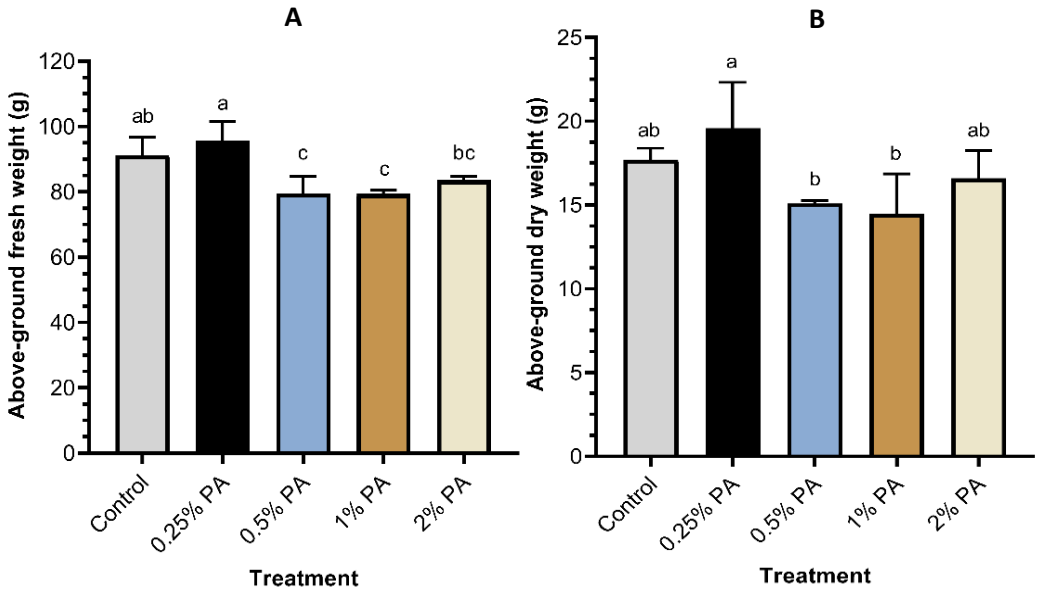

Figure 5.1. Pyroligneous acid effect on tomato plant above-ground biomass. (A) fresh weight (B) dry weight. Values are means ± SD of four replicates and different letters indicate significant ($p < 0.05$) difference according to Fisher least significant difference (LSD). Error bars show standard deviations.

5.3.3 Fruit yield and quality

The 0.5% PA treatment increased the total fruit weight by *ca*. 26% although not significantly different from that of the 0.25% PA and the control (Figure 5.2A). However, the 2% PA had a

significant reduction in total fruit weight, which is not different from that of the 1% PA treated plants. Similarly, the number of fruits was significantly ($p < 0.005$) increased by *ca*. 66% and *ca*. 34% by the 0.5% and the 0.25% PA respectively, compared to the control (Figure 5.2B). Nevertheless, the application of the 2% PA and the control reduced the number of fruits compared to the other PA treatments. Fruit morphological characteristics including polar (Figure 5.2C) and equatorial diameters (Figure 5.2D) were not significantly ($p > 0.05$) affected by PA.

Table 5.2. Physiological response of tomato 'Scotia' plants treated with pyroligneous acid (PA).

Treatment	F_v/F_o	F_v/F_m	SPAD	Intracellular CO_2 (µmol mol $^{-1}$)	A (µmol m^{-2} s^{-1})	E (mol m^{-2} s^{-1})	Ci (µmol mol $^{-1}$)	g_s (mol m^{-2} s^{-1})
Control	4.16 ± 0.41a	0.80 ± 0.01a	34.14 ± 5.80a	410.56 ± 6.13a	2.15 ± 0.60a	2.53 ± 0.52a	360.70 ± 30.46ab	0.11 ± 0.02a
0.25% PA	4.06 ± 0.27a	0.81 ± 0.01a	36.59 ± 3.74a	417.74 ± 8.72a	1.80 ± 0.84a	2.16 ± 0.60ab	370.27 ± 19.04a	0.09 ± 0.01ab
0.5% PA	3.96 ± 0.33a	0.80 ± 0.01a	34.07 ± 2.96a	410.85 ± 6.61a	2.19 ± 0.80a	1.95 ± 0.71b	343.01 ± 35.68bc	0.08 ± 0.03b
1% PA	4.07 ± 0.34a	0.80 ± 0.01a	35.57 ± 5.14a	413.55 ± 13.84a	1.80 ± 0.79a	1.28 ± 1.03c	325.23 ± 42.80c	0.05 ± 0.04c
2% PA	3.91 ± 0.24a	0.80 ± 0.01a	37.13 ± 6.32a	415.68 ± 14.65a	1.84 ± 1.38a	1.35 ± 0.59c	332.50 ± 41.80c	0.05 ± 0.04c
p-value	0.196	0.188	0.262	0.226	0.534	<0.001	<0.001	<0.001

A, photosynthetic rate; E, transpiration rate; g_s, stomatal conductance; Ci, Sub-stomatal CO_2. Values are means ± SD of four replicates and different letters indicates significant ($p < 0.05$) difference according to Fisher least significant difference (LSD).

Tomato fruit juice pH, °Brix, salinity, electric conductivity (EC), total dissolved solids (TDS) and titratable acidity (TA) were significantly ($p < 0.001$) affected by PA (Table 5.3). Juice pH was significantly ($p < 0.001$) increased by 3.3% and 1.3% following application of 0.25% and 0.5% PA to the plants, respectively compared to the control. An increase in PA concentration from 1% to 2% did not alter fruit juice pH. °Brix content of the fruits was increased by *ca*. 13% following application of 2% PA compared to the control (Table 5.3). However, °Brix content was significantly ($p < 0.001$) reduced in fruits following application of the 0.25% PA by 45% compared to the control.

Table 5.3. Chemical quality of tomato 'Scotia' fruits from plants treated with pyroligneous acid (PA).

Treatment	Juice pH	°Brix	Salinity (g L^{-1})	EC (mS)	TDS (g L^{-1})	TA (% citric acid)
Control	3.60 ± 0.04c	5.67 ± 0.05b	2.95 ± 0.02b	5.42 ± 0.03b	3.80 ± 0.01b	0.26 ± 0.01b
0.25% PA	3.72 ± 0.01a	3.12 ± 0.05d	1.66 ± 0.02e	3.11 ± 0.08e	2.20 ± 0.02e	0.23 ± 0.03c
0.5% PA	3.67 ± 0.01b	5.62 ± 0.13b	2.68 ± 0.03c	5.01 ± 0.07c	3.44 ± 0.07c	0.24 ± 0.01bc
1% PA	3.62 ± 0.03c	5.20 ± 0.14c	2.50 ± 0.03d	4.65 ± 0.04d	3.22 ± 0.02d	0.23 ± 0.01bc
2% PA	3.62 ± 0.03c	6.42 ± 0.10a	3.01 ± 0.03a	5.71 ± 0.04a	3.94 ± 0.04a	0.36 ± 0.01a
***p*-value**	<0.001	<0.001	<0.001	<0.001	<0.001	<0.001

EC, electrical conductivity; TDS, total dissolved solids; TA; titratable acidity. Values are means ± SD of four replicates and different letters indicates significant ($p < 0.05$) difference according to Fisher least significant difference (LSD).

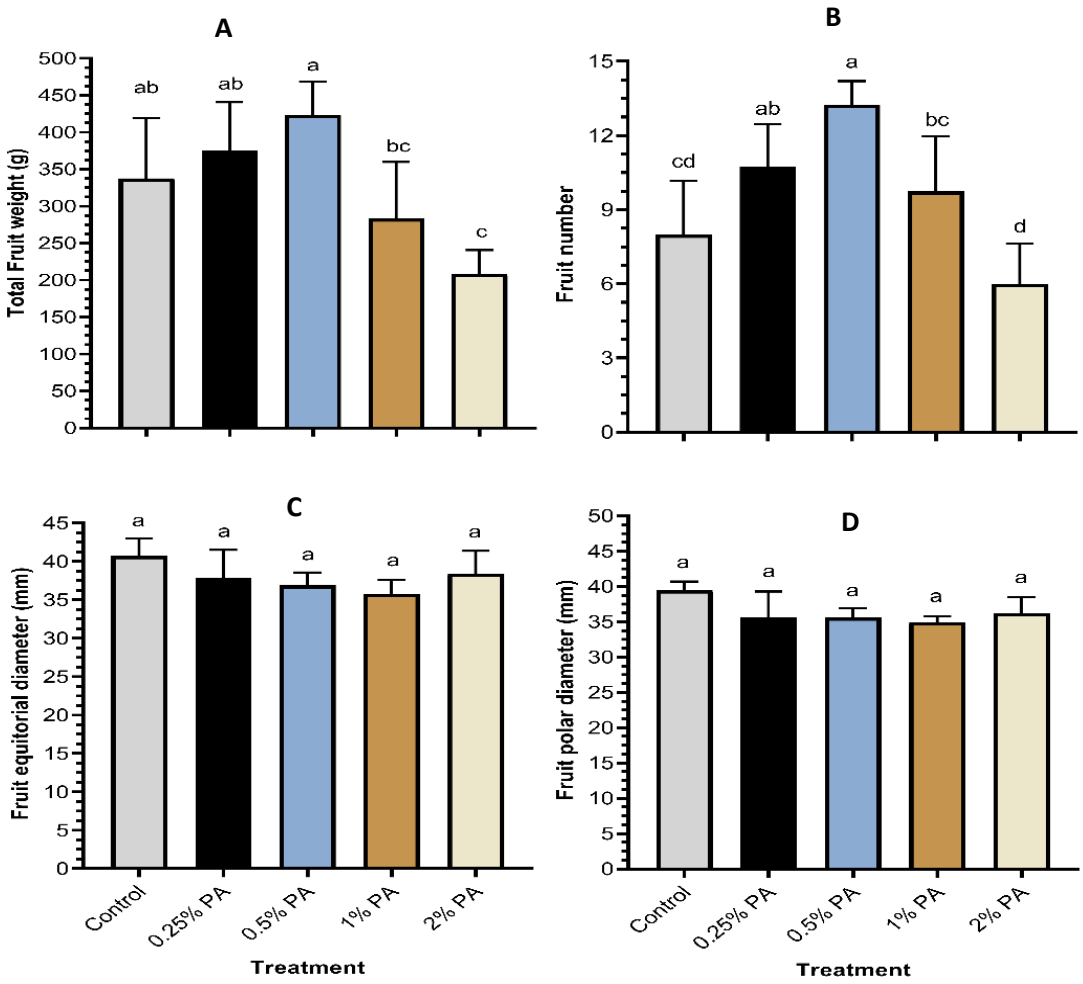

Figure 5. 2. Fruit yield of tomato 'Scotia' in response to pyroligneous acid treatment. (A) Total fruit weight (B) fruit number (C) fruit polar diameter (D) fruit equatorial diameter. Values are means ± SD of four replicates and different letters indicate significant ($p < 0.05$) difference according to Fisher least significant difference (LSD). Error bars show standard deviations.

A significantly ($p < 0.001$) high fruit juice salinity was noticed with the 2% PA treatment compared to the control, while the 0.25% PA recorded the least salinity (Table 5.3). A considerable increase in fruit electrical conductivity was recorded with the 2% PA, while the least PA of 0.25% reduced fruit juice electrical conductivity. Likewise, the 2% PA recorded the highest fruit juice total dissolved solids (Table 5.3). Moreover, fruit titratable acidity was significantly ($p < 0.001$) increased by *ca*. 39% upon application of 2% PA compared to the control (Table 5.3).

Nevertheless, the 0.25% PA had a significant ($p < 0.001$) reduction on fruit TA, which was not different from those of 0.5% PA and 1% PA treatments.

5.3.4 Fruit biochemicals and peroxidase activities

Carotenoid was significantly ($p < 0.05$) increased by the 0.5% PA and 1% PA by *ca*. 20% and 22% respectively, compared to that of the control (Figure 5.3A). The carotenoid contents of the 0.5% and 1% PA fruits were not statistically ($p > 0.05$) different from that of the 2% PA; while the carotenoid content of the 0.25% PA fruits was low and comparable to the control. Tomato fruit total phenolics (Figure 5.3B) and flavonoid were significantly ($p < 0.001$) influenced with PA (Figures 5.3C). The application of 2% PA exhibited a considerably higher fruit total phenolic compounds (*ca*. 23%) and flavonoid content (*ca*. 39%) compared to the control. The 0.5% PA reduced fruit TPC and flavonoid contents. Total ascorbate was increased by *ca*. 377%, *ca*. 177%, *ca*. 165% and *ca*. 129% following application of 2%, 0.25%, 1% and 0.5% PA respectively, compared to the control (Figure 5.3D). Although 0.5% PA had the highest impact on total fruit protein, it was not statistically ($p > 0.05$) different from those of the 0.25% PA and the control treatments (Figure 3E). However, the 2% PA significantly ($p < 0.001$) reduced total fruit protein content compared to the control. Furthermore, PA caused a significant ($p < 0.001$) reduction in total fruit sugar content (Figure 5.3F). The 1% PA treated plants exhibited the least total fruit sugar content, while the 2% PA slightly increased total fruit sugar but was approximately 4.8% lower than that of the control. Furthermore, PA application exhibited a significant ($p < 0.001$) reduction in fruit peroxidase activity (Figure 5.4). The reduction in peroxidase activity was more obvious in the 0.25% PA fruits followed by the 1% PA and the 2% PA fruits.

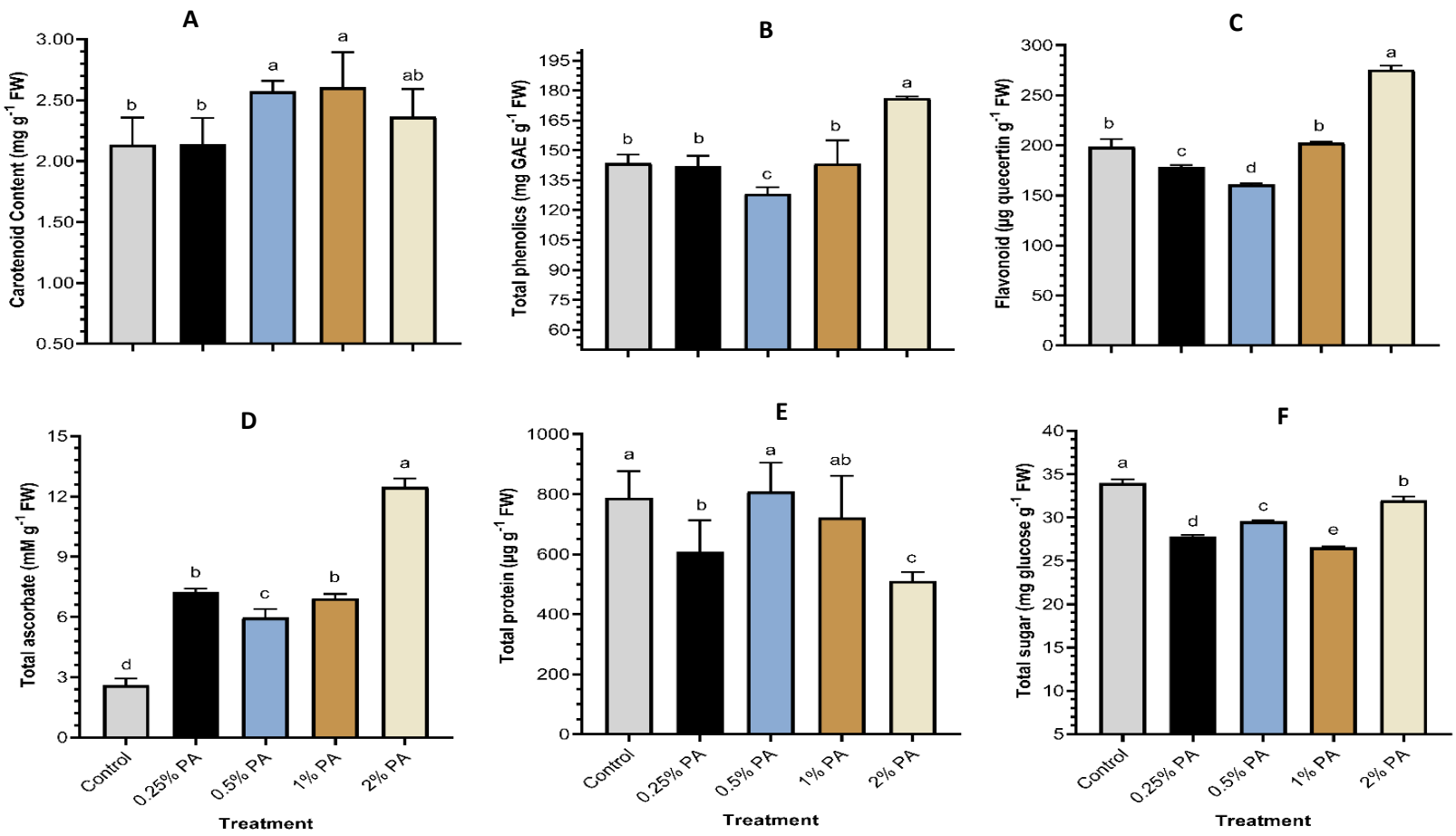

Figure 5.3. Tomato 'Scotia' fruit biochemical content in response to pyroligneous acid treatment. (A) Carotenoid content (B) Total phenolic content (C) Flavonoid content (D) Total ascorbate content (E) Total protein content (F) total sugar content. Values are means ± SD of four replicates and different letters indicate significant ($p < 0.05$) difference according to Fisher least significant difference (LSD). Error bars show standard deviations.

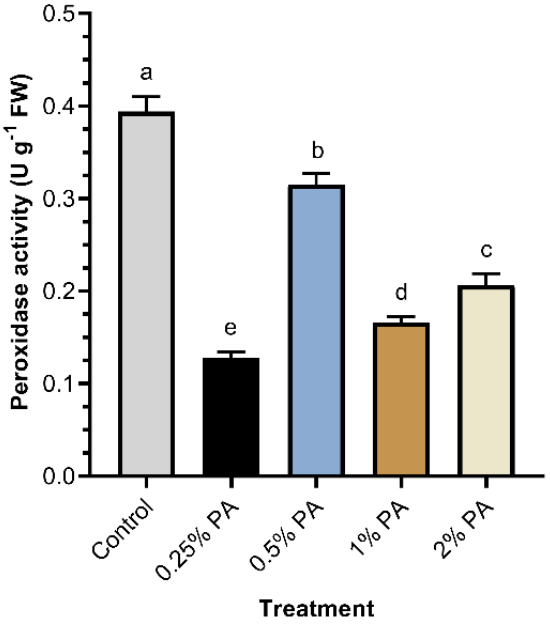

Figure 5.4. Peroxidase activity of tomato 'Scotia' fruit in response to pyroligneous acid treatment. Values are means ± SD of four replicates and different letters indicate significant ($p < 0.05$) difference according to Fisher least significant difference (LSD). Error bars show standard deviations.

5.3.5 Fruit elemental composition

Tomato 'Scotia' fruit N content was increased by ca. 10% upon plant application with the 0.25% PA compared to the control but was reduced by the 0.5% PA (Table 5.4). Fruit Ca was markedly increased by *ca*. 29% upon plant treatment with the 1% PA, but was reduced by the 0.5% PA. Generally, PA had no effect on fruit K compared to the control. However, fruit Mg was increased by *ca*. 13% with the 0.25% PA but was reduced by *ca*. 12% with the 0.5% PA compared to the control. Fruit P content was increased slightly by the 2% PA, which was similar to the effect of the 0.25% PA, but was reduced by the 0.5% PA. Fruit Na content increased by *ca*. 59% following the application of 1% PA compared to the control, but was reduced by the 0.5% PA. Variation in PA concentration did not change fruit B content. Overall, Fe, Zn, Mn and Cu, contents were

increased with the application of 0.25% PA by *ca*. 8%, *ca*. 8%, *ca*. 9% and *ca*. 15%, respectively compared to the control. However, the 0.5% PA markedly reduced these four elements in the fruits.

Table 5.4. Tomato 'Scotia' fruit elemental composition in response to pyroligneous acid (PA) treatments.

Element	Treatment						
	Control	**0.25% PA**	0.5% PA	1% PA	2% PA	Mean	CV (%)
Nitrogen (N %)	1.68	**1.84**	1.44	1.61	1.56	1.63	9.12
Calcium (Ca %)	0.24	0.29	0.23	0.31	0.28	0.27	12.39
Potassium (K %)	2.68	2.27	2.67	2.32	2.59	2.51	7.91
Magnesium (Mg %)	0.17	0.19	0.15	0.17	0.17	0.17	8.21
Phosphorus (P %)	0.44	0.46	0.41	0.42	0.47	0.44	5.60
Sodium (Na %)	0.02	0.03	0.02	0.04	0.02	0.02	26.28
Boron (B mg L^{-1})	12.61	13.61	12.59	13.91	13.62	13.27	4.69
Copper (Cu mg L^{-1})	7.51	8.86	5.98	6.53	7.02	7.18	15.29
Iron (Fe mg L^{-1})	42.46	49.87	40.08	43.37	45.00	44.16	8.28
Manganese (Mn mg L^{-1})	26.14	28.37	22.58	27.49	25.06	25.93	8.71
Zinc (Zn mg L^{-1})	14.81	17.71	14.80	14.68	16.25	15.65	8.44

CV = coefficient of variation.

5.3.6. Association between morpho-physiological properties of tomato plants and productivity and quality in response to PA application

Pearson correlation coefficients (r) was used to further assess the association amongst the morpho-physiological, yield and quality of tomato plants in response to PA application (Table S5.2). The PCA biplot showed a projection of response variables in the factor spaces and explained 68.93% of the total variations in the data set. The results revealed that the number of suckers had a significantly ($p < 0.05$) stronger positive correlation with number of flowers (r=0.903) and fruit K content (r = 0.914), while SPAD had a significantly ($p < 0.05$) stronger positive association with

leaf intracellular CO_2 content (r = 0.927) and a negative correlation with photosynthetic rate (r = -0.891). Similarly, leaf transpiration had a significantly ($p < 0.05$) strong positive correlation with sub-stomatal CO_2 content (r = 0.888) and stomatal conductance (r = 0.996) and moderate association with photosynthetic rate (r = 0.608) and total fruit weight (r = 0.651) although this was not statistically significant. Total fruit weight exhibited a significant ($p < 0.05$) and strong positive correlation with plant height (r = 0.943) and fruit number (r = 0.887). However, it had a significantly ($p < 0.05$) strong negative interaction with total phenolics (r = -0.915) and flavonoid content (r = -0.953). Also, fruit number has similar association with plant height (r = 0.915), total phenolics (r = -0.897) and flavonoid content (r = -0.906). Fruit salinity content showed a significantly ($p < 0.05$) strong positive correlation with EC (r = 0.998), TDS (r = 0.999) and Brix (r = 0.979), and a negative association with pH (r = -0.864).

5.4 DISCUSSION

Current crop production practices make use of natural products that can boost plant growth and the desirable dietary and nutritional quality without compromising the environment and agroecological production systems. Therefore, the functional properties of various natural materials such as PA has recently attracted the interest of farmers and researchers. In this study, although drench application of PA had no statistically significant effect on tomato 'Scotia' plant morphological parameters, they were slightly increased by 0.25% and 0.5% PA concentrations. These results agree with other studies where foliar application of PA influenced the morphological growth of several plant species including tomato (Mungkunkamchao et al., 2013), soybean (Travero & Mihara, 2016), rockmelon (Zulkarami et al., 2011), and rapeseed (Zhu et al., 2021b). The discovery of karrikins in PA has revolutionized its use in crop production because its

signalling and biophysiological activities in plants mimic that of known phytohormones (Van Staden et al., 2004; Chiwocha et al., 2009; Dixon et al., 2009; Flematti et al., 2009). Moreover, karrikins have been demonstrated to stimulate seed germination and plant growth (Chiwocha et al., 2009; Kulkarni et al., 2010). Hence, the increase in plant growth although not significant, can be ascribed to the presence of karrikins. The increase in plant growth with PA treatment was reflected in the above-ground fresh and dry weights, which can be attributed to increased nutrient uptake and promotion of cell division and elongation (Mungkunkamchao et al., 2013).

Stomatal conductance and transpiration rate play a pivotal role in thermoregulation and photosynthesis (Tuzet et al., 2003; Urban et al., 2017). It was demonstrated that PA and other biostimulant affects stomatal conductance in plants under both stress and non-stress conditions (Francesca et al., 2021; Zhu et al., 2021b). We observed that lower concentrations of PA i.e., 0.25% or 0.5% PA exhibited a comparable stomatal conductance and leaf transpiration effect while higher PA concentrations i.e., > 1% reduced these parameters drastically. A reduction in stomatal conductance is an adaptive strategy used by plants to minimize water loss during water-deficit and other related climatic stress conditions. This scenario adversely affect CO_2 diffusion and net photosynthesis (Hasanuzzaman et al., 2021). Although in the present study photosynthesis rate was not affected by PA treatment, we surmised that the reduction in stomatal conductance with PA treatment could be due to adaptive thermoregulation of the photosynthesis system and stress mitigation mechanism (Urban et al., 2017), which will require further investigation.

Plant productivity (i.e., total number of fruits and yield) were increased with PA application as widely reported by many authors (Kulkarni et al., 2010; Zulkarami et al., 2011; Mungkunkamchao

et al., 2013; Zhu et al., 2021b). The composition of PA is complex and consists of numerous bioactive compounds including organic acids, phenolics, alcohol, alkane, and ester (Kulkarni et al., 2010; Zhu et al., 2021b). This suggests that plants with varying genotypic characteristics will respond differently to PA application. In the present study, an increase in the number of tomato fruits and fruit yield were observed with the application of 0.5% PA. The application of 0.5% and 0.25% PA may be considered less toxic to root systems and may promote root growth and thereby, enhancing plant nutrient uptake and utilization (Ofoe et al., 2022b). Although data on trusses number were not considered, the increase in fruit number in plants treated with lower PA concentrations could suggests that fruit setting was higher in low PA-treated plants compared to those treated with higher PA concentrations. This was reflected in the correlation analyses where total fruit weight had a strong association with fruit number. From the farmers perspective, a slight increase in total fruit yield is considered significant improvement to the overall cashflow. Furthermore, the chemical components of PA might have interacted with and stimulated the activities of various phytohormones including gibberellin, cytokinin, auxin, and various enzymes to enhance plant growth and development as previously reported (Zhu et al., 2021b).

Interestingly, determinants of fruit quality such as $^{\circ}$Brix, titratable acidity, flavonoid, phenolics, and ascorbate were increased by the 2% PA. This suggests that PA could be used to enhance crop quality for human health and nutritional purposes. These results are inconsistent with the report by Kulkarni et al. (2008). The discrepancies may be due to differences in the tested concentration, time of application, and tomato variety. Generally, tomato fruits are considered an excellent source of phytochemicals including phenolics, flavonoids, and ascorbates, which exhibit high antioxidant properties by scavenging reactive oxygen species (ROS) radicals (Chaudhary et al., 2018). Studies

demonstrated that higher PA concentration increases the availability of phenolics and organic acids that could affect plant growth (Loo et al., 2008). Thus, the increased tomato fruits antioxidants in the present study was highly expected since previous studies have demonstrated that phenolic compound in PA exhibited high ROS-scavenging activities, reducing power, and anti-lipid peroxidation capacity (Loo et al., 2007; Wei et al., 2010).

Accordingly, the present finding may be attributed to the increased phenolics and organic acids as reported in *Citrus limon* (Rouina et al., 2009) and *Olea europaea* (Pedrero et al., 2012). The ROS-scavenging abilities of these phytochemicals protect cells against oxidative stress, which are crucial for preventing chronic diseases including cancers, atherosclerosis, and inflammation disorders (Das & Roychoudhury, 2014; Chaudhary et al., 2018; Nowak et al., 2018). Moreover, fruit carotenoids are lipophilic pigments essential for human health (Young & Lowe, 2018). Carotenoid content was higher in fruits harvested from plants that were treated with 0.5% and 1% PA compared to the control. This beneficial effect of PA can be attributed to the activation of pathways involved in N metabolism (Ertani et al., 2014). Furthermore, most plants adapt to stress conditions by accumulating these compounds, which ultimately enhances fruit dietary and nutritional quality. For instance, salinity stress increase TDS, sugar, and antioxidant compounds in tomato fruits (Yin et al., 2010; Li et al., 2019). Hence, it is plausible that although the 2% PA did not alter the growth of the tomato plants, it stimulated the plants to accumulate these phytochemicals in the fruits.

Mineral elements represent a minute fraction of the fruit dry matter content but constitute a vital component of the quality and nutritional profile of vegetables (Abou Chehade et al., 2018). The

present study demonstrated that the application of 0.25% PA enhanced tomato fruit N, Mg, P, and all the analyzed micronutrients except B. Also, the 1% PA increased Ca and Na in the tomato fruits. Some possible explanations could be (1) PA increased the uptake and translocation of mineral elements due to enhanced root growth and root functional activities (Wang et al., 2019b); (2) PA activated and promoted the expression of transporter genes in root cells for efficient nutrient element transport (not determined); and (3) some bioactive compounds in PA intensified the sink effect resulting in continuous flow and accumulation of these elements (Calvo et al., 2014; Zhu et al., 2021b). Therefore, it can be suggested that the optimal application rate of PA for enhancing tomato fruit elemental composition may range between 0.25% and 1% PA. Similar observations were made following application of other biostimulants that enhanced the elemental composition of numerous crops including tomato (Abou Chehade et al., 2018; Caruso et al., 2019) and eggplant (Alicja et al., 2019). Therefore, increased yield and dietary and nutrition quality of tomato can be obtained when the appropriate concentration of PA is applied in a greenhouse production system.

5.5 CONCLUSION

In conclusion, drench application of low PA concentrations of 0.25% and 0.5% increases the morpho-physiological response of tomato plants. Overall, the application of 0.5% PA enhances the number of fruits and yield of tomato but reduces the quality of the fruits. Alternatively, application of 0.25% PA will increase elemental composition of tomato fruits. Additionally, drench application of 2% PA can be considered stressful to tomato plants, but significantly enhanced fruit phytochemical contents including total phenolics and flavonoids and can be adopted to improve the nutritional and health benefits of tomato fruits. Hence, PA represents a novel natural product for improvement of plant growth, productivity, and nutritional content of tomato and other

plants. However, further investigation is required to elucidate the molecular basis of PA effect on different plant species.

CHAPTER 6: FOLIAR APPLICATION OF PYROLIGNEOUS ACID ACTS SYNERGISTICALLY WITH FERTILIZER TO IMPROVE THE PRODUCTIVITY AND PHYTOCHEMICAL PROPERTIES OF GREENHOUSE-GROWN TOMATO

A version of this chapter has been submitted to **Scientific Report Journal**. The citation is:

Ofoe, R., Mousavi, S. M. N., Thomas, R. H., & Abbey, L. (2023). Foliar application of pyroligneous acid acts synergistically with fertilizer to improve the productivity and phytochemical properties of greenhouse-grown tomato. *Scientific Report*. (Under review). https://doi.org/10.21203/rs.3.rs-2640142/v1. (Impact factor = 4.6)

6. ABSTRACT

Pyroligneous acid (PA) is rich in bioactive compounds and known to have the potential to improve crop productivity and phytochemical content. However, the synergistic effect of PA and fertilizer has not been thoroughly studied. In this study, we assessed the biostimulatory effect of different rates of foliar PA application (i.e., 0, 0.25, 0.5, 1, and 2% PA/ddH_2O (*v/v*)) combined with full rate (i.e., 0.63, 0.28, 1.03 g) and half rate of nitrogen-phosphorus-potassium (NPK) fertilizer on the yield and nutritional quality of greenhouse-grown tomato (*Solanum lycopersicum* 'Scotia'). Plants treated with 0.25% and 0.5% PA showed a significantly ($p < 0.001$) higher maximum quantum efficiency of PSII (*Fv/Fm*) and increased potential photosynthetic capacity (*Fv/Fo*), especially when combined with the full NPK rate. Leaf chlorophyll was significantly ($p < 0.001$) increased by *ca.* 60% and 49% in plants treated with 2% PA and full NPK rate compared to no spray and

water, respectively. Total number of fruits was significantly ($p < 0.001$) increased by *ca.* 56% with the 2% PA irrespective of the NPK rate. The combined 2% PA and full NPK rate enhanced total fruit weight and the number of marketable fruits. Similarly, fruit protein, sugar and 2,2-diphenyl-1-picrylhydrazyl (DPPH) activity were significantly ($p < 0.001$) enhanced by the combined 2% PA and full NPK rate. In contrast, the 0.5% PA combined with half NPK rate increased fruit carotenoid and phenolic contents, while the 2% PA plus half NPK rate enhanced fruit flavonoid content. Generally, the synergistic effect of PA and NPK fertilizer increased fruit elemental composition. These showed that foliar application of PA can be a novel and environmentally friendly strategy to increase the productivity and quality of tomato fruits.

Keywords: Biostimulant; wood vinegar; vegetable quality, phytochemicals; *Solanum lycopersicum*; sustainable agriculture; nutritional quality

6.1 INTRODUCTION

Tomato (*Solanum lycopersicum*) is the most cultivated greenhouse and consumed vegetable worldwide due to its diverse use in sauces, soups and puree. Its fruits are known as a potent source of health-enhancing phytochemicals including phenolics, flavonoids, polysaccharides, vitamins and carotenoids, which makes it a good model for studying fruit quality (Chaudhary et al., 2018). These compounds are known to mitigate the destructive effects of reactive oxygen radicals produced during cellular oxidative stress. Dietary intake of tomato fruits has been reported to stimulate antioxidant effects and help prevent chronic diseases in humans including cancers, atherosclerosis, cardiovascular, neurodegenerative and inflammation disorders (Chaudhary et al., 2018; Nowak et al., 2018).

Moreover, tomato productivity and phytochemical properties are highly dependent on growing medium fertility status, growing conditions and plant genetic characteristics (Ye et al., 2020). It has been reported that appropriate fertilization enhances soil fertility and promotes crop yield (Ye et al., 2020). Additionally, the high demand for horticultural crops has resulted in an extensive use of chemical fertilizers for crop production (Pretty & Bharucha, 2014). However, the indiscriminate use of chemical fertilizers coupled with their negative impact on the environment has become a major concern not only to growers but also to consumers and the public (Fan et al., 2014). Evidence suggests that synthetic chemical fertilizers can affect fruit quality including nutritional and phytochemical potentials (Carvalho, 2006; Dudaš et al., 2016; Ye et al., 2020). Consequently, the horticultural industry is seeking alternative strategies to boost crop productivity without compromising nutritional qualities while ensuring environmental sustainability (Tripathi et al., 2019).

One of the most promising inputs to tackle the concerns of indiscriminate use of chemical fertilizers is the use of pyroligneous acid (PA), which is also known as wood distillate, wood vinegar or liquid smoke (Grewal et al., 2018). PA is an aqueous translucent reddish-brown liquid that is produced during the pyrolysis of organic biomass (Grewal et al., 2018). As a natural byproduct of pyrolysis, it contains 80-90% water and rich in over 200 water-soluble bioactive compounds including organic acids, esters, polyphenols, alcohols, sugar derivatives and mineral elements (Wei et al., 2010; Grewal et al., 2018; Ofoe et al., 2022a). However, these chemical properties are dependent on the feedstock, heating rate, temperature and resident time (Grewal et al., 2018; Ofoe et al., 2022a). PA has been used extensively in agriculture as a biostimulant to increase seed germination and seedling growth (Wang et al., 2019a; Wang et al., 2019b; Ofoe et

al., 2022b), crop photosynthetic performance (Berahim et al., 2014; Vannini et al., 2021; Fedeli et al., 2022a; Ye et al., 2022), crop biomass, crop yield (fruit number and weight) (Zulkarami et al., 2011; Mungkunkamchao et al., 2013; Zhu et al., 2021b; Ofoe et al., 2022c) and the nutrition and phytochemical properties of food crops (Kårlund et al., 2014; Benzon & Lee, 2016; Maach et al., 2021; Fedeli et al., 2022a). Additionally, PA has recently been used as a herbicide (Liu et al., 2021b) and antimicrobial agent to control major plant diseases (Jung, 2007; Mourant et al., 2007). Intriguingly, several studies have reported that PA contains a thermal-resistant biologically active compound known as karrikins, which can remain efficacious at a broad array of concentrations (Chiwocha et al., 2009; Dixon et al., 2009). The mode of action of karrikins in plants has been suggested to resemble that of known phytohormones and demonstrated to stimulate seed germination and plant growth (Van Staden et al., 2004; Kulkarni et al., 2008; Chiwocha et al., 2009; Dixon et al., 2009). Also, the high phenolic content of PA has been proven to exhibit high scavenging activities of reactive oxygen species (ROS) radicals, anti-lipid peroxidation and reducing power activities (Loo et al., 2008; Wei et al., 2010; Ofoe et al., 2022a). This suggests that a suitable PA rate and concentration can enhance plant growth and productivity.

According to Drobek et al. (2019), crop production utilizes a huge proportion of fertilizer nutrients with a significant amount not taken up by plants. As such, biostimulants including PA have become feasible alternatives to promote efficient nutrient uptake for increasing crop growth and productivity. Like other biostimulants, PA cannot be defined as a fertilizer since it might not supply direct nutrients to plants but can be treated as an additive fertilizer which facilitates nutrient uptake *via* stimulation of metabolic and biochemical processes in plants and soils (Lashari et al., 2013; Drobek et al., 2019). It was demonstrated that co-application of PA with other soil

amendments including manure (Chen et al., 2010; Lashari et al., 2013), biochar (Shen et al., 2020) and compost (Lashari et al., 2013; Liu et al., 2018a) synergistically improves growth and productivity of crops. Nevertheless, studies on biostimulatory effect of foliar PA application in combination with varying fertilizer regimes on greenhouse tomato yield and fruit quality are limited. Besides, the complex composition of PA with its high acidity makes the concentration for use in crop production critical. Therefore, a low PA concentration can contain the right amounts of bioactive compounds which can maximise its effectiveness on improving crop performance during cultivations.

In the present study, we investigated the biostimulatory effect of PA at varying concentrations and in combination with different application rates of NPK fertilizer on the yield and nutritional quality of greenhouse-grown tomato 'Scotia'. Additionally, the phytochemical levels of leaf tissues can be influenced by mineral nutrition and have been demonstrated to increase following PA application in the leaves of several crops including lettuce (Fedeli et al., 2022b), strawberry (Kårlund et al., 2014) and tobacco (Ye et al., 2022). As such, we examined the phytochemical contents in treated leaf tissues in comparison to fruit tissue as an alternative strategy for enhancing bioactive compounds accumulation or biosynthesis in plants.

6.2 MATERIALS AND METHODS

6.2.1 Plant material and growing condition

This study was carried out from August to December 2021 and repeated from February to June 2022 in the Department of Plant, Food, and Environmental Sciences, Faculty of Agriculture greenhouse. Tomato (*Solanum lycopersicum* "Scotia") seeds were purchased from Halifax seeds

(Halifax, Canada). Seeds were sterilized with 10% NaClO for 10 min, thoroughly washed three times with sterile distilled water (ddH2O) followed by 70% ethanol sterilization for 5 min, and subsequently washed 5 times with sterile distilled water. The PA was derived from white pine biomass and prepared by Proton Power Inc (Lenoir City, USA). The seeds were sown in 32-cell packs containing Pro-Mix® BX (Premier Tech Horticulture, Québec, Canada). The germinated seedlings were grown for 4 weeks in a growth chamber with a day/night temperature regime of 24/22°C, 16/8 h d^{-1} illumination at a light intensity of 300 µmol $m^{-2} \cdot s^{-1}$ and relative humidity of 70%. The seedlings were transplanted into 11.35 L-plastic pots at one plant per pot containing Pro-Mix® BX medium and acclimatized for a week under greenhouse conditions before treatment application. The greenhouse condition was day/night temperature of 28°C/20°C, 16/8 h d^{-1} photoperiod, relative humidity of 70% and supplemental lighting provided by a 600 W HS2000 high-pressure sodium lamp with NAH600.579 ballast (P.L. Light Systems, Beamsville, Canada).

6.2.2 Experimental treatment and design

The study was arranged in a 4 × 2 factorial completely randomized design with four replications. The treatment factors were varying PA concentrations (0%, 0.25%, 0.5%, 1% and 2% PA: ddH_2O) and water-soluble fertilizer (NPK (15:15:30)) (Botaflora, Groupe Bmr, Boucherville, Québec, Canada) applied at a full rate (2.5 g/L) and half rate (1.25 g/L). The full rate of 2.5 g/L was based on manufacturers' recommendations for tomato production. The full rate consisted of 0.63, 0.28, 1.03 g NPK/L and half of the recommended rate contained 0.32, 0.14, 0.52 g NPK/L. PA was applied bi-weekly as foliar sprayed using an 8-L capacity sprayer until the leaves started dripping. The liquid NPK fertilizer was applied as a soil drench every 21 days. The potted plants were

rearranged weekly on the bench to offset unpredictable occurrences due to variations in microclimate.

6.2.3 Plant physiology and yield measurements

Chlorophyll fluorescence indices were determined from five fully expanded leaves per plant at 50 days after transplanting (DAT) using a chlorophyll fluorometer (Optical Science, Hudson, NH, USA). Briefly, leaves were first dark adapted for 25 min before the initial fluorescence yield (F_o) was measured, followed by the maximum chlorophyll fluorescence (F_m) emitted during a saturating light pulse. Variable chlorophyll fluorescence (F_v) was calculated as $F_v = F_m - F_o$. Fluorometric parameters including maximum quantum efficiency (F_v/F_m) and potential photosynthetic capacity (F_v/F_o) were determined at each saturating pulse (Maxwell & Johnson, 2000). At 80 DAT, ripe fruits were harvested and the total fresh weight per plant was recorded using an XT portable balance (Ohaus navigator®, ITM Instruments Inc., Sainte-Anne-de-Bellevue, QC, Canada). Fruit equatorial and polar diameters were measured with a digital Vernier caliper (Mastercraft®, Ontario, Canada). The harvested fruits were graded according to the Canadian Food Inspection Agency (CFIA) grade compendium for fresh vegetables (CFIA, 2021). After harvest, the total above ground (i.e., leaves and shoot) was weighed followed by oven-drying at 65^{o}C for 72 h for dry weight determination.

6.2.4 Fruit quality and leaf tissue biochemical analysis

During the first fruit harvest, leaf samples (15 leaves from four plants/treatment) were collected, flash-frozen in liquid nitrogen and stored in a -80^{o}C freezer. Ten ripe fruits of average size and colour were randomly selected, and surface sterilized with 70% ethanol. The fruit pericarp

(consisting of the epidermis) was excised from the longitudinal section using a sterilized scalpel blade, flash-frozen in liquid nitrogen and stored in a -80^{o}C freezer for biochemical analysis. The remaining portion of the fruit was kept at -20^{o}C until further quality analysis. The fruit quality analyses were performed as described by Ofoe et al. (2022c). The frozen fruits were thawed at room temperature and hand-squashed in a clear Ziplock bag. Total soluble solids (TSS) of the fruit juice was determined using a handheld refractometer (Atago, Tokyo, Japan) and expressed as degree Brix (^{o}Brix). Fruit juice pH, salinity, total dissolved solids (TDS), and electric conductivity (EC) were measured with a 3-in-1 pH meter (Extech Instrument, Taiwan). The complete macro- and micro-nutrient contents of the fruits were determined using inductively coupled plasma mass spectrometry (PerkinElmer Perkin Elmer 2100DV, USA) at the Nova Scotia Department of Agriculture Laboratory, Truro, NS (Donohue et al., 1992).

6.2.4.1 Chlorophyll a and b, and carotenoid content

Chlorophyll a and b of the leaves, and carotenoid content of leaves and fruits were determined as described by Lichtenthaler (1987) with little modification. A 0.2 g of both ground leaf tissues and fruit pericarp were separately homogenized in 2 mL of 80% acetone. The mixture was centrifuged at 15000 × *g* for 15 min and the absorbance of the supernatant was measured at 646.8, 663.2, and 470 nm using a UV-vis spectrophotometer (Jenway, Staffordshire, UK) against 80% acetone as blank. Leaf chlorophyll a and b, and the total carotenoid content of both leaves and fruits were expressed as a µg/g FW of the sample.

6.2.4.2 Leaf and fruit total soluble sugar contents

Total soluble sugar content was estimated according to the phenol-sulphuric acid method described by Dubois et al. (1956). 0.2 g of ground leaf and fruit tissues were separately mixed in 10 mL of 90% ethanol. The mixture was vortexed for 3 min and incubated in a water bath at 60°C for 60 min. The final volume of the mixture was adjusted to 5 mL with 90% ethanol and centrifuged at 12000 × *g* for 3 min. A 1 mL aliquot of the supernatant was transferred into a thick-walled glass test tube containing 1 mL of 5% phenol and mixed thoroughly. A 5 mL of concentrated sulphuric acid was added to the reaction mixture, vortexed for 20 s, and incubated in the dark for 15 min. The mixture was cooled at room temperature and the absorbance measured at 490 nm against a blank containing deionised water, phenol and sulphuric acid. Total sugar was calculated using a standard glucose curve (0 – 300 µg glucose) and expressed as µg of glucose/g FW.

6.2.4.3 Leaf and fruit total phenolics

Total phenolics content (TPC) was determined by the Folin-Ciocalteu assay described by Ainsworth and Gillespie (2007) with little modification. 0.2 g of ground leaf and fruit tissues were separately homogenized in 2 mL of ice-cold 95% methanol and incubated in the dark at room temperature for 48 h. The mixture was centrifuged at 13000 × *g* for 5 min before adding 100 µL of the supernatant to 200 µL of 10% (v/v) Folin-Ciocalteau reagent. The mixture was vortexed for 5 min, mixed with 800 µL of 700 mM Na_2CO_3, and incubated in the dark at 25ºC for 2 h. The absorbance of the supernatant was measured at 765 nm against a blank. TPC was calculated using a gallic acid standard curve (0 – 50 mg gallic acid) and expressed as mg gallic acid equivalents per g fresh weight (i.e., mg GAE/g FW).

6.2.4.4 Leaf and fruit total flavonoid

Total flavonoid was estimated following the colorimetric method described by Chang et al. (2002). 0.2 g of ground leaf and fruit tissues were separately homogenized in 2 mL of ice-cold 95% methanol followed by centrifugation at 15000 × *g* for 10 min. 500 µL of the supernatant was added to a reaction mixture containing 1.5 mL of 95% methanol, 0.1 mL of 10% $AlCl_3$, 0.1 mL of 1 M potassium acetate, and 2.8 mL of distilled water. The mixture was incubated at room temperature for 30 min and the absorbance was measured at 415 nm against a blank lacking $AlCl_3$. Total flavonoid content was estimated using the quercetin standard curve (0 – 250 µg quercetin) and expressed as µg quercetin equivalents per g fresh weight (µg quercetin/g FW).

6.2.4.5 Leaf and fruit total protein content

For leaf and fruit total protein content, 0.2 g of ground leaf tissues and fruit pericarp were homogenized in 1.8 mL ice-cold extraction buffer (50 mM potassium phosphate buffer at a pH 7.0, 1% polyvinylpyrrolidone, and 0.1 mM EDTA). The homogenate was centrifuged at 15000 × *g* for 20 min at 4°C. The supernatant (crude enzyme extract) was transferred to a new microfuge tube on ice and the protein content was measured at 595 nm after 5 min of mixing with Bradford's reagent (Bradford, 1976). Protein content was estimated from a standard curve of bovine serum albumin (BSA) (0 – 900 µg BSA) and expressed as mg BSA/g FW.

6.2.4.6 DPPH free radical scavenging capacity

The DPPH radical scavenging capacity was determined using the method described by Dudonne et al. (2009) with little modification. Briefly, 0.2 g of ground leaf tissue and fruit pericarp were homogenized in 1.5 mL pure methanol. The mixture was centrifuged at 12000 × *g* for 10 min and

100 µL of supernatant was added to 2.9 mL of 60 µM fresh DPPH methanolic solution. The mixture was vortexed and incubated in the dark at room temperature for 30 min. The absorbance of the reaction mixture was measured at 515 nm against methanol blank and the radical scavenging activity was calculated using the formula:

Inhibition (%) = $[(A_B – A_S)/ A_B] \times 100\%$; where A_B is the absorbance of the blank sample and A_S is the absorbance of the sample.

6.2.5 Statistical analysis

All data collected from the experiments were subjected to a two-way analysis of variance (ANOVA) using Minitab (Minitab 19 Statistical Software, USA). Means with significant differences were separated using the Fisher Least Significant Differences (LSD) test at $\alpha = 0.05$. A multivariate analysis including Pearson correlation and two-dimensional principal component analysis (PCA) biplot was performed using XLSTAT version 2022.1.

6.3 RESULTS

6.3.1 Plant physiology and biomass response

Chlorophyll fluorescence indices were significantly ($p < 0.001$) affected by PA treatment but not its interaction with NPK (Figure 6.1). The results showed F_v/F_o was significantly ($p < 0.001$) increased by *ca.* 12% and 15% in the 0.25% and 0.5% PA-treated plants respectively, compared to no spray plants (Figure 6.1A). Similarly, F_v/F_m was substantially ($p < 0.001$) enhanced in the 0.25% and 0.5% PA-treated plants compared to no spray plants (Figure 6.1B). However, the values of these parameters were reduced as PA was increased to 1% and 2% but was not significantly (*p*

> 0.05) different from those of the no spray and water alone treatments (Figure 6.1). Analysis of leaf chlorophyll content indicates that PA application had a significant ($p < 0.001$) interaction with NPK (Table 6.1). The 2% PA with full NPK rate increased total chlorophyll content by *ca*. 60% and 49% compared to the no spray and water alone treatments (Table 6.1).

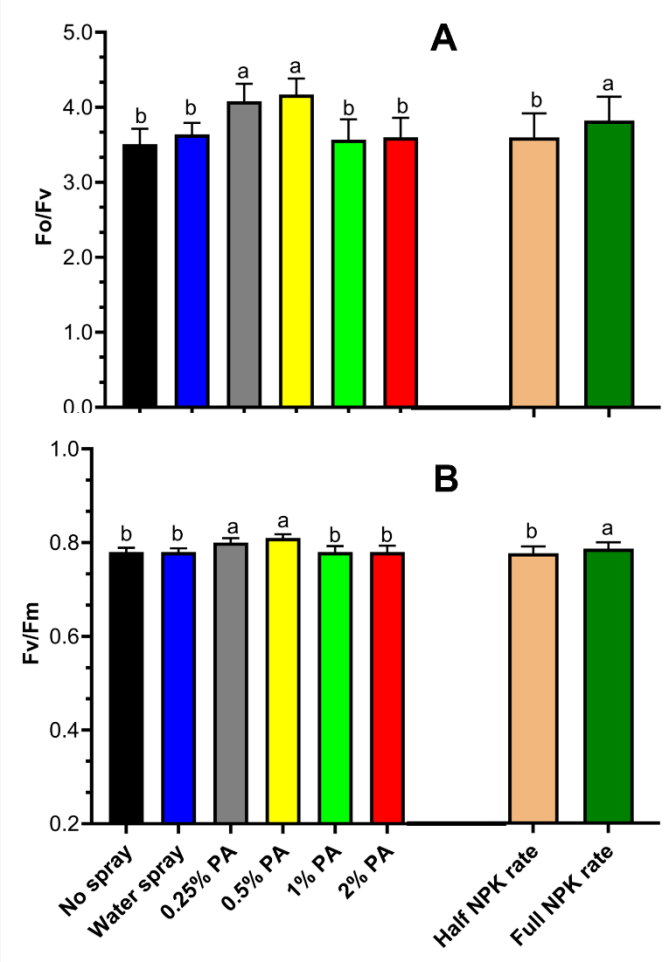

Figure 6.1. Chlorophyll fluorescence of tomato 'Scotia' in response to pyroligneous acid treatment under varying NPK rates. (A) Potential photosynthetic capacity (F_v/F_o) (B) Maximum quantum efficiency (F_v/F_m). Values are means ± SD of four replicates and the different letters indicate significant ($p < 0.05$) difference according to Fisher's least significant difference (LSD) post hoc test.

Moreover, 0.5% PA with full NPK rate significantly ($p < 0.001$) increased only chlorophyll a by *ca.* 39% and 32% compared to no spray and water treatments. Also, the 2% PA treatment with full

NPK rate considerably enhanced both chlorophyll a and b contents by *ca*. 43% and 36% and 104% and 83% compared to no spray and water treatments respectively. On the contrary, 0.25% PA in addition to the full NPK rate recorded the least leaf chlorophyll content and was not significantly ($p > 0.05$) different from no spray treatment (Table 6.1). It was clear that PA slightly increased chlorophylls a and b although they were reduced in plants applied with half NPK rate.

Table 6.1. Morpho-physiological response of tomato 'Scotia' sprayed with pyroligneous acid (PA) under varying NPK rates.

PA	NPK rate	Chlorophyll a (mg g^{-1} FW)	Chlorophyll b (mg g^{-1} FW)	Total chlorophyll (mg g^{-1} FW)	Above-ground fresh weight (g)
0.25%	Full	191.36±12.53 e	83.81±5.02 g	274.76±17.55 f	562.52±40.80 a
	Half	241.14±12.15 c	118.28±7.36 c	359.02±19.51 c	449.41±63.60 bcd
0.5%	Full	278.48±1.28 a	152.11±1.32 b	419.23±23.80 b	542.29±69.90 ab
	Half	207.04±10.95 de	96.64±5.81 def	303.35±16.75 def	411.41±67.60 cd
1%	Full	253.72±10.33 b	122.32±7.46 c	375.70±17.80 c	558.47±124.40 a
	Half	191.73±14.30 e	86.31±6.67 fg	277.47±21.00 f	378.59±69.70 d
2%	Full	286.20±7.18 a	178.83±1.59 a	458.29±21.20 a	480.85±49.20 abc
	Half	214.47±4.33 d	100.93±3.32 d	302.22±28.90 def	471.22±64.00 abc
No spray	Full	200.00±13.97 de	87.75±6.83 efg	287.21±20.80 ef	428.57±52.80 cd
	Half	215.24±14.53 d	99.25±8.05 d	313.90±22.60 de	426.94±65.10 cd
Water	Full	210.93±12.88 d	97.69±7.23 de	308.14±20.00 def	551.14±24.70 ab
	Half	233.58±1.12 c	101.51±8.87 d	327.02±25.30 d	413.31±22.40 cd
Sources of Variation					
PA		0.001	<0.001	<0.001	0.313
NPK		<0.001	<0.001	<0.001	<0.001
PA x NKP		<0.001	<0.001	<0.001	0.044

Values are means ± SD of four replicates and the different letters indicate significant ($p < 0.05$) difference according to Fisher's least significant difference (LSD) post hoc test.

Total above-ground fresh weight was significantly ($p < 0.05$) increased by the interaction of PA and NPK but not PA alone (Table 6.1; Table S6.1). Overall, the application of PA significantly ($p < 0.05$) increased the above-ground fresh weight under full NPK rate in the range 31% and 12% compared to no spray but not significantly ($p > 0.05$) different from the water-sprayed plants (Table 1). Furthermore, the interaction between PA and NPK had no significant ($p > 0.05$) effect on the aboveground dry weight. However, the aboveground dry weight of 0.25% PA-treated plants under full NPK rate increased by *ca.* 54% and 11% compared to no spray and water treatment, respectively.

6.3.2 Fruit yield and marketability

The total number of fruits per plant was significantly ($p < 0.001$) affected by PA and NPK interaction (Figure 6.2A; Table S6.1). The application of both PA and full NPK rate had the most significant ($p < 0.001$) increase in the total number of fruits compared to water and no spray treatments. Notably, PA increased the number of fruits under full NPK rate by *ca.* 44% to 56% and 30% to 40% compared to no spray and water alone treatment, respectively. Similarly, the number of fruits was significantly ($p < 0.001$) increased with 2% PA under half NPK rate by *ca.* 40% and 56% compared to no spray and water treatment, respectively (Figure 6.2A). However, 0.5% PA and 1% PA slightly reduced the number of fruits although this was not significantly ($p > 0.05$) different from the no spray and water treatments (Figure 6.2A). Moreover, total fruit weight was highest in 2% PA-treated plants under full NPK rate although not significantly ($p > 0.05$) different from 0.25% PA-treated plants (Figure 6.2B). The 2% PA significantly ($p < 0.001$) increased total fruit weight by *ca.* 104% and 62%, while the 0.25% PA substantially ($p < 0.001$) increased the total fruit weight by *ca.* 93% and 53% compared to no spray and water treatment respectively (Figure 6.2B). Also, the total fruit weight of 0.5% PA-treated plants under full NPK

rate was slightly higher than those of the no-spray and water-treated plants but was not significantly ($p > 0.05$) different from that of water-treated plants (Figure 6.2B). Nevertheless, under half NPK rate, the total fruit weight of PA-treated plants was significantly ($p < 0.001$) reduced compared to their full NPK rate counterpart.

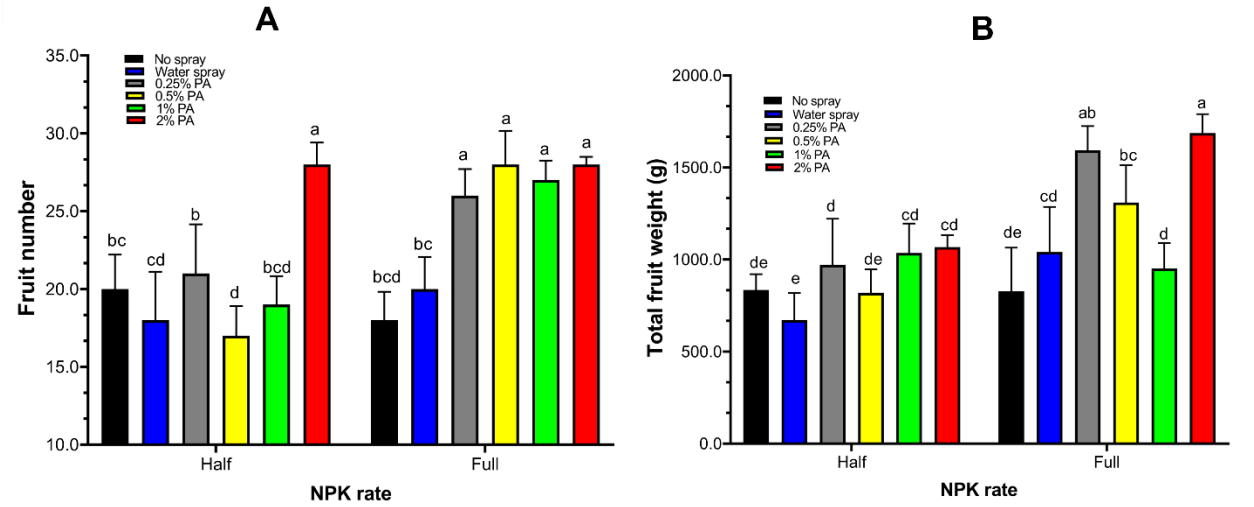

Figure 6.2. Fruit yield of tomato 'Scotia' in response to pyroligneous acid treatment under varying NPK rates. (A) Fruit number (B) Total fruit weight. Values are means ± SD of four replicates and the different letters indicate significant ($p < 0.05$) difference according to Fisher's least significant difference (LSD) post hoc test.

To examine the effect of PA on the marketability of tomato fruits, the harvested fruits were graded according to the CFIA grade compendium for fresh vegetables (CFIA, 2021). The results revealed that majority of the fruits (*ca*. 73%) were categorised under Canada No.2 with an equatorial diameter greater than or equal to 38 mm but less than 63 mm, while 27% and 0.2% constituted non-marketable fruits and Canada commercial with an equatorial diameter of less than 38 mm and greater than or equal to 63 mm respectively (Figure 6.3; Table S6.2). Among the various treatment, the 2% PA with full NPK rate recorded the highest increase in the number of Canada No.2 marketable fruits by *ca.* 115% and 63% while non-marketable fruit was reduced by *ca.* 57% and

44% compared to no spray and water treatments, respectively (Figure 6.3; Table S6.2). A similar increase in the number of Canada No.2 marketable fruits was noted with 0.25% and 0.5% PA in combination with the full NPK rate. Nonetheless, the number of Canada No.2 marketable fruits were slightly reduced by 0.25%, 0.5% and 2% PA in combination with half NPK rate compared to full NPK (Figure 6.3). Besides, the number of Canada No.2 marketable fruits from 0.25%, 0.5% and 2% PA-treated plants under half NPK rate were comparable to those of no spray and water alone treatments. The number of non-marketable fruits was lower in 0.25% and 0.5% PA-treated plants under half NPK rate but increased in the 1% and 2% PA-treated plants compared to that of no spray and water-treated plants (Figure 6.3).

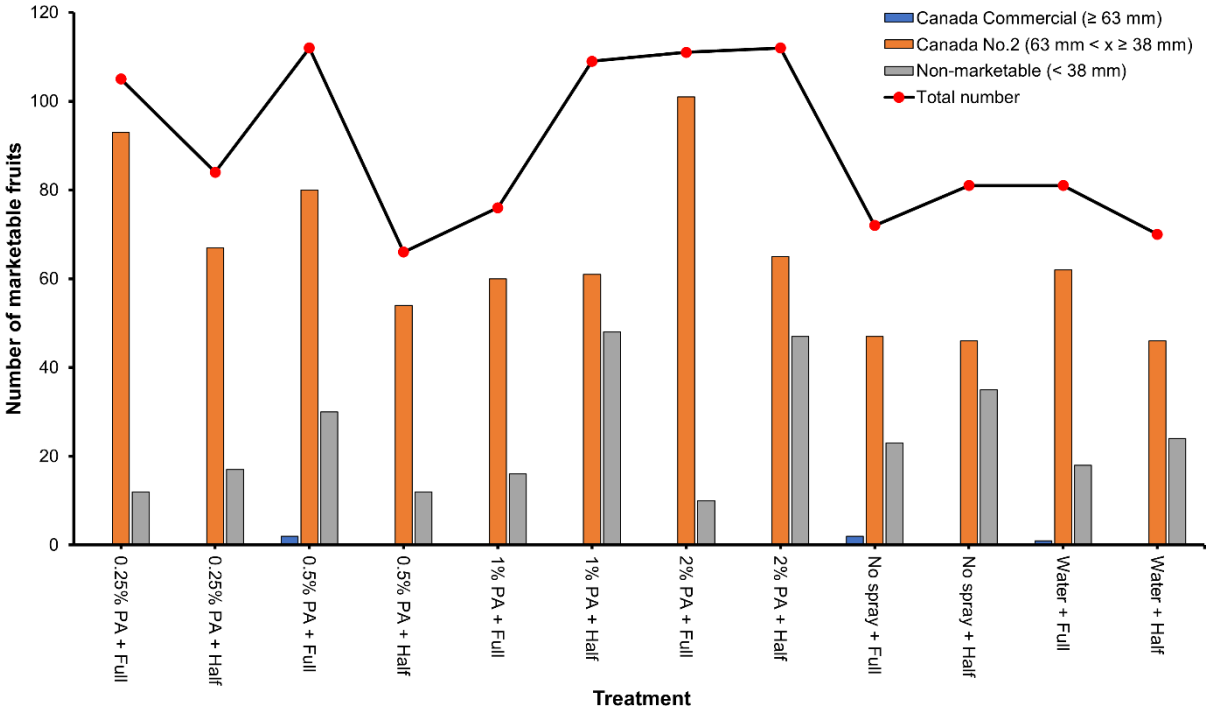

Figure 6.3. Fruit marketability of tomato 'Scotia' plants treated with pyroligneous acid (PA) under varying NPK rates. Values are the total fruit grades from four plants.

6.3.3 Fruit chemical composition

Fruit chemical quality parameters including juice °Brix, pH, TDS, salinity and EC were significantly ($p < 0.001$) affected by PA and NPK fertilizer interaction (Figure 6.4; Figure 6.5). Juice Brix content was significantly ($p < 0.001$) increased by *ca.* 14% following 2% PA with half NPK rate application compared to no spray treatment (Figure 6.4). Fruit °Brix content of the 2% PA-treated plants was comparable to that of the water-treated plants under half NPK rate. However, the 0.25% PA combined with half NPK rate significantly ($p < 0.001$) reduced Brix content compared to the water treatment but was not different from no spray-treated plants (Figure 6.4). Comparatively, °Brix content was not significantly ($p > 0.05$) altered in PA-treated plants with full NPK rate except for the 0.25% PA which reduced the Brix content compared to water-treated plants. On the other hand, all PA treatments (except 0.25% PA) with full NPK rate significantly ($p < 0.001$) increased Brix content compared to no spray-treated plants (Figure 6.4).

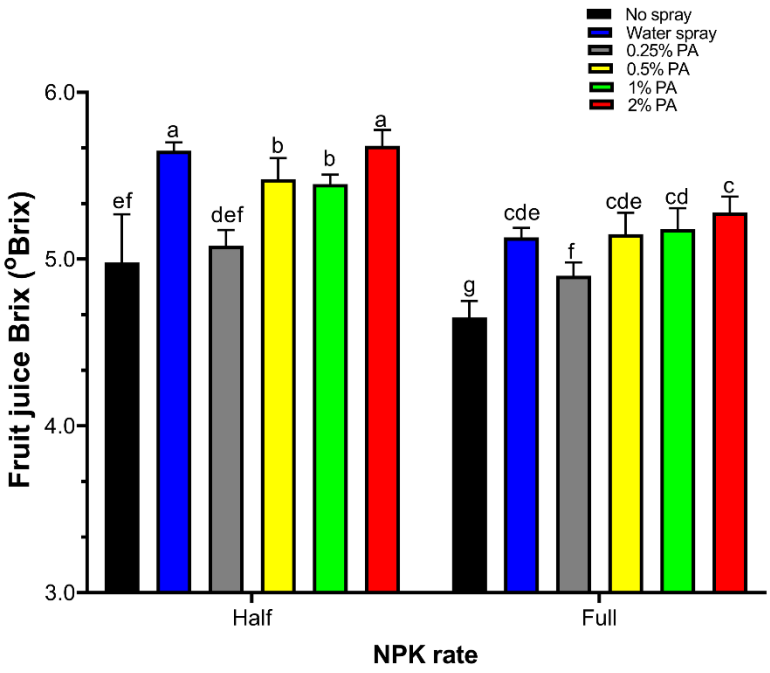

Figure 6.4. Fruit Brix content of tomato 'Scotia' plants treated with pyroligneous acid (PA) under varying NPK rates. Values are means ± SD of four replicates and the different letters indicate significant ($p < 0.05$) difference according to Fisher's least significant difference (LSD) post hoc test.

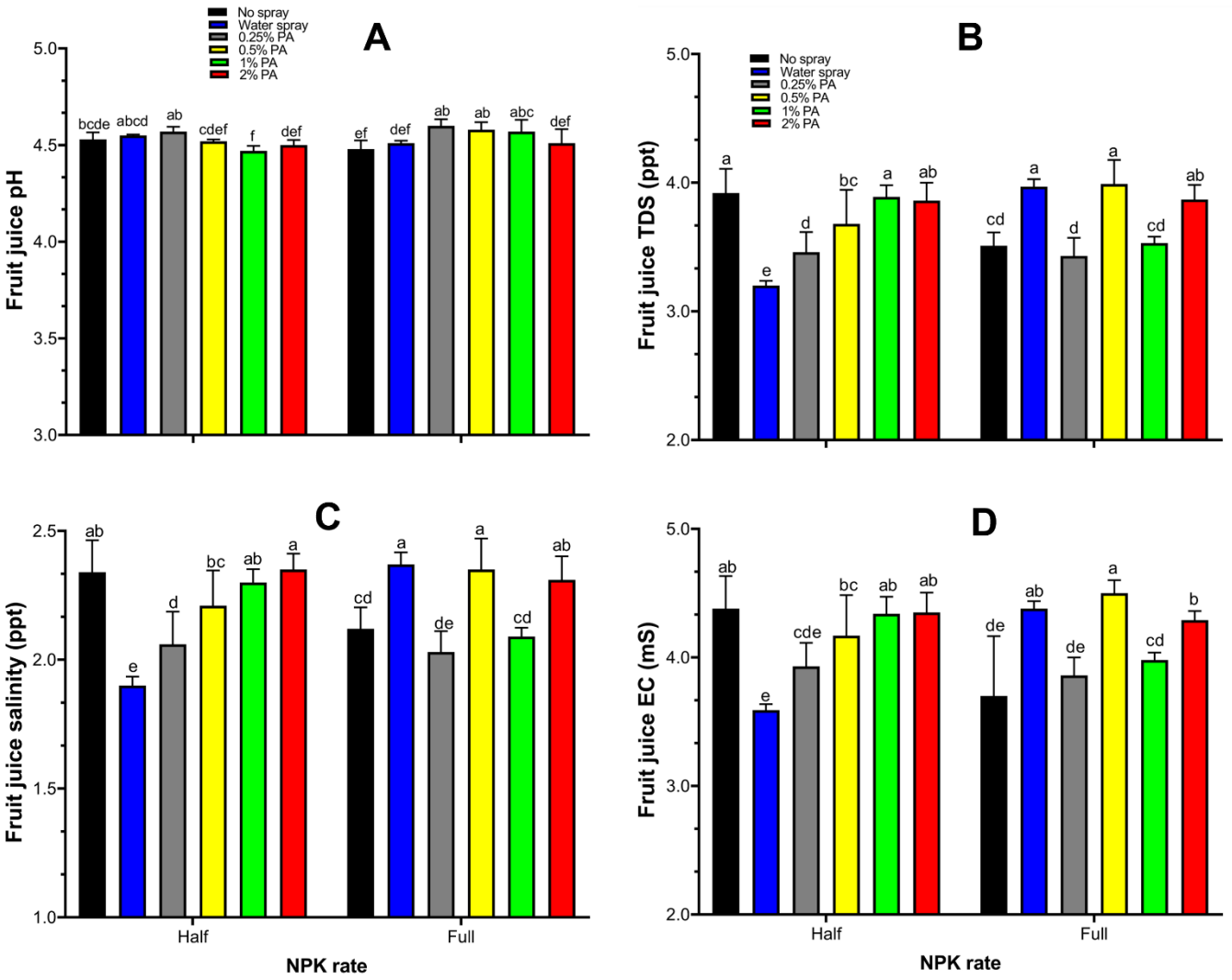

Figure 6.5. Chemical quality of tomato 'Scotia' fruits from plants treated with pyroligneous acid (PA) under varying NPK rates. Values are means ± SD of four replicates and the different letters indicate significant ($p < 0.05$) difference according to Fisher's least significant difference (LSD) post hoc test.

Similarly, 0.25% PA with half NPK rate enhanced fruit juice pH although not significantly ($p > 0.05$) different from the no spray and water treatment (Figure 6.5A). Under NPK rate, all PA treatments significantly ($p < 0.001$) increased fruit juice pH while 2% PA showed no significant ($p > 0.05$) effect compared to no spray and water treatment (Figure 6.5A). Moreover, fruit juice TDS and salinity were significantly ($p < 0.001$) higher in the fruits of 1% and 2% PA-treated plants under half NPK rate but comparable to no spray-treated plants (Figure 6.5B; Figure 6.5C). The 0.5% and 2% PA under full NPK rate significantly ($p < 0.001$) increased both fruit juice TDS and salinity compared to no spray treatment (Figure 6.5B; Figure 6.5C). Nevertheless, 0.25% PA with full NPK rate significantly ($p < 0.001$) decreased fruit juice TDS and salinity compared to water treatment although not significantly ($p > 0.05$) different from the no spray treatment (Figure 5B; Figure 6.5C). Likewise, 1% and 2% PA combined with half NPK rate considerably increased fruit juice EC by *ca*. 17% and 18% respectively compared to water treatment but was comparable to that of the no spray treatment (Figure 6.5D). Furthermore, 0.5% and 2% PA with full NPK rate significantly ($p < 0.001$) improved fruit juice EC compared to no spray treatment but was not different from water treatment (Figure 5D). However, 0.25% PA had no effect on fruit juice EC, irrespective of NPK rate (Figure 6.5D).

6.3.4 Leaf and fruit tissue phytochemical analysis

Leaf carotenoid content was significantly ($p < 0.001$) increased in 0.5% PA-treated plants under full NPK rate by *ca*. 33% and 19% compared to no spray and water treatment, respectively (Table 6.2). Similarly, 0.5% PA in addition to half NPK rate significantly ($p < 0.001$) enhanced fruit carotenoid content by *ca.* 30% and 13% compared to no spray and water treatment, respectively, but was not significantly ($p > 0.05$) different from that of the 2% PA (Table 6.3). On the contrary,

0.5% PA combined with full NPK rate significantly ($p < 0.001$) reduced fruit carotenoid content by *ca.* 17% and 15% compared to no spray and water treatment respectively (Table 6.3). Overall, leaf carotenoid content was *ca.* 2631% higher than fruit carotenoid content (Table S6.3). Both leaf and fruit protein contents were significantly ($p < 0.001$) affected by PA and NPK interaction (Table 6.2; Table 6.3). In general, total leaf protein content was significantly ($p < 0.001$) higher (*ca.* 119%) than fruit total protein (Table S6.3). Among the applied treatments, 2% PA with half NPK rate enhanced leaf protein content by *ca.* 13% and 12% compared to no spray and water treatment respectively (Table 6.2). However, 0.25% PA combined with full NPK rate markedly reduced leaf protein content. Besides, 2% PA with full NPK rate recorded the highest fruit protein content (*ca*. 40% and 67%) followed by 1% PA with full NPK rate (*ca.* 33% and 59%) compared to no spray and water treatment respectively (Table 3). Leaf and fruit sugar contents were significantly ($p < 0.001$) affected by PA and NPK interaction (Table 6.2; Table 6.3). Relative tissue analysis revealed that fruit sugar content was significantly ($p < 0.001$) increased by *ca.* 148% compared to leaf sugar content (Table S6.3). All the PA treatments with full NPK rate considerably reduced leaf sugar contents which 0.5% PA recorded the lowest. Contrarily, 0.5% PA with half NPK rate increased leaf sugar content by *ca.* 26% compared to no spray treatment but not different from water treatment (Table 6.2). Besides, 2% PA with full NPK rate recorded the highest (*ca.* 32% and 15%) fruit sugar content compared to no spray and water treatment (Table 6.3).

Table 6.2. Phytochemical composition and ROS scavenging activities of tomato 'Scotia' leaf sprayed with pyroligneous acid (PA) under varying NPK rates.

PA	NPK rate	Carotenoid (mg g^{-1} FW)	Protein (mg g^{-1} FW)	Sugar (mg glucose g^{-1} FW)	Phenolics (mg GAE g^{-1} FW)	Flavonoid (µg quercetin g^{-1} FW)	DPPH (%)
0.25%	Full	64.21±4.75 g	2.00±0.04 f	6.86±0.11 ef	604.69±6.12 de	820.55±0.01 g	55.57±3.30 f
	Half	86.40±0.41 b	2.41±0.28 bcd	7.69±0.27 d	606.55±0.85 d	1030.91±0.03 bc	48.35±3.71 g
0.5%	Full	89.52±2.05 a	2.31±0.03 cde	6.74±0.08 f	529.74±2.84 g	899.81±0.03 e	42.56±4.74 h
	Half	79.26±3.94 cd	2.18±0.14 ef	9.01± 0.54 b	580.66±1.99 f	1085.57±0.02 a	71.18±2.25 b
1%	Full	83.93±3.41 b	2.52±0.08 b	7.11±0.54 e	602.49±8.90 de	755.51±0.01 h	64.11±2.60 cd
	Half	71.05±4.97 fg	2.43±0.02 bcd	7.16±0.17 e	691.98±11.98 a	944.17±0.02 d	82.76±1.40 a
2%	Full	86.18±0.25 b	2.29±0.07 de	8.53±0.07 bc	460.21±18.27 h	1079.25±0.02 a	66.03±2.62 c
	Half	74.37±6.07 ef	2.64±0.04 a	7.96±0.17 cd	685.04±15.46 ab	931.02±0.03 d	72.49±2.01 b
No spray	Full	67.23±4.68 g	2.32±0.05 cde	8.82±0.87 b	657.47±12.62 c	1059.24±0.01 ab	58.62±2.88 ef
	Half	76.78±4.46 cde	2.33±0.15 cde	7.17±0.342 e	593.52±3.77 def	858.10±0.01 f	55.51±3.25 f
Water	Full	75.14±4.31def	2.44±0.05 bc	9.95±0.56 a	592.51±7.02 ef	870.92±0.01 f	61.42±2.75 de
	Half	79.85±0.31 c	2.37±0.04 cd	8.37±0.50 bc	674.05±7.12 b	1028.33±0.02 c	61.10±2.91 de
Sources of variation				***p*-value**			
PA		<0.001	<0.001	<0.001	<0.001	<0.001	<0.001
NPK		0.043	0.008	0.560	<0.001	<0.001	<0.001
PA x NPK		<0.001	<0.001	<0.001	<0.001	<0.001	<0.001

Values are means ± SD of four replicates and the different letters indicate significant ($p < 0.05$) difference according to Fisher's least significant difference (LSD) post hoc test.

Table 6.3. Phytochemical composition and ROS scavenging activities of tomato 'Scotia' fruit from plants sprayed with pyroligneous acid (PA) under varying NPK rates.

PA	NPK rate	Carotenoid (mg g^{-1} FW)	Protein (mg g^{-1} FW)	Sugar (mg glucose g^{-1} FW)	Phenolic (mg GAE g^{-1} FW)	Flavonoid (µg quercetin g^{-1} FW)	DPPH (%)
0.25%	Full	2.88±0.16 cde	1.16±0.02 c	20.29±0.61 d	134.91±8.81 d	57.92±2.02 e	24.05±0.62 i
	Half	2.51±0.10 fg	1.23±0.05 bc	13.43±0.33 f	106.64±4.42 g	59.28±1.90 e	25.50±0.34 h
0.5%	Full	2.38±0.20 g	1.14±0.06 c	21.21±0.32 c	259.46±9.80 a	58.58±2.68 e	29.46±0.15 f
	Half	3.39±0.04 a	1.13±0.03 cd	13.47±0.46 f	152.43±11.12 c	66.39±2.62 d	30.68±0.11 e
1%	Full	2.70±0.26 defg	1.30±0.10 ab	12.28±0.24 g	67.80±0.51 h	26.87±1.99 f	32.95±0.11 b
	Half	2.78±0.29 def	1.04±0.04 de	21.77±0.11 c	181.77±3.40 b	94.37±5.47 b	33.14±0.19 b
2%	Full	3.08±0.28 bc	1.37±0.17 a	26.46±0.58 a	129.82±2.31 de	81.86±5.97 c	34.17±0.22 a
	Half	3.29±0.26 ab	1.13±0.08 cd	22.93±0.95 b	164.59±4.70 bc	108.95±5.20 a	31.82±0.45 c
No spray	Full	2.85±0.14 cde	0.98±0.06 e	20.14±0.36 d	158.03±8.31 c	70.17±4.73 d	31.01±0.18 de
	Half	2.61±0.24 efg	0.77±0.06 f	19.04±0.65 e	112.24±2.90 f	66.13±5.25 d	30.91±0.72 de
Water	Full	2.79±0.26 def	0.82±0.07 f	22.98±0.17 b	167.67±4.61 bc	104.84±5.01 a	28.57±0.52 g
	Half	3.00±0.05 bcd	0.78±0.05 f	19.44±0.48 e	122.96±4.34 e	21.41±1.00 g	31.30±0.32 d
Sources of variation				***p*-value**			
PA		<0.001	<0.001	<0.001	<0.001	<0.001	<0.001
NPK		0.016	<0.001	<0.001	<0.001	0.663	0.001
PA x NPK		<0.001	<0.001	<0.001	<0.001	<0.001	<0.001

Values are means ± SD of four replicates and the different letters indicate significant ($p < 0.05$) difference according to Fisher's least significant difference (LSD) post hoc test.

PA with NPK fertilizer interaction significantly ($p < 0.001$) affected total phenolic and flavonoid contents (Table 6.2; Table 6.3). Leaf total phenolic and flavonoid contents were significantly ($p < 0.001$) increased by *ca.* 331% and 1297% respectively compared to the tomato fruits (Table S6.3). The 1% PA combined with half NPK rate recorded a significantly ($p < 0.001$) higher (i.e., *ca.* 17% and 30%) leaf phenolic content while the 2% PA with full NPK rate recorded the least compared to no spray and water treatment (Table 6.2). Conversely, the 0.5% PA with full NPK rate significantly ($p < 0.001$) increased fruit phenolic content by *ca*. 65% and 55% while the 1% PA with full NPK rate recorded the least compared to no spray and water treatment respectively (Table 6.3). Furthermore, leaf flavonoid content was significantly ($p < 0.001$) increased with 0.5% PA under half NPK rate compared to no spray and water alone treatments (Table 6.2). The flavonoid content of the 0.5% PA-treated leaves was comparable to that of 2% PA and no spray treatments with half NPK rate. Nevertheless, the flavonoid content of 2 % PA-treated leaves was significantly ($p < 0.001$) higher (*ca*. 5%) than that of water treatment (Table 6.2). Tomato fruit flavonoid content was significantly ($p < 0.001$) increased by *ca*. 65% and 409% following the application of 2% PA and half NPK rate compared to no spray and water treatment respectively (Table 3). Nevertheless, PA application with full NPK rate reduced fruit flavonoid content compared to water treatment but not the no spray treatment (Table 6.3). The ROS scavenging activity of leaf and fruit tissue extracts using DPPH scavenging activity showed a significant effect ($p < 0.001$) of PA and NPK fertilizer interaction (Table 6.2; Table 6.3). The total DPPH scavenging activity of leaf tissues was significantly ($p < 0.001$) higher (*ca*. 103%) than that of the fruit (Table S6.3). All PA treatments with half NPK rate except for 0.25% PA significantly ($p < 0.001$) increased leaf DPPH scavenging activity by up to 49% and 36% compared to no spray and water treatment, respectively (Table 6.2). Likewise, a significantly ($p < 0.001$) high fruit DPPH scavenging activity (*ca*. 10% and 20%)

was noticed in 2% PA-treated plants in combination with full NPK rate, whereas 0.25% PA recorded the least fruit DPPH scavenging activity compared to no spray and water treatments (Table 6.3).

6.3.5 Fruit mineral element composition

Fruit elemental composition was highly influenced by PA and NPK fertilizer interaction (Table 6.4). Fruit N content was increased by up to *ca*. 10% in 0.25%, 0.5% and 1% PA-treated plants in combination with full NPK rate compared to water-treated plants (Table 6.4). Fruit Ca content was slightly increased in 1% PA-treated plants with full NPK while 0.5% recorded the least Ca content (Table 6.4). Also, high fruit K content was noticed in fruits of the 1% PA-treated plants followed by 2% PA with half NPK rate compared to no spray and water treatment (Table 6.4). Besides, PA and NPK application had no obvious effect on fruit Mg, P and Na content. Fruit B content was increased by *ca.* 8% in fruits of 2% PA with full NPK rate compared to no spray and water treatment. Fruit Cu content was reduced in fruits of PA with full NPK rate treated plants compared to no spray treatment but was slightly increased with 1% and 2% PA when compared to water treatment. Moreover, 2% PA markedly increased fruit Fe content by *ca*. 626% and 416% under full NPK rate and by *ca*. 513% and 108% under half NPK rate compared to no spray and water treatment respectively (Table 6.4). However, 0.25% PA reduced fruit Fe content irrespective of NPK rate. Fruit Mn content was marginally reduced with PA application under full NPK rate compared to no spray treatment but increased considerably with all PA treatments compared to water treatment. Under half NPK rate, fruit Mn content was not altered with PA application compared with no spray and water treatments (Table 6.4).

Table 6.4. Tomato 'Scotia' fruit elemental composition in response to pyroligneous acid (PA) under varying NPK rates.

PA	NPK rate	Fruit mineral element										
		N (%)	Ca (%)	K (%)	Mg (%)	P (%)	Na (%)	B (mg L^{-1})	Cu (mg L^{-1})	Fe (mg L^{-1})	Mn (mg L^{-1})	Zn (mg L^{-1})
0.25%	Full	1.62	0.17	2.68	0.14	0.41	0.03	11.39	5.47	43.35	26.44	22.91
	Half	1.33	0.15	2.72	0.13	0.40	0.04	11.87	5.18	40.06	21.82	17.63
0.5%	Full	1.60	0.14	2.94	0.14	0.44	0.03	11.91	5.56	40.68	24.47	21.31
	Half	1.38	0.18	2.82	0.14	0.42	0.03	11.62	ND	100.07	20.54	17.6
1%	Full	1.52	0.19	2.64	0.14	0.39	0.03	10.65	5.38	57.36	25.62	22.17
	Half	1.27	0.20	3.09	0.14	0.42	0.03	12.33	5.01	107.47	24.22	24.35
2%	Full	1.46	0.16	2.98	0.13	0.43	0.03	12.36	5.69	309.67	25.64	18.72
	Half	1.42	0.20	2.99	0.15	0.42	0.03	11.99	ND	267.86	24.9	20.28
No spray	Full	1.72	0.17	2.61	0.15	0.44	0.03	11.58	7.07	42.68	27.62	18.86
	Half	1.24	0.22	2.96	0.14	0.41	0.03	12.41	ND	43.69	25.42	18.53
Water	Full	1.47	0.18	2.83	0.13	0.41	0.02	11.43	5.47	59.99	18.04	18.46
	Half	1.12	0.22	2.61	0.13	0.36	0.05	11.58	ND	128.67	23.56	15.36
Mean		1.43	0.18	2.82	0.14	0.41	0.03	11.76	5.60	103.46	24.02	19.68
CV (%)		12.12	13.29	5.93	4.30	5.21	19.99	4.26	11.24	88.90	11.22	13.09

Values are based on pooled samples from four replicates. ND, Not determined.

Furthermore, 1% PA with half NPK rate enhanced fruit Zn content by *ca.* 32% and 59% followed by 2% PA compared to no spray and water treatments, respectively (Table 6.4).

6.3.6 Association between morpho-physiological properties, productivity and phytochemicals

A two-dimension (2-D) principal component analysis and Pearson correlation coefficients (r) were used to further asses the association amongst the morpho-physiological, yield and phytochemical properties of tomato plants in response to PA and NPK fertilizer interaction (Figures 6.6 – 6.7; Table S6.4). The correlation analysis showed that *Fv*/*Fm* had a significant ($p < 0.001$) positive association with *Fv*/*Fo*, fruit weight, and fruit juice pH, but exhibited a significant ($p < 0.01$) negative correlation with leaf protein content, phenolic content and leaf and fruit DPPH. Similarly, total number of fruits had a significant ($p < 0.01$) positive correlation with total fruit weight, chlorophyll a and b and fruit protein content and a negative association with leaf sugar content. Total fruit weight had a significant ($p < 0.01$) negative association with leaf phenolic content but a positive association with fruit protein content. Above-ground fresh weight had a significant ($p < 0.01$) positive correlation with aboveground dry weight and a negative association with leaf flavonoid content (Figure 6.6; Table S6.4). Likewise, fruit juice Brix content exhibited a significant ($p < 0.01$) positive correlation with fruit juice TDS, EC, salinity, leaf sugar, leaf DPPH and fruit flavonoid contents (Figure 6.6; Table S6.4). However, fruit juice pH showed a significant ($p < 0.01$) negative association with leaf DPPH, fruit flavonoid and fruit DPPH (Figure 6). Fruit juice TDS had a significantly ($p < 0.01$) positive association with fruit juice EC, salinity, fruit total sugar, phenolics and flavonoid contents. Similar to TDS, EC had a significantly ($p < 0.01$) strong positive association with fruit juice salinity while both fruit juice EC and salinity had a

significantly ($p < 0.01$) positive association with fruit total sugar, phenolics and flavonoid contents (Figure 6.6; Table S6.4).

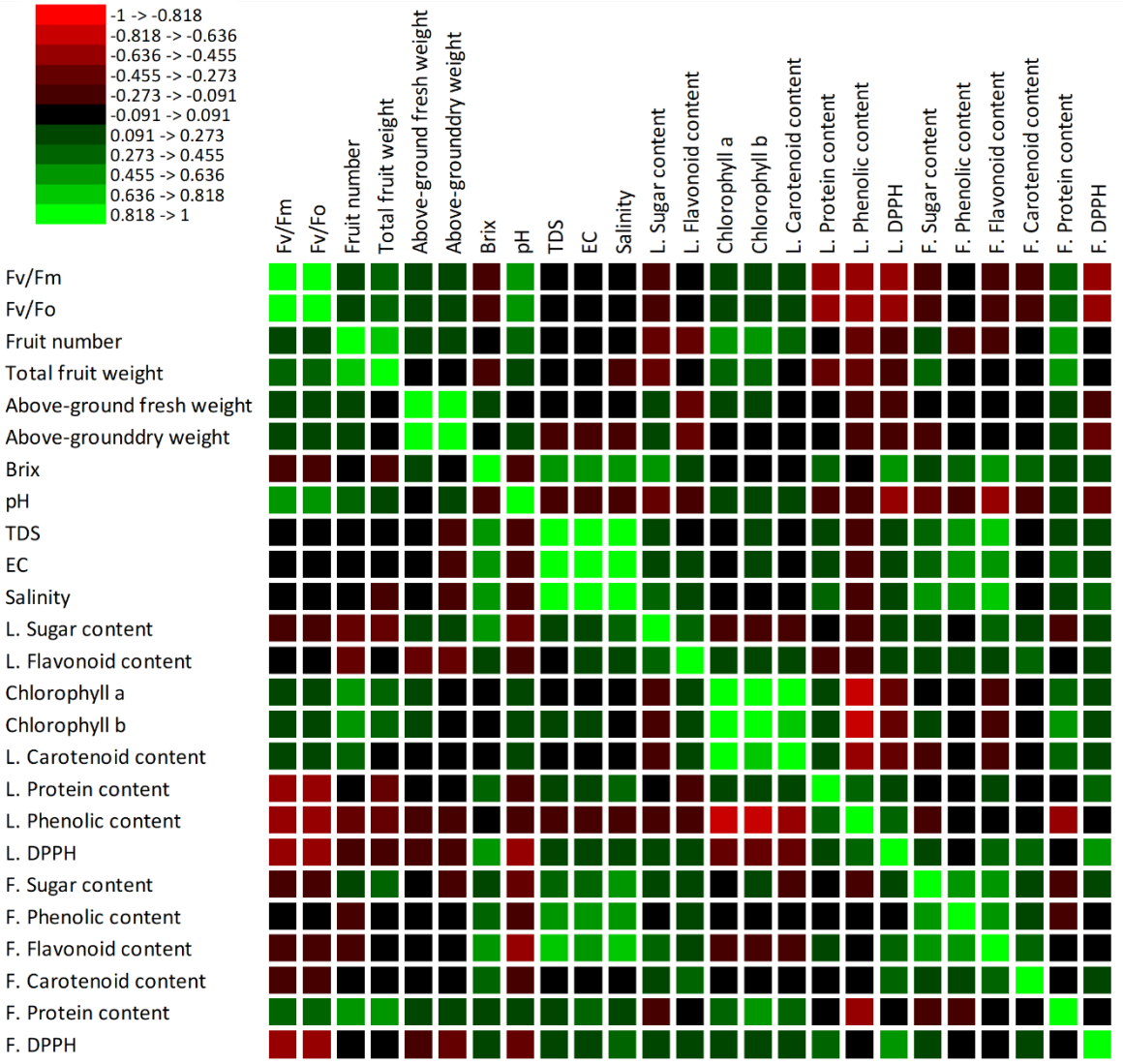

Figure 6.6. Pearson correlation matrix among the morpho-physiological, yield, quality, and phytochemical properties of tomato plants in response to PA and NPK combination. The red colour represents a strong negative association, and the green colour represents a strong positive association.

Moreover, chlorophyll a exhibited a significant ($p < 0.01$) association with chlorophyll b and total leaf carotenoid. Both chlorophyll a and b and leaf carotenoid contents had a significant ($p < 0.01$) negative and positive correlation with leaf total phenolic and DPPH content, and total fruit protein

respectively (Figure 6.6; Table S6.4). Also, both leaf total protein and leaf DPPH had a significant ($p < 0.01$) positive association with fruit DPPH while leaf total phenolic content had a negative correlation with fruit protein. Additionally, fruit total sugar content showed a significant ($p < 0.01$) positive correlation with fruit total phenolic and flavonoid content while fruit total phenolic content exhibited a significant ($p < 0.01$) positive association with fruit flavonoid (Figure 6.6; Table S6.4).

The 2D PCA biplot explained *ca*. 95% of the total variations in the dataset (Figure 6.7). Response variables and treatments that are closer to the arrow had the maximum effect on the overall plant productivity while those that are distant from the arrow exhibit a minimum effect. The results revealed that fruit juice EC, TDS, salinity, Brix, fruit total phenolic content, leaf and fruit total sugar, fruit total flavonoid content, fruit total protein, leaf and fruit carotenoid content, fruit DPPH, chlorophyll a and b, fruit number and total fruit weight were strongly influenced by PA and NPK fertilizer treatments (Figure 6.7). However, fruit juice pH and leaf total phenolics were weakly affected by the treatments. Additionally, chlorophyll fluorometric indices, aboveground fresh and dry weights, leaf total protein, leaf total sugar, leaf total flavonoid and leaf DPPH were moderately affected by the treatment applications (Figure 6.7). Moreover, 0.5% PA and 2% PA combined with full NPK rate had the maximum positive effect on the overall performance of tomato plants while no spray and water treatments with half NPK rate had the least effect on the growth and productivity of the greenhouse-grown tomato plants (Figure 6.7).

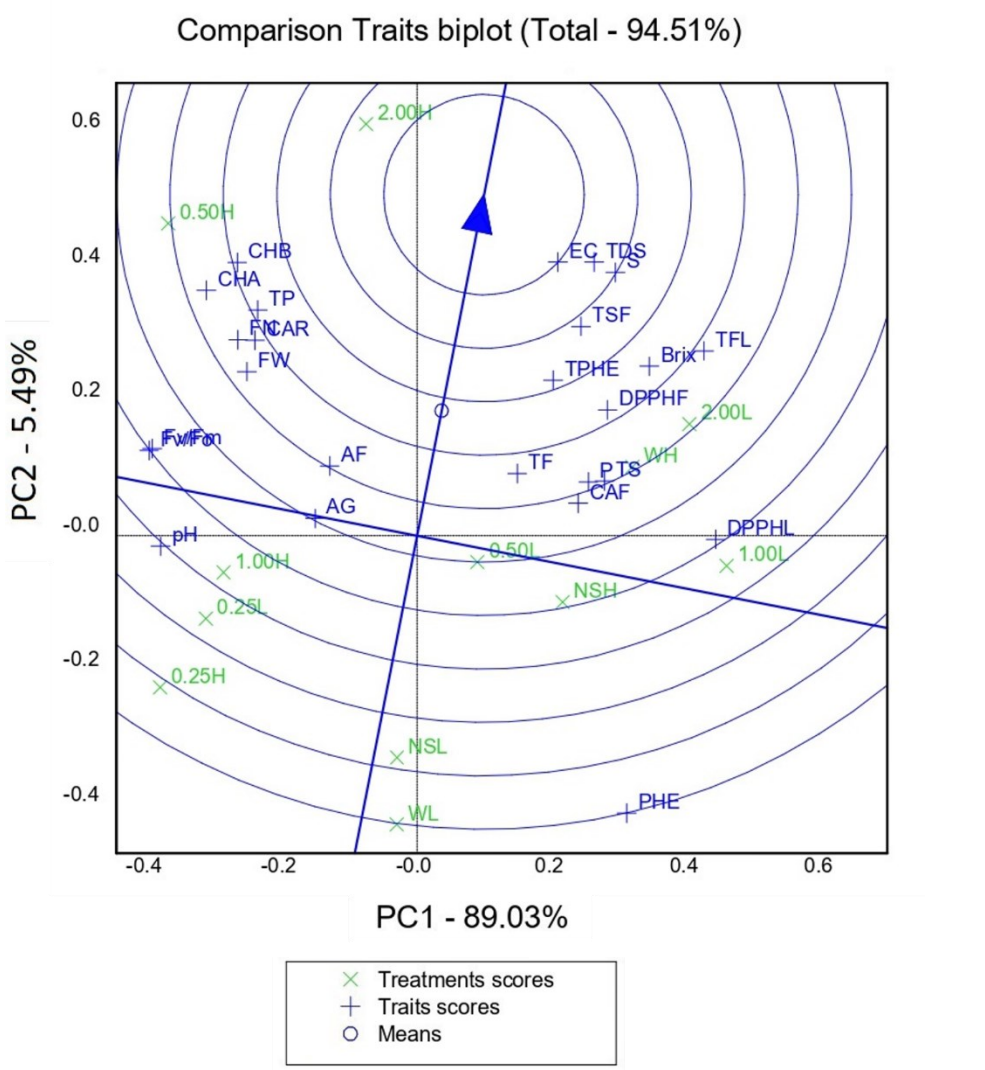

Figure 6.7. A two-dimensional principal component (2-D PCA) analysis biplot shows relationships amongst tomato plants' morpho-physiological, yield, quality, and phytochemical properties in response to pyroligneous acid (PA) and NPK combination. Projection of the variables in the principal component (PC1 and PC2) explained a total of 94.51% of the variations in the dataset. Variables that are closely located are not different compared to variables located at a distance within a quadrant or between quadrants. Total fruit number, FN; Total fruit weight, FW; Above-ground fresh weight, AF; Above-ground dry weight, AG; Fruit juice Brix, Brix; fruit juice pH, pH; fruit juice total dissolved solids, TDS; fruit juice electrical conductivity, EC; fruit juice salinity, S; Leaf total sugar, TS; Leaf total flavonoid content, TF; Chlorophyll a, CHA; Chlorophyll b, CHB; Leaf carotenoid, CAR; Leaf total protein, P; Leaf total phenolics, PHE; Leaf DPPH, DPPHL; Fruit total sugar, TSF; Fruit total phenolic content, TPHE; Fruit total flavonoid content, TFL; Fruit carotenoid, CAF; Fruit total protein, TP; Fruit DPPH, DPPHF. No spray + Full NPK rate, NSH; No spray + Half NPK rate, NSL; Water + Full NPK rate, WH; Water + Half NPK rate, WL; 0.25% PA + Full NPK rate, 0.25H; 0.25% PA + Half NPK rate, 0.25L; 0.5% PA + Full NPK rate, 0.5H; 0.5% PA + Half NPK rate, 0.5L; 1% PA + Full NPK rate, 1H; 1% PA + Half NPK rate, 1L; 2% PA + Full NPK rate, 2H; 2% PA + Half NPK rate, 2L.

6.4 DISCUSSION

The use of PA as a biostimulant to boost plant productivity and phytochemical properties in edible plant parts has spiked the interest of farmers and researchers. This is motivated by the quest for environmentally friendly strategies for sustainable crop production. The results of this study clearly revealed that foliar application of 0.25% and 0.5% PA increased *Fv*/*Fo* and *Fv/Fm* but were higher when combined with the full NPK rate which is recommended for tomato production. Chlorophyll fluorescence has been widely used to determine the photosynthesis performance of plants (Maxwell & Johnson, 2000). Previous studies revealed that PA application increased *Fv*/*Fm* values in rice (*Oryza sativa*) (Berahim et al., 2014), tobacco (*Nicotiana tabacum*) (Ye et al., 2022), and lettuce (*Lactuca sativa*) (Vannini et al., 2021).

Chlorophyll plays a crucial role in photosynthesis and the overall productivity of crops (Liu et al., 2019) and its level in plant leaves reflects the strength of the photosynthetic process (Fromme et al., 2003; Liu et al., 2019). In this study, 2% PA with full NPK rate increased chlorophylls a and b, suggesting that PA and NPK applications exhibited a synergistic effect on plant photosynthetic capacity. This result is consistent with previous studies where a similar increase in chlorophyll content with different PA concentrations have been reported (Berahim et al., 2014; Wang et al., 2019a; Vannini et al., 2021; Fedeli et al., 2022b; Ye et al., 2022). Besides, the PA used in this study was previously revealed to contain high levels of N, K and Ca, as well as other bioactive compounds (Ofoe et al., 2022a). In plants, N is a key modulator of nitrogenous compounds biosynthesis including chlorophyll and proteins, K is critical in enzyme activation, stomatal regulation and photosynthesis, while Ca facilitate nutrient uptake and cell elongation (Morgan et

al., 2013; Tripathi et al., 2014). Moreover, high polyphenol has been correlated with high chlorophyll content in leaf tissues due to the former's significant contribution to reducing oxidative stress-induced photorespiration (Meyer et al., 2006). PA is known to contain high levels of polyphenols, which have been suggested to mediate increased chlorophyll content in lettuce (Vannini et al., 2021). Hence, the increase in chlorophyll parameters with foliar PA application can be attributed to its rich bioactive compounds that can stimulate root nutrient uptake, reduce oxidative stress-induced photorespiration, and enhance the biosynthesis of chlorophyll.

The impact of PA on crop yield has been reported extensively by several authors (Kulkarni et al., 2008; Zulkarami et al., 2011; Mungkunkamchao et al., 2013; Zhu et al., 2021b; Fedeli et al., 2022a; Ofoe et al., 2022c). Similarly, our results showed that 2% PA irrespective of NPK fertilizer rate increased the total number of fruits and fruit weight followed by 0.5% PA combined with full NPK rate. Although the positive effect of NPK cannot be neglected, a similar increase in fruit number and weight have been reported in tomato (Mungkunkamchao et al., 2013; Benzon & Lee, 2016; Ofoe et al., 2022c) and sweet pepper (*Capsicum annuum*) (Jeong et al., 2006). Although the exact mechanism of the PA-mediated increase in fruit yield is still under investigation, it can be suggested that the increase in fruit yield could be due to increased chlorophyll content which indicates high photosynthetic translocation of assimilates into the increased number of fruits (Gifford & Evans, 1981; Liu et al., 2019). This was revealed in the correlation analysis that total fruit weight and number of fruits had a significant association with chlorophyll a and b content. Furthermore, PA is a complex mixture of numerous bioactive compounds including alkanes, phenolics, esters, organic acids and alcohol (Grewal et al., 2018). Previous study revealed that karrikins present in PA behave similarly to other phytohormones and interact with gibberellins,

ethylene and cytokinin to regulate plant growth and productivity (Van Staden et al., 2004). This indicates that PA might have induced and cooperated with the functions of enzymes and hormones to increase plant yield.

Chemical properties and phytochemical composition of edible plant portions are important parameters considered in the marketability of crops. This study showed that 2% PA with half NPK increased fruit Brix content while both fruit TDS and salinity were higher in 1% PA-treated plants under half NPK rate, and 0.5% and 2% PA-treated plants irrespective of NPK rate. Brix content is commonly used to determine the quality of tomato concentrate and correlates with the fruit TDS (Maach et al., 2021). Consistently, PA and other biostimulants were reported to increase the Brix of tomato fruits (Maach et al., 2021; Ofoe et al., 2022c). This indicates that PA can be used to enhance tomato fruit flavour and taste (Maach et al., 2021). Moreover, our correlation analysis confirmed that fruit salinity content exhibits a significantly positive association with its Brix, TDS and EC. Intriguingly, tissue sugar analysis revealed that the total fruit sugar content was higher than that of the leaf tissue. While PA application alone reduced leaf sugar content, 2% PA combined with full NPK rate recorded the highest fruit sugar content. It is well known that sugar production begins with leaf photosynthesis and the assimilate is translocated to the developing fruit in the case of tomato. Sugar distribution to fruits depends on several bioprocesses including photosynthesis rate, carbohydrate absorption and metabolism in sink organ, and phloem loading and unloading (Liesche & Patrick, 2017; Falchi et al., 2020). The overall reduction in leaf tissue sugar content suggests that PA application increased photo-assimilation and translocation of sugar into the fruits. Fedeli et al. (2022b) reported a similar reduction of sugar content in lettuce leaves following PA treatment. Also, some studies have shown an increase in fruit sugar content in tomato

(Ofoe et al., 2022c) and rock melon (Zulkarami et al., 2011). It is therefore plausible to indicate that the increased fruit sugar content can be linked to the high photosynthetic performance of PA-treated plants.

Moreover, leaves of some crops have been reported to contain a high content of phytochemicals (e.g., flavonoids and phenolics) than fruit tissues (Harris et al., 2007; Dawson, 2017). An increase in phytochemicals in leaf tissues following PA application has been reported in lettuce (Fedeli et al., 2022b) and strawberry (*Fragaria* × *ananassa*) (Kårlund et al., 2014). The increase in tomato leaves phytochemicals in the present study can be attributed to the high phenolic and organic acid content in PA as previously reported by Loo et al. (2008). This finding indicates that PA can be adopted as a strategy to increase the nutritional and health value of leafy vegetables. Generally, tomato fruits are deemed as a good reservoir of phytochemicals including carotenoids, phenolics and flavonoids (Chaudhary et al., 2018). In this study, 0.5% PA with half and full NPK rates enhanced fruit carotenoid and phenolics contents respectively, while 2% PA increased fruit flavonoid content. Accordingly, several studies have reported that PA application increased phenolics and flavonoid contents in tomato fruits (Benzon & Lee, 2016; Ofoe et al., 2022c).

Carotenoids are lipophilic antenna pigments in photosynthesis and are crucial for maintaining good human health (Young & Lowe, 2018). The increased carotenoid content with PA application can be attributed to the stimulation of physiological and molecular pathways involved in nitrogen metabolism (Ertani et al., 2014; Young & Lowe, 2018). Besides, these compounds are known to exhibit high antioxidant properties by scavenging reactive oxygen species (ROS) radicals and thereby, protecting cells against oxidative stress (Chaudhary et al., 2018; Nowak et al., 2018). High

ROS scavenging activity was recorded following 2% PA treatment. The increase in DPPH activity was highly expected and may be correlated with enhanced phytochemical content as previously reported (Benzon & Lee, 2016; Fedeli et al., 2022a). Additionally, it was reported that the high phenolic content of PA exhibited high anti-lipid peroxidation and antioxidant capacity (Loo et al., 2008; Wei et al., 2010; Ofoe et al., 2022a). These findings suggest that foliar PA application with NPK fertilizer combination may be considered as an environmentally friendly plant growth promotion technique to increase fruit nutritional quality and promote health benefits.

Fruit mineral elements are crucial for numerous plant physiological and biochemical processes, and constitute a relatively small portion of dry fruit tissues (Abou Chehade et al., 2018; Bhat et al., 2020). This study showed that both 0.25% and 0.5% PA combined with full NPK rate enhanced fruit N content while 0.5% PA increased fruit P. The 1% PA with half NPK increased fruit K and Zn content whereas 2% PA increased fruit K and Fe irrespective of NPK rate. Additionally, 2% PA with half NPK rate increased fruit Mg content. According to Bhat et al. (2020), the uptake of these nutrients by plants is dependent on the soil constituents and/or supplied when plants are foliar sprayed with fertilizers or biostimulants. Besides, the increase in N, P and K content can be attributed to increased soil supply of NPK fertilizer rate. Also, increased nutrient uptake is promoted by increased primary or secondary metabolism and enhanced enzyme activities for physiological growth (Bhat et al., 2020). These results agree with previous studies where PA and other biostimulants were reported to increase fruit mineral elements in tomato (Abou Chehade et al., 2018; Ofoe et al., 2022c). Although the mechanism by which PA increase these elements remains unknown, it can be speculated that the bioactive composition of PA could: (1) promote sink strength for continuous mineral element flow and accumulation (Calvo et al., 2014); (2)

stimulate genes encoding nutrient transporters in cell membranes; and (3) stimulate root system to facilitate intense nutrient uptake and translocation (Wang et al., 2019b).

6.5 CONCLUSION

The present study clearly showed a synergistic effect of foliar PA application and soil-drenched NPK in enhancing tomato productivity and phytochemical composition. Foliar application of 0.25% and 0.5% PA increased chlorophyll fluorometric parameters, while 2% PA with full NPK rate increased leaf chlorophyll content. Also, 2% PA increased the total number of fruits irrespective of NPK rate but increased the overall fruit weight and marketable number of fruits with full NPK rate. The PA-treated plants accumulated higher phytochemical content in their leaves than in fruit tissues except for total sugar. The 2% and 0.5% PA with various NPK combinations enhanced fruit phytochemical contents. Besides, the synergistic effect of PA and fertilizer increased fruit mineral elemental composition. Taken together, this study demonstrated that 2% PA with full NPK rate is the best treatment combination that can be adopted to increase the productivity and nutritional benefits of greenhouse-grown tomato plants and can be extended to improve the nutritional and health value of leafy vegetables. However, further study is required to investigate the molecular basis of PA biostimulatory effect on plants. Furthermore, PA application in mainstream agriculture represents an eco-friendly novel natural product that can contribute to the achievement of the United Nations' sustainable development goals by enhancing the production of nutrient-dense vegetables, promoting sustainable crop production, and ending world hunger.

CHAPTER 7: PYROLIGNEOUS ACID IMPROVES TOMATO GROWTH AND ALLEVIATES AL STRESS BY ENHANCING OSMOLYTE ACCUMULATION AND ANTIOXIDANT DEFENCE SYSTEM

A version of this chapter has been submitted to **Plant and Soil Journal**. The citation is:

Ofoe, R., Thomas, R. H. And Abbey, L. (2023). Pyroligneous acid improves tomato growth and alleviates Al stress by enhancing osmolyte accumulation and antioxidant defence system. *Plant and Soil*. Under review.

7. ABSTRACT

Pyroligneous acid (PA) is an aqueous mixture of bioactive compounds that improve crop productivity and resilience to several environmental stresses. However, its mechanism of action in plants under aluminum (Al) stress is unknown. In this study, we examined the morpho-physiological and biochemical response of tomato (*Solanum lycopersicum* 'Scotia') seedlings treated to varying PA concentrations (0, 0.25, 0.5 and 1% PA/ddH_2O (*v*/*v*)) under Al stress (1- and 4-mM aluminum chloride ($AlCl_3$)). The results indicate that Al stress at 4 mM considerably reduced plant height, root growth, aboveground fresh weight, and photosynthetic efficiency compared to the control. However, plants treated with 0.25% and 0.5% PA mitigated Al stress and enhanced root growth, leaf gas exchange parameters and chlorophyll content compared to the control. In most cases, the effect of 1 mM Al was comparable to that of the control while a high PA concentration (1% PA) aggravated Al phytotoxicity on plant morphology. Also, Al-induced hydrogen peroxide and malonaldehyde contents were reduced while proline, sugar and antioxidant

compounds were enhanced in PA-treated plants. Additionally, PA-treated plants showed increased peroxidase and ascorbate peroxidase and reactive oxygen species-scavenging activities. Furthermore, PA treatment restricted Al uptake and facilitated the availability and translocation of boron, manganese, sodium and phosphorus in tomato plants. These findings suggest that PA can be used as a novel strategy to detoxify Al and improve plant tolerance in agricultural production systems.

Keywords: Wood vinegar; biostimulant; aluminum toxicity; root growth; Solanaceae; pyrolysis

7.1 INTRODUCTION

Crop growth and productivity are faced with frequent occurrences of several environmental factors. Among these factors, soil acidity with pH < 5.0 is prevalent as a major limiting factor to field crop production (Kochian et al., 2015). Acid soils comprise over 50% of the world's arable land that sustains up to 80% of global vegetable production (Sade et al., 2016; Slessarev et al., 2016). Acid soils are notably marked by nutrient deficiencies and increased presence of toxic metals including aluminum (Al), manganese (Mn) and iron (Fe), with Al being the major constraint for crop production on such soils (Bojórquez-Quintal et al., 2017; Ofoe et al., 2023). Aluminum is abundant in the earth's crust and its availability can be associated with the acidity level of the soil (Kochian et al., 2015). Al occurs in most soils as non-toxic oxides and silicates which interact with plant roots. However, at soil pH below 5, Al solubilizes into trivalent forms to which most plants including tomato (*Solanum lycopersicum*) are sensitive to even at low concentrations, leading to a wide range of Al-induced phytotoxicity (Kochian et al., 2015). The danger posed by Al stress is further aggravated by climate change and the intensive use of synthetic agrochemicals (Bojórquez-Quintal et al., 2017; Bungau et al., 2021).

The primary symptom of Al stress is the inhibition of root growth and disruption of root systems (Kochian et al., 2015). Such interference with root systems restricts water and nutrient uptake and thereby, reducing the development of aerial parts. This toxic effect of Al on plant morphology has been widely reported in several crop species such as tomato (Wang et al., 2020b; Ofoe et al., 2022b), common bean (*Phaseolus vulgaris*), rice (*Oryza sativa*) (Awasthi et al., 2017), highbush blueberry (Cárcamo et al., 2019) and wheat (*Triticum aestivum*) (Hossain et al., 2006). Nevertheless, the maintenance of root growth under Al stress is an important indication of Al tolerance (Cárcamo et al., 2019; Siqueira et al., 2020). Also, Al stress damages leaf thylakoid structures, decreased chlorophyll content, photosynthetic and transpiration rates, and stomatal conductance thereby, disrupting photosynthesis (Chen et al., 2005a; Zhao et al., 2017; Cheng et al., 2020). Additionally, Al stress induces the production and accumulation of reactive oxygen species (ROS), which causes oxidative impairment of cellular and metabolic processes (Sharma et al., 2012; Du et al., 2020). Excessive ROS accumulation promotes loss of plasma membrane integrity *via* lipid peroxidation and damage of macromolecules including proteins and nucleic acids (Sharma et al., 2012; Yamamoto, 2019). Accordingly, these phytotoxic effects result in considerable yield reduction and total crop loss if not managed (Siqueira et al., 2020; Ofoe et al., 2023).

To counter the destructive effect of Al stress, most plants have evolved adaptive mechanisms to promote tolerance. Al tolerance mechanisms have been studied extensively in several plant species (Kochian et al., 2015). Al tolerant plants may possess an Al exclusion mechanism that restricts Al entry and/or retain Al in roots and reduces its translocation to aerial parts or an internal tolerance

mechanism which promotes Al entry, detoxification with organic acid and storage in subcellular compartments (Kochian et al., 2015; Ofoe et al., 2023). Additionally, internal tolerance also involves the accumulation of osmolytes including proline and sugar, and the activation of antioxidant enzymes (peroxidases (POD), superoxide dismutase (SOD), catalase (CAT) and ascorbate peroxidases (APX) and metabolites such as phenolics, carotenoids, and ascorbate (Gill & Tuteja, 2010; Waszczak et al., 2018; Wei et al., 2021). These osmolytes and antioxidants function together to promote water retention, scavenge ROS radicals and stabilize membranes and macromolecules (Pirzadah et al., 2019; Ejaz et al., 2020). However, these adaptive strategies usually affect the growth and productivity of plants.

Consequently, farmers in recent years have begun to shift toward sustainable practices that emphasize alternative strategies to enhance plant productivity and resilience to environmental stresses (Dudaš et al., 2016). One such promising strategy is the use of biostimulants that promote plant growth and resilience to environmental stresses, which have attracted the interest of farmers and researchers (Hasanuzzaman et al., 2021; Ma et al., 2022). An example is pyroligneous acid (PA), which has been used extensively used as a plant biostimulant (Grewal et al., 2018). PA is an aqueous reddish-brown liquid produced through the carbonation of organic biomass in the presence of limited oxygen (Grewal et al., 2018). It is a complex mixture which contains 80-90% water and over 200 water-soluble bioactive compounds such as organic acids, phenolics, sugar and alcohol derivatives, and mineral elements (Wei et al., 2010; Grewal et al., 2018; Ofoe et al., 2022a). However, the chemical constituent of PA depends on the pyrolytic temperature, heating rate and feedstock. Also, PA contains a biologically active compound called butenolide, which belongs to a novel family of growth regulators known as karrikins (Dixon et al., 2009; Grewal et al., 2018).

Besides, its mode of action and signalling are similar to that of known plant hormones and have been demonstrated to enhance plant growth and development (Chiwocha et al., 2009; Dixon et al., 2009). Moreover, PA application has been reported to enhance seed germination, vegetative and reproductive growth, and yield of several crops (Grewal et al., 2018; Wang et al., 2019b).

Recently, the use of PA in mitigating abiotic stresses has gained attention in scientific literature. PA has been reported to enhance plant growth and tolerance to drought, heavy metal and salinity stress (Benzon & Lee, 2017; Wang et al., 2019b; Ma et al., 2022). Under drought stress, Wang et al. (2019b) showed that PA priming enhanced wheat seedling root growth and facilitates the activation of antioxidants and stress-related proteins. Likewise, Ma et al. (2022) reported that PA treatment of rapeseed (*Brassica napus*) under salinity improved plant biomass, leaf chlorophyll content, and transpiration and photosynthesis. Additionally, PA treatment reduced ROS accumulation and lipid peroxidation, and enhanced osmolyte and antioxidant activities that promoted salinity tolerance (Ma et al., 2022). Also, under Al stress, seed priming with PA was demonstrated to increase tomato seedling root growth and reduced ROS-induced oxidative stress by increasing the expression of antioxidant genes (Ofoe et al., 2022b). Moreover, the high antioxidant activities of PA are related to its high phenolic content, which induces high ROS-scavenging activities, anti-lipid peroxidation capacity and reducing power (Loo et al., 2007; Wei et al., 2010). Furthermore, the rich organic acids in PA are reported to chelate metals and thereby, restrict their uptake and toxic effects on Indian mustard (*Brassica juncea*) growth and productivity (Benzon & Lee, 2017). These reports indicate that PA has the potential not only to enhance plant growth and development, but also to promote tolerance to environmental stresses. Despite the positive effect of PA on plant growth, its effects on Al tolerance remain unknown. To date, no

studies have investigated the morpho-physiological and biochemical responses of PA-treated plants on Al stress. In this study, we examine the effect of PA on tomato seedling growth under Al stress.

7.2 MATERIALS AND METHODS

7.2.1 Plant material and experimental condition

The experiment was conducted from January to March 2022 and repeated from March to May 2022 at the Department of Plant, Food, and Environmental Sciences, Faculty of Agriculture, Dalhousie University, Truro. Tomato "Scotia" seeds were purchased from Halifax Seeds (Halifax, NS, Canada) and PA derived from white pine (*Pinus strobus*) biomass was obtained from Proton Power Inc (Lenoir City, TN, USA). The seeds were sterilized with 10% sodium hypochlorite for 10 min and thoroughly washed three times with sterile distilled water. The seeds were further sterilized with 70% ethanol for 5 mins and washed five times with sterile distilled water. The sterilized seeds were sown in a Pro-Mix® BX (Premier Tech Horticulture, Rivière-du-Loup, QC, Canada) and grown for four weeks in a growth chamber (Conviron Controlled Environments Ltd, Winnipeg, MB, Canada) with 16/8 h day/night photoperiod, 24/22°C day/night temperature cycle, 300 µmol m^{-2}•s^{-1} light intensity and 70% relative humidity. Uniformly grown seedlings with 8-cm root length at the three to four true-leaf stage were transplanted into a 10.2-cm plastic pot containing 500 g of sterilized sand with an average particle size of 0.5–1.0 mm. The seedlings were maintained with a 25% strength Hoagland nutrient solution at a pH of 5 for a week in the growth chamber.

7.2.2 Experimental treatment and design

After one week of acclimation, half-strength followed by full-strength nutrient solutions were amended with varying PA and Al concentrations and applied every week. PA treatment was applied to the nutrient solution at 0%, 0.25%, 0.5% and 1% PA/ddH_2O (*v/v*) with Al ($AlCl_3$) at 0, 1 mM and 4 mM. The nutrient solution (pH=4.5) was renewed every 3 days to maintain adequate moisture content. During the entire study period, the pH of the amended nutrient solution (PA with or without Al) was monitored frequently and adjusted to 4.5, using either sodium hydroxide (NaOH) or HCl. The study was arranged in a 4 × 3 factorial completely randomized design with five replications at one plant per replication.

7.2.3 Plant physiological measurement

Chlorophyll content was measured on three fully expanded leaves per plant using a SPAD 502-plus chlorophyll meter (Spectrum Technologies, Inc., Aurora, IL, USA). Chlorophyll fluorescence indices were measured on the same leaves using a chlorophyll fluorometer (Optical Science, Hudson, NH, USA). During each fluorometric measurement, a clip was fixed to the leaf and dark-adapted for 25 mins before initial fluorescence yield (*Fo*) was measured, followed by the maximum chlorophyll fluorescence (*Fm*) emitted when a saturating light pulse was increased from 0 to 3000 μmol m^{-2}•s^{-1}. Variable chlorophyll fluorescence (*Fv*) was calculated as $Fv = Fm - Fo$. Other fluorometric parameters including maximum quantum efficiency of PSII (*Fv*/*Fm*) and potential photosynthetic capacity (*Fv*/*Fo*) were determined at each saturating pulse (Maxwell & Johnson, 2000). Leaf gas exchange parameters including net photosynthetic rate (A) and transpiration rate (E) were measured from the same three leaves per plant using LCi portable photosynthesis system (ADC BioScientific Ltd., Hoddesdon, UK).

7.2.4 Morphological measurement

Plant growth parameters were measured 40 DAT. Plant height was measured with a ruler from the stem collar to the highest leaf tip. Stem girth was measured at 3 cm from the collar with a Vernier caliper (Mastercraft®, Toronto, ON, Canada). The number of flower buds was recorded for each plant. Root growth parameters were analyzed for each plant using an STD4800 Pant Root Scanner (Epson Perfection V850 Pro, Epson Canada Ltd, Markham, ON, Canada) equipped with WinRHIZO^{TM}2000 software (Regent Instruments, Sainte Foy, QC, Canada). Root tissues were taken out of the sand culture and washed several times in deionized water. The WinRHIZO^{TM}2000 software was used to take digital root images and for the analyses of morphological traits including total root length, surface area and volume for a defined region (Himmelbauer, 2004). The total fresh weight of both shoots and roots tissues was estimated using a portable balance (Ohaus navigator®, ITM Instruments Inc., Sainte-Anne-de-Bellevue, QC, Canada) followed by oven drying at 65°C for 72 h for dry weight determination. Leave tissues (15 leaves from 5 plants per treatment) were collected and immediately frozen in liquid nitrogen. The frozen samples were ground into a fine powder and stored in a -80°C freezer for biochemical analyses.

7.2.4.1 Chlorophyll a, b and carotenoid contents

Leaf tissue chlorophyll and carotenoid contents were determined as described by Lichtenthaler (1987). Approximately, 0.2 g of ground leaf tissue was homogenized in 2 mL of 80% acetone. The mixture was centrifuged at 15000 × *g* for 15 min and the supernatant was diluted in a ratio of 1:1 with 80% acetone. The absorbance of the supernatant was measured at 646.8, 663.2, and 470 nm using a UV-Vis spectrophotometer (Cole-Parmer®, Vernon Hills, IL, USA) against 80% acetone

as blank. Chlorophyll and carotenoid contents were expressed as μg g^{-1} fresh weight (FW) of the sample.

7.2.4.2 Hydrogen peroxide production and lipid peroxidation determination

Hydrogen peroxide (H_2O_2) content of the leaf tissues was determined according to the method described by Alexieva et al. (2001). Briefly, 0.2 g of ground leaf tissue was homogenized in 1.8 mL 0.1% (*w/v*) trichloroacetic acid (TCA) and centrifuged at 16000 × *g* at 4ºC for 10 min. 200 μL of supernatant was added to 200 μL of 100 mM potassium phosphate buffer (pH 7.0) and 800 μL of 1 M potassium iodide. The reaction was incubated in the dark for 60 min. The absorbance of the mixture was measured at 390 nm and the H_2O_2 content was defined using a H_2O_2 standard curve. Malondialdehyde (MDA) content was used as an indication of lipid peroxidation. MDA content was determined following the procedures described by Hodges et al. (1999) with slight modifications. A 0.2 g ground leaf tissue was mixed with 1.8 mL of 0.1% (*w/v*) TCA and centrifuged at 16000 × *g* for 10 mins at 4ºC. 500 μL of the supernatant was added to an equal volume of 0.5% thiobarbituric acid (TBA) in 20% TCA. The reaction mixture was then incubated at 95ºC for 30 mins, cooled on ice, and centrifuged at 12000 × *g* for 5 min. The absorbance of the resultant mixture was measured at 532 nm and non-specific absorption at 600 nm using UV-VIS spectrophotometer. The MDA content was estimated from the extinction coefficient 155 m/M cm as $C = [Abs\ (535–600) \div 155{,}000] \times 10^6$. Total MDA content was expressed as nmol MDA g^{-1} FW.

7.2.4.3 Total ascorbate content

Total ascorbate was determined following the procedure described by Gillespie and Ainsworth (2007) with slight modification. Briefly, 0.2 g of ground leaf tissue was mixed with 1.5 mL ice-

cold freshly prepared 5% TCA and centrifuged at 12000 × *g* for 10 min at 4°C. 100 µL of the supernatant was transferred into a new tube and 200 µL of 75 mM phosphate buffer (pH 7.0) was added. A 100 µL of 10 mM dithiothreitol (DTT) was added, vortexed for 30 s and incubated at room temperature for 15 min. 100 µL of 0.5% (*w/v*) N-ethylmaleimide was then added to remove excess DTT and vortexed for 30 s. A reaction mixture containing 400 µL of 10% (*w/v*) TCA, 400 µL of 44% orthophosphoric acid, 400 µL of 4% (*w/v*) α-α-1-dipyridyl in 70% ethanol and 200 µL of 30 g/L ferric chloride was added to obtain colour. The mixture was further incubated at 40°C for 60 min in a shaking incubator and the absorbance was read at 525 nm using a UV-VIS spectrophotometer. The total ascorbate content was determined using an L-ascorbic acid standard curve and expressed as µmol g^{-1} FW.

7.2.4.4 Soluble sugar content

Total sugar content was determined using the phenol-sulphuric acid procedure described by Dubois et al. (1956). A 0.2 g of ground leaf tissue was mixed with 10 mL of 90% ethanol and incubated in a water bath at 60°C for 60 min. The volume of the mixture was re-adjusted to 10 mL with 90% ethanol and centrifuged at 12000 × *g* for 3 min. 1 mL of the supernatant was thoroughly mixed with 1 mL of 5% phenol in a thick-walled glass test tube and 5 mL of concentrated sulphuric acid was added. The reaction mixture was vortexed for 20 s and incubated in the dark for 15 min before cooling to room temperature. The absorbance was read at 490 nm against a blank using a UV-VIS spectrophotometer. Total sugar content was estimated using a sugar standard curve and expressed as µg of glucose g^{-1} FW.

7.2.4.5 Total phenolic content

Total phenolic content was determined using the Folin-Ciocalteu assay procedure described by Ainsworth and Gillespie (2007) with slight modification. Briefly, a 0.2 g of ground leaf tissue was homogenized in 2 mL of ice-cold 95% methanol and incubated in the dark at room temperature for 48 h. The mixture was centrifuged at 12000 × *g* for 5 min and 100 µL of supernatant was added to 200 µL of 10% (*v/v*) Folin-Ciocalteau reagent. The mixture was vortexed for 5 min, and 800 µL of 700 mM sodium carbonate was added and incubated in a dark at room temperature for 2 h. The absorbance was read at 765 nm against a blank using a UV-VIS spectrophotometer. Total phenolic content was estimated using a gallic acid standard curve and expressed as mg gallic acid equivalents per g fresh weight (mg GAE g^{-1} FW).

7.2.4.6 Total flavonoid

Total flavonoid content was estimated according to the colorimetric method described by Chang et al. (2002). A 0.2 g of ground leaf tissue was mixed with 2 mL of ice-cold 95% methanol and centrifuged at 15000 × *g* for 10 min. 500 µL of supernatant was added to a reaction mixture containing 1.5 mL 95% methanol, 0.1 mL of 10% $AlCl_3$, 0.1 mL of 1 M potassium acetate and 2.8 mL distilled water. The resulting mixture was incubated at room temperature for 30 min and the absorbance was measured at 415 nm against a blank lacking $AlCl_3$ using a UV-VIS spectrophotometer. Total flavonoid content was estimated using quercetin standard curve and expressed as µg quercetin g^{-1} FW.

7.2.4.7 Proline content

Proline content was estimated following the method described by Bates et al. (1973). A 0.2 g of ground leaf tissue was homogenized in 3 mL of 3% sulfosalicylic acid followed by centrifugation at 12000 × *g* for 10 min. 400 µL of the supernatant was mixed in a container with 400 µL of 3% sulfosalicylic acid, 800 µL glacial acetic acid, and 800 µL acidic ninhydrin and the mixture was incubated at 96ºC for 1 h. The reaction was cooled on ice and mixed with 4 mL of toluene to extract red chromophore. After 5 min, the red chromophore containing toluene was transferred into a new vial and the absorbance was measured at 520 nm using toluene as a blank using UV-VIS spectrophotometer. The proline content was calculated using an L-proline standard curve and expressed as mmol g^{-1} FW.

7.2.4.8 DPPH free radical scavenging capacity

The DPPH radical scavenging capacity of PA-treated plants under Al stress was determined using the method described by Dudonne et al. (2009) with little modification. A 0.2 g of ground leaf tissue was homogenized with 1.5 mL of pure methanol and centrifuged at 12000 × *g* for 10 min. Aliquots of 100 µL of the supernatant was mixed with 2.9 mL of 60 µM fresh DPPH methanolic solution and the resultant mixture incubated in the dark at room temperature. After 30 min, the absorbance was measured at 515 nm against a methanol blank using a UV-VIS spectrophotometer and radical scavenging activity was determined as Inhibition (%) = $[(A_B – A_S)/ A_B] \times 100\%$; where A_B is the absorbance of the blank sample and A_S is the absorbance of the samples.

7.2.4.9 Protein content and antioxidant enzyme activity

To determine protein content, 0.2 g of ground leaf tissue was mixed with 1.8 mL ice-cold extraction buffer (50 mM potassium phosphate buffer (pH 7.0), 1% polyvinylpyrrolidone, and 0.1 mM EDTA) and centrifuged at 12000 × *g* for 20 min at 4ºC. The supernatant (crude enzyme extract) was transferred into a new vial and 1 mL of Bradford's reagent was added. The absorbance of the mixture was read at 595 nm after 5 min using UV-VIS spectrophotometer and the protein content was calculated from a bovine serum albumin standard curve ranging from 200 to 900 µg mL^{-1} (Bradford, 1976). POD (EC 1.11.1.7) activity was measured according to the procedure described by Chance and Maehly (1955) with little modification. A 100 µL of crude enzyme extract was added to a reaction mixture containing 100 mM potassium-phosphate buffer (pH 6.0), 5% pyrogallol, and 0.5% H_2O_2. The reaction mixture was incubated at room temperature for 5 min and 1 mL of 2.5 N H_2SO_4 was added to terminate the reaction. The absorbance was measured at 420 nm against a blank (Milli-Q water) using UV-VIS spectrophotometer. One unit of POD forms 1 mg of purpurogallin from pyrogallol in 20 s at pH 6.0 and 20°C.

For ascorbate peroxidase (APX) activity, 100 µL of the crude enzyme extract was added to a reaction mixture containing 50 mM potassium phosphate (pH 7.0), 0.5 mM ascorbic acid and 1 mM H_2O_2. The mixture was allowed to stand at room temperature for 30 s and the decrease in absorbance of ascorbate was read at 290 nm against the reaction mixture without H_2O_2 and enzyme extract at 20 s intervals for 1 min using a UV-VIS spectrophotometer. The amount of APX that was able to oxidize 1 µmol of ascorbate at 25°C within 1 min is defined as 1 unit of the enzyme (U/min /mg) (Nakano & Asada, 1981)

7.2.5 Aluminum and other mineral element uptake and translocation

To examine Al and other mineral elements uptake from root to shoot translocation, leaves, stem and root tissues were separated and oven dried at 65°C for 72 h before grinding into a fine powder using a bead mill (Retsch, Haan, Germany). Approximately 0.5 g of each ground tissue was digested with a microwave-assisted nitric acid digestion method using Mars 6 Microwave (CEM, USA) (Huang et al., 2004). Trace element contents were analyzed with an Inductively Coupled Plasma Mass Spectrometry using a Varian model 820MS ICP Mass Spectrometer (Varian, Mulgrave, VIC, Australia) at the Prince Edward Island Analytical Laboratories (PEIAL), Charlotte town, Canada. Mineral element translocation was calculated as the ratio of specific metal content in the shoot (leaves and stems) to that of the root as:

Translocation factor (TF) = C_{shoot} / C_{root}; where, C_{shoot} is the concentration of metal in shoot and C_{root} = concentration of metal in root (Bose & Bhattacharyya, 2008).

7.2.6 Statistical analysis

All data collected from the experiments were subjected to two-way analysis of variance (ANOVA) for Al and PA interaction using Minitab (Minitab 19 Statistical Software, Minitab, State College, PA, USA). A Kruskal-Wallis test was performed for number of flower buds. Means with significant differences were separated using Tukey's honestly significant difference (HSD) post hoc test at $p \leq 0.05$.

7.3 RESULTS

7.3.1 Morphological characteristics

Tomato plant morphological characteristics were significantly ($p < 0.001$) affected by PA and Al but not their interaction (Table 7.1; Figure 7.1). The application of 0.25% PA slightly increased plant height (*ca*. 1.0%), flower number (*ca*. 3.8%), root fresh (*ca*. 10.4%) and dry (*ca*. 15.0%) weight, and root volume (*ca*. 15.4%) compared to the control (Table 7.1). However, 1% PA significantly ($p < 0.001$) reduced these morphological parameters compared to the control (Table 7.1). Under 1 mM Al, the morphological parameters were comparable to that of the 0 mM Al while the 4 mM Al significantly ($p < 0.001$) reduced plant height, root volume and aboveground fresh weight by *ca.* 9.8%, 10.0% and 25.7%, respectively compared to the control (Table 7.1; Figure 7.1). Additionally, stem diameter, flower bud number, root fresh weight and aboveground dry weight of the plants under 4 mM Al were non-significantly ($p > 0.05$) reduced by *ca*. 4.3%, 17.4%, 4.5%, 10.0% and 14.5% respectively compared to plants under 0 mM Al. On the average, total root length and surface area were significantly ($p < 0.001$) reduced in PA-treated plants under 0 mM Al (Figure 7.1&2). Nevertheless, 0.25% PA significantly ($p < 0.001$) increased total root length by *ca.* 29.3% and 65.1% under both 1 mM Al and 4 mM Al, respectively compared to their respective Al alone treatments (Figure 7.2A). Similarly, total root surface area was significantly ($p < 0.001$) increased in 0.25% PA-treated plants under 1 mM Al by *ca*. 46.0% and non-significantly ($p > 0.05$) increased by *ca.* 39.1% under 4 mM Al compared to 1 mM Al and 4 mM Al alone respectively (Figure 7.2B).

Table 7.1. Morphological response of tomato 'Scotia' seedlings treated with pyroligneous acid (PA) under aluminum (Al) stress.

PA (%)	Plant height (cm)	Stem diameter (mm)	Flower bud[1] number	Root fresh weight (g)	Root dry weight (g)	Root volume (cm^3)	Above-ground fresh weight (g)	Above-ground dry weight (g)
0	38.07±2.29 ab	5.91±0.42 a	42.2±2.59 a	4.42±0.99 a	0.40±0.12 a	4.95 ±1.64 a	26.21±4.83 a	2.56±0.64 a
0.25	38.37±3.40 a	5.91±0.48 a	43.8±1.60 a	4.88±0.61 a	0.46±0.07 a	5.71±1.29 a	24.36±3.55 a	2.50±0.65 a
0.5	35.80±3.07 b	5.11±0.52 b	25.6±1.12 b	2.68±0.83 b	0.40±0.85 a	2.83±1.35 b	13.24±3.51 b	1.41±0.44 b
1	27.48±2.55 c	4.33 ±0.59 c	10.4±1.44 c	1.28±0.32 c	0.19±0.06 b	1.39±0.45c	5.84±1.50 c	0.58±0.18 c
Al (mM)	**Plant height (cm)**	**Stem diameter (mm)**	**Flower bud[1] number**	**Root fresh weight (g)**	**Root dry weight (g)**	**Root volume (cm^3)**	**Above-ground fresh weight (g)**	**Above-ground dry weight (g)**
0	36.58±5.68 a	5.41±0.86 a	33.40±3.06 a	2.89±1.72 a	0.32±0.16 a	3.20±2.34 ab	16.46±9.02 a	1.59±1.15 a
1	34.81±4.07 ab	5.47±0.79 a	30.60±2.74 a	3.16±1.64 a	0.36±0.15 a	3.72±2.22 a	16.46±8.09 a	1.60±0.94 a
4	33.00±5.48 b	5.18±0.86 a	27.60±2.48 a	2.76±1.56 a	0.32±0.75 a	2.88±1.85 b	12.23±6.78 b	1.36±0.86 a
Significant level								
PA	<0.001	<0.001	<0.001	<0.001	<0.001	<0.001	<0.001	<0.001
Al	<0.001	0.159	0.574	0.154	0.429	0.038	<0.001	0.072
PA × Al	0.415	0.667	-	0.592	0.211	0.774	0.576	0.615

Values are means ± standard deviation of five replicates and the different letters indicate significant differences according to Tukey's honestly significant difference (HSD) post hoc test at $p < 0.05$.[1] Non-parametric analysis has no p-value for interaction.

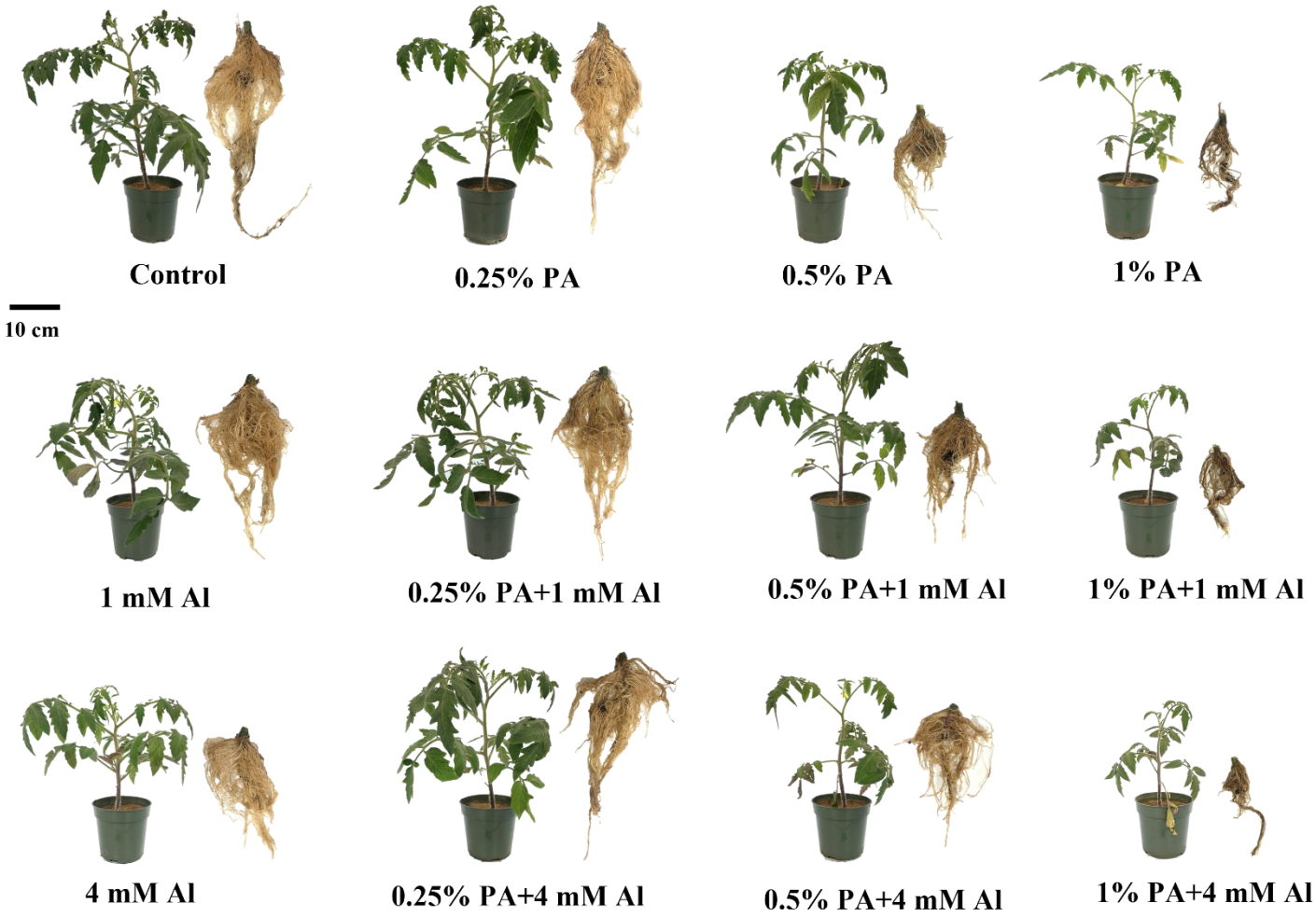

Figure 7.1. Growth response of tomato 'Scotia' seedlings treated with or without pyroligneous acid (PA) under aluminum (Al) stress.

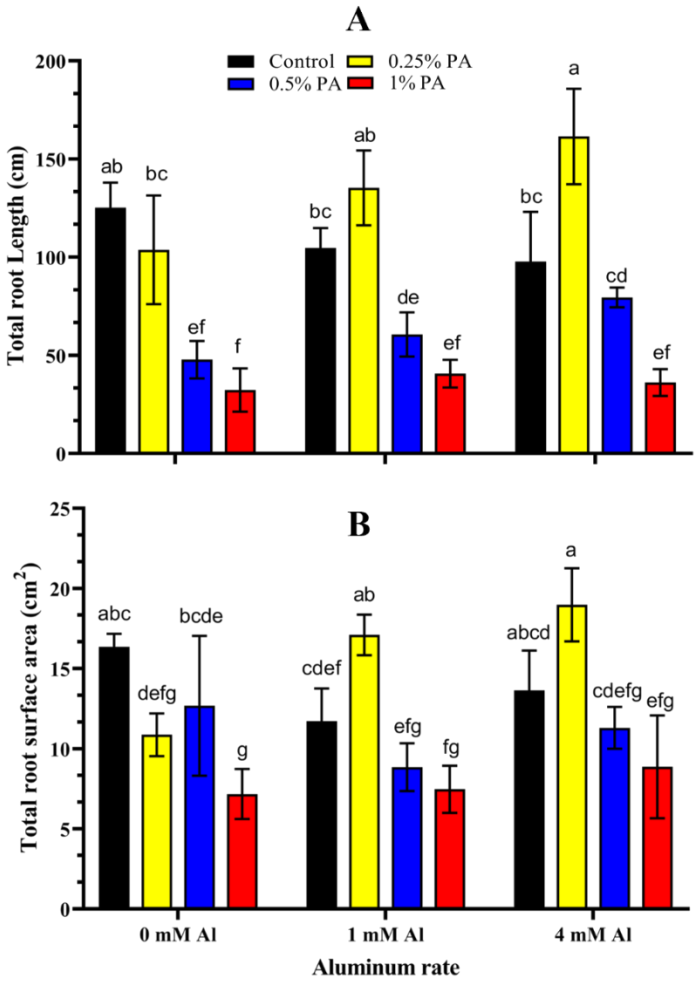

Figure 7.2. Root growth characteristics of tomato 'Scotia' seedlings treated with pyroligneous acid (PA) under aluminum (Al) stress. (A) Total root length; (B) Total root surface area. Values are means ± standard deviation of five replicates and the different letters indicate significant differences according to Tukey's honestly significant difference (HSD) post hoc test at $p < 0.05$.

7.3.2 Fluorescence, chlorophyll, and leaf gas exchange parameters

Chlorophyll fluorometric indices including maximum quantum efficiency of PSII (*Fv*/*Fm*) and potential photosynthetic capacity (*Fv*/*Fo*) were significantly ($p < 0.001$) affected by PA under Al stress (Table 7.2). *Fv/Fm* was significantly ($p < 0.001$) reduced by *ca*. 1.2% in 1% PA-treated plants under 0 mM Al concentration while 0.25% and 0.5% PA treatment exhibited no significant ($p > 0.05$) effect on the plants compared to the control (Table 7.2). However, exposure of plants

treated with 0.5% PA and 1% PA to 1 mM and 4 mM Al considerably reduced *Fv/Fm* by *ca*. 1.2% and 6.2%, and 6.2% and 3.7%, respectively compared to the control under the same conditions. Similarly, the 0.25% PA alone slightly increased *Fv*/*Fo* while the 1% PA alone significantly ($p < 0.001$) reduced it by *ca*. 8.1% compared to the control. Under 1 mM and 4 mM Al stress, both 0.5% PA and 1% PA significantly ($p < 0.001$) reduced *Fv*/*Fo* compared to their respective Al alone treatment (Table 2). With exposure to 1 mM Al stress, 0.25% PA treatment slightly increased *Fv/Fo* by *ca*. 3.7% while the 1% PA significantly ($p < 0.001$) reduced *Fv/Fo* by *ca*. 19% compared to 1 mM Al alone. Nevertheless, PA treatment had no significant ($p > 0.05$) effect on *Fv/Fo* under 4 mM Al treatment compared to the 4 mM Al alone. Also, SPAD index was increased with 0.25% PA treatment by *ca*. 12.5% and reduced by *ca*. 4.1% following 1% PA treatment under 0 mM Al compared to the control (Table 7.2). Overall, SPAD index was not significantly ($p > 0.05$) altered following plant exposure to Al.

Chlorophyll analysis indicated that chlorophyll a was non-significantly ($p > 0.05$) increased by *ca.* 1.8% in 0.25% PA-treated plants but reduced significantly ($p < 0.001$) by *ca*. 11.4% in 1% PA-treated plants under 0 mM Al compared to the control (Table 7.2). Likewise, upon exposure to 1 mM Al stress, the 0.25% PA treatment significantly ($p < 0.001$) enhanced chlorophyll a by *ca.* 10.1% but it decreased with application of 0.5% PA and 1% PA compared to the 1 mM Al alone (Table 7.2). Also, upon exposure to 4 mM Al, the 0.5% PA significantly ($p < 0.001$) increased chlorophyll a by *ca*. 9.2% but was reduced by the 0.25% PA treatment compared to the 4 mM Al alone. Additionally, chlorophyll b was significantly ($p < 0.001$) increased by *ca.* 24.3% with 0.25% PA treatment under 0 mM Al compared to the control (Table 7.2).

Table 7.2. Physiological response of tomato 'Scotia' seedlings treated with pyroligneous acid (PA) under aluminum (Al) stress.

Treatment	*Fv*/*Fm*	*Fv*/*Fo*	SPAD	Chlorophyll a (mg/g FW)	Chlorophyll b (mg/g FW)	E (mol m^{-2} s^{-1})	A (µmol m^{-2} s^{-1})
Control	0.81±0.01 a	4.32±0.22 a	53.58±2.44 abc	2415.62±43.60 a	1234.08±87.20 b	0.46±0.53 ab	2.24±1.09 a
0.25% PA	0.81±0.01 a	4.40±0.16 a	60.09±1.64 a	2459.43±38.70 a	1533.71±59.80 a	1.05±0.58 a	2.05±1.15 ab
0.5% PA	0.81±0.01 ab	4.30±0.21 a	54.89±2.31 abc	2327.63±11.10 b	1035.75±79.00 c	0.22±0.20 bcd	1.00±0.44 cde
1% PA	0.80±0.01 b	3.97±0.29 b	51.40±2.67 cd	2141.05±22.8 cd	921.4±16.20 cd	0.07±0.06 de	0.42±0.36 e
1 mM Al	0.81±0.01 a	4.38±0.19 a	57.10±3.80 abc	2214.13±90.90 bcd	947.04±79.60 cd	0.36±0.30 abc	1.02±0.37 bcde
0.25% PA + 1 mM Al	0.81±0.01 a	4.38±0.22 a	59.19±2.89 ab	2437.15±6.40 a	1251.53±18.70 b	0.32±0.45 abc	1.91±0.55 abc
0.5% PA + 1 mM Al	0.80±0.02 b	3.98±0.27 b	56.11±2.27 abc	2146.41±115.7 cd	957.84±10.44 cd	0.33±0.31 abc	1.44±0.69 abcd
1% PA + 1 mM Al	0.76±0.06 c	2.91±1.14 c	46.27±2.92 d	2198.31±9.58 cd	1044.95±7.02 c	0.17±0.22 bcd	1.02±0.50 bcde
4 mM Al	0.81±0.01 ab	4.26±0.24 ab	56.52±3.91 abc	2259.92±11.20 bc	1021.84±8.33 c	0.12±0.07 cd	0.93±0.36 cde
0.25% PA + 4 mM Al	0.81±0.01 a	4.39±0.18 a	57.13±3.66 abc	2050.28±92.8 d	841.24±57.90 d	0.16±0.23 bcd	1.57±0.76 abcd
0.5% PA + 4 mM Al	0.78±0.03 c	3.42±0.77 c	52.55±3.49 bcd	2468.58±17.5 a	1606.25±116.60 a	0.11±0.15 cd	1.92±1.06 abc
1% PA + 4 mM Al	0.78±0.04 c	3.39±0.57 c	54.42±2.32 abc	2133.65±110.9 cd	945.88±74.50 cd	0.03±0.04 e	0.76±0.33 de
Significant level							
PA	<0.001	<0.001	<0.001	<0.001	<0.001	<0.001	<0.001
Al	<0.001	<0.001	0.204	<0.001	<0.001	<0.001	0.889
PA × Al	<0.001	<0.001	<0.001	<0.001	<0.001	0.016	<0.001

Values are means ± standard deviation of five replicates and the different letters indicate significant differences according to Tukey's honestly significant difference (HSD) post hoc test at $p < 0.05$..SPAD, soil plant analysis development; A, photosynthetic rate; E, transpiration rate.

However, the 1% PA significantly ($p < 0.001$) reduced chlorophyll b under the 0 mM Al treatment compared to the control. Treatment with 0.25% PA significantly ($p < 0.001$) increased chlorophyll b content by *ca*. 32.2% under 1 mM Al while 0.5% PA increased this content by *ca*. 57.2% under the 4 mM Al compared to their respective Al alone treatments. Furthermore, transpiration rate was significantly ($p < 0.001$) increased by *ca*. 128.3% in 0.25% PA-treated plants but reduced in 1% PA-treated plants by *ca.* 84.8% compared to the control (Table 7.2). Similarly, the photosynthetic rate was significantly ($p < 0.001$) reduced with 1% PA treatment while 0.25% PA displayed no significant ($p > 0.05$) effect under 0 mM Al compared to the control. The presence of Al significantly ($p < 0.001$) reduced both transpiration and photosynthetic rate, especially under 4 mM Al (Table 7.2). However, the application of 0.25% PA slightly increased transpiration rate. Both 0.25% PA and 0.5% PA increased photosynthetic rate under 4 mM Al while 1% PA drastically reduced transpiration rate compared to the 4 mM Al alone (Table 7.2). Notwithstanding, exposure of both control and PA-treated plants to 1 mM Al did not significantly ($p > 0.05$) affect transpiration and photosynthesis.

7.3.3 ROS content and lipid peroxidation

Hydrogen peroxide determination was used to assess the extent of oxidative stress damage induced by Al stress (Figure 7.3A). The results showed that PA significantly ($p < 0.001$) increased H_2O_2 under 0 mM Al compared to the control. Also, Al stress significantly ($p < 0.001$) increased ROS under 4 mM Al compared to 0 mM Al (Figure 7.3A). Under both 1 mM and 4 mM Al, the 1% PA considerably increased H_2O_2 content by *ca*. 90% and 33% respectively, compared to their respective Al alone treatment. The 0.25% PA treatment remarkably reduced H_2O_2 content of the tomato seedlings under 4 mM Al treatment (Figure 7.3A).

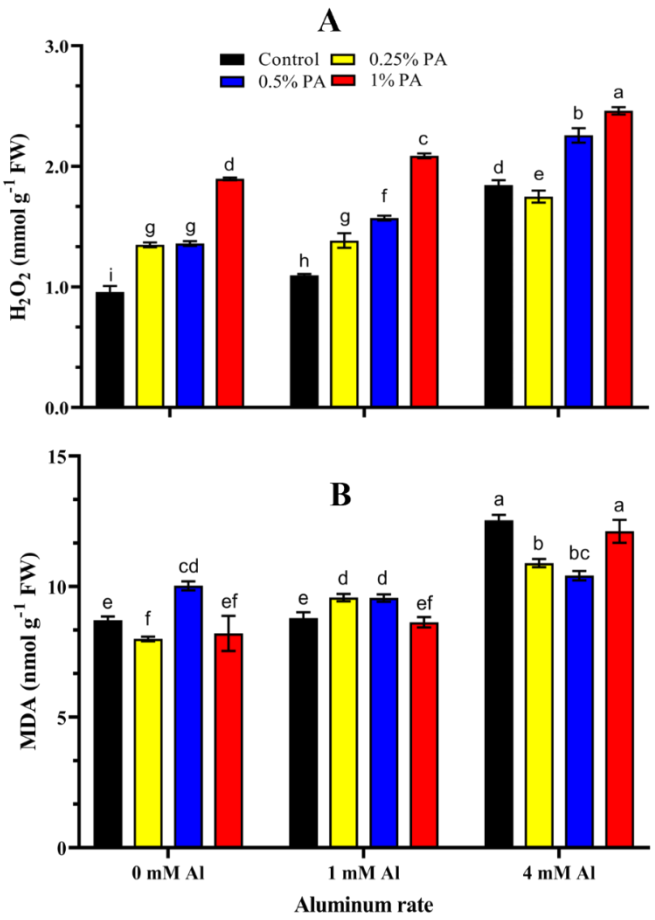

Figure 7.3. Oxidative stress of tomato 'Scotia' seedlings treated with pyroligneous acid (PA) under aluminum (Al) stress. (A) H_2O_2, hydrogen peroxide content; (B) MDA, malonaldehyde content. Values are means ± SD of five replicates and the different letters indicate significant differences according to Tukey's honestly significant difference (HSD) post hoc test at $p < 0.05$.

MDA which indicates the degree of ROS-induced lipid peroxidation was reduced in plants treated with 0.25% PA alone but was increased with 0.5% PA compared to the control (Figure 7.3B). Besides, exposure to 4 mM Al stress significantly ($p < 0.001$) resulted in higher MDA production in control plants and 1% PA-treated plants. On the other hand, 0.25% PA and 0.5% PA treatments significantly ($p < 0.001$) reduced MDA content by *ca*. 13.1% and 16.1%, respectively compared to the 4 mM Al alone (Figure 7.3B).

7.3.4 Osmolyte accumulation

Osmolytes including proline, soluble sugar and proteins were assessed. Proline content was significantly ($p < 0.001$) reduced in PA-treated plants under 0 mM Al, but increased by *ca*. 15% with 0.25% PA treatment under 1 mM Al compared to the 1 mM Al alone (Table 7.3). Under 4 mM Al stress, the 1% PA treatment considerably increased proline content by *ca*. 18.5% but was reduced following 0.5% PA treatment compared to the 4 mM Al alone (Table 7.3).

Table 7.3. Osmolyte accumulation in tomato 'Scotia' seedlings treated with pyroligneous acid (PA) under aluminum (Al) stress.

Treatment	Proline (nmol/ g/FW)	Sugar (mg glucose/ g FW)	Total Protein (mg/g FW)
Control	2.26±0.01 a	2.85±0.06 g	4.24±0.06 efg
0.25% PA	1.94±0.01 d	4.38±0.19 de	4.42±0.06 def
0.5% PA	1.93±0.02 d	4.94±0.21 cd	4.82±0.01 ab
1% PA	1.91± 0.00 d	6.31±0.60 b	4.69±0.13 bc
1 mM Al	1.93±0.01 d	3.29±0.15 f	4.04±0.21 gh
0.25% PA + 1 mM Al	2.22±0.00 b	4.07±0.17 e	4.63±0.08 bcd
0.5% PA + 1 mM Al	1.14±0.01 h	4.45±0.17 cde	4.96±0.18 a
1% PA + 1 mM Al	1.85±0.02 e	7.41±0.16 ab	4.49±0.10 cde
4 mM Al	1.73±0.02 f	5.00±0.26 c	3.73±0.11 h
0.25% PA + 4 mM Al	1.46±0.01 g	4.02±0.22 e	4.19±0.10 fg
0.5% PA + 4 mM Al	0.65±0.00 i	4.67±0.28 cd	4.48±0.04 cde
1% PA + 4 mM Al	2.05±0.03 c	7.80±1.02 a	4.27±0.10 efg
Significant level			
PA	<0.001	<0.001	<0.001
Al	<0.001	<0.001	<0.001
PA × Al	<0.001	<0.001	<0.001

Values are means ± SD of five replicates and the different letters indicate significant differences according to Tukey's honestly significant difference (HSD) post hoc test at $p < 0.05$.

Likewise, PA treatment significantly ($p < 0.001$) affected sugar accumulation following plant exposure to Al. Notably, sugar content increased significantly ($p < 0.001$) by *ca*. 121.4%, 125.2% and 56.0% in the 1% PA-treated plants under 0 mM, 1 mM and 4 mM Al, respectively compared to the control and Al alone treatments (Table 7.3). Furthermore, total protein was significantly ($p < 0.001$) enhanced with 0.5% PA treatment under 0 mM although not significantly ($p > 0.05$) different from that of the 0.25% PA-treated plants compared to the control (Table 7.3). The 4 mM Al treatment significantly ($p < 0.001$) reduced total protein by *ca.* 12% compared to the 0 mM Al alone. Conversely, PA-treated plants accumulated higher levels of total protein under 1 mM and 4 mM compared to the control. Accordingly, 0.5% PA treatment increased total protein content by *ca*. 22.8% and 20.1% in response to 1 mM and 4 mM Al, respectively compared to their respective Al alone treatment (Table 7.3).

7.3.5 Antioxidant compound accumulation

The antioxidant compounds were significantly ($p < 0.001$) affected by PA and Al treatment (Figure 7.4). Al exposure increased total phenolic content under 4 mM Al compared to 0 mM Al (Figure 7.4). Similarly, the total phenolic content was considerably higher in PA-treated plants irrespective of Al treatment (Figure 7.4A). The 0.5% and 1% PA treatments recorded the highest phenolic contents (*ca*. 36.5%), especially upon exposure to 4 mM Al (Figure 7.4A). Moreover, Al stress showed no obvious effect on flavonoid content while the PA treatment significantly ($p < 0.001$) increased flavonoid content irrespective of Al treatment. The 0.5% PA treatment enhanced flavonoid content by *ca.* 43.9% under 4 mM Al compared to the control (Figure 7.4B). Also, ascorbate content was not significantly ($p > 0.05$) altered by PA under 0 mM Al but was significantly ($p < 0.001$) increased with 1% PA treatment under 1 mM Al (Figure 7.4C). Ascorbate content was significantly ($p < 0.01$) increased with or without PA under 4 mM Al.

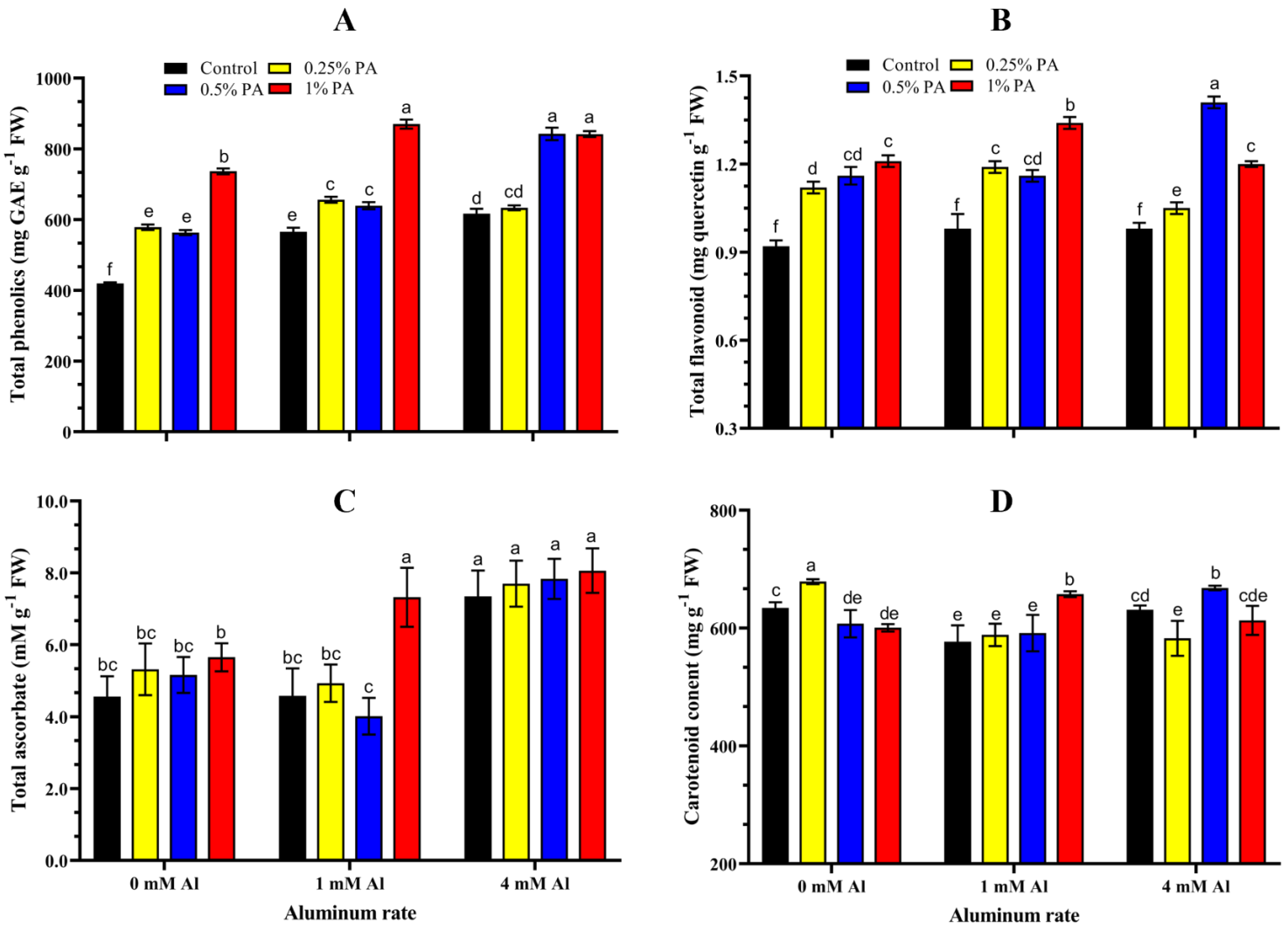

Figure 7.4. Antioxidant compound accumulation in tomato 'Scotia' seedlings treated with pyroligneous acid (PA) under aluminum (Al) stress. (A) Total phenolic content; (B) Total flavonoid content; (C) Total ascorbate content; (D) Carotenoid content. Values are means ± SD of five replicates and the different letters indicate significant differences according to Tukey's honestly significant difference (HSD) post hoc test at $p < 0.05$.

Similarly, carotenoid content was significantly ($p < 0.001$) increased in 0.25% PA-treated plants under 0 mM Al but was reduced with or without PA under 1 mM Al (Figure 7.4D). Although the 1% and 0.5% PA-treated plants accumulated high carotenoid content under 1 mM Al and 4 mM Al, respectively compared to the control, these were significantly ($p < 0.001$) lower than what was recorded for the 0.25% PA-treated plants under 0 mM Al (Figure 7.4D).

7.3.6 Antioxidant enzymes and ROS scavenging activity

Antioxidant enzymes including POD and APX, and ROS scavenging activities were significantly ($p < 0.001$) stimulated by PA treatment under Al stress (Figure 7.5). POD activities were significantly ($p < 0.001$) reduced irrespective of PA treatment under no Al treatment alone i.e., 0 mM Al. However, the 0.5% PA treatment recorded the highest POD activity (*ca*. 71.9% and 36.2%) followed by the 1% PA treatment (*ca*. 63.8 and 32.3%) upon exposure to 1 mM Al and 4 mM Al, respectively, compared to their respective Al alone treatments (Figure 7.5A). APX activity was not significantly ($p > 0.05$) affected by PA treatments under 0 mM Al, but was reduced in PA-treated plants under 4 mM Al (Figure 7.5B). It was found that the 0.25% PA increased APX activity by *ca.* 126.9% and 96.4% under 0 mM and 1 mM Al, respectively compared to the control and 1 mM alone treatment (Figure 7.5B). Besides, ROS scavenging activity using DPPH scavenging assay showed a significant ($p < 0.001$) effect of PA treatment under Al stress (Figure 7.5C). PA treatment significantly ($p < 0.001$) increased DPPH scavenging activity irrespective of Al treatment in a dose-dependent manner. Notably, the 1% PA-treated plants exhibited a substantial increase in DPPH scavenging activity by *ca*. 61.6%, 98.9% and 116% under 0, l and 4 mM Al, respectively compared to the control and their respective Al alone treatment (Figure 7.5C).

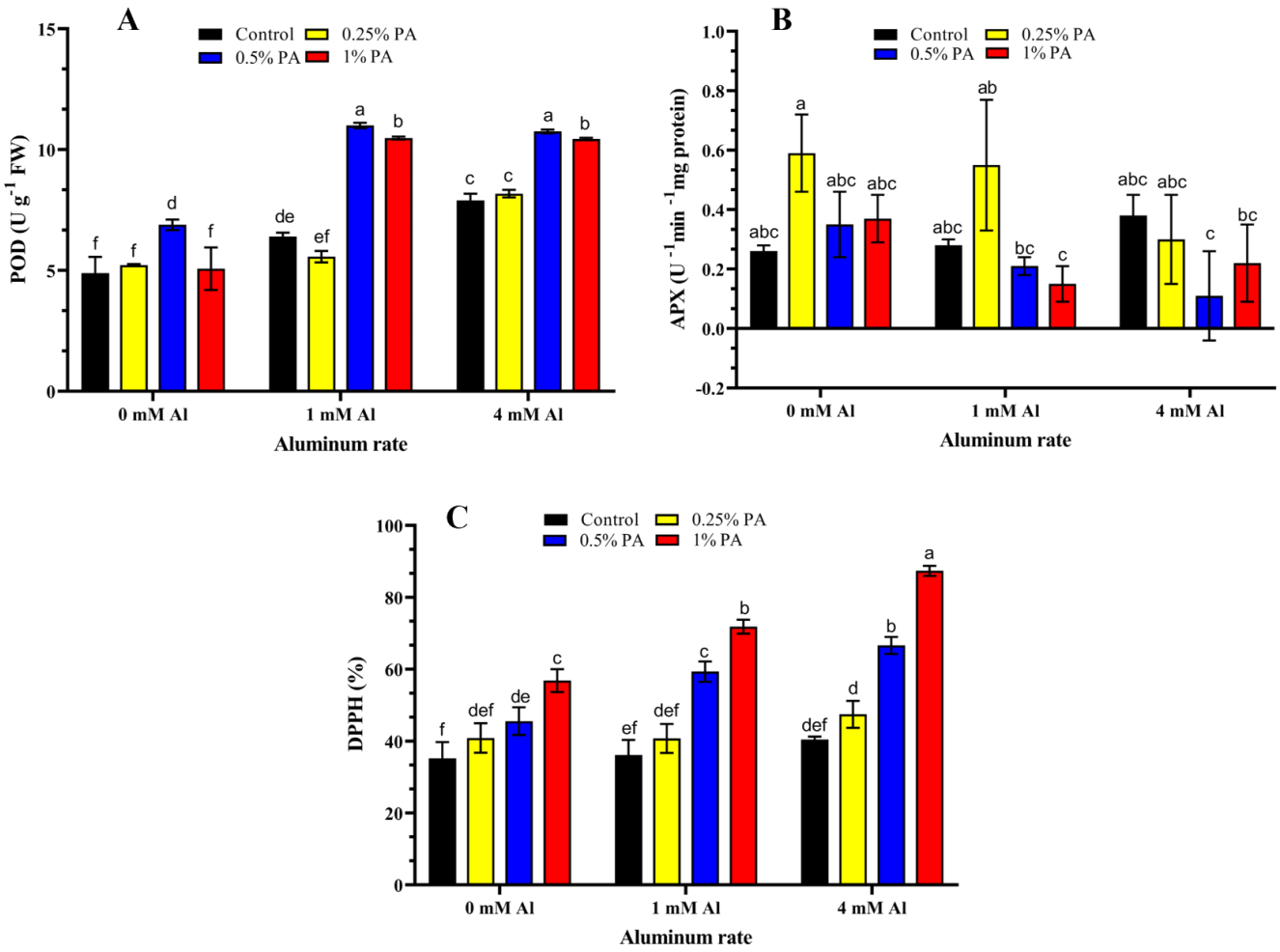

Figure 7.5. Antioxidant enzymes and reactive oxygen species (ROS) scavenging activities in tomato 'Scotia' seedlings treated with pyroligneous acid (PA) under aluminum (Al) stress. (A) POD, peroxidase; (B) APX, ascorbate peroxidase; (C) ROS-scavenging activity (DPPH). Values are means ± SD of five replicates and the different letters indicate significant differences according to Tukey's honestly significant difference (HSD) post hoc test at $p < 0.05$.

7.3.7 Mineral element accumulation

Mineral elements in the different parts of the tomato 'Scotia' plants were highly influenced by PA treatment under varying Al concentrations (Table 7.4). Al and Mg contents were increased in the leaves of 0.25% PA-treated plants while high leaf B, Mn, Na, P and Zn contents were accumulated in all PA-treated plants under 0 mM Al. Al treatment markedly increased Al and Cu accumulation in control plants but reduced Al and Cu content substantially in the leaf PA-treated plants. Conversely, B was increased in leaves of the 0.5% PA-treated plants under both 1 mM and 4 mM Al, while high leaf P and Zn contents were recorded in 0.25% PA-treated plants under 1 mM and 4 mM Al, respectively (Table 7.4). Both Mn and Na contents were increased in the leaves of PA-treated plants under all Al concentrations but higher in 0.5% PA and 1% PA-treated plants (Table 7.4). However, leaf Fe content was not altered with PA and Al treatments. Similarly, Al, Cu and Fe contents were higher in the stems of the 1% PA-treated plants under 0 mM Al compared to the control. These elements were unaffected in both control and PA-treated plants under Al stress (Table 7.4). On the contrary, stem B was reduced in all PA-treated plants under 0 mM but increased in PA-treated plants under Al stress (Table 7.4). Plant stem Mn, Na, P and Zn contents were increased in all PA-treated plants under 0 mM Al. Although all PA-treated plants accumulated high stem Mn and Na under Al stress, the 1% PA increased stem P content under the 4 mM Al while the 0.25% PA increased both stem P and Zn under 4 mM Al (Table 7.4). Nevertheless, stem Mg content was not affected by both PA or Al. Furthermore, while Mn and Na contents were increased, B and P contents were reduced in the roots of PA-treated plants under both 0 mM and Al treatments. Root Cu and Fe contents were increased in 0.25% PA and 1% PA-treated plants under 0 mM Al but reduced with Al treatment.

Table 7.4. Mineral element accumulation in tomato 'Scotia' seedlings treated with pyroligneous acid (PA) under aluminum (Al) stress.

Plant tissue	Treatment	Al (mg /kg)	B (mg /kg)	Cu (mg /kg)	Fe (mg /kg)	Mg (mg /kg)	Mn (mg /kg)	Na (mg /kg)	P (mg /kg)	Zn (mg /kg)
Leaves	Control	39.84	230.52	31.70	48.31	7932.74	98.73	1120.19	3640.90	29.71
	0.25% PA	48.66	415.87	31.44	49.96	8598.15	317.71	1865.72	4351.35	45.64
	0.5% PA	24.52	406.08	32.88	49.05	7755.93	485.49	3381.82	5480.22	45.09
	1% PA	40.14	365.63	25.07	50.14	6231.03	502.60	7279.92	4249.30	52.49
	1 mM Al	73.00	331.59	37.03	49.26	6760.03	109.45	953.59	4232.96	39.38
	0.25% PA + 1 mM AL	51.06	392.13	33.31	49.60	7072.59	351.65	1780.48	5309.53	43.55
	0.5% PA + 1 mM AL	25.67	427.35	27.22	50.21	6770.95	514.87	2718.91	4550.09	46.16
	1% PA + 1 mM AL	27.59	377.93	25.09	50.18	5628.36	526.39	7967.68	2722.92	42.54
	4 mM Al	52.78	421.61	40.56	48.72	7444.33	180.91	689.58	3843.45	50.20
	0.25% PA + 4 mM AL	59.05	379.99	37.22	49.86	7000.68	409.04	1232.59	4576.88	53.44
	0.5% PA + 4 mM AL	48.76	429.89	32.58	49.34	5793.86	551.79	2967.09	2271.99	48.58
	1% PA + 4 mM AL	25.40	381.83	26.06	48.76	4414.86	467.41	7819.77	2874.30	44.05
Mean		44.64	379.87	32.19	49.51	6998.97	368.06	2905.23	4111.78	45.16
CV (%)		34.37	14.52	15.72	1.30	16.32	44.89	95.24	24.12	14.06
Stem	Control	24.81	145.13	24.81	49.62	8845.78	107.19	1254.78	2576.10	21.27
	0.25% PA	24.77	99.30	27.23	49.53	10024.26	189.02	3496.33	2803.86	29.22
	0.5% PA	24.30	114.88	24.30	48.60	9846.63	244.60	6829.66	4062.03	32.48
	1% PA	41.60	135.68	41.60	83.19	9898.09	266.54	15469.92	3343.07	64.27
	1 mM Al	24.92	106.23	27.17	49.83	9910.96	67.10	1210.01	3288.09	24.10
	0.25% PA + 1 mM AL	23.66	118.22	23.66	47.32	9874.27	248.26	3431.53	4509.92	33.07
	0.5% PA + 1 mM AL	24.84	135.64	24.84	49.68	8936.48	246.45	5382.83	3628.02	19.83
	1% PA + 1 mM AL	24.65	137.18	24.65	49.30	9169.07	293.89	12119.89	2963.94	20.89
	4 mM Al	24.66	95.57	22.91	49.33	10171.42	78.25	683.18	2329.47	28.51
	0.25% PA + 4 mM AL	24.73	101.37	24.73	49.46	9617.69	229.30	2513.21	2161.56	33.10
	0.5% PA + 4 mM AL	24.74	127.33	24.74	49.49	9789.10	366.95	5640.56	2278.74	17.90
	1% PA + 4 mM AL	24.29	140.99	24.29	48.58	9515.45	249.32	11764.28	3035.17	15.11
Mean		26.15	119.68	26.42	52.31	9643.98	212.50	5275.63	3085.89	29.51
CV (%)		18.83	14.85	18.89	18.83	4.48	42.37	92.14	23.56	43.76
Root	Control	2169.49	80.05	47.51	1688.75	8131.55	391.85	1303.08	6458.24	42.33
	0.25% PA	1333.82	74.56	58.10	1409.03	5991.45	475.51	1967.07	3504.70	63.28
	0.5% PA	1907.34	79.67	43.82	2369.43	9537.39	850.43	2199.78	4305.16	27.89
	1% PA	1948.33	67.56	42.80	2276.70	10763.57	974.77	2397.83	3321.07	34.58
	1 mM Al	1340.18	88.64	52.70	1128.90	8916.12	289.13	1465.52	5083.86	57.81
	0.25% PA + 1 mM AL	1477.30	58.33	38.12	1377.50	6778.74	399.89	1501.62	3535.97	56.28
	0.5% PA + 1 mM AL	2235.93	51.79	45.31	2547.97	7498.29	494.58	1666.22	3273.53	40.83
	1% PA + 1 mM AL	2027.35	27.95	28.40	4048.29	8676.66	819.69	2173.70	1224.77	34.84
	4 mM Al	1514.63	71.66	38.97	1709.08	10226.13	526.32	1250.70	4532.59	38.97
	0.25% PA + 4 mM AL	1680.46	56.04	29.67	1885.51	8294.53	740.16	1665.88	3528.86	25.33
	0.5% PA + 4 mM AL	1810.08	47.27	31.67	2398.52	7614.90	521.89	2257.98	3573.94	42.19

	1% PA + 4 mM AL	1915.51	30.50	28.94	3314.78	7241.01	881.56	2374.28	1524.76	33.92
Mean		1767.72	63.96	41.55	2076.34	8402.67	589.47	3032.67	3849.34	42.21
CV (%)		17.47	30.35	23.29	40.81	16.73	38.49	125.69	36.62	28.24

CV, coefficient of variation; Al, aluminum; B, boron; Cu, copper; Fe, iron; Mg, magnesium; Mn, manganese; Na, sodium; Zn, zinc.

Besides, root of 0.5% PA- and 1% PA-treated plants accumulated high levels of Fe under both 0 mM and all Al treatments compared to control plants. Al contents were reduced drastically in the roots of 0.25% PA-treated plants under 0 mM Al but was slightly increased in PA-treated plant in the presence of Al (Table 7.4). On the other hand, the 0.25% PA-treated plants accumulated high levels of Zn in their roots under 0 mM Al, while exposure to Al had no effect on Zn levels in both the control and PA-treated plants (Table 7.4).

7.3.8 Mineral element translocation

Mineral element translocation factor (TF) varied among the treatments (Table 7.5). The results showed that the TFs of B, Mn, Na and P were markedly increased following PA treatments under all Al treatments. Notably, the 1% PA recorded the highest TFs for B, Na and P followed by the 0.5% PA, while both 0.25% PA and 0.5% PA recorded the highest TF for Mn compared to the control. Although the TF for Cu was not altered by PA under both 0 mM Al and 1 mM Al treatments, it was increased substantially with the application of 0.25% PA under 4 mM Al. Besides, the TF for Mg was higher in 0.25% PA-treated plants under both 0 mM Al and all Al treatments, while the TF for Zn was higher in the 1% PA-treated plants under 0 mM Al and 1 mM Al and 0.25% PA-treated plants under 4 mM Al (Table 7.5). On the other hand, the TFs for Al and Fe were much lower than the other mineral elements but reduced in PA-treated plants under both 0 mM Al and all Al treatments.

Table 7.5. Translocation factors (TF) of mineral element accumulation in tomato 'Scotia' seedlings treated with pyroligneous acid (PA) under aluminum (Al) stress.

Treatment	Al	B	Cu	Fe	Mg	Mn	Na	P	Zn
Control	0.03	4.69	1.19	0.06	2.06	0.53	1.82	0.96	1.20
0.25% PA	0.06	6.91	1.01	0.07	3.11	1.07	2.73	2.04	1.18
0.5% PA	0.03	6.54	1.30	0.04	1.85	0.86	4.64	2.22	2.78
1% PA	0.04	7.42	1.56	0.06	1.50	0.79	9.49	2.29	3.38
1 mM Al	0.07	4.94	1.22	0.09	1.87	0.61	1.48	1.48	1.10
0.25% PA + 1 mM Al	0.05	8.75	1.49	0.07	2.50	1.50	0.35	2.78	1.36
0.5% PA + 1 mM Al	0.02	10.87	1.15	0.04	2.09	1.54	4.86	2.50	1.62
1% PA + 1 mM Al	0.03	18.43	1.75	0.02	1.71	1.00	9.24	4.64	1.82
4 mM Al	0.05	7.22	1.63	0.06	1.72	0.49	1.10	1.36	2.02
0.25% PA + 4 mM Al	0.05	8.59	2.09	0.05	2.00	0.86	2.25	1.91	3.42
0.5% PA + 4 mM Al	0.04	11.79	1.81	0.04	2.05	1.76	3.81	1.27	1.58
1% PA + 4 mM Al	0.03	17.14	1.74	0.03	1.92	0.81	8.25	3.88	1.74
Mean	0.04	9.44	1.50	0.05	2.03	0.98	4.17	2.28	1.93
CV (%)	37.93	46.89	21.71	35.02	20.68	41.91	77.26	47.48	42.45

CV, coefficient of variation; Al, aluminum; B, boron; Cu, copper; Fe, iron; Mg, magnesium; Mn, manganese; Na, sodium; Zn, zinc.

7.4 DISCUSSION

Aluminum stress is one of the most limiting factors of crop production in acidic soils. However, improving crop productivity and resilience to Al stress through environmentally friendly strategies is imperative for expanding food production and meeting the high food demand of the ever-growing population. As a result, the use of PA as a biostimulant has gained tremendous attention in sustainable crop production and environmental stress mitigation (Grewal et al., 2018; Wang et al., 2019a; Wang et al., 2019b; Zhu et al., 2021a). This is the first study to explore the functional role of PA on the growth and development of tomato seedlings under Al stress. Although no interaction between PA and Al stress was observed for the tomato 'Scotia' plant morphological traits, the application of 0.25% PA alone increased root fresh and dry weights and volumes while 1% PA alone reduced these parameters. This result is consistent with previous studies where PA treatment at lower concentrations was reported to enhance root growth and development in tomato (Ofoe et al., 2022b) and wheat (Wang et al., 2019b) plants. PA contains numerous bioactive compounds including karrikins that have been proven to stimulate plant growth and development (Dixon et al., 2009; Grewal et al., 2018). However, the effectiveness of PA depends on the concentration used, which suggests that an appropriate concentration can contain the right proportion of bioactive compounds to positively improve plant growth.

Also, our results showed that 4 mM Al drastically reduced tomato 'Scotia' plant morphological parameters, which confirms that Al induces toxicity in plants (Awasthi et al., 2017; Wang et al., 2020b; Ofoe et al., 2022b). Besides, the reduction of root growth and distortion of root systems is the primary symptoms of Al stress (Kochian et al., 2015). Such disruption restricts water and nutrient uptake and thereby, reducing the development of aerial parts. However, the maintenance

of root growth under Al stress is an important induction of Al tolerance (Cárcamo et al., 2019; Siqueira et al., 2020). As a result, the application of 0.25% increased both root length and root surface areas under Al stress. This shows that 0.25% had a positive role in ameliorating root activities under Al stress. It has been reported that the rich organic compound in PA chelates heavy metal and renders them less toxic (Benzon & Lee, 2017; Grewal et al., 2018). Hence, the increase in root growth following 0.25% PA treatment under Al stress can be attributed to the restriction of Al rhizotoxicity. Likewise, plants exposed to 1 mM Al showed a similar morphological effect to both control and 0.25% PA treatment, suggesting that 1 mM Al stimulated the growth of the tomato plants. This finding is consistent with previous reports where low Al concentrations increased plant growth and development of tomato (Simon et al., 1994; Ofoe et al., 2022b), maize (*Zea mays*) (Wang et al., 2015b), and rice (*Oryza sativa*) (Famoso et al., 2011) seedlings.

Photosynthesis is an integral part of a plant survival to changes in the environment. The photosynthetic process is considered sensitive and affected by several environmental stress. Previous studies have revealed that Al stress impairs photosynthesis by reducing chlorophyll content, photosynthetic and transpiration rates, and stomatal conductance in pepper (*Capsicum annuum*) (Konarska, 2010), tomato (Simon et al., 1994), alfalfa (Cheng et al., 2020) and peanut (Shen et al., 2014). In the present study, tomato plants showed similar trends of reduced chlorophyll content, and photosynthetic and transpiration rates under 4 mM Al treatments. Al stress instigates osmotic stress which could damage mesophyll cells, limit stomatal conductance and inhibit enzymes involved in carbohydrate metabolism (Li et al., 2012; Kochian et al., 2015). As such, the reduction in photosynthetic rate under Al stress in the present study was not solely due to Al-induced impairment of mesophyll cells but also, a reduction in chlorophyll (Yang et al.,

2015). However, low concentration of PA significantly improved photosynthesis and leaf gas exchange parameters under Al stress, which indicates that high PA concentration aggravates the phytotoxic effect of Al stress. A similar improvement in photosynthesis and leaf gas exchange effects of PA was reported in rapeseed under salinity stress (Ma et al., 2022) and mustard grown in heavy metal-contaminated soils (Benzon & Lee, 2017). Although the exact mechanism of PA-mediated improvement in photosynthesis is unknown, it is plausible that PA mediates stomatal reopening for more carbon dioxide capture to promote photosynthesis and carbohydrate production for Al stress adaptation (Ma et al., 2022).

Al stress facilitates rapid production and accumulation of ROS including H_2O_2 radicals, which ultimately causes oxidative damage to cell integrity. Al-induced oxidative stress is a decisive event that promotes disruption of cellular components including membrane lipids, nucleic acids and proteins leading to cell death (Huang et al., 2014b; Yamamoto, 2019). Membrane lipids peroxidation aggravates cell structural damage through excessive production of MDA (Sharma et al., 2012). Our results showed that Al stress (4 mM Al) increased H_2O_2 accumulation and MDA production in tomato plants while 0.25% PA treatment remarkably reduced these levels under Al stress. However, 1% PA increased both H_2O_2 and MDA levels irrespective of the Al concentration. This suggests that 1% PA applied to roots is toxic to plants and could result in cellular damage. This is consistent with previous studies where Al stress increased ROS and MDA in several plants (Sharma et al., 2012; Huang et al., 2014b; Yamamoto, 2019). Additionally, seed priming with PA was reported to reduce ROS accumulation and MDA production in wheat and tomato under drought (Wang et al., 2019b) and Al stress (Ofoe et al., 2022b), respectively. Similarly, a recent study showed that exogenous PA treatment of rapeseeds inhibits lipid peroxidation and reduced

ROS accumulation under salinity stress (Ma et al., 2022). This illustrates that PA could promote Al tolerance in plants by maintaining ROS homeostasis.

To counter oxidative damage, plants have evolved an efficient defensive mechanism to detoxify ROS radicals and maintain cellular homeostasis (Gill & Tuteja, 2010; Ejaz et al., 2020). Osmolytes including proline and sugars are known to accumulate under Al stress conditions to promote water retention, and stabilize membranes and macromolecules (Pirzadah et al., 2019; Ejaz et al., 2020). In the present study, PA treatment reduced proline content in the absence of Al stress but 0.25% and 1% PA increased the proline content under 1 mM and 4 mM Al, respectively. Likewise, Al stress increased sugar content while 1% PA enhanced its accumulation further under both 1 mM and 4 mM Al. PA-mediated increase in osmolytes could have protected macromolecules and stabilized cellular membranes. Thus, improving plant performance under Al stress. Such osmoprotectant helps plants to optimize the preserved carbohydrate to sustain essential metabolism under Al stress (Mishra & Dubey, 2008). Previous studies have demonstrated that Al stress inflicts energy starvation on plants. Accordingly, Al-tolerant plants accumulate increased levels of sugar to produce sufficient ATP required by cells (Koch, 2004; Li et al., 2016a; Pinto et al., 2021). In Al-tolerant citrus (*Citrus sinensis* and *C. grandis*), Li et al. (2016a) showed a similar increase in glucose content in the leaves upon Al exposure. This indicates that the high sugar and proline accumulation in 1% PA-treated plants could indicate a switch from growth to survival mode. Moreover, sugars are the primary end-product of photosynthesis and are used as metabolite signalling molecules and to support leaf cell turgor (Couée et al., 2006). Accumulation of sugar in the leaves may also be associated with callose biosynthesis as reported by Silva et al. (2012).

Antioxidant defence system consists of diverse metabolites (i.e., phenolics, ascorbate and carotenoid) and proteins (i.e., POD and APX), which act together to enhance plant tolerance to Al stress (Gill & Tuteja, 2010; Waszczak et al., 2018; Wei et al., 2021b). Our results showed that phenolics, ascorbate and POD activities were increased following exposure to Al stress as previously reported for other plants such as wheat (Liu et al., 2018b), watermelon (Malangisha et al., 2020), maize (Du et al., 2020), and soybean (Du et al., 2010). Similarly, PA treatment further boosted phenolics, ascorbate and POD and APX activities under Al stress conditions. This effect of PA was expected as previous studies showed that PA contains high phenolic compounds which induced high antioxidant properties (Loo et al., 2007; Wei et al., 2010). The increase in POD activities with PA under Al stress is consistent with the findings of Wang et al. (2019b) and Ma et al. (2022). POD activities function in mediating signal transduction, fortifying cell walls and detoxifying accumulated H_2O_2 into H_2O (Sharma et al., 2012; Waszczak et al., 2018). Also, APX detoxifies H_2O_2 into H_2O using ascorbate as an electron donor in the first level of the ascorbate-glutathione cycle (Sharma et al., 2012). Besides, it was suggested that these phenolic compounds have a high affinity to Al ions and could chelate Al in the leaves (Tolrà et al., 2005). The increase in antioxidants plays a vital role in scavenging ROS radicals as confirmed by our DPPH assay, which suggests that PA contributes to Al tolerance.

Al tolerance mechanisms have been extensively studied in several plant species (Kochian et al., 2015). Al tolerant plants may possess an Al exclusion mechanism that restricts Al entry and/or retain Al in roots to limit its transport to the aerial parts or an internal tolerance mechanism that promotes Al entry, detoxification with organic acid and storage in subcellular compartments (Kochian et al., 2015; Ofoe et al., 2023). Our results revealed that Al stress reduced root Al content

but increased leaf Al content as previously reported for maize (Siqueira et al., 2020). However, PA treatment decreased leaf Al content and increases root Al content, which suggests that PA enhances the retention of Al in roots, which can be a tolerance strategy in Al tolerance (Kichigina et al., 2017). The higher Al retention in PA-treated roots and lower translocation to aerial parts indicates higher efficiency of the exclusion mechanism (Kochian et al., 2015). Moreover, PA is known to be rich in numerous organic acids including malate, citrate and oxalic which has been demonstrated to exhibit high adsorption to heavy metals and render them immobile (Benzon & Lee, 2017; Grewal et al., 2018; Ofoe et al., 2022a). As such, the high Al retention could indicate PA immobilization of Al in tomato root to restrict its translocation, which should be investigated further.

Previous studies have established that Al stress induces mineral element deficiencies and restricts their transport (Mariano et al., 2015; Moustaka et al., 2016; Kichigina et al., 2017). In this study, Na and Mn were reduced upon Al exposure in all tissues as reported by Kichigina et al. (2017) and Bernal and Clark (1997); while PA treatment increased their contents in both root and shoot. Similarly, B and P were reduced in the tomato plant shoot but increased in the roots following Al exposure. This indicates that Al stress indeed disturbs the homeostasis and transport of mineral elements in plants. However, PA treatments enhanced B and P translocation to aerial parts and decreased their accumulation in the roots. This is consistent with the finding of Zhao et al. (2017) who showed that Al stress reduced P in shoot of maize plants under Al stress. The increased P in roots of Al-alone treated tomato plants is a major concern in acidic soils and has been reported that Al exhibits a high affinity to P and forms Al-P complexes and thereby, restricting P uptake (Bose et al., 2015; Magalhaes et al., 2018). Besides, we can surmise that the rich organic functional

groups in PA including carboxyl, phenoxyl and hydroxyl with adsorption sites can (1) form non-toxic compounds in the rhizosphere; and (2) increase P availability and uptake by chelating Al and releasing P from Al-P complexes (Bose et al., 2015; Benzon & Lee, 2017; Grewal et al., 2018).

7.5 CONCLUSION

The present study revealed that Al stress significantly affects the morphology and physiological performance of tomato seedlings. However, the application of a low PA concentration of 0.25% alleviated the toxic effect of Al stress and enhanced tomato plant growth while a high PA concentration of 1% PA exacerbates the phytotoxic effect of Al. Furthermore, PA treatment mitigated the toxic effects of Al stress by reducing H_2O_2 and MDA levels while concomitantly enhancing the accumulation of osmolytes, antioxidant compounds and ROS-scavenging enzyme activities. PA treatment restricted Al uptake and facilitated the availability and translocation of B, Mn, Na and P in tomato plants. These findings suggest that PA could be used as a novel strategy to detoxify Al in soils and improve plant tolerance to this edaphic stressor in agricultural production systems. Nevertheless, further work are required to elucidate the molecular basis of PA-mediated Al tolerance and the direct role of PA in Al-binding in tomato plants cultivated in the presence of this stressor.

CHAPTER 8: COORDINATED REGULATION OF CENTRAL CARBON METABOLISM IN PYROLIGNEOUS ACID-TREATED TOMATO PLANTS UNDER ALUMINUM STRESS

A version of this chapter has been published in **Metabolite Journal**. The citation is:

Ofoe, R., Thomas, R. H. and Abbey, L. (2023). Coordinated regulation of central carbon metabolism in pyroligneous acid-treated tomato plants under aluminum stress. *Metabolites, 13,* 770. https://doi.org/10.3390/metabo13060770 . (Impact factor = 4.1)

8. ABSTRACT

Aluminum (Al) toxicity is a major threat to global crop production in acidic soils, which can be mitigated by natural substances such as pyroligneous acid (PA). However, the effect of PA in regulating plant central carbon metabolism (CCM) under Al stress is unknown. In this study, we investigated the effects of varying PA concentrations (0, 0.25 and 1% PA/ddH_2O (*v/v*)) on intermediate metabolites involved in CCM in tomato (*Solanum lycopersicum* L. 'Scotia') seedlings under varying Al concentrations (0, 1 and 4 mM $AlCl_3$). A total of 48 differentially expressed metabolites of CCM were identified in the leaves of both control and PA-treated plants under Al stress. Calvin-Benson cycle (CBC) and pentose phosphate pathway (PPP) metabolites were considerably reduced under 4 mM Al stress, irrespective of the PA treatment. Conversely, the PA treatment markedly increased glycolysis and tricarboxylic acid cycle (TCA) metabolites compared to the control. Although glycolysis metabolites in the 0.25% PA-treated plants under Al stress were

comparable to the control, the 1% PA-treated plants accumulated the highest glycolysis metabolites. Furthermore, all PA treatments increased TCA metabolites under Al stress. Electron transport chain (ETC) metabolites were higher in PA-treated plants alone and under 1 mM Al but were reduced under a higher Al treatment of 4 mM. Pearson correlation analysis revealed that CBC metabolites had a significantly strong positive (r = 0.99; p <0.001) association with PPP metabolites. Additionally, glycolysis metabolites showed a significantly moderate positive (r = 0.76; p <0.05) association with TCA metabolites while ETC metabolites exhibited no association with any of the determined pathways. The coordinated association between CCM pathway metabolites suggests that PA can stimulate alteration in plant metabolism to modulate energy production and biosynthesis of organic acids under Al stress conditions.

Keywords: Wood vinegar; metabolomics; TCA cycle; carbohydrate metabolism; *Solanum lycopersicum*

8.1 INTRODUCTION

Soil acidity is widespread and accounts for 50% of the global agricultural lands that support up to 80% of world vegetable production (Slessarev et al., 2016). Aluminum (Al) is the most abundant metal in the lithosphere, and its availability is dependent on soil acidity levels (Kochian et al., 2015). Al exists in soils as non-toxic oxides and Al-silicates to which several plant roots are exposed. However, as soil pH drops below 5, Al dissociates into trivalent forms which most plants including tomato plants are sensitive to even at low concentrations (Kochian et al., 2015). These sensitive plants exhibit a wide range of Al-induced phytotoxicity with the inhibition of root growth being the most significant effect (Kochian et al., 2015; Ofoe et al., 2022b). Al disrupts root cells

leading to physiological drought by restricting water and nutrient uptake (Ofoe et al., 2023). It also reduces leaf elongation, impairs the photosynthetic ability of plants and instigates the accumulation of reactive oxygen species (ROS) (Peixoto et al., 2002; Chen et al., 2005a). Al-induced buildup of ROS facilitates membrane lipid peroxidation, loss of cell membrane integrity and damage to cellular components including nucleic acids and proteins (Pandey et al., 2016). Consequently, these phytotoxic effects result in marked yield reduction and total crop failure (Siqueira et al., 2020; Ofoe et al., 2023).

Generally, plants have evolved cellular and metabolic mechanisms to mitigate Al-induce phytotoxicity. The exclusion and internal detoxification mechanisms of Al tolerance have been well-characterized in plants (Kochian et al., 2015; Ofoe et al., 2023). The exclusion mechanism involves preventing Al entry into root cells by secreting organic acids (OA) to chelate Al within the rhizosphere. The internal tolerance mechanism involves intracellular detoxification of Al and sequestration of the non-toxic Al – OA complexes in the vacuole (Ofoe et al., 2023). These key mechanisms of Al tolerance can be linked to the central carbon metabolism (CCM) and its associated mitochondrial activity, but they are understudied. Furthermore, plant exposure to stress requires a rapid metabolic shift to maintain appropriate metabolism. As a result, several regulatory mechanisms must interact with various metabolic routes to regulate fluxes through the different intermediate pathways associated with CCM (Timm & Arrivault, 2021). The CCM pathway supplies the fundamental carbon needed to sustain growth and productivity under stress conditions and comprises the Calvin-Benson cycle (CBC), glycolysis, pentose phosphate pathway and tricarboxylic acid (TCA) cycle followed by oxidative phosphorylation for ATP production through the electron transport chain (ETC) (Fernie et al., 2004; Fuchs & Berg, 2014; Timm & Arrivault, 2021). Recently, several studies have demonstrated that Al stress alters metabolic profiles in plants

which may enhance Al tolerance (Wang et al., 2014; Li et al., 2016a; Pinto et al., 2021). Although most of these studies have focused on the root metabolism of Al tolerance, the effects of Al stress on metabolic changes in aerial parts or plants are poorly understood.

Mitochondrial metabolism plays an important role in Al tolerance by facilitating carbohydrate consumption for OA and cellular ATP biosynthesis (Kochian et al., 2015; Siqueira et al., 2020). Consequently, the glycolytic influx is increased under stress conditions to support not only energy production but also, OA generation during Al – detoxification. Notably, the TCA cycle produces high malic and citric acids in response to Al stress. These organic acids bind to Al ions to reduce Al toxicity both in the intracellular environment and around the rhizosphere (Kochian et al., 2015). Therefore, the end-products of photosynthesis are highly utilised for OA generation during Al stress (Peixoto et al., 2002; Wang et al., 2015b; Li et al., 2016a), which suggests that Al tolerance is linked to improved photosynthesis. Similarly, leaf metabolism under Al stress represents an important characteristic of plant growth and productivity and thus, the identification of metabolic alterations modulating photosynthesis and respiration may contribute to improving Al tolerance in plants.

Recent research and development have focused on the use of novel strategies to improve plant growth and resilience due to the multicomplex interaction of various environmental stresses (Pareek et al., 2020). As a result, the use of biostimulants to enhance crop growth and productivity, and tolerance to environmental stresses has attracted the interest of both researchers and farmers (Francesca et al., 2021; Hasanuzzaman et al., 2021). Pyroligneous acid (PA) is one of the widely used biostimulants that is known to improve crop growth, resilience to environmental stresses and productivity (Grewal et al., 2018; Ofoe et al., 2022c). PA is a translucent reddish-brown liquid produced through the carbonation of organic biomass in the presence of limited oxygen (Grewal

et al., 2018). It consists of a complex mixture of over 200 water-soluble bioactive compounds including organic acids, phenolics, sugar and alcohol derivatives (Wei et al., 2010; Grewal et al., 2018; Ofoe et al., 2022a). However, its chemical composition depends on the feedstock, temperature, residence time and heating rate. In agriculture, PA has been demonstrated to promote seed germination, vegetative growth and yield in several crops (Grewal et al., 2018; Wang et al., 2019b; Ofoe et al., 2022b).

Accumulating evidence has revealed that seed priming with PA treatments enhances plant tolerance to Al and drought stress by regulating genes and proteins involved in energy production and antioxidant defense systems (Grewal et al., 2018; Wang et al., 2019b; Ofoe et al., 2022b). Under drought stress, Wang et al. (2019b) reported that PA stimulates the differential accumulation of proteins involved in carbohydrate metabolism in wheat (*Triticum aestivum* L.) seedlings. This increase in drought tolerance was related to increased activities of enzymes related to glycolysis and the TCA cycle. Similarly, Ofoe et al. (2022b) showed that PA enhances peroxidase activities, and promotes the expression of auxin response factor and antioxidant genes in primed seedlings under Al stress, thus promoting Al tolerance. These findings suggest that PA can promote normal cellular balance and metabolic processes under stress conditions but requires further investigation. Despite the accumulating efforts to study the stimulation effects of PA on plant growth and stress tolerance, the metabolic mechanism underlying plant response to PA and Al stress remains unknown. Furthermore, no studies to date have explored the impact of PA on CCM regulation in plants under Al stress. In this study, we examined the metabolic profile involved in the CCM of PA-treated Scotia tomato seedlings under varying Al stress conditions. This investigation provides metabolic insights governing biochemical pathways that are crucial for understanding how PA mediates Al – tolerance in plants.

8.2 MATERIALS AND METHODS

8.2.1 Plant material and experimental conditions

The experiment was conducted from January to March 2022 and repeated from March to May 2022 at the Department of Plant, Food, and Environmental Sciences, Faculty of Agriculture, Dalhousie University, Truro. Scotia tomato seeds were purchased from Halifax seeds (Halifax, Canada) and PA derived from white pine (*Pinus strobus*) biomass was produced by Proton Power Inc (Lenoir City, USA). Details of the PA and its chemical constituents were previously published by Ofoe et al. (2022a).

The Scotia tomato seeds were initially sterilized with 10% NaClO for 10 min and thoroughly washed 3 times with sterile distilled water. The seeds were further sterilized with 70% ethanol for 5 mins and washed thoroughly with sterile distilled water. The sterilized seeds were sown in a Pro-Mix® BX (Premier Tech Horticulture, Rivière-du-Loup, Québec, Canada) and grown for four weeks in a growth chamber (Conviron Controlled Environments Ltd, Winnipeg, Canada) with 16/8 h day/night photoperiod, 24/22 °C day/night temperature regime, 300 μmol m^{-2} s^{-1} light intensity and a relative humidity of 70%. Uniform seedlings with an 8-cm root length at the 3rd to 4th true leaf stage were transplanted into a 10.2-cm plastic pot containing 500 g of sterilized sand with an average particle size of 0.5–1.0 mm. The seedlings were maintained with a 25% strength Hoagland nutrient solution (pH=5.0) at planting for a week under a growth chamber to acclimatize.

8.2.2 Experimental treatment and design

After one week of acclimation, half-strength followed by full-strength Hoagland nutrient solutions were amended with varying PA and Al concentrations and applied every week. PA treatments

were applied to the nutrient solution at 0%, 0.25% and 1% PA/ddH_2O (*v/v*) with Al ($AlCl_3$) concentrations at 0, 1 and 4 mM. The nutrient solution (pH=4.5) was renewed every 3 days to maintain adequate moisture content. Throughout the entire study period, the pH of the amended nutrient solution (PA with or without Al) was monitored frequently and adjusted to 4.5, using either sodium hydroxide (NaOH) to increase the pH or HCl to reduce the pH. The study was arranged in a 3 × 3 factorial completely randomized design with five replications at one plant per replication.

8.2.3 Plant sample preparation

The fully expanded leaf tissues on the third and fourth petioles from the top (15 leaves from 5 plants per treatment) were collected 40 days after transplanting and immediately frozen in liquid nitrogen. The frozen samples were ground into a fine powder and stored in a -80°C freezer for central carbon metabolite analyses.

8.2.4 Metabolite quantitation using LC-MRM/MS

Targeted metabolite quantitation was performed at the University of Victoria Genome BC – Proteomics Centre of The Metabolomics Innovation Centre, Canada. Ground samples (50 mg) of each ground sample were mixed with 80% methanol and homogenized with two metal balls on an MM400 mill mixer (Retsch, Haan, Germany) for 3 min at a shaking frequency of 30 Hz. The mixture was then sonicated in an ice-water bath for 5 min and centrifuged at 12000 × *g* at 5°C for 20 min. Next, 250 µL of the supernatant was mixed with 150 µL of water and 150 µL of dichloromethane. The mixture was vortexed for 30 s and centrifuged at 21000 × *g* for 20 min.

Subsequently, 80 µL aliquots of the supernatant were dried under a nitrogen gas flow and the residues were used for the following assay.

8.2.4.1 TCA cycle

A standard solution of all targeted carboxylic acids was prepared using 80% methanol with concentrations ranging from 200 to 1000 µM. For each sample, 50 µL of both the standard solution and the sample supernatant were mixed with an equal volume of 200 mM 3-nitrophenyl hydrazines (NPH) solution and 150 mM carbodiimide hydrochloride (EDC)-6% pyridine solution. The mixture was then incubated at 30°C for 40 min. After the reaction, 450 µL of water was added to each solution and 10 µL of the resulting solution was injected into a C18 liquid chromatography (LC) column (2.1 x 100 mm, 1.8 µm) for quantification of carboxylic acids using ultrahigh LC-multiple reaction monitoring/mass spectroscopy (UPLC-MRM/MS) with (−) ion detection. The UPLC-MRM/MS was performed on an Agilent 1290 UHPLC system coupled to a Sciex 4000 QTRAP MS instrument (AB Sciex, Concord, ON, Canada). The metabolite-dependent parameters used in the UPLC-MRM/MS were based on the procedure described by Han et al. (2013a).

8.2.4.2 Glucose and selected sugar phosphates

The dried residue of each sample was mixed with 50 µL of 50% methanol. The solution and 50 µL of each serially diluted standard solution of glucose, ribose, ribose-5-phosphate, glucose-6-phosphate and mannose-6-phosphate were mixed with 100 µL of 25 mM 3-amino-9-ethyl carbazole (AEC), 50 µL of 50 mM sodium cyanoborohydride ($NaCBH_3$) and 20 µL of LC/MS grade acetic acid. The mixtures were incubated at 60°C for 70 min and 200 µL of water and 300 µL of chloroform were added. Following centrifugation at 12500 × *g* for 5 min, 50 µL of each

supernatant was mixed with an equal volume of water and 10 μL of the resulting solution was injected into a pentafluorophenylpropyl (PFP) LC column (2.1 x 150 mm, 1.7 μm) for UPLC-MRM/MS analysis. The UPLC-MRM/MS analysis was performed on an Agilent 1290 UHPLC system coupled to an Agilent 6495B QQQ instrument (Conquer Scientific, Poway, CA, USA) with positive-ion detection. The metabolite-dependent parameters used in the UPLC-MRM/MS were based on the procedure described by Han et al. (2013b).

8.2.4.3 Other metabolites

An internal standard (IS) solution containing 25 isotope-labelled metabolites including adenosine diphosphate (ADP), adenosine triphosphate (ATP), fructose-6-phosphate (fructose-6P), fructose-bisphosphate, glycerol-3-phosphate, nicotinamide adenine dinucleotide (NAD), NADH, glucose-1-phosphate, ribose-5-phosphate and others was prepared in 50% methanol with concentrations ranging from 0.00002 to 10 μM. The dried residue of each sample was dissolved in 100 μL of the IS solution. Then, 10 μL of the resulting solution and standard solutions were injected into a C18 LC column (2.1 x 100 mm, 1.9 μm) for UPLC-MRM/MS with (−) ion detection. The UPLC-MRM/MS analysis was performed on a Waters Acquity UPLC system coupled to a Sciex QTRAP 6500 Plus MS instrument. A tributylamine acetate buffer – acetonitrile/methanol (1:1, *v/v*) was used as the mobile phase for gradient elution (10% to 50% B over 25 min) at 0.25 mL/min and a temperature of 60 ºC.

8.2.5 Data analysis

The concentrations of the detected analytes in the above assays were calculated using internal standard calibration. This involved interpolating the constructed linear regression curves of

individual compounds using the analyte-to-internal standard peak area ratios measured from injections of the sample solution. The data analysis of the metabolites was performed using Analyst 1.6.2. A multivariate statistical analysis including two-dimensional (2D) principal component analysis (PCA) and hierarchical clustering was performed to assess the differential metabolism per group. The analysis was performed using XLSTAT version 2022.3 (Addinsoft, New York, NY, USA), and Euclidean distance was utilized for constructing the hierarchical clustering analysis.

8.3 RESULTS AND DISCUSSION

8.3.1 Overall metabolic changes in PA-treated plants under Al stress

Metabolites are the end products of cellular processes, and their levels are influenced by coordinated responses of biological systems to changes in internal and external conditions (Das et al., 2017). Although the metabolic analysis of plant responses to both PA and Al stress is relatively unknown, this study provides a comprehensive understanding of the complex metabolic changes that occur in PA-treated tomato plants under Al stress. Our cluster analysis of both PA-treated and control plants under Al stress revealed two main groupings based on the global metabolic profile (Figure 8.1B). While the effect of PA was somewhat comparable to the control group, distinct metabolic changes were observed with 1% PA under 1 mM Al stress, but not with 0.25% PA and 1 mM Al alone (Figure 8.1A&B). Moreover, the clustering of the control group, PA alone, 0.25% PA under 1 mM Al and 1 mM Al alone treatments indicated that the effect of 1 mM Al was less toxic to the tomato plants and resulted in a stable metabolic profile. In contrast, a considerable alteration in metabolic profile was observed in PA-treated and control groups under 4 mM Al stress with the 1% PA treatment exhibiting the most pronounced effect (Figure 8.1A&B). These results were expected, as previous studies have shown that high PA and Al concentrations induced

phytotoxic effects, while lower concentrations stimulate plant growth and productivity (Li et al., 2016a; Muhammad et al., 2019; Liu et al., 2020; Liu et al., 2021b; Ofoe et al., 2022c).

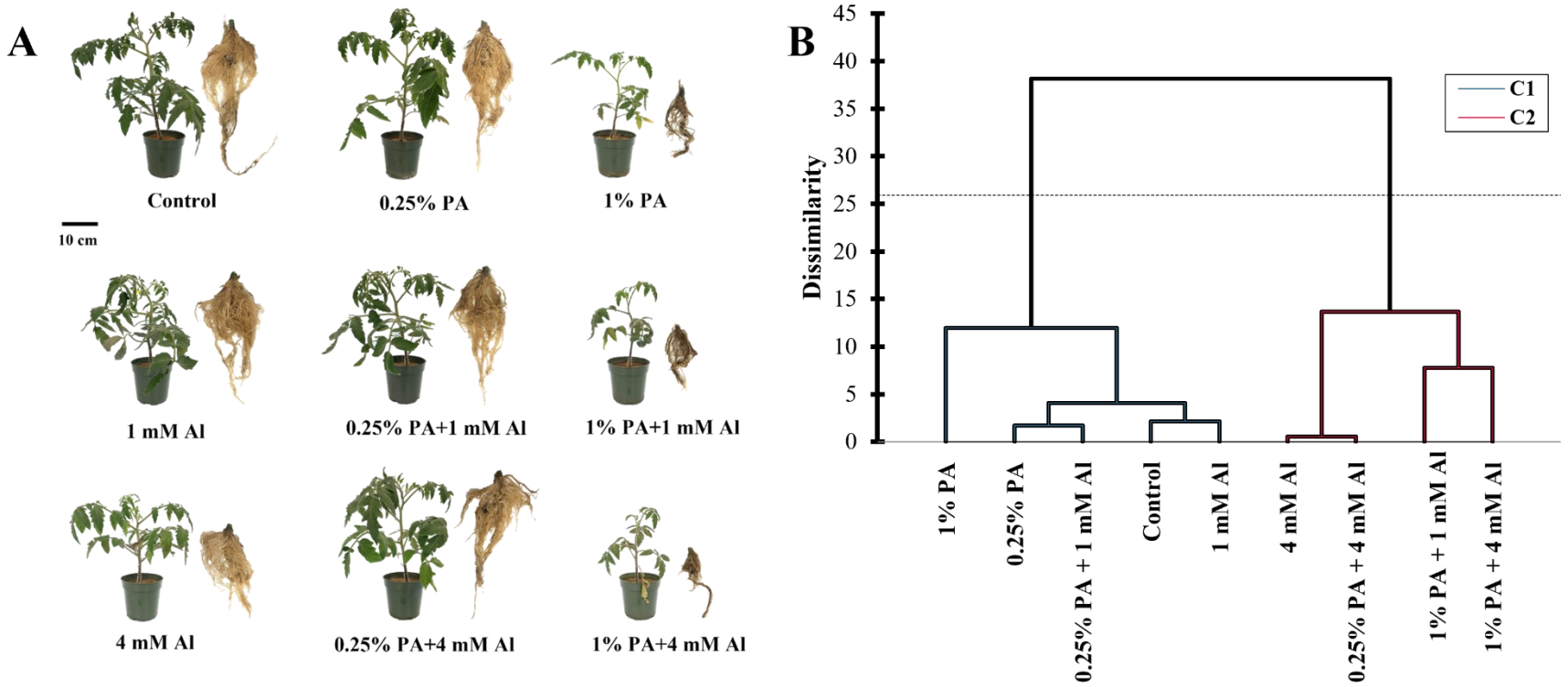

Figure 8.1. Response of Scotia tomato seedlings to pyroligneous acid (PA) treatment under aluminum stress (Al). (A) Morphological effect on tomato growth. (B) Cluster analysis of overall central carbon metabolites composition in the leaves.

8.3.2 Differential accumulation of metabolites in PA-treated plants under Al stress

Exposure of plants to adverse environmental conditions, including Al stress necessitates rapid metabolic reprogramming to stimulate stress tolerance. These metabolic changes are coordinated among diverse pathways to alter fluxes related to the different CCM routes (Timm & Arrivault, 2021). Table 8.1 shows the total differential abundance of metabolites involved in specific pathways within the CCM. In total, 48 metabolites were detected (Figure S8.1; Table S8.1) and categorized into five groups based on their biological function in the CCM routes: CBC, glycolysis, PPP, TCA cycle and ETC (Table 8.1). Among these groups, glycolysis was the main differentially expressed metabolic pathway, accounting for approximately 75% of the total identified metabolites (Figure S8.2). Additionally, the TCA cycle accounted for approximately 25%, while the remaining groups comprised less than 1% of the total differentially expressed metabolites (Figure S8.2).

Table 8.1. Total metabolites involved in central carbon metabolic pathways in the leaves of tomato (*Solanum lycopersicum* 'Scotia') seedlings treated with pyroligneous acid (PA) under aluminum (Al) stress.

Treatment	CBC (nmol g^{-1} FW)	Glycolysis (µmol g^{-1} FW)	PPP (nmol g^{-1} FW)	TCA (µmol g^{-1} FW)	ETC (nmol g^{-1} FW)
Control	23.79	21.72	30.01	6.97	5.63
1 mM Al	15.54	15.18	20.70	6.08	5.38
4 mM Al	6.10	20.63	5.97	7.77	4.88
0.25% PA	16.15	20.72	22.90	8.66	6.51
0.25% PA + 1 mM Al	11.10	15.81	13.40	7.99	6.05
0.25% PA + 4 mM Al	5.30	15.60	5.23	8.03	5.75
1% PA	17.18	38.16	20.97	10.18	8.17
1% PA + 1 mM Al	6.50	32.36	6.33	11.97	7.07
1% PA + 4 mM Al	5.33	56.65	5.13	10.92	3.53
CV (%)	55.70	52.56	64.72	21.97	22.43

CBC, Calvin−Benson cycle; PPP, pentose phosphate pathway; TCA, tricarboxylic acid cycle; ETC, electron transport chain

8.3.2.1 Calvin−Benson cycle

The Calvin−Benson cycle is the main biochemical pathway for carbon fixation in the chloroplast stroma of C3 plants (Michelet et al., 2013). During this process, plants utilize light energy to produce the chemical energy required to synthesize sugars and other carbon intermediates (Sharma et al., 2020). The regulation of CBC under stressful environments has been identified as a survival strategy for plants (Sharma et al., 2020). In the present study, both PA application and Al stress greatly affected the total CBC metabolites in the leaves of tomato seedlings (Table 8.1). PA treatments slightly reduced the total CBC metabolites compared to the control (Table 8.1). Similarly, Al stress exhibited a phytotoxic effect on CBC metabolites, especially under 4 mM Al and this was further pronounced in PA-treated plants, suggesting that PA treatment could lead to decreased photosynthetic capacity under Al stress (Table 8.1). Moreover, the reduction in CBC metabolites under 4 mM Al stress can be attributed to low levels of all CBC metabolites except for sedoheptulose-7P (Figure 8.2A). This result agrees with previous studies that demonstrated a decrease in carbon fixation in tomato (Simon et al., 1994), spinach (*Spinacia oleracea*) (Hampp & Schnabl, 1975), citrus (Chen et al., 2005a; Chen et al., 2005b; Jiang et al., 2009a) and rice (*Oryza sativa*) seedlings (Mishra & Dubey, 2008) under Al stress. Similarly, the decrease in total CBC metabolites caused by 0.25% PA, irrespective of Al exposure may be attributed to low contents of all CBC metabolites except for DHAP, ribulose-5P and sedoheptulose-7P. While 3-phosphoglyceric acid, DAP, fructose 1,6-bisP and ribulose-bisP were increased in the 1% PA condition under 4 mM Al, the reduction in total CBC metabolites in 1% PA-treated plants under Al stress could be due to decreased glyceraldehyde-3P, fructose 6-phosphate, sedoheptulose-bisP,

sedoheptulose-7P, ribose-5P and ribulose-5P (Figure 8.2A). Although PA treatment led to a reduction in total CBC metabolites, the impact of PA under Al stress could be considered slightly lower compared to 4 mM Al alone.

Previous research has suggested that the Al-induced downregulation of CBC results from both stomatal and non-stomatal factors (Chen et al., 2005b; Sharma et al., 2020). Stomatal closure is thought to reduce leaf CO_2 influx, which further impairs CBC processes (Sharma et al., 2020). However, some studies have indicated that stomatal closure alone cannot fully explain the Al-induced reduction in CBC. This is because intracellular CO_2 levels were higher in Al-stressed leaves or comparable to those of control leaves, irrespective of stomatal conductance (Simon et al., 1994; Peixoto et al., 2002; Chen et al., 2005a; Chen et al., 2005b; Jiang et al., 2009b). Pereira et al. (2000) also indicated that Al-induced reduction in CBC was associated with thylakoid structural damage in lemon (*Citrus limon*) seedlings. Although the activities of CBC enzymes were not examined in this study, several studies have reported that heavy metal stress inhibits the activities of CBC enzyme activities leading to a reduction the overall CBC process (Ahsan et al., 2009; D'Alessandro et al., 2013; Manzoor et al., 2022; Sharma et al., 2022). Hence, the decrease in total CBC metabolites in both control and PA-treated plants under Al stress could be due to Al-induced structural damage and reduction in CBC enzyme activities (Pereira et al., 2000; Manzoor et al., 2022).

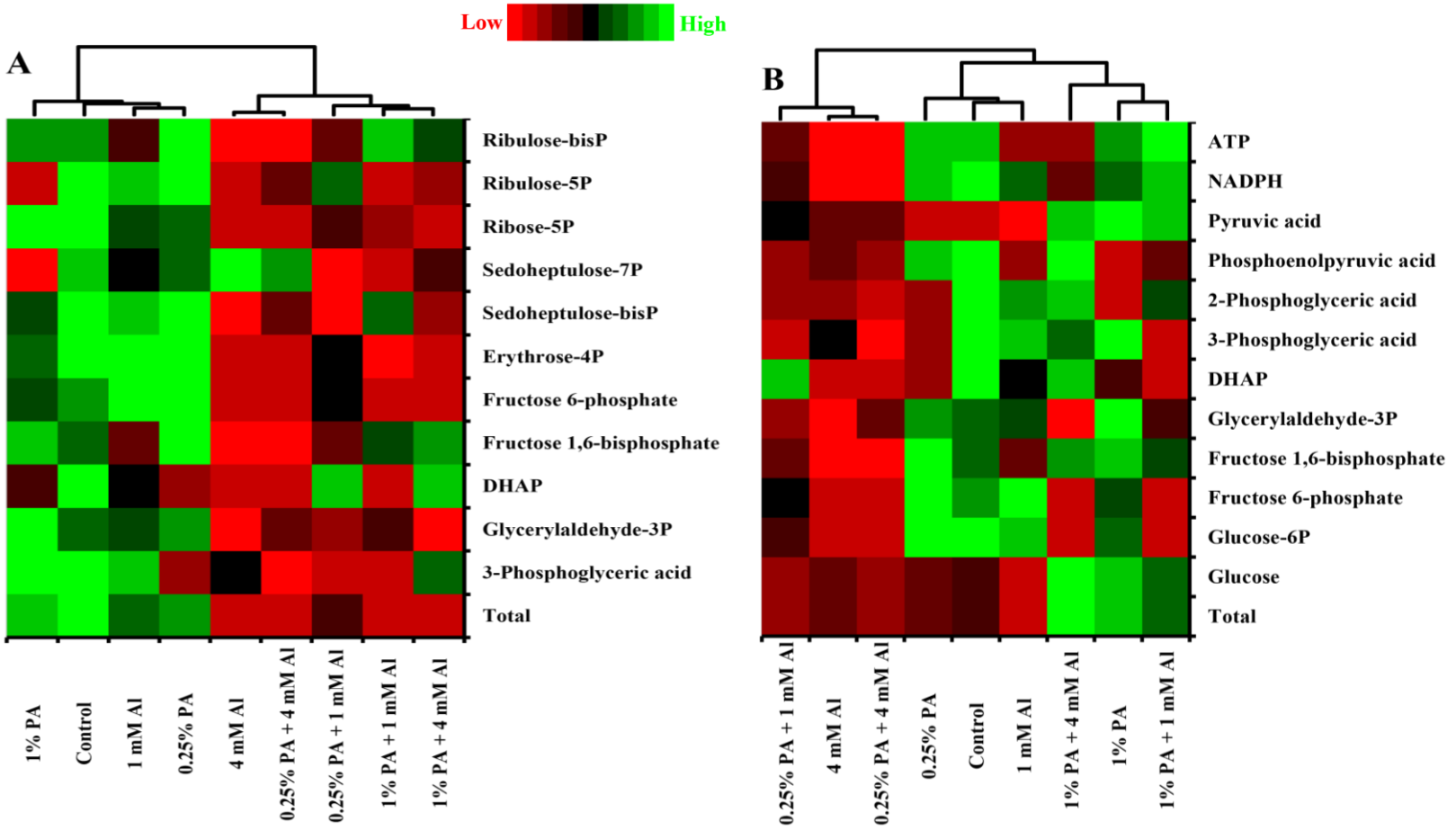

Figure 8.2. Heat map of metabolites involved in (A) the Calvin–Benson cycle and (B) the glycolysis pathway in leaves of Scotia tomato seedlings treated with pyroligneous acid (PA) under aluminum (Al) stress. Metabolite concentrations in each compartment are normalized across all data for an individual metabolite such that similar colour intensities between compounds can represent widely differing concentrations. The red colour represents a lower concentration, and the green colour represents a higher concentration of a particular metabolite.

8.3.2.2 Glycolysis

Balanced energy flow under environmental stress plays a crucial role in plant growth, development and stress tolerance. Glycolysis is a significant catabolic pathway that breaks down carbohydrates to provide energy for physiological and cellular operations in plants (Timm & Arrivault, 2021). In this study, carbohydrate catabolism *via* the glycolysis pathway was higher in 1% PA-treated plants irrespective of Al treatment (Table 8.1). In the absence of Al exposure, the total glycolysis metabolites were markedly increased in the 1% PA-treated plants by approximately 75% compared to the control. When exposed to Al stress, glycolysis metabolites were sightly downregulated in the control plants, while the 1% PA treatment increased the total glycolysis metabolites by approximately 200% and 175% compared to the 1 mM Al and 4 mM Al treatments, respectively (Table 8.1). Moreover, the increase in total glycolysis metabolites with 1% PA treatment in the absence of Al exposure was due to high glucose and pyruvate acid contents (Figure 8.2B). On the other hand, the increase in total glycolysis metabolites in 1% PA-treated plants under Al stress can be ascribed to high levels of glucose, fructose 1, 6-phosphate, DHAP, 3- and 2-phosphoglyceric acid, PEP, pyruvic acid, NADPH and ATP (Figure 8.2B). These findings are consistent with the results reported by Niedziela et al. (2022) who observed that key enzymes of glycolysis were enhanced in Al-treated plants, leading to accelerated production of pyruvate and acetyl CoA.

Studies have shown that Al stress leads to energy deprivation in plant growth and development. As a result, tolerant plants accumulated high levels of glucose to produce adequate ATPs through glycolysis (Koch, 2004; Li et al., 2016a; Pinto et al., 2021). For instance, in Al-tolerant rice, Wang et al. (2014) showed that glycolytic pathway proteins are enhanced, which could maintain basic respiration needs and/or generate ATP for Al-stress tolerance. A similar increase in glycolytic flux

was noted in Al-tolerant citrus leaves (Li et al., 2016a). The magnitude of glucose production in plants through the CBC is crucial in confirming Al stress tolerance (Mishra & Dubey, 2008). Accumulation of glucose under Al stress also functions as an osmoprotectant, which decreases osmotic potential, regulates turgor dynamics and promotes the maintenance of membrane integrity and overall cellular homeostasis (Pandey et al., 2016; Ejaz et al., 2020). This osmoregulation enables plants to maintain sufficient adequate carbohydrate reserves for sustaining essential metabolism under Al stress (Mishra & Dubey, 2008). These findings indicate that the 1% PA treatment can trigger a metabolic switch from growth to survival mode *via* glucose metabolism for energy generation. Furthermore, biostimulants have been reported to enhance plant tolerance to various stresses (Conselvan et al., 2018). Similar to many other biostimulants, PA has been reported to enhance the production of proteins and metabolites associated with carbohydrate metabolism and energy production (Wang et al., 2019b; Ofoe et al., 2022b). Consistent with the study of Wang et al. (2019b), PA treatment increased the abundance of glycolytic metabolic pathway proteins, increasing plant tolerance to drought. Additionally, the bioactive compounds in PA may act as signalling molecules to regulate key metabolic pathways including CCM and/or stimulate differential gene expression to promote plant growth and resilience to Al stress (Wang et al., 2019b; Ofoe et al., 2022a; Ofoe et al., 2022b). Hence, increasing glycolytic metabolites with 1% PA treatment can be considered as an effective strategy to meet the energy demand for Al tolerance and adaptation.

8.3.2.3 Pentose phosphate pathway

The PPP is a critical metabolic pathway for glucose degradation and is important for providing reducing power and intermediate metabolites for other pathways (Lehmann et al., 2012). The

present study showed that the total PPP metabolites were affected by both PA and Al treatment (Table 8.1; Figure 8.3A). The total PPP metabolites were reduced by approximately 23% and 30% with 0.25% PA and 1% PA respectively, compared to the control. The decrease in total PPP metabolites in 1% PA-treated plants can be attributed to low levels of ribulose-5P and sedoheptulose-7P, although 6-phosphogluconate levels was higher compared to the control (Figure 8.3A). On the other hand, Al stress markedly reduced total PPP metabolites and PA treatment could not alleviate such effects compared to the control (Table 8.1). For instance, under 1 mM Al, the total PPP metabolites were substantially reduced by approximately 35% and 69% with 0.25% PA and 1% PA treatments respectively, compared to 1 mM Al treatment alone. The reduction in total PPP metabolites in 0.25% PA-treated plants can be attributed to low glucose-6P, ribose-5P, glyceraldehyde-3P, fructose-6P, erythrose-4P, and sedoheptulose-7P contents. Similarly, the reduction to total PPP metabolites following the application of 1% PA can be attributed to low glucose-6P, ribulose-5P, ribose 5-P, glyceraldehyde-3P, fructose-6P, erythrose-4P, and sedoheptulose-7P contents, although 6-phosphogluconate levels were higher compared to the 1 mM Al treatment alone (Figure 8.3A).

The 4 mM Al significantly reduced the total PPP metabolites, which were not different from those of 0.25% and 1% PA-treated plants under the same conditions of Al stress (Table 8.1). Furthermore, the substantial reduction in total PPP metabolites in both control and PA-treated plants under 4 mM Al can be attributed to low levels of all PPP metabolites except 6-phosphogluconate and sedoheptulose-7P contents (Figure 8.3A). Nicotinamide adenine dinucleotide phosphate (NADPH) is the primary reducing power in the PPP pathway and is used to maintain cellular redox homeostasis *via* antioxidant production (Lehmann et al., 2012).

However, the levels of NADPH were not affected by PA treatment but were reduced under 4 mM Al stress (Figure 3A). It has been established that Al stress leads to ROS accumulation which causes cellular damage and programmed cell death (Huang et al., 2014b). The results of this study indicate that a reduction in NADPH levels under Al stress could increase ROS generation and compromise the antioxidant defence system in plants.

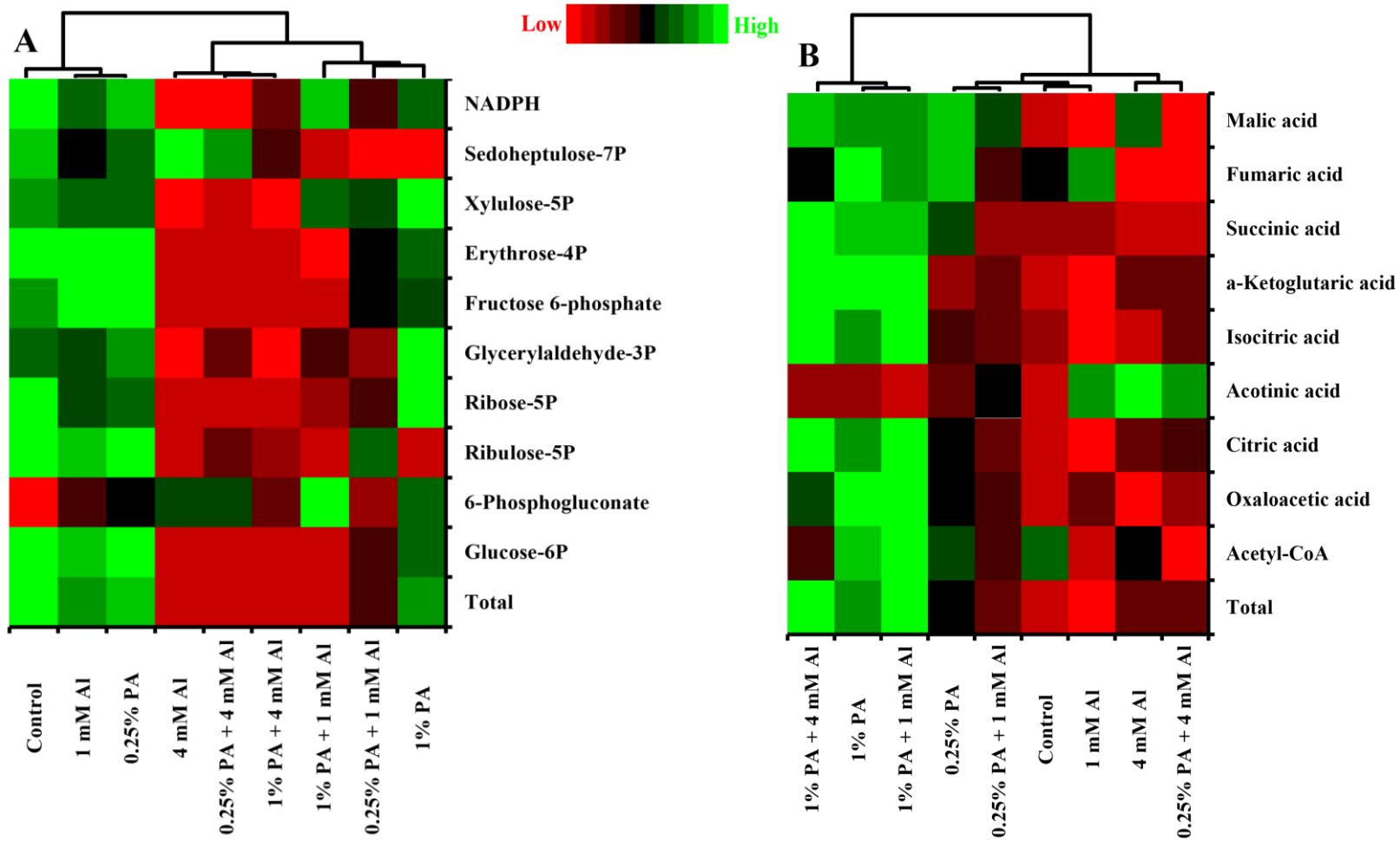

Figure 8.3. Heat map of metabolites profile involved in (A) pentose phosphate pathway and (B) tricarboxylic acid (TCA) cycle in leaves of Scotia tomato seedlings treated with pyroligneous acid (PA) under aluminum (Al) stress. Metabolite concentrations in every compartment are normalized across all data for an individual metabolite such that similar colour intensities between compounds can represent widely differing concentrations. The red colour represents a lower concentration, and the green colour represents a higher concentration of a particular metabolite.

8.3.2.4 Tricarboxylic acid cycle

The TCA cycle is a central biochemical pathways for respiratory substrate oxidation and the production of ATP for all cellular functions (Sweetlove et al., 2010). In response to Al stress, the TCA cycle serves as a reservoir for organic acids (OA) production, which has been strongly linked to Al tolerance in most plants (Kochian et al., 2015; Ofoe et al., 2023). Our study revealed that the total TCA cycle intermediate metabolites were affected by PA and Al treatment (Table 8.1; Figure 8.3B). In the absence of Al stress, the total TCA cycle metabolites increased by approximately 24% and 46% with PA treatment compared to the control. The increased total TCA cycle metabolites with 0.25% PA could be due to increased levels of oxaloacetic acid, citric acid, succinic acid, fumaric acid and malic acid (Figure 8.3B). Likewise, the increased total TCA cycle metabolites with 1% PA treatment can be ascribed to high contents of all TCA cycle metabolites except for acetyl-CoA and aconitic acid, which were not altered compared to the control (Figure 8.3B). Similarly, in response to Al stress, PA-treated plants accumulated high levels of TCA cycle metabolites compared to plants treated with Al alone. Exposing the plants to 4 mM Al without PA increased the total TCA cycle metabolites by approximately 11% due to high levels of citric acid, aconitic acid, α-ketoglutaric acid and malic acid (Figure 8.3B). It has been established that primary metabolic constituents associated with Al tolerance are strongly linked to mitochondrial metabolism and OA production (Kochian et al., 2015; Siqueira et al., 2020; Ofoe et al., 2023). Organic acid production in response to Al stress is the most-characterized mechanism for Al tolerance with citrate and malate being the common TCA cycle metabolites identified in several plants (Siqueira et al., 2020; Pinto et al., 2021; Ofoe et al., 2023). For instance, tomato plants produce and secrets malate, which chelate Al ions into non-toxic forms (Ye et al., 2017). The increased OA production observed under Al stress in this study is consistent with previous studies

in which mitochondrial citrate and malate levels were enhanced and shown to improve Al tolerance in tomato (Ye et al., 2017), maize (*Zea mays*) (Wang et al., 2015b; Siqueira et al., 2020; Pinto et al., 2021), buckwheat (*Fagopyrum esculentum*) (Wang et al., 2015a), cabbage (*Brassica oleracea*) (Zhang et al., 2018) and wheat (*Triticum aestivum*) (Sasaki et al., 2004).

Furthermore, both 0.25% PA and 1% PA treatments resulted in the accumulation of approximately 31% and 97% of the total TCA cycle metabolites, respectively, under 1 mM Al compared to plants treated with 1 mM Al alone. Under 4 mM Al, the total TCA cycle metabolites increased by approximately 3% and 41% in 0.25% PA and 1% PA-treated plants, respectively, compared to plants exposed to 4 mM Al alone (Table 8.1). The increase in total TCA cycle metabolites with 1% PA treatment under Al stress could be due to high levels of all the TCA metabolites except for aconitic acid which was reduced (Figure 8.3B). Similarly, Wang et al. (2019b) reported that PA treatment enhanced the TCA cycle in wheat seedlings under drought stress due to increased activities of malate dehydrogenase. Additionally, Sweetlove et al. (2010) suggested that the activities of the different TCA cycle enzymes are independent of each other, and the TCA metabolites vary in their flux levels. Although the activities of these enzymes were not examined in this study, the increased TCA cycle metabolites following PA treatment could be associated with an increase in enzyme activities. This indicates that PA can promote the TCA cycle to produce sufficient ATP to accommodate the energy demand of plants under Al stress (Wang et al., 2019b). Evidence from numerous studies revealed that some plants accumulate high levels of TCA cycle metabolites internally to detoxify Al in roots and leaf cells, and compartmentalize Al−OA complexes into the vacuole (Kochian et al., 2015; Wang et al., 2015a). This internal Al complexation could prevent Al from interacting with macromolecules, including nucleic acids and

proteins. Although this an Al tolerance mechanism is mostly associated with hyperaccumulators (Wang et al., 2015a; Ofoe et al., 2023), the increased TCA cycle metabolites in the leaves of both PA and control-treated plants under Al stress could suggest the stimulation of internal detoxification of Al ions, thereby promoting Al tolerance. Moreover, the TCA cycle metabolites are not only known to chelate Al ion. For instance, citrate is plays an important role in antioxidant production is involved in respiratory assimilation to produce energy for stress defense (Zhao et al., 2015). Additionally, α-ketoglutaric acid is critical in respiration and nitrogen metabolism for amino acid biosynthesis, which regulate osmotic potential and mediate stress tolerance in plants (Xu & Fu, 2022). Hence, the increased TCA cycle metabolites in PA and control plants under Al stress can also be linked to amino acid and nucleic acid biosynthesis for Al tolerance.

8.3.2.5 Electron transport chain

The electron transport chain is one of the most critical pathways for both cellular respiration and photosynthesis (Sweetlove et al., 2010). It consists of an array of electron transporters that oxidize reducing equivalents for energy generation *via* ATP biosynthesis (Fernie et al., 2004). The results of this study revealed that PA and Al treatment altered the total ETC metabolites in tomato leaves (Table 8.1; Figure 8.4). The total ETC metabolites were increased by approximately 16% and 45% in 0.25% PA and 1% PA-treated plants, respectively, compared to the control in the absence of Al stress (Table 8.1). This increase in ETC metabolites following PA treatments could be due to high levels of FMN, FAD, NAD and NADH contents (Figure 8.4). Nonetheless, the levels of ADP and ATP remained unchanged with PA treatments (Figure 8.4). When exposed to Al stress, the tomato plants slightly reduced their total ETC metabolites by approximately 13% under 4 mM Al, while those under 1 mM Al exhibited no considerable change. The reduction in total ETC metabolites

with 4 mM Al can be attributed to low ADP and ATP contents compared to the control (Figure 8.4). Accumulating evidence has revealed that Al stress impairs the activities of ETC complexes and could result in decreased metabolite production (Pereira et al., 2000; Li & Xing, 2011; Li et al., 2012; Su et al., 2019).

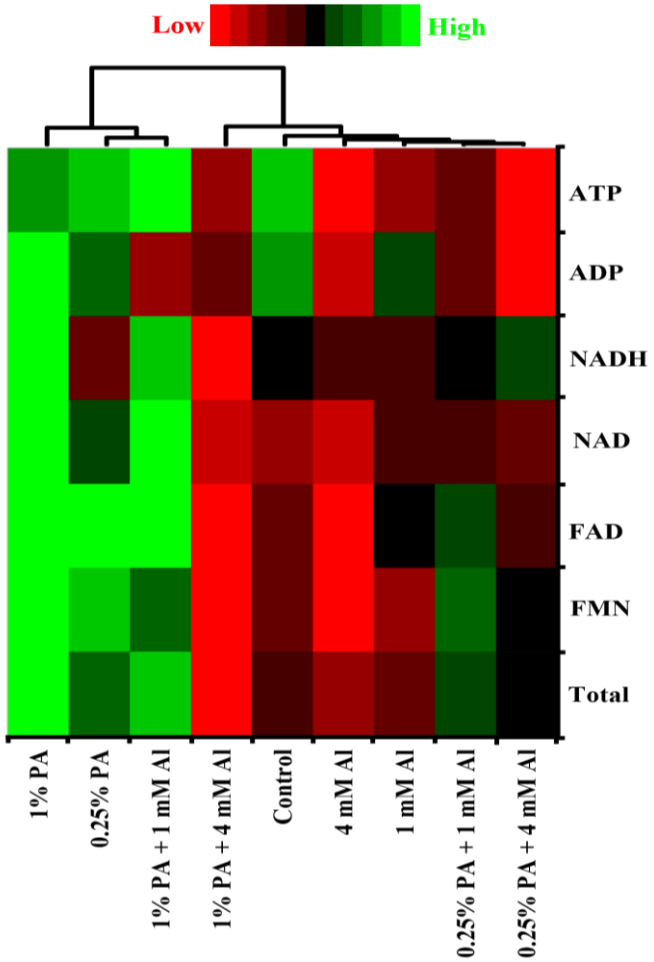

Figure 8.4. Heat map of metabolites profile involved in electron transport chain in the leaves of Scotia tomato seedlings treated with pyroligneous acid (PA) under aluminum (Al) stress. Metabolite concentrations in each compartment are normalized across all data for an individual metabolite such that similar colour intensities between compounds can represent widely differing concentrations. The red colour represents a lower concentration, and the green colour represents a higher concentration of a particular metabolite.

Moreover, both 0.25% and 1% PA treatments under 1 mM Al increased the total ETC metabolites by approximately 12% and 31%, respectively, compared to 1 mM Al plants. The increased total ETC metabolites in the 0.25% PA-treated plants can be associated with increased FMN, FAD, NAD and ATP contents while that of 1% PA-treated plants is due to high FMN, FAD, NAD, NADH and ATP contents (Figure 4). However, the total ETC metabolites were slightly increased in plants treated with 0.25% PA plants under 4 mM Al while 1% PA decreased the total ETC metabolites compared to 4 mM Al alone (Table 8.1). Additionally, the increase in ETC metabolites with 0.25% PA can be attributed to a slight increase in FMN, FAD, NAD and, NADH contents, while the reduction in ETC metabolites with 1% PA treatments was due to low NADH contents (Figure 8.4). ATP synthase is critical for ATP production in ETC (Fernie et al., 2004). According to Su et al. (2019), Al stress targets and damage subunits of ATP synthase, thereby, reducing the amount of ATP generated. With a limitation in ATP production and electron transport, electrons leakage is enhanced, which could result in uncontrollable ROS generation and oxidative stress-induced cell death (Fernie et al., 2004; Li & Xing, 2011). Interestingly, Wang et al. (2019b) reported that the relative abundance of proteins related to ATP synthesis was increased in PA-treated wheat seedlings under drought stress. Although ATP-related proteins were not examined in this study, the increase in ATP production in PA-treated plants alone and with 1 mM Al stress partially aligns with the findings of Wang et al. (2019b). In plant stress adaptation, the energy cost is high and the enhancement of ETC processes with PA treatments suggests that restoring energy supply *via* ATP production is critical to protect several basal metabolic processes under Al stress.

8.3.3 Association between central carbon metabolites

To further examined the association amongst the intermediate metabolites of the CCM routes in the PA-treated tomato seedlings under Al stress, a 2-D PCA and Pearson correlation were used (Table 8.2; Figures 8.5 - 6). The Pearson correlation analysis showed that the total CBC metabolites had a significantly ($p < 0.001$) strong positive association with the total PPP metabolites and a weak negative association with glycolysis and TCA cycle metabolites (Table 8.2). Additionally, the total glycolytic metabolites had a significantly ($p < 0.05$) moderate positive correlation with total TCA cycle metabolites and a weak negative association with total PPP and ETC metabolites (Table 8.2). These findings are consistent with the results reported by Niedziela et al. (2022), who demonstrated that key enzymes of glycolysis were enhanced in Al-treated plants and accelerated pyruvate and acetyl CoA production for OA synthesis. These results suggest that energy production plays a crucial role in supporting basic cellular function under Al stress, and that plants channel their photosynthetic carbon for stress adaption (Wang et al., 2014). On the other hand, total PPP metabolites exhibited non-significantly ($p > 0.05$) weak negative and positive associations with the total TCA cycle and ETC metabolites, respectively (Table 8.2). Similarly, the total TCA cycle metabolites had a weak positive correlation with the total ETC metabolites. The increase in glycolytic flux under Al stress proved that carbon skeletons produced *via* glycolysis are used primarily for OA production to detoxify Al ions, thereby promoting Al tolerance (Wang et al., 2015a; Ye et al., 2017; Pinto et al., 2021).

Table 8.2. Pearson correlation coefficients (r) amongst the specific central carbon metabolic pathways in Scotia tomato seedlings treated with pyroligneous acid (PA) under aluminum (Al) stress and their corresponding significance levels at $p \leq 0.05$.

Variables	CBC	Glycolysis	PPP	TCA
Glycolysis	r = -0.240 p = 0.533			
PPP	**r = 0.993** ***p* = 0.000**	r = -0.274 p = 0.475		
TCA	r = -0.436 p = 0.240	**r =0.762** ***p* = 0.017**	r = -0.461 p = 0.211	
ETC	r = 0.319 p = 0.403	r = -0.303 p = 0.429	r = 0.302 p = 0.430	r = 0.147 p = 0.706

CBC, Calvin−Benson cycle; PPP, pentose phosphate pathway; TCA, tricarboxylic acid cycle.

Although some of the total metabolites showed a non-significant ($p > 0.05$) weak correlation with other metabolites, the CBC, glycolysis and PPP shared common metabolites which showed significant ($p < 0.05$) associations (Figure 8.5; Table S8.2). For example, RuBP had a significantly ($p < 0.01$) strong positive association with fructose 1,6BP and ATP, and a moderate positive association with glucose-6P and xylulose-5P (Figure 8.5; Table S8.2). Similarly, sedoheptulose-7BP showed a significantly ($p < 0.01$) moderate positive correlation with fructose-6P, erythrose-4P and glucose-6P and a non-significant ($p > 0.05$) moderate positive association with ATP and xylulose-5P. Additionally, both ribose-5P and ribulose-5P had a significantly ($p < 0.01$) strong positive association with erythrose-4P and glucose-6P and a moderate association with fructose-6P. However, both sedoheptulose-7P and ribulose-5P exhibited a significantly ($p < 0.01$) strong negative association with pyruvic acid while ribulose-5P had a moderate association with xylulose-5P (Figure 8.5; Table S8.2). Moreover, the correlation analysis among the individual metabolites confirmed that the glycolysis intermediates had a significant ($p < 0.05$) association with the TCA cycle intermediate metabolites (Figure 8.5; Table S8.2). Fructose-1,6BP had a strong positive

association with succinic acid and fumaric acid, and a negative association with aconitic acid. Glucose had a strong association with isocitric acid, α-ketoglutaric acid and succinic acid, and a moderate association with oxaloacetic acid and citric acid (Figure 8.5; Table S8.2). Similarly, pyruvic acid had a strong positive association with oxaloacetic acid, citric acid, isocitric acid and α-ketoglutaric acid, and a moderate positive association with succinic acid and acetyl-CoA (Figure 8.5; Table S8.2).

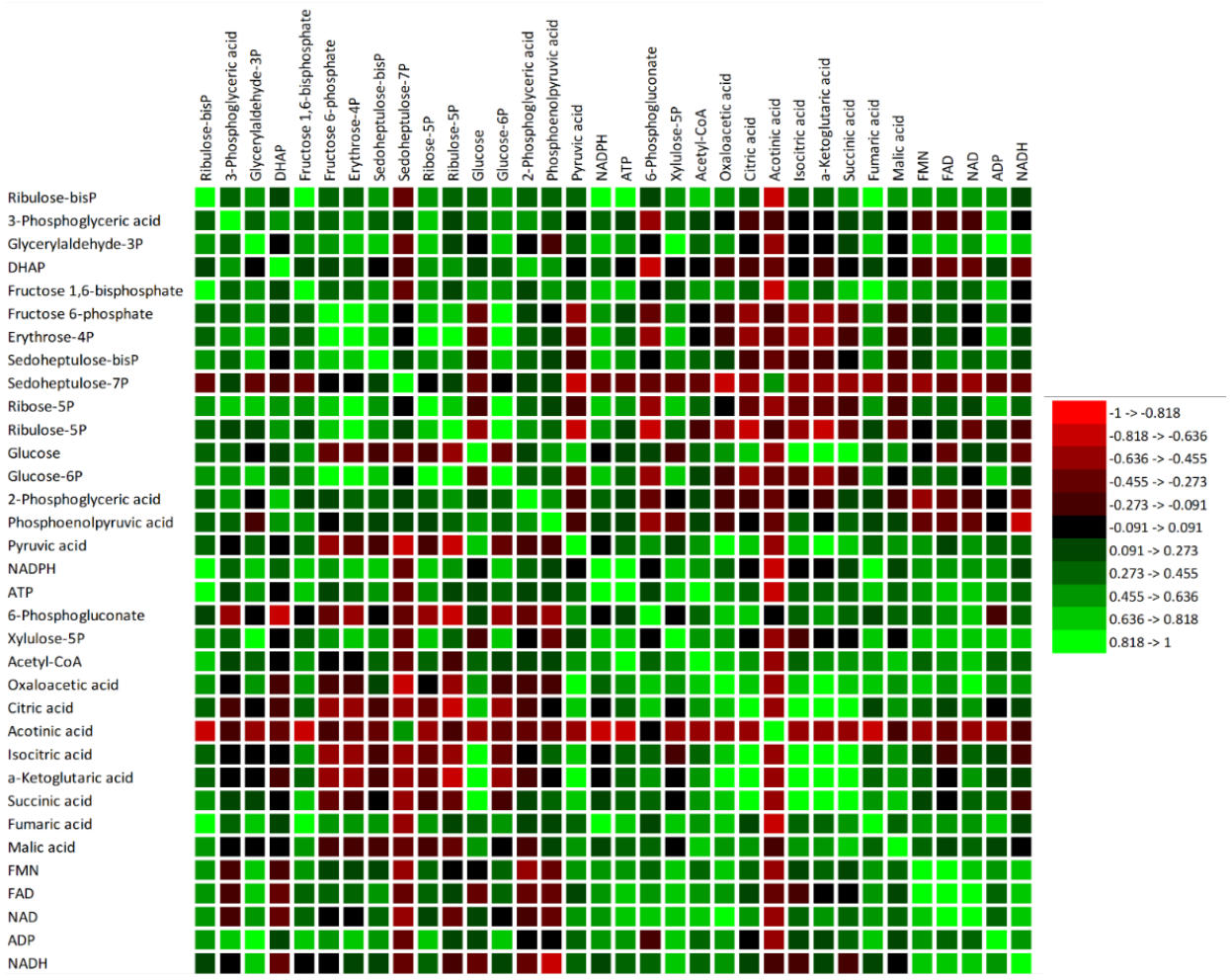

Figure 8.5. Pearson correlation matrix among individual metabolites of the central carbon metabolic pathway in Scotia tomato seedlings treated with pyroligneous acid (PA) under aluminum (Al) stress. The red colour represents a strong negative association, and the green colour represents a strong positive association. DHAP, dihydroxyacetone phosphate; NADP, nicotinamide adenine dinucleotide phosphate;

FMN, flavin mononucleotides; FAD, flavin adenine dinucleotide; ADP, adenosine diphosphate; ATP, adenosine triphosphate.

A 2D PCA biplot revealed a projection of response variables in the factor spaces (F1 and F2) and explained approximately 82% of the total disparity in the dataset (Figure 8.6). The control treatment exhibited a strong influence on both the CBC and PPP and a moderate influence on ETC. Similarly, both 0.25% PA and 1% PA showed a strong influence on ETC and a moderate influence on the CBC and PPP (Figure 8.6). However, under Al stress, 0.25% PA and 1 mM Al moderately influenced the CBC and PPP, while 1% PA showed a strong influence on TCA and glycolysis. Additionally, 1% PA under 4 mM Al showed a moderate influence on glycolysis and TCA while both 0.25% PA under 4 mM Al and 4 mM alone had no influence on the CCM metabolites (Figure 8.6). These findings are consistent with the results of Wang et al. (2019b), who reported that PA promotes the glycolysis pathway which fuels the TCA cycle to produce sufficient energy for stress tolerance. In summary, the coordinated association between the determined metabolites confirmed that PA stimulates alterations in plant metabolism to increase energy production and organic acids biosynthesis for Al stress tolerance (Figure 8.7).

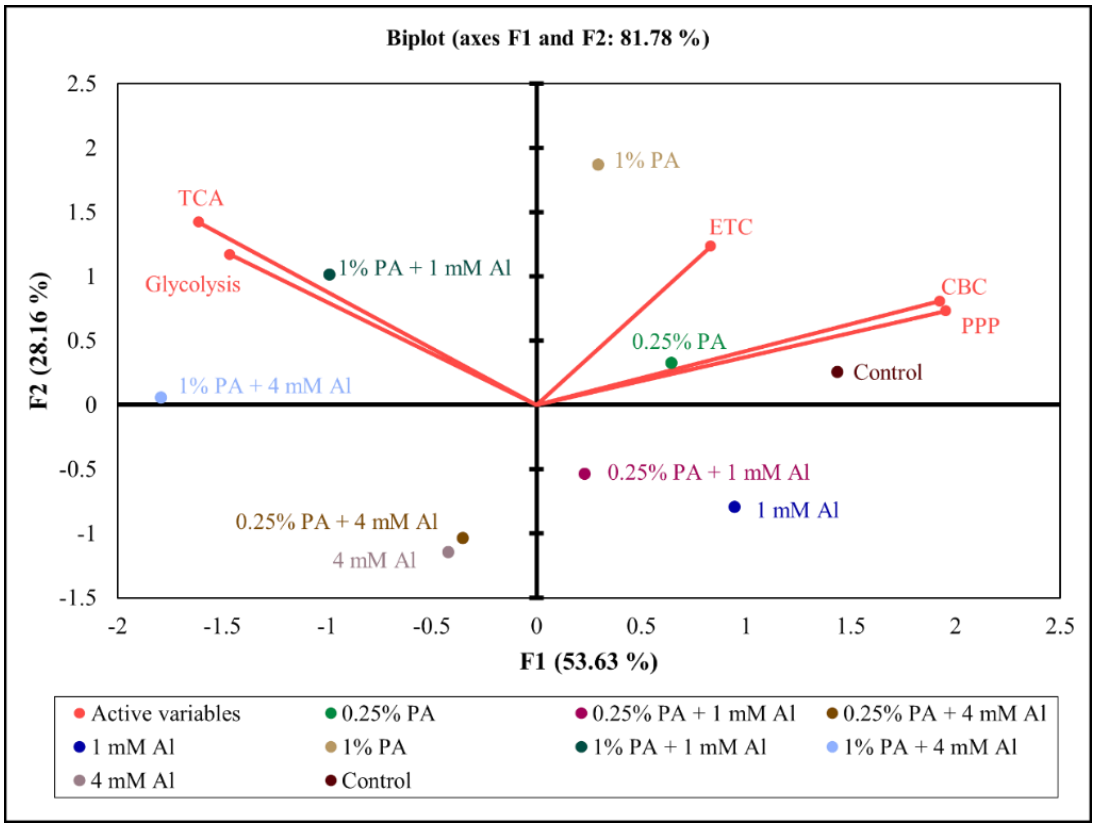

Figure 8.6. A two-dimensional principal component analysis (2-D PCA) biplot showing relationships amongst the explanatory variables (total metabolites involved in specific central carbon metabolic pathways) Calvin−Benson cycle (CBC), glycolysis, pentose phosphate pathway (PPP), tricarboxylic acid (TCA) cycle and electron transport chain (ETC) of Scotia tomato seedlings treated with pyroligneous acid (PA) under aluminum (Al) stress. The projection of the variables in the 2-D factor space (F1 and F2) explained a total of 81.78% of the variations in the dataset. Variables that are closely located are not different compared to variables located at a distance within a quadrant or between quadrants.

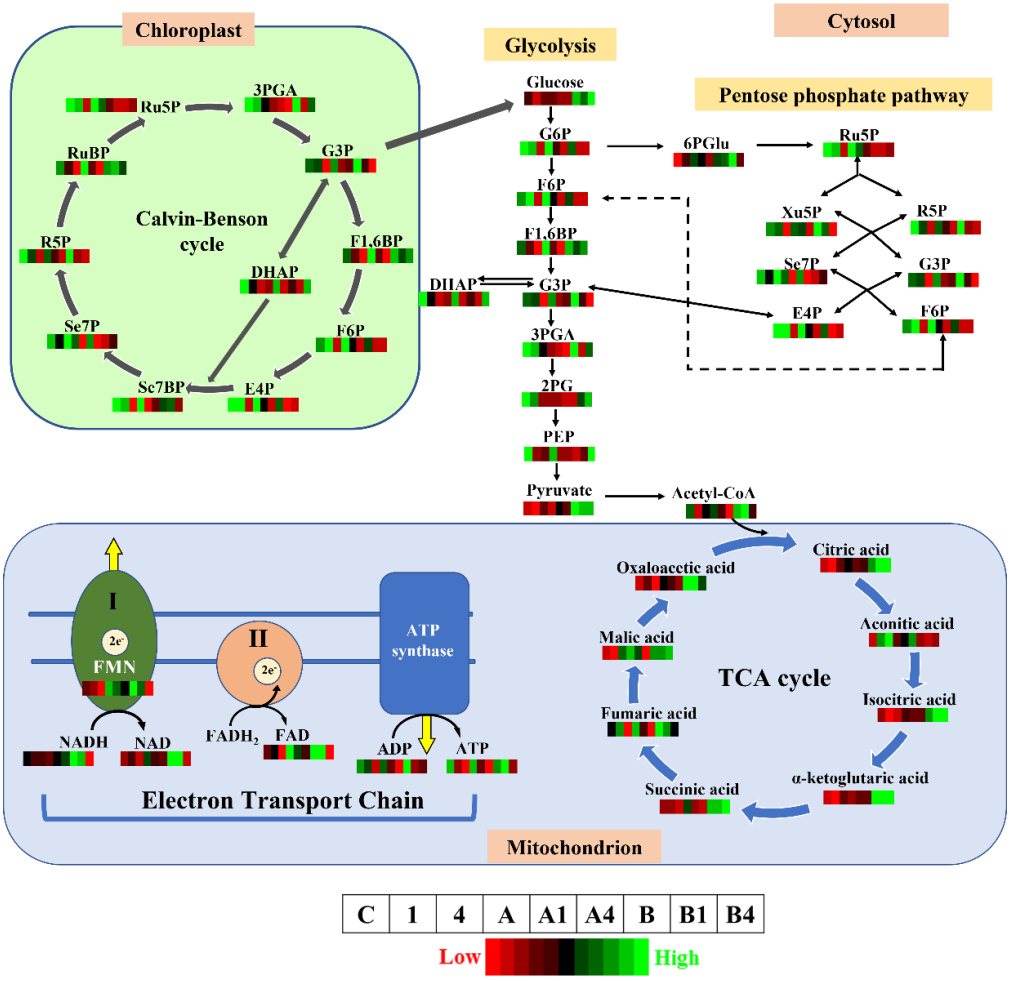

Figure 8.7. Overview of metabolic changes of key central carbon pathways in the leaves of Scotia tomato seedlings treated with pyroligneous acid (PA) under aluminum (Al) stress. Ru5P, ribulose-5-phosphate; 3PGA, 3-phosphoglyceric acid; G3P, glyceraldehyde-3-phosphate; F1,6BP, fructose-1,6-bisphosphate; F6P, fructose-6-phosphate; E4P, erythrose-4-phosphate; Se7BP, sedoheptulose-1,7-bisphosphate; Se7P, sedoheptulose-7-phosphate; R5P, ribose-5-phosphate; RuBP, ribulose-1,5-bisphosphate; G6P, glucose-6-phosphate; DHAP, dihydroxyacetone phosphate; 2PG, 2-phosphoglyceric acid; PEP, phosphoenolpyruvic acid; 6PGlu, 6-phosphogluconate; Xu5P, xylulose-5-phosphate; NADP, nicotinamide adenine dinucleotide phosphate; FMN, flavin mono-nucleotides; FAD, flavin adenine dinucleotide; ADP, adenosine diphosphate; ATP, adenosine triphosphate. The red colour of the metabolic pattern represents a lower concentration, and the green colour represents a higher concentration of a particular metabolite. The treatments that match the corresponding colour patterns were arranged from left to right as control (C), 1 mM Al (1), 4 mM Al (4), 0.25% PA (A), 0.25% PA + 1 mM Al (A1), 0.25% PA + 4 mM Al (A4), 1% PA (B), 1% PA + 1 mM Al (B1) and 1% PA + 4 mM Al (B4).

8.4 CONCLUSIONS

Acidic soils are widespread and Al stress is a major limiting factor for plant growth and productivity in acidic soils. In the present study, we comprehensively investigated the metabolic response of key intermediate metabolites in the central carbon metabolism routes in PA-treated tomato seedlings under Al stress. A total of 48 differentially expressed metabolites involved in the Calvin−Benson cycle, glycolysis, pentose phosphate pathway, tricarboxylic acid cycle and electron transport chain were identified in the leaves of both control and PA-treated tomato plants under Al stress. Aluminum stress considerably reduced the levels of these metabolites, while PA treatment triggered dynamic metabolic alterations and played an important role in Al stress adaptation. The coordinated association among these identified metabolites revealed that PA stimulates changes in plant metabolism to modulate energy production and the biosynthesis of organic acids for Al stress tolerance. However, further investigation is required to examine how PA treatment influences the genes and enzymes involved in these CCM routes under Al stress.

CHAPTER 9: CONCLUSION

9.1 Thesis findings

The impact of food security has been an important topic for the past decades and a major concern in several countries of the world. The current increase in global population has a significant consequence on the demand for nutrient-dense food which must be doubled by 2050. However, global crop production is significantly constrained by numerous environmental stresses including acidic soils and its associated aluminum (Al) toxicity. Numerous crops are hypersensitive to micromolar concentrations of Al which inhibit root growth, reduce water and nutrient uptake and alter several physiological, metabolic and molecular processes and thereby, leading to ultimate crop loss. The negative impact of this stress has been predicted to be aggravated by climate change and the intensive use of synthetic chemical fertilizers, which is estimated to affect over 50% of global agricultural lands by 2050 (Jamil et al., 2011; Daliakopoulos et al., 2016). Furthermore, the intensive use of synthetic chemical fertilizers for boosting crop yields has stimulated greater public concern about its side effects on the environment and human health. Accordingly, recent developments in agriculture rely on reduced synthetic chemical use while seeking alternative strategies that stimulate plant productivity and resilience to environmental stresses as well as ensure environmental sustainability. One such strategy is the use of PA which is used as a biostimulant to enhance crop growth and productivity. The overall aim of the thesis was to advance our knowledge of the biostimulatory effect of PA on crop productivity under greenhouse conditions and its regulatory mechanism in promoting aluminum stress tolerance in plants.

In this study, the PA used was produced from white pine (*Pinus strobus*) using fast pyrolysis at 1100°C (Chapter 3). Although no studies have examined the chemical and metabolite profile of

PA produced at such a high temperature, the study revealed that PA from *P. strobus* had lower electrical conductivity (EC), total dissolved solids (TDS) and salinity but higher Brix content. Also, the PA contained high contents of phenolics and flavonoids and exhibited a higher antioxidant activity which was characterized by increased DPPH radical scavenging activity. This high phenolic content and its associated antioxidant activity were expected as such properties have been reported by several authors. The metabolite analysis indicates the presence of 156 metabolites, which were grouped into four main classes including organic acids, hexose, carnitine and phospholipids. Additionally, the mineral elements analysis revealed that the PA contained high concentrations of N, K, Ca and Zn, while the content of Na and trace/heavy metals including Al, Cd, Pb, Ni and As were present at low levels and/or below the reported limit. This finding clearly indicates that PA derived from *P. strobus* produced at high pyrolysis temperatures can be used as a promising sustainable alternative to enhance plant productivity and resilience to diverse environmental stresses.

In Chapter 4, tomato "Scotia" seeds were primed with different PA concentrations to investigate its effect on seed germination and seedling growth, and Al tolerance. Seed priming with 2% PA for 24 h considerably increased seed germination indices and seedling growth in the absence of Al stress. Irrespective of the level of Al stress imposed, 2% PA priming significantly enhanced seed germination index and seedling vigour but not seed germination percentage compared to the control. Similarly, under Al stress, PA priming increased the total lengths and surface areas of seedling shoots and roots, root volume and overall seedling fresh weight. Also, PA priming mitigated the negative impact of Al stress on tomato seedlings by reducing ROS and MDA contents while enhancing osmotic regulation through increased proline and soluble protein

contents in PA-primed seedlings compared to the control. Moreover, PA priming enhanced POD activities and increased the expression of auxin response factor and antioxidant genes (i.e., *GR, POD, SOD, CAT,* and *APX1*). These establish that seed priming with PA can be a feasible strategy to enhance tomato seed germination and seedling growth under Al stress.

To explore the biostimulatory effect of PA on crop productivity, tomato "Scotia" plants were drenched (soil-applied) with different PA concentrations under greenhouse conditions (Chapter 5). Also, foliar PA application combined with a full and half rate of NPK fertilizer was used to assess the synergistic effect of PA and NPK on tomato productivity under greenhouse conditions (Chapter 6). Soil application of low PA concentrations of 0.25% and 0.5% increased the morpho-physiological responses of tomato plants compared to the control. The application of 0.5% PA substantially increased the number of fruits and total fruit weight while 0.25% PA enhanced the elemental content of the fruits. The application of 0.5% and 0.25% PA may be considered less toxic to root systems and may promote root growth and thereby, facilitating plant nutrient uptake. However, the soil application of 2% PA reduced the growth and yield but considerably increased the chemical qualities and phytochemical composition of fruits. All PA-treated plants accumulated high levels of ascorbate in their fruits with considerably low POD enzyme activities. This indicates that soil application of 2% PA can instigate a deleterious effect on tomato growth and productivity. Most plants adapt to stress conditions by accumulating these compounds, which ultimately enhances fruit dietary and nutritional quality (Li et al., 2019). Therefore, this study confirms that increased yield and dietary and nutritional quality of tomato can be obtained when the appropriate concentration of PA is applied in a greenhouse production system (Chapter 5).

Furthermore, foliar application of 0.25% and 0.5% PA enhanced the maximum quantum efficiency of PSII and potential photosynthetic capacity, particularly when combined with fully recommended NPK rate. The foliar application of 2% PA with full NPK rate increased leaf chlorophyll contents while the total number of fruits was increased, irrespective of the NPK rate. Similarly, the 2% PA combined with a full NPK rate increased total fruit weight and the number of total marketable fruits compared to water and no-spray treatments. The 2% PA with full NPK rate significantly enhanced fruit soluble protein, sugar and DPPH activities while 0.5% PA with a half NPK rate increased fruit phenolic and carotenoid content. The PA-treated plants accumulated higher levels of phytochemicals in their leaves than the fruit tissues except for sugar. Overall, the study demonstrated that 2% PA with a full NPK rate is the best treatment combination that can be adopted to increase the productivity and nutritional benefits of greenhouse-grown tomato (Chapter 6).

In Chapter 7, the morpho-physiological and biochemical response of tomato "Scotia" seedlings treated with different PA concentrations and Al stress was investigated. Al stress significantly reduced the morphological and physiological performance of tomato seedlings. Nevertheless, the 0.25% and 0.5% PA improved tomato seedling root growth, leaf gas exchange parameters and chlorophyll contents under Al stress. The effect of 1 mM Al was comparable to that of the control while 1% PA exacerbated Al phytotoxicity effect on plant morphology. The accumulation of osmolytes, and antioxidant enzymes and compounds due to PA treatment reduced Al-induced oxidative stress and maintain cellular homeostasis. Also, PA treatment restricted Al uptake and promoted the availability and transport of B, Mn, Na and P in tomato plants. The study of Chapter 8 further confirmed that PA regulates Al stress tolerance by coordinating intermediate metabolites

involved in the CCM of tomato seedlings under Al stress. The CBC and PPP metabolites were reduced in both control and PA-treated plants under 4 mM Al stress. Although glycolysis metabolites of 0.25% PA-treated plants under Al stress were comparable to the control, the 1% PA-treated plants accumulated the highest glycolysis metabolites while all the other PA treatments increased TCA metabolites under Al stress. Besides, ETC metabolites were increased in PA-treated plants alone and when treated with 1 mM Al, but were decreased under 4 mM Al. The Pearson correlation and PCA analysis showed a coordinated association between the central carbon metabolism pathway metabolites (Chapter 8). These findings establish that PA stimulates metabolic alteration in plants to regulate organic acid and energy production, and PA can be used as a novel strategy to detoxify Al and improve plant tolerance in agricultural production systems.

9.2 Thesis contributions

The studies reported in this thesis addressed several gaps and contributed to the understanding of the biostimulatory effects of PA on plant growth and environmental stress mitigation. Although previous studies have examined varying quantities of bioactive compounds produced from different plant species (Wei et al., 2010; Theapparat et al., 2014), this study is the first to investigate the metabolic profile of PA and has undeniably extended the understanding of bioactive compounds and chemical elements that contributes to the biostimulatory effect of PA (Chapter 3). This finding further confirms PA as a potential alternative source of plant growth promoter for improving crop productivity and resilience to diverse environmental stresses.

Several studies have utilized PA in different areas of agriculture including insect repellent (Chalermsan et al., 2009), soil enhancement (Lashari et al., 2013) and antimicrobial agents (Jung,

2007; Mourant et al., 2007). Additionally, it has been proven that co-application of PA with other soil amendments improves growth and productivity of several crops (Chen et al., 2010; Lashari et al., 2013; Liu et al., 2018a; Fedeli et al., 2022b). Nevertheless, studies on the biostimulatory effect of soil-applied and foliar-applied PA in combination with varying fertilizer regimes on tomato productivity and quality is limited (Grewal et al., 2018). Therefore, these studies (Chapter 4; Chapter 5) indisputably provide insight into the potential use of PA for enhancing the productivity and quality of greenhouse grown tomato. Furthermore, this thesis established that the rate of PA required to improve the productivity and quality of tomato is dependent on the mode of application (Figure 9.1). For instance, the optimum rates for improving yield with soil application is 0.5% PA while 2% PA enhances the fruit chemical qualities and phytochemical content. Also, foliar application of 2% PA combined with full NPK rate is the best PA-fertilizer combination that can be adopted by greenhouse tomato farmers to increase not only the growth and yield but also, improve the nutritional qualities.

Moreover, the use of PA in alleviating environmental stresses in plants has recently gained attention in the literature (Benzon & Lee, 2017; Wang et al., 2019b; Ma et al., 2022). Despite the positive effect of PA on plant growth, this thesis is the first to investigate the effect of PA on Al stress mitigation using both seed priming and nutrient amendment techniques (Figure 9.1). This study clearly established that priming seeds with 2% PA for 24 h enhances seed germination and seedling growth under Al stress (Figure 9.1). Seed priming is a technique used to enhance the performance of seedlings (Cao et al., 2019; Bortolin et al., 2020) and this study indicates that priming with PA can be extended for use in nursery and/or agricultural fields with high Al to enhance crop establishment and alleviate Al stress (Chapter 6). Biochemical and molecular

evidence for this study further enlightened the understanding of the mechanisms of PA-mediated Al stress mitigation.

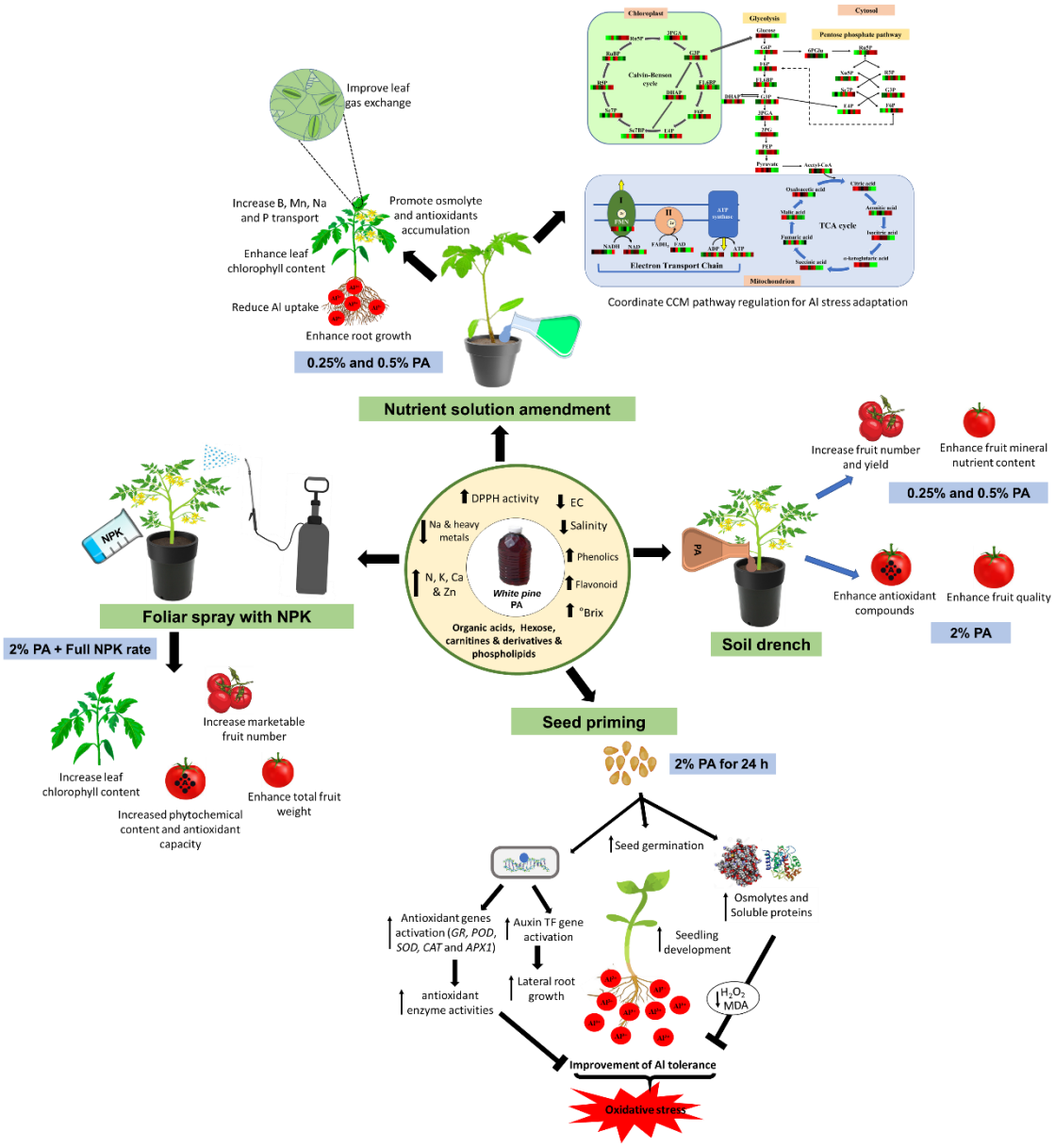

Figure 9.1. Overview of thesis contributions to agricultural systems and aluminum (Al) stress mitigation. The efficacy of pyroligneous acid (PA) on plant growth and productivity depends on the mode of application and the concentration used. Overall, the optimum rate to improve tomato productivity is 0.5% soil drenched and 2% PA with full NPK for foliar application. Seed priming with 2% PA and soil application of 0.25% and 0.5% PA promoted increased tomato growth and Al tolerance.

Accordingly, the PA-mediated Al tolerance with seed priming is governed by the accumulation of osmolytes and antioxidant compounds, and the activation of antioxidant and auxin transcription factor gene expressions. In four-week-old seedlings, PA enhances growth and Al tolerance when applied at lower concentrations (0.25 and 0.5%; Chapter 7). With such mode of PA application, this study showed that PA treatment promotes the coordinated association of CCM pathway metabolites which obviously ascertains that PA stimulates plant metabolism to produce organic acids and sufficient energy for Al stress adaptation (Chapter 8).

The use of PA in Canada is at its infancy stage and the finding of this thesis revealed that PA application can be adopted for enhancing the productivity and quality of greenhouse-grown crops. From the farmers' perspective, the increase in crop productivity and quality can result in significant improvement in the overall farm cash flow. Also, the thesis established that PA can be used as a partial substitute and/or in combination with chemical fertilizer which could reduce production costs and ensure environmental sustainability. In Al spike soils, PA has the potential to improve early crop establishment and Al tolerance which can be utilized in field crop production. Overall, this thesis indicates that PA application in mainstream agriculture represents an eco-friendly novel natural product that can contribute to the achievement of the United Nations' sustainable development goals by enhancing the production of nutrient-dense vegetables, promoting sustainable crop production, and ending world hunger.

9.3. Thesis limitations and recommendation for future studies

This thesis accomplished all the aims in expanding the knowledge and understanding of the biostimulatory effect of PA on plant growth and Al stress mitigation. However, there are some experimental limitations and recommendations that future studies can explore further. For

example, the chemical properties of the feedstocks used to produce the PA at higher temperatures were not investigated. According to Grewal et al. (2018), the chemical properties of PA are strongly influenced by the feedstock. Therefore, examining such properties will further strengthen the evidence obtained as the high organic acid composition of PA has been linked to a high hemicellulose content of feedstocks (Stefanidis et al., 2014; Hu et al., 2017). Additionally, PA have been reported to contains butenolide, which has been shown to induce numerous biostimulatory effects in plants (Van Staden et al., 2004; Chiwocha et al., 2009; Dixon et al., 2009; Flematti et al., 2009). However, the content of butenolide was not examined in this study and future studies can investigate how its content may by affected especially at such a high pyrolytic temperature. Furthermore, this thesis established that various PA concentrations depending on the mode of application can enhance the productivity and nutritional qualities of tomato under greenhouse conditions (Chapter 5; Chapter 6). Nevertheless, these recommendations can be tested on other tomato genotypes and explored under field conditions and on other crops of importance. Although different plant may respond to difference PA concentration (Grewal et al., 2018), this will form the baseline for adopting PA for field crop cultivation.

Despite the effect of PA in enhancing tomato seed germination and tolerance to Al stress, the molecular basis of the biostimulatory effect of PA was not investigated. A similar molecular mechanism was not investigated upon exposure of tomato seedlings to varying PA and Al treatments. However, the results of this thesis revealed the biochemical and physiological responses of seedlings of PA-primed seeds (Chapter 4) and PA-treated seedlings to Al stress (Chapter 7). Although the targeted metabolic analysis was used to elucidate the mechanism of how PA regulate CCM under Al stress (Chapter 8), further study is required to examine how PA

treatment influences genes and enzymes involved in these CCM routes under Al stress. The use of transcriptomic or proteomic approaches could have extended the finding of this study. Also, future studies could focus on the seed priming with PA effect and soil treatment on tomato productivity upon exposure to long-term Al stress. Additionally, such a study needs to examine Al and other heavy metal contents in the fruits of PA-treated tomato plants under Al stress as this could play a vital role in the dietary intake of tomato fruits from plants grown on acidic soils. Furthermore, the use of PA in alleviating abiotic stresses is in its infancy stage (Theerakulpisut et al., 2016; Wang et al., 2019a; Wang et al., 2019b; Ma et al., 2022). The studies conducted in this thesis should be extended to other environmental stresses (e.g. high temperature, flooding, heavy metal toxicity) that limit crop growth and productivity. Future studies that also examine the effect of PA on multiple environmental stresses (e.g., Al and drought, Al-salinity and drought or low temperature) can advance knowledge and promote PA use as a biostimulant. These studies will provide more insight into not only the mechanism of PA-mediated Al tolerance but also, its importance in stimulating crop productivity in acidic soils.

REFERENCES

AAFC. (2022a). *Statistical Overview of the Canadian Field Vegetable Industry*. Retrieved from https://publications.gc.ca/collections/collection_2023/aac-aafc/A1-37-2021-eng.pdf

AAFC. (2022b). *Statistical Overview of the Canadian Greenhouse Vegetable and Mushroom Industry*. Retrieved from https://agriculture.canada.ca/sites/default/files/documents/2022-12/GreenhouseVegetable_Report_2021_EN.pdf

Abou Chehade, L., Al Chami, Z., De Pascali, S. A., Cavoski, I., & Fanizzi, F. P. (2018). Biostimulants from food processing by-products: agronomic, quality and metabolic impacts on organic tomato (Solanum lycopersicum L.). *Journal of the Science of Food and Agriculture*, *98*(4), 1426-1436. https://doi.org/10.1002/jsfa.8610

Agarwal, P., Singh, P. C., Chaudhry, V., Shirke, P. A., Chakrabarty, D., Farooqui, A., Nautiyal, C. S., Sane, A. P., & Sane, V. A. (2019). PGPR-induced OsASR6 improves plant growth and yield by altering root auxin sensitivity and the xylem structure in transgenic *Arabidopsis thaliana* [Article]. *Journal of Plant Physiology*, *240*, 11, Article 153010.https://doi.org/10.1016/j.jplph.2019.153010

Aghaee, P., & Rahmani, F. (2019). Biochemical and molecular responses of flax to 24-epibrassinosteroide seed priming under drought stress. *Journal of Plant Interactions*, *14*(1), 242-253.https://doi.org/10.1080/17429145.2019.1618503

Aguilera, J. G., Teodoro, P. E., da Silva, J. P., Pereira, J. F., Zuffo, A. M., & Consoli, L. (2019). Selection of Aluminum-Resistant Wheat Genotypes Using Multienvironment and Multivariate Indices [Article]. *Agronomy Journal*, *111*(6), 2804-2810.https://doi.org/10.2134/agronj2019.06.0470

Ahadiyat, Y. R., Hadi, S. N., & Herliana, O. (2018). Application of wood vinegar coconut shell and NPK fertilizer to maintain sustainable agriculture of upland rice production. *Journal of Degraded and Mining Lands Management*, *5*(3), 1245.https://doi.org/10.15243/jdmlm.2018.053.1245

Ahsan, N., Renaut, J., & Komatsu, S. (2009). Recent developments in the application of proteomics to the analysis of plant responses to heavy metals. *Proteomics*, *9*(10), 2602-2621.https://doi.org/10.1002/pmic.200800935.

Ainsworth, E. A., & Gillespie, K. M. (2007). Estimation of total phenolic content and other oxidation substrates in plant tissues using Folin–Ciocalteu reagent. *Nature Protocols*, *2*(4), 875-877.https://doi.org/10.1038/nprot.2007.102

Alcantara, B. K., Machemer-Noonan, K., Silva Junior, F. G., & Azevedo, R. A. (2015). Dry priming of maize seeds reduces aluminum stress. *PloS One*, *10*(12), e0145742.https://doi.org/10.1371/journal.pone.0145742

Alexieva, V., Sergiev, I., Mapelli, S., & Karanov, E. (2001). The effect of drought and ultraviolet radiation on growth and stress markers in pea and wheat. *Plant, Cell & Environment*, *24*(12), 1337-1344.https://doi.org/10.1046/j.1365-3040.2001.00778.x

Ali, S., Zeng, F., Qiu, L., & Zhang, G. (2011). The effect of chromium and aluminum on growth, root morphology, photosynthetic parameters and transpiration of the two barley cultivars. *Biologia Plantarum*, *55*(2), 291-296.https://doi.org/10.1007/s10535-011-0041-7

Alia, F. J., Shamshuddin, J., Fauziah, C. I., Husni, M. H. A., & Panhwar, Q. A. (2015). Effects of aluminum, iron and/or low pH on rice seedlings grown in solution culture. *International Journal of Agriculture and Biology*, *17*(4).https://doi.org/10.17957/IJAB/14.0019

Alicja, P., Grabowska, A., Kalisz, A., & Sekara, A. (2019). The eggplant yield and fruit composition as affected by genetic factor and biostimulant application. *Notulae Botanicae Horti Agrobotanici Cluj-Napoca*, *47*(3), 929-938. https://doi.org/10.15835/nbha47311468

Alves Silva, G. E., Toledo Ramos, F., de Faria, A. P., & Costa França, M. G. (2014). Seeds' physicochemical traits and mucilage protection against aluminum effect during germination and root elongation as important factors in a biofuel seed crop (Ricinus communis). *Environmental Science and Pollution Research*, *21*(19), 11572-11579.https://doi.org/10.1007/s11356-014-3147-6

Amaral, E., Sales, J. F., Pinto, J. F. N., Barbosa, L. C. S., Reis, E. F., & Vasconcelos, S. C. (2018). Growth evaluation and anatomical root structure of Campomanesia pubescens (Mart. ex DC.) O. Berg (Myrtaceae) under different concentrations of aluminum.*Acta Horticulturae* VIII International Symposium on Mineral Nutrition of Fruit Crops, Leuven 1.

Amenós, M., Corrales, I., Poschenrieder, C., Illéš, P., Baluška, F., & Barceló, J. (2009). Different effects of aluminum on the actin cytoskeleton and brefeldin A-sensitive vesicle recycling in root apex cells of two maize varieties differing in root elongation rate and aluminum tolerance. *Plant and Cell Physiology*, *50*(3), 528-540.https://doi.org/10.1093/pcp/pcp013

Andrivon, D. (1995). Inhibition by aluminum of mycelial growth and of sporangial production and germination in Phytophthora infestans. *European Journal of Plant Pathology*, *101*(5), 527-533.https://doi.org/10.1007/BF01874477

Angelidis, A. S., & Smith, G. M. (2003). Role of the glycine betaine and carnitine transporters in adaptation of Listeria monocytogenes to chill stress in defined medium. *Applied and Environmental Microbiology*, *69*(12), 7492-7498.https://doi.org/10.1128/AEM.69.12.7492-7498.2003

Arasimowicz-Jelonek, M., Floryszak-Wieczorek, J., Drzewiecka, K., Chmielowska-Bąk, J., Abramowski, D., & Izbiańska, K. (2014). Aluminum induces cross-resistance of potato to Phytophthora infestans. *Planta*, *239*(3), 679-694.https://doi.org/10.1007/S00425-013-2008-8

Arenhart, R. A., Schunemann, M., Bucker Neto, L., Margis, R., Wang, Z. Y., & Margis-Pinheiro, M. (2016). Rice ASR1 and ASR5 are complementary transcription factors regulating aluminium responsive genes. *Plant, Cell & Environment*, *39*(3), 645-651.https://doi.org/10.1111/pce.12655

Ariffin, A., McNeil, P. H., Cooke, R. J., Wood, C., & Thomas, D. R. (1982). Carnitine content of greening barley leaves. *Phytochemistry*, *21*(6), 1431-1432.https://doi.org/10.1016/0031-9422(82)80156-8

Audran-Delalande, C., Bassa, C., Mila, I., Regad, F., Zouine, M., & Bouzayen, M. (2012). Genome-wide identification, functional analysis and expression profiling of the Aux/IAA gene family in tomato. *Plant and Cell Physiology*, *53*(4), 659-672.https://doi.org/10.1093/pcp/pcs022

Awasthi, J. P., Saha, B., Panigrahi, J., Yanase, E., Koyama, H., & Panda, S. K. (2019). Redox balance, metabolic fingerprint and physiological characterization in contrasting North East Indian rice for Aluminum stress tolerance. *Scientific Reports*, *9*(1), 1-21.https://doi.org/10.1038/s41598-019-45158-3

Awasthi, J. P., Saha, B., Regon, P., Sahoo, S., Chowra, U., Pradhan, A., Roy, A., Panda, S. K., Jp, A., B, S., P, R., S, S., U, C., A, P., A, R., & Sk, P. (2017). Morpho-physiological analysis of tolerance to aluminum toxicity in rice varieties of North East India. *PloS One*, *12*(4), e0176357-e0176357. https://doi.org/10.1371/journal.pone.0176357

Bai, B., Bian, H., Zeng, Z., Hou, N., Shi, B., Wang, J., Zhu, M., & Han, N. (2017). miR393-Mediated Auxin Signaling Regulation is Involved in Root Elongation Inhibition in Response to Toxic Aluminum Stress in Barley. *Plant and Cell Physiology*, *58*(3), 426-439.https://doi.org/10.1093/PCP/PCW211

Balat, M. (2008). Mechanisms of thermochemical biomass conversion processes. Part 1: reactions of pyrolysis. *Energy Sources, Part A*, *30*(7), 620-635.https://doi.org/10.1080/15567030600817258

Balzergue, C., Dartevelle, T., Godon, C., Laugier, E., Meisrimler, C., Teulon, J.-M. M., Creff, A., Bissler, M., Brouchoud, C., Hagège, A., Müller, J., Chiarenza, S., Javot, H., Becuwe-Linka, N., David, P., Péret, B., Delannoy, E., Thibaud, M.-C. C., Armengaud, J., Abel, S., Pellequer, J.-L. L., Nussaume, L., & Desnos, T. (2017). Low phosphate activates STOP1-ALMT1 to rapidly inhibit root cell elongation. *Nature Communications*, *8*(1), 1-16.https://doi.org/10.1038/ncomms15300

Baranova, E. N., Christov, N. K., Kurenina, L. V., Khaliluev, M. R., Todorovska, E. G., & Smirnova, E. A. (2016). Formation of atypical tubulin structures in plant cells as a nonspecific response to abiotic stress. *Bulgarian Journal of Agricultural Science*, *22*(6), 987-992.

Basit, F., Liu, J., An, J., Chen, M., He, C., Zhu, X., Li, Z., Hu, J., & Guan, Y. (2021). Seed priming with brassinosteroids alleviates aluminum toxicity in rice via improving antioxidant defense system and suppressing aluminum uptake. *Environmental Science and Pollution Research*, 1-15.https://doi.org/10.1007/s11356-021-16209-y

Bates, L. S., Waldren, R. P., & Teare, I. D. (1973). Rapid determination of free proline for water-stress studies. *Plant and Soil*, *39*(1), 205-207.https://doi.org/10.1007/BF00018060

Beecher, G. R. (1998). Nutrient content of tomatoes and tomato products. *Proceedings of the Society for Experimental Biology and Medicine*, *218*(2), 98-100.https://doi.org/10.3181/00379727-218-44282a

Benzon, H. R. L., & Lee, S. C. (2016). Potential of wood vinegar in enhancing fruit yield and antioxidant capacity in tomato. *Korean Journal of Plant Resources*, *29*(6), 704-711.https://doi.org/10.7732/kjpr.2016.29.6.704

Benzon, H. R. L., & Lee, S. C. (2017). Pyroligneous acids enhance phytoremediation of heavy metal-contaminated soils using mustard. *Communications in Soil Science and Plant Analysis*, *48*(17), 2061-2073.https://doi.org/10.1080/00103624.2017.1406102

Bera, S., De, A. K., & Adak, M. K. (2019). Modulation of Glycine Betaine Accumulation with Oxidative Stress Induced by Aluminium Toxicity in Rice. *Proceedings of the National Academy of Sciences India Section B - Biological Sciences*, *89*(1), 291-301.https://doi.org/10.1007/s40011-017-0948-7

Berahim, Z., Panhwar, Q. A., Ismail, M. R., Saud, H. M., Monjurul, M., Mondal, A., Naher, U. A., & Islam, M. R. (2014). Rice yield improvement by foliar application of phytohormone. *Journal of Food Agriculture and Environment*, *12*, 399-404.

Bernal, J. H., & Clark, R. B. (1997). Mineral acquisition of aluminum-tolerant and -sensitive sorghum genotypes grown with varied aluminum. *Communications in Soil Science and Plant Analysis*, *28*(1-2), 49-62.https://doi.org/10.1080/00103629709369771

Bewley, J. D. (1997). Seed germination and dormancy. *The Plant Cell*, *9*(7), 1055.https://doi.org/10.1105/tpc.9.7.1055

Bewley, J. D., Bradford, K., & Hilhorst, H. (2012). *Seeds: physiology of development, germination and dormancy*. Springer Science & Business Media. https://doi.org/https://doi.org/10.1007/978-1-4899-1002-8

Bhat, B. A., Islam, S. T., Ali, A., Sheikh, B. A., Tariq, L., Islam, S. U., & Hassan Dar, T. U. (2020). Role of micronutrients in secondary metabolism of plants. In *Plant Micronutrients* (pp. 311-329). Springer. https://doi.org/https://doi.org/10.1007/978-3-030-49856-6_13

Bindraban, P. S., Dimkpa, C. O., & Pandey, R. (2020). Exploring phosphorus fertilizers and fertilization strategies for improved human and environmental health. *Biology and Fertility of Soils*, *56*(3), 299-317.https://doi.org/10.1007/s00374-019-01430-2

Bojórquez-Quintal, E., Escalante-Magaña, C., Echevarría-Machado, I., & Martínez-Estévez, M. (2017). Aluminum, a friend or foe of higher plants in acid soils. *Frontiers in plant science*, *8*, 1767.https://doi.org/10.3389/fpls.2017.01767

Bojórquez-Quintal, J. E. A., Sánchez-Cach, L. A., Ku-González, Á., de los Santos-Briones, C., de Fátima Medina-Lara, M., Echevarría-Machado, I., Muñoz-Sánchez, J. A., Sotomayor, S. M. T. H., & Estévez, M. M. (2014). Differential effects of aluminum on in vitro primary root growth, nutrient content and phospholipase C activity in coffee seedlings (Coffea arabica). *Journal of Inorganic Biochemistry*, *134*, 39-48.https://doi.org/10.1016/j.jinorgbio.2014.01.018

Borges, C. E., Cazetta, J. O., Sousa, F. B. F. d., & Oliveira, K. S. (2020). Aluminum toxicity reduces the nutritional efficiency of macronutrients and micronutrients in sugarcane seedlings. *Ciência e Agrotecnologia*, *44*.https://doi.org/10.1590/1413-7054202044015120

Borgo, L., Rabelo, F. H., Carvalho, G., Ramires, T., Righetto, A. J., Piotto, F. A., Boaretto, L. F., & Azevedo, R. (2020). Antioxidant performance and aluminum accumulation in two genotypes of Solanum lycopersicum in response to low pH and aluminum availability and under their combined stress [Article]. *Scientia Horticulturae*, *259*, 11, Article 108813.https://doi.org/10.1016/j.scienta.2019.108813

Bortolin, G. S., Teixeira, S. B., de Mesquita Pinheiro, R., Ávila, G. E., Carlos, F. S., da Silva Pedroso, C. E., & Deuner, S. (2020). Seed Priming with Salicylic Acid Minimizes Oxidative Effects of Aluminum on Trifolium Seedlings [Article]. *Journal of Soil Science and Plant Nutrition*, *20*(4), 2502-2511.https://doi.org/10.1007/s42729-020-00316-9

Boscolo, P. R. S., Menossi, M., & Jorge, R. A. (2003). Aluminum-induced oxidative stress in maize. *Phytochemistry*, *62*(2), 181-189.https://doi.org/10.1016/S0031-9422(02)00491-0

Bose, J., Babourina, O., Ma, Y., Zhou, M., Shabala, S., & Rengel, Z. (2015). Specificity of Ion Uptake and Homeostasis Maintenance During Acid and Aluminium Stresses. In S. K. Panda & F. Baluška (Eds.), *Aluminum Stress Adaptation in Plants* (pp. 229-251). Springer International Publishing. https://doi.org/https://doi.org/10.1007/978-3-319-19968-9_12

Bose, J., Babourina, O., Shabala, S., & Rengel, Z. (2010). Aluminum-dependent dynamics of ion transport in *Arabidopsis*: specificity of low pH and aluminum responses. *Physiologia plantarum*, *139*(4), 401-412.https://doi.org/10.1111/j.1399-3054.2010.01377.x

Bose, S., & Bhattacharyya, A. K. (2008). Heavy metal accumulation in wheat plant grown in soil amended with industrial sludge. *Chemosphere*, *70*(7), 1264-1272.https://doi.org/10.1016/j.chemosphere.2007.07.062

Bourdin, B., Adenier, H., & Perrin, Y. (2007). Carnitine is associated with fatty acid metabolism in plants. *Plant Physiology and Biochemistry*, *45*(12), 926-931.https://doi.org/10.1016/j.plaphy.2007.09.009

Bradford, M. M. (1976). A rapid and sensitive method for the quantitation of microgram quantities of protein utilizing the principle of protein-dye binding. *Analytical Biochemistry*, *72*(1-2), 248-254.https://doi.org/10.1016/0003-2697(76)90527-3

Bressan, A. C. G., de Oliveira Carvalho Bittencourt, B. M., Silva, G. S., & Habermann, G. (2021). Could the absence of aluminum (Al) impair the development of an Al-accumulating woody species from Brazilian savanna? *Theoretical and Experimental Plant Physiology*, *33*(3), 281-292.https://doi.org/10.1007/s40626-021-00216-y

Bridgwater, A. V., Meier, D., & Radlein, D. (1999). An overview of fast pyrolysis of biomass. *Organic geochemistry*, *30*(12), 1479-1493.https://doi.org/10.1016/S0146-6380(99)00120-5

Brunner, I., & Sperisen, C. (2013). Aluminum exclusion and aluminum tolerance in woody plants. *Frontiers in plant science*, *4*, 172.https://doi.org/10.3389/fpls.2013.00172

Buchanan, B. B., Gruissem, W., & Jones, R. L. (2015). *Biochemistry and molecular biology of plants*. John wiley & sons.

Bungau, S., Behl, T., Aleya, L., Bourgeade, P., Aloui-Sossé, B., Purza, A. L., Abid, A., & Samuel, A. D. (2021). Expatiating the impact of anthropogenic aspects and climatic factors on long-term soil monitoring and management. *Environmental Science and Pollution Research*, *28*(24), 30528-30550.https://doi.org/10.1007/s11356-021-14127-7

Burklew, C. E., Ashlock, J., Winfrey, W. B., & Zhang, B. (2012). Effects of aluminum oxide nanoparticles on the growth, development, and microRNA expression of tobacco (*Nicotiana tabacum*). *PloS One*, *7*(5), e34783.https://doi.org/10.1371/journal.pone.0034783

Cai, K., Jiang, S., Ren, C., & He, Y. (2012a). Significant damage-rescuing effects of wood vinegar extract in living Caenorhabditis elegans under oxidative stress. *Journal of the Science of Food and Agriculture*, *92*(1), 29-36.https://doi.org/10.1002/jsfa.4624

Cai, M.-Z., Zhang, S.-N., Xing, C.-H., Wang, F.-M., Zhu, L., Wang, N., & Lin, L.-Y. (2012b). Interaction between iron plaque and root border cells ameliorates aluminum toxicity of Oryza sativa differing in aluminum tolerance. *Plant and Soil*, *353*(1), 155-167.https://doi.org/10.1007/s11104-011-1019-0

Cai, M., Wang, N., Xing, C., Wang, F., Wu, K., & Du, X. (2013). Immobilization of aluminum with mucilage secreted by root cap and root border cells is related to aluminum resistance in Glycine max L. *Environmental Science and Pollution Research*, *20*(12), 8924-8933.https://doi.org/10.1007/s11356-013-1815-6

Cai, Z. D., Xian, P. Q., Lin, R. B., Cheng, Y. B., Lian, T. X., Ma, Q. B., & Nian, H. (2020). Characterization of the Soybean GmIREG Family Genes and the Function of GmIREG3 in Conferring Tolerance to Aluminum Stress [Article]. *International Journal of Molecular Sciences*, *21*(2), 14, Article 497.https://doi.org/10.3390/ijms21020497

Calvo, P., Nelson, L., & Kloepper, J. W. (2014). Agricultural uses of plant biostimulants. *Plant Soil*, *383*(1), 3-41.https://doi.org/10.1007/s11104-014-2131-8

Canovas, M., Bernal, V., Sevilla, A., Torroglosa, T., & Iborra, J. L. (2007). Salt stress effects on the central and carnitine metabolisms of Escherichia coli. *Biotechnology and bioengineering*, *96*(4), 722-737.https://doi.org/10.1002/bit.21128

Cao, Q., Li, G., Cui, Z., Yang, F., Jiang, X., Diallo, L., & Kong, F. (2019). Seed priming with melatonin improves the seed germination of waxy maize under chilling stress via promoting the antioxidant system and starch metabolism. *Scientific Reports*, *9*(1), 1-12.https://doi.org/10.1038/s41598-019-51122-y

Cárcamo, M. P., Reyes-Díaz, M., Rengel, Z., Alberdi, M., Omena-Garcia, R. P., Nunes-Nesi, A., & Inostroza-Blancheteau, C. (2019). Aluminum stress differentially affects physiological performance and metabolic compounds in cultivars of highbush blueberry. *Scientific Reports*, *9*(1), 1-13.https://doi.org/10.1038/s41598-019-47569-8

Cardoso, T. B., Pinto, R. T., & Paiva, L. V. (2020). Comprehensive characterization of the ALMT and MATE families on Populus trichocarpa and gene co-expression network analysis of its members during aluminium toxicity and phosphate starvation stresses [Article]. *3 Biotech*, *10*(12), 16, Article 525.https://doi.org/10.1007/s13205-020-02528-3

Caruso, G., De Pascale, S., Cozzolino, E., Cuciniello, A., Cenvinzo, V., Bonini, P., Colla, G., & Rouphael, Y. (2019). Yield and nutritional quality of Vesuvian Piennolo tomato PDO as affected by farming system and biostimulant application. *Agronomy*, *9*(9), 505.https://doi.org/10.3390/agronomy9090505

Carvalho, F. P. (2006). Agriculture, pesticides, food security and food safety. *Environmental science & policy*, *9*(7-8), 685-692.https://doi.org/10.1016/j.envsci.2006.08.002

CFIA. (2021). *Canadian Grade Compendium: Volume 2 – Fresh Fruit or Vegetables*. Retrieved 10/09/2022 from https://inspection.canada.ca/about-cfia/acts-and-regulations/list-of-acts-and-regulations/documents-incorporated-by-reference/canadian-grade-compendium-volume-2/eng/1519996239002/1519996303947?chap=3#s34c3

Chalermsan, Y., Peerapan, S., & Agro-Industry. (2009). Wood vinegar: by-product from rural charcoal kiln and its role in plant protection. *Asian Journal of Food*, *2*(Special Issue).

Chance, B., & Maehly, A. C. (1955). Assay of catalases and peroxidases. *Methods in Enzymology*, *2*, 764-775.https://doi.org/10.1016/S0076-6879(55)02300-8.

Chang, C.-C., Yang, M.-H., Wen, H.-M., & Chern, J.-C. (2002). Estimation of total flavonoid content in propolis by two complementary colorimetric methods. *Journal of food and drug analysis*, *10*(3).https://doi.org/10.38212/2224-6614.2748

Charrier, A., Rippa, S., Yu, A., Nguyen, P. J., Renou, J. P., & Perrin, Y. (2012). The effect of carnitine on Arabidopsis development and recovery in salt stress conditions. *Planta*, *235*(1), 123-135.https://doi.org/10.1007/s00425-011-1499-4

Chaudhary, P., Sharma, A., Singh, B., & Nagpal, A. K. (2018). Bioactivities of phytochemicals present in tomato. *Journal of Food Science and Technology*, *55*(8), 2833-2849.https://doi.org/10.1007/s13197-018-3221-z

Chauhan, D. K., Yadav, V., Vaculik, M., Gassmann, W., Pike, S., Arif, N., Singh, V. P., Deshmukh, R., Sahi, S., & Tripathi, D. K. (2021). Aluminum toxicity and aluminum stress-induced physiological tolerance responses in higher plants. *Critical Reviews in Biotechnology*, *41*(5), 715-730.https://doi.org/10.1080/07388551.2021.1874282

Che, J., Tsutsui, T., Yokosho, K., Yamaji, N., & Ma, J. F. (2018a). Functional characterization of an aluminum (Al)-inducible transcription factor, ART2, revealed a different pathway for Al tolerance in rice [Article]. *New Phytologist*, *220*(1), 209-218.https://doi.org/10.1111/nph.15252

Che, J., Yamaji, N., Shen, R. F., & Ma, J. F. (2016). An Al-inducible expansin gene, OsEXPA10 is involved in root cell elongation of rice. *Plant Journal*, *88*(1), 132-142.https://doi.org/10.1111/tpj.13237

Che, J., Yamaji, N., Yokosho, K., Shen, R. F., & Ma, J. F. (2018b). Two Genes Encoding a Bacterial-Type ATP-Binding Cassette Transporter are Implicated in Aluminum Tolerance in Buckwheat [Article]. *Plant and Cell Physiology*, *59*(12), 2502-2511.https://doi.org/10.1093/pcp/pcy171

Chen, L.-S., Qi, Y.-P., & Liu, X.-H. (2005a). Effects of aluminum on light energy utilization and photoprotective systems in citrus leaves. *Annals of botany*, *96*(1), 35-41.https://doi.org/10.1093/aob/mci145.

Chen, L.-S., Qi, Y.-P., Smith, B. R., & Liu, X.-H. (2005b). Aluminum-induced decrease in CO2 assimilation in citrus seedlings is unaccompanied by decreased activities of key enzymes involved in CO2 assimilation. *Tree Physiology*, *25*(3), 317-324.https://doi.org/10.1093/treephys/25.3.317.

Chen, L., Cai, Y. P., Liu, X. J., Guo, C., Yao, W. W., Sun, S., Wu, C. X., Jiang, B. J., Han, T. F., & Hou, W. S. (2018a). GmGRP-like gene confers Al tolerance in *Arabidopsis* [Article]. *Scientific Reports*, *8*, 12, Article 13601.https://doi.org/10.1038/s41598-018-31703-z

Chen, L., Liu, Y., Liu, H., Kang, L., Geng, J., Gai, Y., Ding, Y., Sun, H., & Li, Y. (2015). Identification and expression analysis of MATE genes involved in flavonoid transport in blueberry plants. *PloS One*, *10*(3), e0118578.https://doi.org/10.1371/journal.pone.0118578

Chen, P., Sjogren, C. A., Larsen, P. B., & Schnittger, A. (2019a). A multi-level response to DNA damage induced by aluminium. *The Plant Journal*, *98*(3), 479-491.https://doi.org/10.1111/tpj.14231

Chen, Q., Wu, K.-H., Wang, P., Yi, J., Li, K.-Z., Yu, Y.-X., & Chen, L.-M. (2013). Overexpression of MsALMT1, from the aluminum-sensitive Medicago sativa, enhances malate exudation and aluminum resistance in tobacco. *Plant Molecular Biology Reporter*, *31*(3), 769-774.https://doi.org/10.1007/s11105-012-0543-2

Chen, Q. Q., Wu, W. W., Zhao, T., Tan, W. Q., Tian, J., & Liang, C. Y. (2019b). Complex Gene Regulation Underlying Mineral Nutrient Homeostasis in Soybean Root Response to Acidity Stress [Article]. *Genes*, *10*(5), 21, Article 402.https://doi.org/10.3390/genes10050402

Chen, S.-Y., Tang, Y.-M., Hu, Y.-Y., Wang, Y., Sun, B., Wang, X.-R., Tang, H.-R., & Chen, Q. (2018b). FaTT12-1, a multidrug and toxin extrusion (MATE) member involved in proanthocyanidin transport in strawberry fruits. *Scientia Horticulturae*, *231*, 158-165.https://doi.org/10.1016/j.scienta.2017.12.032

Chen, Y., Huang, L., Liang, X., Dai, P. B., Zhang, Y. X., Li, B. H., Lin, X. Y., & Sun, C. L. (2020). Enhancement of polyphenolic metabolism as an adaptive response of lettuce (Lactuca sativa) roots to aluminum stress [Article]. *Environmental Pollution*, *261*, 8, Article 114230.https://doi.org/10.1016/j.envpol.2020.114230

Chen, Y. X., Huang, X. D., Han, Z. Y., Huang, X., Hu, B., Shi, D. Z., & Wu, W. X. (2010). Effects of bamboo charcoal and bamboo vinegar on nitrogen conservation and heavy metals immobility during pig manure composting. *Chemosphere*, *78*(9), 1177-1181.https://doi.org/10.1016/j.chemosphere.2009.12.029

Chen, Z. C., Yamaji, N., Motoyama, R., Nagamura, Y., & Ma, J. F. (2012). Up-regulation of a magnesium transporter gene OsMGT1 is required for conferring aluminum tolerance in rice. *Plant physiology*, *159*(4), 1624-1633.https://doi.org/10.1104/pp.112.199778

Cheng, X. Q., Fang, T. Y., Zhao, E. H., Zheng, B. G., Huang, B. R., An, Y., & Zhou, P. (2020). Protective roles of salicylic acid in maintaining integrity and functions of photosynthetic photosystems for alfalfa (Medicago sativa L.) tolerance to aluminum toxicity [Article]. *Plant Physiology and Biochemistry*, *155*, 570-578.https://doi.org/10.1016/j.plaphy.2020.08.028

Chiwocha, S. D. S., Dixon, K. W., Flematti, G. R., Ghisalberti, E. L., Merritt, D. J., Nelson, D. C., Riseborough, J.-A. M., Smith, S. M., & Stevens, J. C. (2009). Karrikins: a new family of plant growth regulators in smoke. *Plant Science*, *177*(4), 252-256.https://doi.org/10.1016/j.plantsci.2009.06.007

Choi, Y. S., Johnston, P. A., Brown, R. C., Shanks, B. H., & Lee, K.-H. (2014). Detailed characterization of red oak-derived pyrolysis oil: Integrated use of GC, HPLC, IC, GPC and Karl-Fischer. *Journal of Analytical and Applied Pyrolysis*, *110*, 147-154.https://doi.org/10.1016/j.jaap.2014.08.016

Chowra, U., Yanase, E., Koyama, H., Panda, S. K., & Kumar Panda, S. (2017). Aluminium-induced excessive ROS causes cellular damage and metabolic shifts in black gram Vigna mungo (L.) Hepper. *Protoplasma*, *254*(1), 293-302.https://doi.org/10.1007/s00709-016-0943-5

Chumpookam, J., Lin, H.-L., & Shiesh, C.-C. (2012). Effect of Smoke-water on Seed Germination and Seedling Growth of Papaya (Carica papaya cv. Tainung No. 2). *HortScience horts*, *47*(6), 741-744.https://doi.org/10.21273/HORTSCI.47.6.741

Colla, G., & Rouphael, Y. (2015). Biostimulants in horticulture. *Scientia Horticulturae*, *196*, 1-2.https://doi.org/10.1016/j.scienta.2015.10.044

Collins, N. C., Shirley, N. J., Saeed, M., Pallotta, M., & Gustafson, J. P. (2008). An ALMT1 gene cluster controlling aluminum tolerance at the Alt4 locus of rye (Secale cereale L.). *Genetics*, *179*(1), 669-682.https://doi.org/10.1534/genetics.107.083451

Conselvan, G. B., Fuentes, D., Merchant, A., Peggion, C., Francioso, O., & Carletti, P. (2018). Effects of humic substances and indole-3-acetic acid on Arabidopsis sugar and amino acid metabolic profile. *Plant and Soil*, *426*(1), 17-32.https://doi.org/10.1007/s11104-018-3608-7.

Couée, I., Sulmon, C., Gouesbet, G., & El Amrani, A. (2006). Involvement of soluble sugars in reactive oxygen species balance and responses to oxidative stress in plants. *Journal of Experimental Botany*, *57*(3), 449-459.https://doi.org/10.1093/jxb/erj027

Cowan, A. K. (2006). Phospholipids as plant growth regulators. *Plant Growth Regulation*, *48*(2), 97-109.https://doi.org/10.1007/s10725-005-5481-7

Crepier, J., Le Masle, A., Charon, N., Albrieux, F., Duchene, P., & Heinisch, S. (2018). Ultra-high performance supercritical fluid chromatography hyphenated to atmospheric pressure chemical ionization high resolution mass spectrometry for the characterization of fast pyrolysis bio-oils. *Journal of Chromatography B*, *1086*, 38-46.https://doi.org/10.1016/j.jchromb.2018.04.005

Cui, Z., & Houweling, M. (2002). Phosphatidylcholine and cell death. *Biochimica et Biophysica Acta (BBA)-Molecular and Cell Biology of Lipids*, *1585*(2-3), 87-96.https://doi.org/10.1016/S1388-1981(02)00328-1

D'Alessandro, A., Taamalli, M., Gevi, F., Timperio, A. M., Zolla, L., & Ghnaya, T. (2013). Cadmium Stress Responses in Brassica juncea: Hints from Proteomics and Metabolomics. *Journal of proteome research*, *12*(11), 4979-4997.https://doi.org/10.1021/pr400793e.

Daliakopoulos, I., Tsanis, I., Koutroulis, A., Kourgialas, N., Varouchakis, A., Karatzas, G., & Ritsema, C. (2016). The threat of soil salinity: A European scale review. *Science of the Total Environment*, *573*, 727-739.https://doi.org/10.1016/j.scitotenv.2016.08.177

Das, A., Rushton, P. J., & Rohila, J. S. (2017). Metabolomic profiling of soybeans (Glycine max L.) reveals the importance of sugar and nitrogen metabolism under drought and heat stress. *Plants*, *6*(2), 21.https://doi.org/10.3390/plants6020021.

Das, K., & Roychoudhury, A. (2014). Reactive oxygen species (ROS) and response of antioxidants as ROS-scavengers during environmental stress in plants. *Frontier in Environmental Science*, *2*, 53.https://doi.org/10.3389/fenvs.2014.00053

Das, N., Bhattacharya, S., Bhattacharyya, S., & Maiti, M. K. (2018). Expression of rice MATE family transporter OsMATE2 modulates arsenic accumulation in tobacco and rice [Article]. *Plant Molecular Biology*, *98*(1-2), 101-120.https://doi.org/10.1007/s11103-018-0766-1

Daspute, A. A., Kobayashi, Y., Panda, S. K., Fakrudin, B., Kobayashi, Y., Tokizawa, M., Iuchi, S., Choudhary, A. K., Yamamoto, Y. Y., & Koyama, H. (2018). Characterization of CcSTOP1; a C2H2-type transcription factor regulates Al tolerance gene in pigeonpea [Article]. *Planta*, *247*(1), 201-214.https://doi.org/10.1007/s00425-017-2777-6

Dawson, J. (2017). *Concentration and Content of Secondary Metabolites* [PhD Thesis, University of Saskatchewan].

De Angeli, A., Baetz, U., Francisco, R., Zhang, J., Chaves, M. M., & Regalado, A. (2013). The vacuolar channel VvALMT9 mediates malate and tartrate accumulation in berries of Vitis vinifera. *Planta*, *238*(2), 283-291.https://doi.org/10.1007/s00425-013-1888-y

de Sousa, A., AbdElgawad, H., Fidalgo, F., Teixeira, J., Matos, M., Hamed, B. A., Selim, S., Hozzein, W. N., Beemster, G. T. S., & Asard, H. (2020). Al exposure increases proline levels by different pathways in an Al-sensitive and an Al-tolerant rye genotype [Article]. *Scientific Reports*, *10*(1), 11, Article 16401.https://doi.org/10.1038/s41598-020-73358-9

de Sousa, A., AbdElgawad, H., Han, A., Teixeira, J., Matos, M., & Fidalgo, F. (2016). Oxidative metabolism of rye (Secale cereale L.) after short term exposure to aluminum: uncovering the glutathione–ascorbate redox network. *Frontiers in plant science*, *7*, 685.https://doi.org/10.3389/fpls.2016.00685

de Souza, M. C., Williams, T. C. R., Poschenrieder, C., Jansen, S., Pinheiro, M. H. O., Soares, I. P., & Franco, A. C. (2020). Calcicole behaviour of Callisthene fasciculata Mart., an Al-accumulating species from the Brazilian Cerrado [Article]. *Plant Biology*, *22*(1), 30-37.https://doi.org/10.1111/plb.13036

Devi, S. S., Saha, B., Awasthi, J. P., Regon, P., & Panda, S. K. (2020). Redox status and oxalate exudation determines the differential tolerance of two contrasting varieties of 'Assam tea' Camelia sinensis (L.) O. Kuntz in response to aluminum toxicity [Article]. *Horticulture Environment and Biotechnology*, *61*(3), 485-499.https://doi.org/10.1007/s13580-020-00241-x

Dissatian, A., Sanitchon, J., Pongdontri, P., Jongrungklang, N., & Jothityangkoon, D. (2018). Potential of wood vinegar for enhancing seed germination of three upland rice varieties by suppressing malondialdehyde production. *AGRIVITA, Journal of Agricultural Science*, *40*(2), 371-380.http://doi.org/10.17503/agrivita.v40i2.1332

Dixon, K. W., Merritt, D. J., Flematti, G. R., & Ghisalberti, E. L. (2009). Karrikinolide–a phytoreactive compound derived from smoke with applications in horticulture, ecological restoration and agriculture. *Acta Horticulturae*, *813*, 155-170.https://doi.org/10.17660/ActaHortic.2009.813.20

Djuric, M., Mladenovic, J., Pavlovic, R., Murtic, N., Murtic, S., Milic, V., & Šekularac, G. (2011). Aluminium content in leaf and root of oat (Avena sativa L.) grown on pseudogley soil. *African Journal of Biotechnology*, *10*(77), 17837-17840.https://doi.org/10.5897/AJB11.156

Dong, B. Y., Niu, L. L., Meng, D., Song, Z. H., Wang, L. T., Jian, Y., Fan, X. H., Dong, M. Z., Yang, Q., & Fu, Y. J. (2019). Genome-wide analysis of MATE transporters and response to metal stress in Cajanus cajan [Article]. *Journal of Plant Interactions*, *14*(1), 265-275.https://doi.org/10.1080/17429145.2019.1620884

Donohue, S. J., Aho, D. W., & Plank, C. O. (1992). Determination of P, K, Ca, Mg, Mn, Fe, Al, B, Cu, and Zn in plant tissue by inductively coupled plasma (ICP) emission spectroscopy. *Plant analysis reference procedures for the southern region of the United States*, 34-37.

dos Santos, A. L., Chaves-Silva, S., Yang, L., Maia, L. G. S., Chalfun-Júnior, A., Sinharoy, S., Zhao, J., & Benedito, V. A. (2017). Global analysis of the MATE gene family of metabolite transporters in tomato. *BMC Plant Biology*, *17*(1), 1-13.https://doi.org/10.1186/s12870-017-1115-2

Drobek, M., Frąc, M., & Cybulska, J. (2019). Plant biostimulants: Importance of the quality and yield of horticultural crops and the improvement of plant tolerance to abiotic stress—A review. *Agronomy*, *9*(6), 335.https://doi.org/10.3390/agronomy9060335

Du, B., Nian, H., Zhang, Z., & Yang, C. (2010). Effects of aluminum on superoxide dismutase and peroxidase activities, and lipid peroxidation in the roots and calluses of soybeans differing in aluminum tolerance. *Acta Physiologiae Plantarum*, *32*(5), 883-890.https://doi.org/10.1007/s11738-010-0476-z

Du, H., Ryan, P., Liu, C., Li, H., Hu, W., Yan, W., Huang, Y., He, W., Luo, B., Zhang, X., Gao, S., Zhou, S., & Zhang, S. (2021). ZmMATE6 From Maize Encodes a Citrate Transporter That Enhances Aluminum Tolerance in Transgenic *Arabidopsis Thaliana*. *Plant Science*, *311*, 111016.https://doi.org/10.21203/rs.3.rs-141756/v1

Du, H. M., Huang, Y., Qu, M., Li, Y. H., Hu, X. Q., Yang, W., Li, H. J., He, W. Z., Ding, J. Z., Liu, C., Gao, S. B., Cao, M. J., Lu, Y. L., & Zhang, S. Z. (2020). A Maize ZmAT6 Gene Confers Aluminum Tolerance via Reactive Oxygen Species Scavenging [Article]. *Frontiers in plant science*, *11*, 12, Article 1016.https://doi.org/10.3389/fpls.2020.01016

Dubois, M., Gilles, K. A., Hamilton, J. K., Rebers, P. A. t., & Smith, F. (1956). Colorimetric method for determination of sugars and related substances. *Analytical Chemistry*, *28*(3), 350-356.https://doi.org/10.1021/ac60111a017

Dudaš, S., Šola, I., Sladonja, B., Erhatić, R., Ban, D., & Poljuha, D. (2016). The effect of biostimulant and fertilizer on "low input" lettuce production. *Acta Botanica Croatica*, *75*(2), 253-259. https://doi.org/10.1515/botcro-2016-0023

Dudonne, S., Vitrac, X., Coutiere, P., Woillez, M., & Mérillon, J.-M. (2009). Comparative study of antioxidant properties and total phenolic content of 30 plant extracts of industrial interest using DPPH, ABTS, FRAP, SOD, and ORAC assays. *Journal of agricultural and food chemistry*, *57*(5), 1768-1774.https://doi.org/10.1021/jf803011r

EC. (2021). *Regulation (EC) No 2065/2003 of the European Parliament and of the Council of 10 November 2003 on smoke flavourings used or intended for use in or on foods*. Retrieved 16/02 from https://eur-lex.europa.eu/legal-content/EN/ALL/?uri=CELEX%3A32003R2065

Eekhout, T., Larsen, P., & De Veylder, L. (2017). Modification of DNA checkpoints to confer aluminum tolerance. *Trends in Plant Science*, *22*(2), 102-105.https://doi.org/10.1016/j.tplants.2016.12.003

Ejaz, S., Fahad, S., Anjum, M. A., Nawaz, A., Naz, S., Hussain, S., & Ahmad, S. (2020). *Role of Osmolytes in the Mechanisms of Antioxidant Defense of Plants* (Vol. 39). Springer, Cham. https://doi.org/https://doi.org/10.1007/978-3-030-38881-2_4.

Ertani, A., Pizzeghello, D., Francioso, O., Sambo, P., Sanchez-Cortes, S., & Nardi, S. (2014). Capsicum chinensis L. growth and nutraceutical properties are enhanced by biostimulants in a long-term period: chemical and metabolomic approaches. *Frontiers in plant science*, *5*, 375. https://doi.org/10.3389/fpls.2014.00375

EU. (2019). *Regulation of the European parliament and of the council laying down rules on the making available on the market of EU fertilising products and amending Regulations (EC) No 1069/2009 and (EC) No 1107/2009 and repealing Regulation (EC) No 2003/2003*. Retrieved from https://eur-lex.europa.eu/legal-content/EN/TXT/?uri=OJ:L:2019:170:TOC

Ezaki, B., Jayaram, K., Higashi, A., & Takahashi, K. (2013). A combination of five mechanisms confers a high tolerance for aluminum to a wild species of Poaceae, Andropogon virginicus L. *Environmental and Experimental Botany*, *93*, 35-44.https://doi.org/10.1016/j.envexpbot.2013.05.002

Fagernäs, L., Kuoppala, E., Tiilikkala, K., & Oasmaa, A. (2012). Chemical Composition of Birch Wood Slow Pyrolysis Products. *Energy & Fuels*, *26*(2), 1275-1283.https://doi.org/10.1021/ef2018836

Falchi, R., Bonghi, C., Drincovich, M. F., Famiani, F., Lara, M. V., Walker, R. P., & Vizzotto, G. (2020). Sugar metabolism in stone fruit: source-sink relationships and environmental and agronomical effects. *Frontiers in plant science*, *11*, 573982.https://doi.org/10.3389/fpls.2020.573982

Famoso, A. N., Zhao, K., Clark, R. T., Tung, C.-W., Wright, M. H., Bustamante, C., Kochian, L. V., & McCouch, S. R. (2011). Genetic architecture of aluminum tolerance in rice (Oryza sativa) determined through genome-wide association analysis and QTL mapping. *PLoS Genetics*, *7*(8), e1002221.https://doi.org/10.1371/journal.pgen.1002221

Fan, K., Wang, M., Gao, Y. Y., Ning, Q. Y., & Shi, Y. Z. (2019a). Transcriptomic and ionomic analysis provides new insight into the beneficial effect of Al on tea roots' growth and nutrient uptake [Article]. *Plant Cell Reports*, *38*(6), 715-729.https://doi.org/10.1007/s00299-019-02401-5

Fan, N., Wen, W., Gao, L., Lv, A., Su, L., Zhou, P., & An, Y. (2022). MsPG4-mediated hydrolysis of pectins increases the cell wall extensibility and aluminum resistance of alfalfa. *Plant and Soil*.https://doi.org/10.1007/s11104-022-05431-3

Fan, W., Lou, H. Q., Gong, Y. L., Liu, M. Y., Cao, M. J., Liu, Y., Yang, J. L., & Zheng, S. J. (2015). Characterization of an inducible C2H2-type zinc finger transcription factor Vu STOP 1 in rice bean (Vigna umbellata) reveals differential regulation between low pH and aluminum tolerance mechanisms. *New Phytologist*, *208*(2), 456-468.https://doi.org/10.1111/nph.13456

Fan, W., Xu, J. M., Lou, H. Q., Xiao, C., Chen, W. W., & Yang, J. L. (2016). Physiological and molecular analysis of aluminium-induced organic acid anion secretion from grain amaranth (Amaranthus hypochondriacus L.) roots. *International Journal of Molecular Sciences*, *17*(5).https://doi.org/10.3390/IJMS17050608

Fan, W., Xu, J. M., Wu, P., Yang, Z. X., Lou, H. Q., Chen, W. W., Jin, J. F., Zheng, S. J., & Yang, J. L. (2019b). Alleviation by abscisic acid of Al toxicity in rice bean is not associated with citrate efflux but depends on ABI5-mediated signal transduction pathways [Article]. *Journal of Integrative Plant Biology*, *61*(2), 140-154.https://doi.org/10.1111/jipb.12695

Fan, Z., Lin, S., Zhang, X., Jiang, Z., Yang, K., Jian, D., Chen, Y., Li, J., Chen, Q., & Wang, J. (2014). Conventional flooding irrigation causes an overuse of nitrogen fertilizer and low nitrogen use efficiency in intensively used solar greenhouse vegetable production. *Agricultural Water Management*, *144*, 11-19.https://doi.org/10.1016/j.agwat.2014.05.010

Fang, K., Xie, P., Zhang, Q., Xing, Y., Cao, Q., & Qin, L. (2020). Aluminum toxicity-induced pollen tube growth inhibition in apple (Malus domestica) is mediated by interrupting calcium dynamics and modification of cell wall components. *Environmental and Experimental Botany*, *171*, 103928.https://doi.org/10.1016/j.envexpbot.2019.103928

Fang, Q., Zhang, J., Yang, D. L., & Huang, C. F. (2021a). The SUMO E3 ligase SIZ1 partially regulates STOP1 SUMOylation and stability in *Arabidopsis thaliana* [Article]. *Plant Signaling & Behavior*, *16*(5), 7.https://doi.org/10.1080/15592324.2021.1899487

Fang, Q., Zhou, F., Zhang, Y., Singh, S., & Huang, C. F. (2021b). Degradation of STOP1 mediated by the F-box proteins RAH1 and RAE1 balances aluminum resistance and plant growth in *Arabidopsis thaliana*. *Plant Journal*, *106*(2), 493-506.https://doi.org/10.1111/TPJ.15181

FAOSTAT. (2023). *Crops and livestock products*. Food and Agriculture Organization Corporate Statistical Database. https://www.fao.org/faostat/en/#data/QCL

FDA, U. S. (2018). *CFR - Code of Federal Regulations Title 21*. Retrieved from https://www.accessdata.fda.gov/scripts/cdrh/cfdocs/cfcfr/CFRSearch.cfm?fr=172.515

Fedeli, R., Vannini, A., Celletti, S., Maresca, V., Munzi, S., Cruz, C., Alexandrov, D., Guarnieri, M., & Loppi, S. (2022a). Foliar application of wood distillate boosts plant yield and nutritional parameters of chickpea. *Annals of Applied Biology*.https://doi.org/10.1111/aab.12794

Fedeli, R., Vannini, A., Guarnieri, M., Monaci, F., & Loppi, S. (2022b). Bio-Based Solutions for Agriculture: Foliar Application of Wood Distillate Alone and in Combination with Other Plant-Derived Corroborants Results in Different Effects on Lettuce (Lactuca Sativa L.). *Biology*, *11*(3), 404.https://doi.org/10.3390/biology11030404

Feng, Y., Li, X., Guo, S., Chen, X., Chen, T., He, Y., Shabala, S., & Yu, M. (2019). Extracellular silica nanocoat formed by layer-by-layer (LBL) self-assembly confers aluminum resistance in root border cells of pea (Pisum sativum). *Journal of Nanobiotechnology*, *17*(1), 1-11.https://doi.org/10.1186/s12951-019-0486-y

Fernie, A. R., Carrari, F., & Sweetlove, L. J. (2004). Respiratory metabolism: glycolysis, the TCA cycle and mitochondrial electron transport. *Current Opinion in Plant Biology*, *7*(3), 254-261.https://doi.org/10.1016/j.pbi.2004.03.007.

Flematti, G. R., Ghisalberti, E. L., Dixon, K. W., & Trengove, R. D. (2004). A compound from smoke that promotes seed germination. *Science*, *305*(5686), 977-977.https://doi.org/10.1126/science.1099944

Flematti, G. R., Ghisalberti, E. L., Dixon, K. W., & Trengove, R. D. (2009). Identification of alkyl substituted 2 H-furo [2, 3-c] pyran-2-ones as germination stimulants present in smoke. *Journal of agricultural and food chemistry*, *57*(20), 9475-9480.https://doi.org/10.1021/jf9028128

Francesca, S., Raimondi, G., Cirillo, V., Maggio, A., Barone, A., & Rigano, M. M. (2021). A Novel Protein Hydrolysate-Based Biostimulant Improves Tomato Performances under Drought Stress. *Plants*, *10*(4), 783.https://doi.org/10.3390/plants10040783.

Fromme, P., Melkozernov, A., Jordan, P., & Krauss, N. (2003). Structure and function of photosystem I: interaction with its soluble electron carriers and external antenna systems. *Febs letters*, *555*(1), 40-44.https://doi.org/10.1016/S0014-5793(03)01124-4

Fu, Z., Jiang, X., Li, W. W., Shi, Y., Lai, S., Zhuang, J., Yao, S., Liu, Y., Hu, J., Gao, L., & Xia, T. (2020). Proanthocyanidin-Aluminum Complexes Improve Aluminum Resistance and Detoxification of Camellia sinensis. *Journal of agricultural and food chemistry*, *68*(30), 7861-7869.https://doi.org/10.1021/acs.jafc.0c01689

Fuchs, G., & Berg, I. A. (2014). Unfamiliar metabolic links in the central carbon metabolism. *J Biotechnol*, *192 Pt B*, 314-322.https://doi.org/10.1016/j.jbiotec.2014.02.015.

Furlan, F., Borgo, L., Rabêlo, F. H. S., Rossi, M. L., Linhares, F. S., Martinelli, A. P., Azevedo, R. A., & Lavres, J. (2020). Aluminum-induced toxicity in Urochloa brizantha genotypes: A first glance into root Al-apoplastic and -symplastic compartmentation, Al-translocation and antioxidant performance. *Chemosphere*, *243*, 125362.https://doi.org/10.1016/j.chemosphere.2019.125362

Furlan, F., Borgo, L., Rabelo, F. H. S., Rossi, M. L., Martinelli, A. P., Azevedo, R. A., & Lavres, J. (2018). Aluminum-induced stress differently modifies Urochloa genotypes responses on growth and regrowth: root-to-shoot Al-translocation and oxidative stress [Article]. *Theoretical and Experimental Plant Physiology*, *30*(2), 141-152.https://doi.org/10.1007/s40626-018-0109-2

Furukawa, J., Yamaji, N., Wang, H., Mitani, N., Murata, Y., Sato, K., Katsuhara, M., Takeda, K., & Ma, J. F. (2007). An aluminum-activated citrate transporter in barley. *Plant and Cell Physiology*, *48*(8), 1081-1091.https://doi.org/10.1093/pcp/pcm091

Gao, J., Liang, Y. N., Li, J. P., Wang, S. Q., Zhan, M. Q., Zheng, M. H., Li, H., & Yang, Z. M. (2021). Identification of a bacterial-type ATP-binding cassette transporter implicated in aluminum tolerance in sweet sorghum (Sorghum bicolor L.) [Article]. *Plant Signaling & Behavior*, *16*(7), 8.https://doi.org/10.1080/15592324.2021.1916211

Gao, J., Yan, S. Q., Yu, H. Y., Zhan, M. Q., Guan, K. X., Wang, Y. Q., & Yang, Z. M. (2019). Sweet sorghum (Sorghum bicolor L.) SbSTOP1 activates the transcription of a beta-1,3-glucanase gene to reduce callose deposition under Al toxicity: A novel pathway for Al tolerance in plants [Article]. *Bioscience Biotechnology and Biochemistry*, *83*(3), 446-455.https://doi.org/10.1080/09168451.2018.1540290

Garcia-Montoto, V., Verdier, S., Dayton, D. C., Mante, O., Arnaudguilhem, C., Christensen, J. H., & Bouyssière, B. (2021). Phosphorus speciation analysis of fatty-acid-based feedstocks and fast pyrolysis biocrudes via gel permeation chromatography inductively coupled plasma high-resolution mass spectrometry. *RSC Advances*, *11*(43), 26732-26738.https://doi.org/10.1039/D1RA03470G

Garcia-Oliveira, A. L., Benito, C., Prieto, P., de Andrade Menezes, R., Rodrigues-Pousada, C., Guedes-Pinto, H., & Martins-Lopes, P. (2013). Molecular characterization of TaSTOP1 homoeologues and their response to aluminium and proton (H+) toxicity in bread wheat (Triticum aestivumL.). *BMC Plant Biology*, *13*(1), 1-13.https://doi.org/10.1186/1471-2229-13-134

Garcìa-Pèrez, M., Chaala, A., & Roy, C. (2002). Vacuum pyrolysis of sugarcane bagasse. *Journal of Analytical and Applied Pyrolysis*, *65*(2), 111-136.https://doi.org/10.1016/S0165-2370(01)00184-X

Garcia-Oliveira, A. L., Martins-Lopes, P., Tolrá, R., Poschenrieder, C., Tarquis, M., Guedes-Pinto, H., & Benito, C. (2014). Molecular characterization of the citrate transporter gene TaMATE1 and expression analysis of upstream genes involved in organic acid transport under Al stress in bread wheat (Triticum aestivum). *Physiologia plantarum*, *152*(3), 441-452. https://doi.org/10.1111/ppl.12179

Gardiner, J., Overall, R., & Marc, J. (2012). Plant microtubule cytoskeleton complexity: microtubule arrays as fractals. *Journal of Experimental Botany*, *63*(2), 635-642.https://doi.org/10.1093/jxb/err312

Gatahi, D. M. (2020). Challenges and opportunities in tomato production chain and sustainable standards. *International Journal of Horticultural Science and Technology*, *7*(3), 235-262.https://doi.org/10.22059/ijhst.2020.300818.361

Gavassi, M. A., Silva, G. S., da Silva, C. D. S., Thompson, A. J., Macleod, K., Oliveira, P. M. R., Cavalheiro, M. F., Domingues, D. S., & Habermann, G. (2021). NCED expression is related to increased ABA biosynthesis and stomatal closure under aluminum stress [Article]. *Environmental and Experimental Botany*, *185*, 12, Article 104404.https://doi.org/10.1016/j.envexpbot.2021.104404

Gazey, C. (2018). *Effects of soil acidity*. Government of Western Australia. Retrieved 09/02 from https://www.agric.wa.gov.au/soil-acidity/effects-soil-acidity

Geng, X., Horst, W. J., Golz, J. F., Lee, J. E., Ding, Z., & Yang, Z. B. (2017). LEUNIG _ HOMOLOG transcriptional co-repressor mediates aluminium sensitivity through PECTIN METHYLESTERASE 46-modulated root cell wall pectin methylesterification in *Arabidopsis*. *The Plant Journal*, *90*(3), 491-504.https://doi.org/10.1111/tpj.13506

Ghebrehiwot, H. M., Kulkarni, M. G., Kirkman, K. P., & Van Staden, J. (2008). Smoke-Water and a Smoke-Isolated Butenolide Improve Germination and Seedling Vigour of Eragrostis tef (Zucc.) Trotter under High Temperature and Low Osmotic Potential [https://doi.org/10.1111/j.1439-037X.2008.00321.x]. *Journal of Agronomy and Crop Science*, *194*(4), 270-277.https://doi.org/10.1111/j.1439-037X.2008.00321.x

Gifford, R. M., & Evans, L. T. (1981). Photosynthesis, carbon partitioning, and yield. *Annual Review of Plant Physiology*, *32*(1), 485-509.https://doi.org/10.1146/annurev.pp.32.060181.002413

Gill, S. S., & Tuteja, N. (2010). Reactive oxygen species and antioxidant machinery in abiotic stress tolerance in crop plants. *Plant Physiology and Biochemistry*, *48*(12), 909-930.https://doi.org/10.1016/j.plaphy.2010.08.016

Gillespie, K. M., & Ainsworth, E. A. (2007). Measurement of reduced, oxidized and total ascorbate content in plants. *Nature Protocols*, *2*(4), 871-874.https://doi.org/10.1038/nprot.2007.101

Gloria, N. F., Soares, N., Brand, C., Oliveira, F. L., Borojevic, R., & Teodoro, A. J. (2014). Lycopene and beta-carotene induce cell-cycle arrest and apoptosis in human breast cancer cell lines. *Anticancer research*, *34*(3), 1377-1386.

Gomez-Roldan, V., Fermas, S., Brewer, P. B., Puech-Pagès, V., Dun, E. A., Pillot, J.-P., Letisse, F., Matusova, R., Danoun, S., & Portais, J.-C. (2008). Strigolactone inhibition of shoot branching. *Nature*, *455*(7210), 189-194.https://doi.org/10.1038/nature07271

Gonzalez, J. F., Ramiro, A., González-García, C. M., Ganan, J., Encinar, J. M., Sabio, E., & Rubiales, J. (2005). Pyrolysis of almond shells. Energy applications of fractions. *Industrial & engineering chemistry research*, *44*(9), 3003-3012.https://doi.org/10.1021/ie0490942

Goula, A. M., Prokopiou, P., & Stoforos, N. G. (2018). Thermal degradation kinetics of l-carnitine. *Journal of Food Engineering*, *231*, 91-100.https://doi.org/10.1016/j.jfoodeng.2018.03.011

Grewal, A., Abbey, L., & Gunupuru, L. R. (2018). Production, prospects and potential application of pyroligneous acid in agriculture. *Journal of Analytical and Applied Pyrolysis*, *135*, 152-159.https://doi.org/10.1016/j.jaap.2018.09.008.

Gruber, B. D., Ryan, P. R., Richardson, A. E., Tyerman, S. D., Ramesh, S., Hebb, D. M., Howitt, S. M., & Delhaize, E. (2010). HvALMT1 from barley is involved in the transport of organic anions. *Journal of Experimental Botany*, *61*(5), 1455-1467.https://doi.org/10.1093/jxb/erq023

Guilfoyle, T. J., & Hagen, G. (2007). Auxin response factors. *Current Opinion in Plant Biology*, *10*(5), 453-460.https://doi.org/10.1016/j.pbi.2007.08.014

Guillén, M. a. D., & Manzanos, M. a. J. (2002). Study of the volatile composition of an aqueous oak smoke preparation. *Food Chemistry*, *79*(3), 283-292.https://doi.org/10.1016/S0308-8146(02)00141-3

Guimaraes, C. T., Simoes, C. C., Pastina, M. M., Maron, L. G., Magalhaes, J. V., Vasconcellos, R. C. C., Guimaraes, L. J. M., Lana, U. G. P., Tinoco, C. F. S., & Noda, R. W. (2014). Genetic dissection of Al tolerance QTLs in the maize genome by high density SNP scan. *BMC Genomics*, *15*(1), 1-14.https://doi.org/10.1186/1471-2164-15-153

Gul, M., Wakeel, A., Steffens, D., & Lindberg, S. (2019). Potassium-induced decrease in cytosolic Na(+) alleviates deleterious effects of salt stress on wheat (Triticum aestivum L.). *Plant Biology*, *21*(5), 825-831.https://doi.org/10.1111/plb.12999

Guo, D. Y., Zhao, S. Y., Huang, L. L., Ma, C. Y., & Hao, L. (2014). Aluminum tolerance in *Arabidopsis thaliana* as affected by endogenous salicylic acid. *Biologia Plantarum*, *58*(4), 725-732.https://doi.org/10.1007/s10535-014-0439-0

Guo, J., Zhang, Y., Gao, H., Li, S., Wang, Z. Y., & Huang, C. F. (2020). Mutation of HPR1 encoding a component of the THO/TREX complex reduces STOP1 accumulation and aluminium resistance in *Arabidopsis thaliana*. *New Phytologist*, *228*(1), 179-193.https://doi.org/10.1111/NPH.16658

Guo, P., Qi, Y. P., Cai, Y. T., Yang, T. Y., Yang, L. T., Huang, Z. R., & Chen, L. S. (2018). Aluminum effects on photosynthesis, reactive oxygen species and methylglyoxal detoxification in two Citrus species differing in aluminum tolerance [Article]. *Tree Physiology*, *38*(10), 1548-1565.https://doi.org/10.1093/treephys/tpy035

Guo, P., Qi, Y. P., Yang, L. T., Lai, N. W., Ye, X., Yang, Y., & Chen, L. S. (2017). Root adaptive responses to aluminum-treatment revealed by RNA-seq in two citrus species with different aluminum-tolerance. *Frontiers in plant science*, *8*, 330-330.https://doi.org/10.3389/fpls.2017.00330

Guo, T.-R., Zhang, G.-P., Mei-Xue, Z., Fei-Bo, W. U., & Jin-Xin, C. (2007). Influence of aluminum and cadmium stresses on mineral nutrition and root exudates in two barley cultivars. *Pedosphere*, *17*(4), 505-512.https://doi.org/10.1016/S1002-0160(07)60060-5

Gupta, N., Gaurav, S. S., & Kumar, A. (2013). Molecular basis of aluminium toxicity in plants: a review. *American Journal of Plant Sciences*, *2013*.https://doi.org/10.4236/ajps.2013.412A3004

Gyimah, L. A., Amoatey, H. M., Boatin, R., Appiah, V., & Odai, B. T. (2020). The impact of gamma irradiation and storage on the physicochemical properties of tomato fruits in Ghana. *Food Qual. Saf.*, *4*(3), 151-157.https://doi.org/10.1093/fqsafe/fyaa017

Hajiboland, R., Bahrami Rad, S., Barceló, J., & Poschenrieder, C. (2013a). Mechanisms of aluminum-induced growth stimulation in tea (Camellia sinensis). *Journal of Plant Nutrition and Soil Science*, *176*(4), 616-625. https://doi.org/10.1002/jpln.201200311

Hajiboland, R., Barceló, J., Poschenrieder, C., & Tolrà, R. (2013b). Amelioration of iron toxicity: A mechanism for aluminum-induced growth stimulation in tea plants. *Journal of Inorganic Biochemistry*, *128*, 183-187.https://doi.org/10.1016/j.jinorgbio.2013.07.007

Hampp, R., & Schnabl, H. J. Z. f. P. (1975). Effect of aluminium ions on 14CO2-fixation and membrane system of isolated spinach chloroplasts. *Zeitschrift für Pflanzenphysiologie*, *76*(4), 300-306.https://doi.org/10.1016/S0044-328X(75)80056-0.

Han, J., Gagnon, S., Eckle, T., & Borchers, C. H. (2013a). Metabolomic analysis of key central carbon metabolism carboxylic acids as their 3-nitrophenylhydrazones by UPLC/ESI-MS. *Electrophoresis*, *34*(19), 2891-2900.https://doi.org/10.1002/elps.201200601.

Han, J., Tschernutter, V., Yang, J., Eckle, T., & Borchers, C. H. (2013b). Analysis of selected sugars and sugar phosphates in mouse heart tissue by reductive amination and liquid chromatography-electrospray ionization mass spectrometry. *Analytical Chemistry*, *85*(12), 5965-5973.https://doi.org/10.1021/ac400769g.

Harris, C. S., Burt, A. J., Saleem, A., Le, P. M., Martineau, L. C., Haddad, P. S., Bennett, S. A. L., & Arnason, J. T. (2007). A single HPLC-PAD-APCI/MS method for the quantitative comparison of phenolic compounds found in leaf, stem, root and fruit extracts of Vaccinium angustifolium. *Phytochemical Analysis: An International Journal of Plant Chemical and Biochemical Techniques*, *18*(2), 161-169.https://doi.org/10.1002/pca.970

Hasanuzzaman, M., Parvin, K., Bardhan, K., Nahar, K., Anee, T. I., Masud, A. A. C., & Fotopoulos, V. (2021). Biostimulants for the Regulation of Reactive Oxygen Species Metabolism in Plants under Abiotic Stress. *Cell*, *10*(10), 2537.https://doi.org/10.3390/cells10102537.

Hayat, S., Ahmad, H., Nasir, M., Khan, M. N., Ali, M., Hayat, K., Khan, M. A., Khan, F., Ma, Y., & Cheng, Z. (2020). Some Physiological and Biochemical Mechanisms during Seed-to-Seedling Transition in Tomato as Influenced by Garlic Allelochemicals. *Antioxidants*, *9*(3), 235.https://doi.org/10.3390/antiox9030235

Henchion, M., Hayes, M., Mullen, A. M., Fenelon, M., & Tiwari, B. (2017). Future Protein Supply and Demand: Strategies and Factors Influencing a Sustainable Equilibrium. *Foods (Basel, Switzerland)*, *6*(7), 53.https://doi.org/10.3390/foods6070053

Herrero, J., Esteban-Carrasco, A., & Zapata, J. M. (2013). Looking for Arabidopsis thaliana peroxidases involved in lignin biosynthesis. *Plant Physiology and Biochemistry*, *67*, 77-86.https://doi.org/10.1016/j.plaphy.2013.02.019

Heuvelink, E. (2005). *Tomatoes*. CABI Pub.

Heuvelink, E. (2018). *Tomatoes* (2nd edition. ed.). CABI. https://doi.org/https://doi.org/10.1079/9781780641935.0000

Himmelbauer, M. L. (2004). Estimating length, average diameter and surface area of roots using two different image analyses systems. *Plant and Soil*, *260*(1), 111-120.https://doi.org/10.1023/B:PLSO.0000030171.28821.55

Hirschi, K. D. (2004). The calcium conundrum. Both versatile nutrient and specific signal. *Plant physiology*, *136*(1), 2438-2442.https://doi.org/10.1104/pp.104.046490

Ho, C.-L., Lin, C.-Y., Ka, S.-M., Chen, A., Tasi, Y.-L., Liu, M.-L., Chiu, Y.-C., & Hua, K.-F. (2013). Bamboo Vinegar Decreases Inflammatory Mediator Expression and NLRP3 Inflammasome Activation by Inhibiting Reactive Oxygen Species Generation and Protein Kinase C-α/δ Activation. *PloS One*, *8*(10), e75738.https://doi.org/10.1371/journal.pone.0075738

Hodges, D. M., DeLong, J. M., Forney, C. F., & Prange, R. K. J. P. (1999). Improving the thiobarbituric acid-reactive-substances assay for estimating lipid peroxidation in plant tissues containing anthocyanin and other interfering compounds. *Planta*, *207*(4), 604-611.https://doi.org/10.1007/s004250050524

Hon, D. N. S., & Minemura, N. (2001). Color and Discoloration. Dalam: Wood and Cellulosic Chemistry. DNS Hon & N Shiraishi. In *Marcel Dekker, New York. Lukmandaru, G.(2009). Pengukuran kadar ekstraktif dan sifat warna pada kayu teras jati doreng (Tectona grandis). Jurnal Ilmu Kehutanan* (Vol. 3, pp. 67-73).

Hossain, A. K. M. Z., Koyama, H., & Hara, T. (2006). Growth and cell wall properties of two wheat cultivars differing in their sensitivity to aluminum stress. *Journal of Plant Physiology*, *163*(1), 39-47.https://doi.org/10.1016/j.jplph.2005.02.008

Hu, W. J., Wu, Q., Liu, X., Shen, Z. J., Chen, J., Liu, T. W., Chen, J., Zhu, C. Q., Wu, F. H., Chen, L., Wei, J., Qiu, X. Y., Shen, G. X., & Zheng, H. L. (2016a). Comparative Proteomic Analysis Reveals the Effects of Exogenous Calcium against Acid Rain Stress in Liquidambar formosana Hance Leaves. *Journal Proteome Research*, *15*(1), 216-228.https://doi.org/10.1021/acs.jproteome.5b00771

Hu, X., Guo, H., Gholizadeh, M., Sattari, B., & Liu, Q. (2019). Pyrolysis of different wood species: Impacts of C/H ratio in feedstock on distribution of pyrolysis products. *Biomass and Bioenergy*, *120*, 28-39.https://doi.org/10.1016/j.biombioe.2018.10.021

Hu, X., Jiang, S., Wu, L., Wang, S., & Li, C.-Z. (2017). One-pot conversion of biomass-derived xylose and furfural into levulinate esters via acid catalysis. *Chemical Communications*, *53*(20), 2938-2941.https://doi.org/10.1039/C7CC01078H

Hu, Z., Cools, T., & De Veylder, L. (2016b). Mechanisms used by plants to cope with DNA damage. *Annual Review of Plant Biology*, *67*, 439-462.https://doi.org/10.1146/annurev-arplant-043015-111902

Huang, C. F., Yamaji, N., Chen, Z., & Ma, J. F. (2012). A tonoplast-localized half-size ABC transporter is required for internal detoxification of aluminum in rice. *The Plant Journal*, *69*(5), 857-867.https://doi.org/10.1111/j.1365-313X.2011.04837.x

Huang, C. F., Yamaji, N., Mitani, N., Yano, M., Nagamura, Y., & Ma, J. F. (2009). A bacterial-type ABC transporter is involved in aluminum tolerance in rice. *The Plant Cell*, *21*(2), 655-667.https://doi.org/10.1105/tpc.108.064543

Huang, J. J., An, W. J., Wang, K. J., Jiang, T. H., Ren, Q., Liang, W. H., & Wang, H. H. (2019). Expression profile analysis of MATE gene family in rice [Article]. *Biologia Plantarum*, *63*, 556-564.https://doi.org/10.32615/bp.2019.099

Huang, J. W., Shaff, J. E., Grunes, D. L., & Kochian, L. V. (1992). Aluminum effects on calcium fluxes at the root apex of aluminum-tolerant and aluminum-sensitive wheat cultivars. *Plant physiology*, *98*(1), 230-237.https://doi.org/10.1104/pp.98.1.230

Huang, L., Bell, R. W., Dell, B., & Woodward, J. (2004). Rapid Nitric Acid Digestion of Plant Material with an Open-Vessel Microwave System. *Communications in Soil Science and Plant Analysis*, *35*(3-4), 427-440.https://doi.org/10.1081/CSS-120029723

Huang, W., LwinOo, T., He, H., Wang, A., Zhan, J., Li, C., Wei, S.-Q., & He, L. (2014a). Aluminum induces rapidly mitochondria dependent programmed cell death in Al-sensitive peanut root tips. *Botanical Studies*, *55*(1), e67-e67.https://doi.org/10.1186/s40529-014-0067-1

Huang, W., Yang, X., Yao, S., LwinOo, T., He, H., Wang, A., Li, C., & He, L. (2014b). Reactive oxygen species burst induced by aluminum stress triggers mitochondria-dependent programmed cell death in peanut root tip cells. *Plant Physiology and Biochemistry*, *82*, 76-84.https://doi.org/10.1016/j.plaphy.2014.03.037.

Imamura, E., & Watanabe, Y. (2007). Anti-allergy composition comprising wood vinegar-or bamboo vinegar-distilled solution. In: Google Patents.

Ito, H., Kobayashi, Y., Yamamoto, Y. Y., & Koyama, H. (2019). Characterization of NtSTOP1-regulating genes in tobacco under aluminum stress [Article]. *Soil Science and Plant Nutrition*, *65*(3), 251-258.https://doi.org/10.1080/00380768.2019.1603064

Iuchi, S., Koyama, H., Iuchi, A., Kobayashi, Y., Kitabayashi, S., Kobayashi, Y., Ikka, T., Hirayama, T., Shinozaki, K., & Kobayashi, M. (2007). Zinc finger protein STOP1 is critical for proton tolerance in *Arabidopsis* and coregulates a key gene in aluminum tolerance. *Proceedings of the National Academy of Sciences*, *104*(23), 9900-9905.https://doi.org/10.1073/pnas.0700117104

Jacques, F., Rippa, S., & Perrin, Y. (2018). Physiology of L-carnitine in plants in light of the knowledge in animals and microorganisms. *Plant Science*, *274*, 432-440.https://doi.org/10.1016/j.plantsci.2018.06.020

Jain, N., & Van Staden, J. (2007). The potential of the smoke-derived compound 3-methyl-2H-furo [2, 3-c] pyran-2-one as a priming agent for tomato seeds. *Seed Science Research*, *17*(3), 175-181.https://doi.org/10.1017/S0960258507785896

Jamil, A., Riaz, S., Ashraf, M., & Foolad, M. R. (2011). Gene expression profiling of plants under salt stress. *Critical Reviews in Plant Sciences*, *30*(5), 435-458.https://doi.org/10.1080/07352689.2011.605739

Jaskowiak, J., Tkaczyk, O., Slota, M., Kwasniewska, J., & Szarejko, I. (2018). Analysis of aluminum toxicity in Hordeum vulgare roots with an emphasis on DNA integrity and cell cycle [Article]. *PloS One*, *13*(2), 18, Article e0193156.https://doi.org/10.1371/journal.pone.0193156

Javed, M. T., Stoltz, E., Lindberg, S., & Greger, M. (2013). Changes in pH and organic acids in mucilage of Eriophorum angustifolium roots after exposure to elevated concentrations of toxic elements. *Environmental Science and Pollution Research*, *20*(3), 1876-1880.https://doi.org/10.1007/s11356-012-1413-z

Jeong, C., Yun, I., Park, J., Kyoung, J., Kang, J., Lee, S., Jo, T., & Ahn, B. (2006). Effect of wood vinegar and charcoal on growth and quality of sweet pepper. *Korean Journal of Horticultural Science & Technology*, *24*(2), 177-180.

Jiang, H.-X., Chen, L.-S., Zheng, J.-G., Han, S., Tang, N., & Smith, B. R. (2008). Aluminum-induced effects on Photosystem II photochemistry in Citrus leaves assessed by the chlorophyll a fluorescence transient. *Tree Physiology*, *28*(12), 1863-1871.https://doi.org/10.1093/treephys/28.12.1863

Jiang, H.-X., Tang, N., Zheng, J.-G., & Chen, L.-S. (2009a). Antagonistic actions of boron against inhibitory effects of aluminum toxicity on growth, CO2 assimilation, ribulose-1, 5-bisphosphate carboxylase/oxygenase, and photosynthetic electron transport probed by the JIP-test, of Citrus grandis seedlings. *BMC Plant Biology*, *9*, 1-16.https://doi.org/10.1186/1471-2229-9-102.

Jiang, H. X., Tang, N., Zheng, J. G., Li, Y., & Chen, L. S. (2009b). Phosphorus alleviates aluminum-induced inhibition of growth and photosynthesis in Citrus grandis seedlings. *Physiologia plantarum*, *137*(3), 298-311.https://doi.org/10.1111/j.1399-3054.2009.01288.x.

Jin, J. F., He, Q. Y., Li, P. F., Lou, H. Q., Chen, W. W., & Yang, J. L. (2021). Genome-Wide Identification and Gene Expression Analysis of Acyl-Activating Enzymes Superfamily in Tomato (Solanum lycopersicum) Under Aluminum Stress [Original Research]. *Frontiers in plant science*, *12*.https://doi.org/10.3389/fpls.2021.754147

Jung, K.-H. (2007). Growth inhibition effect of pyroligneous acid on pathogenic fungus, Alternaria mali, the agent of alternaria blotch of apple. *Journal of Biotechnology and Bioprocess Engineering*, *12*(3), 318-322.https://doi.org/10.1007/BF02931111

Kader, M. A. (2005). A comparison of seed germination calculation formulae and the associated interpretation of resulting data. *Journal and Proceeding of the Royal Society of New South Wales*, *138*, 65-75.

Kårlund, A., Salminen, J.-P., Koskinen, P., Ahern, J. R., Karonen, M., Tiilikkala, K., & Karjalainen, R. O. (2014). Polyphenols in strawberry (Fragaria× ananassa) leaves induced by plant activators. *Journal of agricultural and food chemistry*, *62*(20), 4592-4600.https://doi.org/10.1021/jf405589f

Kaur, S., Kaur, N., Siddique, K. H. M., & Nayyar, H. (2016). Beneficial elements for agricultural crops and their functional relevance in defence against stresses. *Archives of Agronomy and Soil Science*, *62*(7), 905-920.https://doi.org/10.1080/03650340.2015.1101070

Kawano, T., Kadono, T., Furuichi, T., Muto, S., & Lapeyrie, F. (2003). Aluminum-induced distortion in calcium signaling involving oxidative bursts and channel regulation in tobacco BY-2 cells. *Biochemical and Biophysical Research Communications*, *308*(1), 35-42.https://doi.org/10.1016/S0006-291X(03)01286-5

Kichigina, N. E., Puhalsky, J. V., Shaposhnikov, A. I., Azarova, T. S., Makarova, N. M., Loskutov, S. I., Safronova, V. I., Tikhonovich, I. A., Vishnyakova, M. A., & Semenova, E. V. (2017). Aluminum exclusion from root zone and maintenance of nutrient uptake are principal mechanisms of Al tolerance in Pisum sativum L. *Physiology and Molecular Biology of Plants*, *23*(4), 851-863.https://doi.org/10.1007/s12298-017-0469-0

Kirolinko, C., Hobecker, K. V., Wen, J., Mysore, K., Niebel, A., Blanco, F. A., & Zanetti, M. E. (2021). Auxin Response Factor 2 (ARF2), ARF3 and ARF4 mediate both lateral root and nitrogen fixing nodule development in *Medicago truncatula*. *Frontiers in plant science*, *12*, 465.https://doi.org/10.3389/fpls.2021.659061

Klug, B., & Horst, W. J. (2010). Oxalate exudation into the root-tip water free space confers protection from aluminum toxicity and allows aluminum accumulation in the symplast in buckwheat (Fagopyrum esculentum) [https://doi.org/10.1111/j.1469-8137.2010.03288.x]. *New Phytologist*, *187*(2), 380-391.https://doi.org/10.1111/j.1469-8137.2010.03288.x

Knapp, S., & Peralta, I. E. (2016). The Tomato (Solanum lycopersicum L., Solanaceae) and Its Botanical Relatives. In M. Causse, J. Giovannoni, M. Bouzayen, & M. Zouine (Eds.), *The Tomato Genome* (pp. 7-21). Springer Berlin Heidelberg. https://doi.org/https://doi.org/10.1007/978-3-662-53389-5_2

Koch, K. (2004). Sucrose metabolism: regulatory mechanisms and pivotal roles in sugar sensing and plant development. *Current Opinion in Plant Biology*, *7*(3), 235-246.https://doi.org/10.1016/j.pbi.2004.03.014.

Kochian, L. V., Hoekenga, O. A., & Pineros, M. A. (2004). How do crop plants tolerate acid soils? Mechanisms of aluminum tolerance and phosphorous efficiency. *Annual Review of Plant Biology*, *55*, 459-493.https://doi.org/10.1146/annurev.arplant.55.031903.141655

Kochian, L. V., Piñeros, M. A., Liu, J., & Magalhaes, J. V. (2015). Plant adaptation to acid soils: the molecular basis for crop aluminum resistance. *Annual Review of Plant Biology*, *66*, 571-598.https://doi.org/10.1146/annurev-arplant-043014-114822.

Konarska, A. (2010). Effects of aluminum on growth and structure of red pepper (Capsicum annuum L.) leaves. *Acta Physiologiae Plantarum*, *32*(1), 145-151.https://doi.org/10.1007/s11738-009-0390-4

Kopittke, P. M., Moore, K. L., Lombi, E., Gianoncelli, A., Ferguson, B. J., Blamey, F. P. C., Menzies, N. W., Nicholson, T. M., McKenna, B. A., & Wang, P. (2015). Identification of the primary lesion of toxic aluminum in plant roots. *Plant physiology*, *167*(4), 1402-1411.https://doi.org/10.1104/pp.114.253229

Ku, C. S., & Mun, S. P. (2006). Characterization of pyrolysis tar derived from lignocellulosic biomass. *Journal of Industrial and Engineering Chemistry*, *12*(6), 853-861.

Kulkarni, M. G., Ascough, G. D., & Van Staden, J. (2008). Smoke-water and a smoke-isolated butenolide improve growth and yield of tomatoes under greenhouse conditions. *Horttechnology*, *18*(3), 449-454. https://doi.org/10.21273/HORTTECH.18.3.449

Kulkarni, M. G., Ascough, G. D., Verschaeve, L., Baeten, K., Arruda, M. P., & Van Staden, J. (2010). Effect of smoke-water and a smoke-isolated butenolide on the growth and genotoxicity of commercial onion. *Scientia Horticulturae*, *124*(4), 434-439. https://doi.org/10.1016/j.scienta.2010.02.005

Kulkarni, M. G., Sparg, S. G., Light, M. E., & Van Staden, J. (2006). Stimulation of rice (Oryza sativa L.) seedling vigour by smoke-water and butenolide. *Journal of Agronomy and Crop Science*, *192*(5), 395-398.https://doi.org/10.1111/j.1439-037X.2006.00213.x

Kulkarni, M. G., Sparg, S. G., & Van Staden, J. (2007). Germination and post-germination response of Acacia seeds to smoke-water and butenolide, a smoke-derived compound. *Journal of Arid Environments*, *69*(1), 177-187.https://doi.org/10.1016/j.jaridenv.2006.09.001

Kumar, S., Kumar, S., & Mohapatra, T. (2021). Interaction Between Macro-and Micro-Nutrients in Plants. *Frontiers in plant science*, *12*, 753.https://doi.org/10.3389/fpls.2021.665583

Kundu, A., Das, S., Basu, S., Kobayashi, Y., Kobayashi, Y., Koyama, H., & Ganesan, M. (2019). GhSTOP1, a C2H2 type zinc finger transcription factor is essential for aluminum and proton stress tolerance and lateral root initiation in cotton [Article]. *Plant Biology*, *21*(1), 35-44.https://doi.org/10.1111/plb.12895

Kundu, A., & Ganesan, M. (2020). GhMATE1 expression regulates Aluminum tolerance of cotton and overexpression of GhMATE1 enhances acid soil tolerance of *Arabidopsis* [Article]. *Current Plant Biology*, *24*, 9, Article 100160.https://doi.org/10.1016/j.cpb.2020.100160

Larsen, P. B., Cancel, J., Rounds, M., & Ochoa, V. (2007). *Arabidopsis* ALS1 encodes a root tip and stele localized half type ABC transporter required for root growth in an aluminum toxic environment. *Planta*, *225*(6), 1447-1458.https://doi.org/10.1007/s00425-006-0452-4

Lashari, M. S., Liu, Y., Li, L., Pan, W., Fu, J., Pan, G., Zheng, J., Zheng, J., Zhang, X., & Yu, X. (2013). Effects of amendment of biochar-manure compost in conjunction with pyroligneous solution on soil quality and wheat yield of a salt-stressed cropland from Central China Great Plain. *Field Crops Research*, *144*, 113-118.https://doi.org/10.1016/j.fcr.2012.11.015

Lee, C. S., Yi, E. H., Kim, H. R., Huh, S. R., Sung, S. H., Chung, M. H., & Ye, S. K. (2011). Anti-dermatitis effects of oak wood vinegar on the DNCB-induced contact hypersensitivity via STAT3 suppression. *Journal of ethnopharmacology*, *135*(3), 747-753.https://doi.org/10.1016/j.jep.2011.04.009

Lehmann, M., Laxa, M., Sweetlove, L. J., Fernie, A. R., & Obata, T. (2012). Metabolic recovery of Arabidopsis thaliana roots following cessation of oxidative stress. *Metabolomics*, *8*, 143-153.https://doi.org/10.1007/s11306-011-0296-1.

Lei, G. J., Yokosho, K., Yamaji, N., Fujii-Kashino, M., & Ma, J. F. (2017a). Functional characterization of two half-size ABC transporter genes in aluminium-accumulating buckwheat. *New Phytologist*, *215*(3), 1080-1089.https://doi.org/10.1111/nph.14648

Lei, G. J., Yokosho, K., Yamaji, N., & Ma, J. F. (2017b). Two MATE transporters with different subcellular localization are involved in Al tolerance in buckwheat. *Plant and Cell Physiology*, *58*(12), 2179-2189.https://doi.org/10.1093/pcp/pcx152

Lei, M., Liu, B., & Wang, X. (2018, 2018). Effect of adding wood vinegar on cucumber (*Cucumis sativus* L) seed germination.*IOP Conference Series* IOP Conference Series: Earth and Environmental Science,

Li, C., Liu, G., Geng, X., He, C., Quan, T., Hayashi, K. I., De Smet, I., Robert, H. S., Ding, Z., & Yang, Z. B. (2021). Local regulation of auxin transport in root-apex transition zone mediates aluminium-induced *Arabidopsis* root-growth inhibition. *The Plant Journal*, *108*(1), 55-66.https://doi.org/10.1111/tpj.15424

Li, G. Z., Wang, Z. Q., Yokosho, K., Ding, B., Fan, W., Gong, Q. Q., Li, G. X., Wu, Y. R., Yang, J. L., Ma, J. F., & Zheng, S. J. (2018a). Transcription factor WRKY22 promotes aluminum tolerance via activation of OsFRDL4 expression and enhancement of citrate secretion in rice (Oryza sativa) [Article]. *New Phytologist*, *219*(1), 149-162.https://doi.org/10.1111/nph.15143

Li, H., Yang, L.-T., Qi, Y.-P., Guo, P., Lu, Y.-B., & Chen, L.-S. (2016a). Aluminum Toxicity-Induced Alterations of Leaf Proteome in Two Citrus Species Differing in Aluminum Tolerance. *International Journal of Molecular Sciences*, *17*(7), 118.https://doi.org/10.3390/ijms17071180.

Li, J., Chen, J., Qu, Z., Wang, S., He, P., & Zhang, N. (2019). Effects of alternating irrigation with fresh and saline water on the soil salt, soil nutrients, and yield of tomatoes. *Water*, *11*(8), 1693. https://doi.org/10.3390/w11081693

Li, J., Su, L., Lv, A., Li, Y., Zhou, P., & An, Y. (2020). MsPG1 alleviated aluminum-induced inhibition of root growth by decreasing aluminum accumulation and increasing porosity and extensibility of cell walls in alfalfa (Medicago sativa). *Environmental and Experimental Botany*, *175*.https://doi.org/10.1016/j.envexpbot.2020.104045

Li, J. Y., Liu, J., Dong, D., Jia, X., McCouch, S. R., & Kochian, L. V. (2014). Natural variation underlies alterations in Nramp aluminum transporter (NRAT1) expression and function that play a key role in rice aluminum tolerance. *Proceedings of the National Academy of Sciences of the United States of America*, *111*(17), 6503-6508.https://doi.org/10.1073/pnas.1318975111

Li, L., Li, X., Yang, C., Cheng, Y., Cai, Z., Nian, H., & Ma, Q. (2022). GsERF1 enhances *Arabidopsis thaliana* aluminum tolerance through an ethylene-mediated pathway. *BMC Plant Biology*, *22*(1), 258.https://doi.org/10.1186/s12870-022-03625-6

Li, N., Meng, H., Xing, H., Liang, L., Zhao, X., & Luo, K. (2017). Genome-wide analysis of MATE transporters and molecular characterization of aluminum resistance in Populus. *Journal of Experimental Botany*, *68*(20), 5669-5683.https://doi.org/10.1093/JXB/ERX370

Li, X., Li, Y., Mai, J., Tao, L., Qu, M., Liu, J., Shen, R., Xu, G., Feng, Y., Xiao, H., Wu, L., Shi, L., Guo, S., Liang, J., Zhu, Y., He, Y., Baluška, F., Shabala, S., Yu, M., Balu¡ka, F. e., Shabala, S., & Yu, M. (2018b). Boron alleviates aluminum toxicity by promoting root alkalization in transition zone via polar auxin transport. *Plant physiology*, *177*(3), 1254-1266.https://doi.org/10.1104/pp.18.00188

Li, X., Li, Y., Qu, M., Xiao, H., Feng, Y., Liu, J., Wu, L., & Yu, M. (2016b). Cell wall pectin and its methyl-esterification in transition zone determine Al resistance in cultivars of pea (Pisum sativum). *Frontiers in plant science*, *7*, 39.https://doi.org/10.3389/fpls.2016.00039

Li, Z., & Xing, D. (2011). Mechanistic study of mitochondria-dependent programmed cell death induced by aluminium phytotoxicity using fluorescence techniques. *Journal of Experimental Botany*, *62*(1), 331-343.https://doi.org/10.1093/jxb/erq279.

Li, Z., Xing, F., & Xing, D. (2012). Characterization of target site of aluminum phytotoxicity in photosynthetic electron transport by fluorescence techniques in tobacco leaves. *Plant and Cell Physiology*, *53*(7), 1295-1309.https://doi.org/10.1093/pcp/pcs076.

Liang, C., Piñeros, M. A., Tian, J., Yao, Z., Sun, L., Liu, J., Shaff, J., Coluccio, A., Kochian, L. V., & Liao, H. (2013). Low pH, aluminum, and phosphorus coordinately regulate malate exudation through GmALMT1 to improve soybean adaptation to acid soils. *Plant physiology*, *161*(3), 1347-1361.https://doi.org/10.1104/pp.112.208934

Lichtenthaler, H. K. (1987). Chlorophylls and carotenoids: Pigments of photosynthetic biomembranes. *Methods in Enzymology*, *148*, 350-382.https://doi.org/10.1016/0076-6879(87)48036-1

Liesche, J., & Patrick, J. (2017). An update on phloem transport: a simple bulk flow under complex regulation. *F1000Research*, *6*.https://doi.org/10.12688/f1000research.12577.1

Ligaba, A., Katsuhara, M., Ryan, P. R., Shibasaka, M., & Matsumoto, H. (2006). The BnALMT1 and BnALMT2 genes from rape encode aluminum-activated malate transporters that enhance the aluminum resistance of plant cells. *Plant physiology*, *142*(3), 1294-1303.https://doi.org/10.1104/pp.106.085233

Lin, H.-Y., Huang, B.-R., Yeh, W.-L., Lee, C.-H., Huang, S.-S., Lai, C.-H., Lin, H., & Lu, D.-Y. (2014). Antineuroinflammatory effects of lycopene via activation of adenosine monophosphate-activated protein kinase-α1/heme oxygenase-1 pathways. *Neurobiology of Aging*, *35*(1), 191-202.https://doi.org/10.1016/j.neurobiolaging.2013.06.020

Liu, C., Liu, Y., Lu, Y., Liao, Y., Nie, J., Yuan, X., & Chen, F. (2019). Use of a leaf chlorophyll content index to improve the prediction of above-ground biomass and productivity. *PeerJ*, *6*, e6240.https://doi.org/10.7717/peerj.6240

Liu, G., Gao, S., Tian, H., Wu, W., Robert, H. S., & Ding, Z. (2016a). Local transcriptional control of YUCCA regulates auxin promoted root-growth inhibition in response to aluminium stress in *Arabidopsis*. *PLoS Genetics*, *12*(10), e1006360.https://doi.org/10.1371/journal.pgen.1006360

Liu, J., Li, Y., Wang, W., Gai, J., & Li, Y. (2016b). Genome-wide analysis of MATE transporters and expression patterns of a subgroup of MATE genes in response to aluminum toxicity in soybean. *BMC Genomics*, *17*(1), 1-15.https://doi.org/10.1186/s12864-016-2559-8

Liu, J., Magalhaes, J. V., Shaff, J., & Kochian, L. V. (2009). Aluminum-activated citrate and malate transporters from the MATE and ALMT families function independently to confer Arabidopsis aluminum tolerance. *The Plant Journal*, *57*(3), 389-399. https://doi.org/10.1111/j.1365-313X.2008.03696.x

Liu, J., & Zhou, M. (2018). The ALMT gene family performs multiple functions in plants. *Agronomy*, *8*(2), 20.https://doi.org/10.3390/agronomy8020020

Liu, L., Guo, X., Wang, S., Li, L., Zeng, Y., & Liu, G. (2018a). Effects of wood vinegar on properties and mechanism of heavy metal competitive adsorption on secondary fermentation based composts. *Ecotoxicology and Environmental Safety*, *150*, 270-279.https://doi.org/10.1016/j.ecoenv.2017.12.037

Liu, L. J., Bai, C. M., Chen, Y. L., Palta, J. A., Delhaize, E., & Siddique, K. H. M. (2021a). Durum wheat with the introgressed TaMATE1B gene shows resistance to terminal drought by ensuring deep root growth in acidic and Al3+-toxic subsoils [Article; Early Access]. *Plant and Soil*, 14.https://doi.org/10.1007/s11104-021-04961-6

Liu, M., Xu, J., Lou, H., Fan, W., Yang, J., & Zheng, S. (2016c). Characterization of VuMATE1 expression in response to iron nutrition and aluminum stress reveals adaptation of rice bean (Vigna umbellata) to acid soils through cis regulation. *Frontiers in plant science*, *7*(APR2016).https://doi.org/10.3389/fpls.2016.00511

Liu, W. J., Xu, F. J., Lv, T., Zhou, W. W., Chen, Y., Jin, C. W., Lu, L. L., & Lin, X. Y. (2018b). Spatial responses of antioxidative system to aluminum stress in roots of wheat (Triticum aestivum L.) plants [Article]. *Science of the Total Environment*, *627*, 462-469.https://doi.org/10.1016/j.scitotenv.2018.01.021

Liu, X., Zhan, Y., Li, X., Li, Y., Feng, X., Bagavathiannan, M., Zhang, C., Qu, M., & Yu, J. (2021b). The use of wood vinegar as a non-synthetic herbicide for control of broadleaf weeds. *Industrial Crops and Products*, *173*, 114105.https://doi.org/10.1016/j.indcrop.2021.114105.

Liu, Y. J., Tao, J. Y., Cao, J., Zeng, Y. P., Li, X., Ma, J., Huang, Z., Jiang, M. Y., & Sun, L. X. (2020). The Beneficial Effects of Aluminum on the Plant Growth in Camellia japonica [Article]. *Journal of Soil Science and Plant Nutrition*, *20*(4), 1799-1809.https://doi.org/10.1007/s42729-020-00251-9

Livak, K. J., & Schmittgen, T. D. (2001). Analysis of relative gene expression data using real-time quantitative PCR and the 2− ΔΔCT method. *Methods*, *25*(4), 402-408.https://doi.org/10.1006/meth.2001.1262

Llugany, M., Poschenrieder, C., & Barceló, J. (1995). Monitoring of aluminium-induced inhibition of root elongation in four maize cultivars differing in tolerance to aluminium and proton toxicity. *Physiologia plantarum*, *93*(2), 265-271.https://doi.org/10.1111/j.1399-3054.1995.tb02227.x

Loo, A. Y., Jain, K., & Darah, I. (2007). Antioxidant and radical scavenging activities of the pyroligneous acid from a mangrove plant, Rhizophora apiculata. *Food Chemistry*, *104*(1), 300-307.https://doi.org/10.1016/j.foodchem.2006.11.048

Loo, A. Y., Jain, K., & Darah, I. (2008). Antioxidant activity of compounds isolated from the pyroligneous acid, Rhizophora apiculata. *Food Chemistry*, *107*(3), 1151-1160.https://doi.org/10.1016/j.foodchem.2007.09.044

Lourenço, S. C., Moldão-Martins, M., & Alves, V. D. (2019). Antioxidants of natural plant origins: From sources to food industry applications. *Molecules*, *24*(22), 4132.https://doi.org/10.3390/molecules24224132

Lu, M., Yang, G., Li, P., Wang, Z., Fu, S., Zhang, X., Chen, X., Shi, M., Ming, Z., & Xia, J. (2018). Bioinformatic and Functional Analysis of a Key Determinant Underlying the Substrate Selectivity of the Al Transporter, Nrat1. *Frontiers in plant science*, *9*, 606-606.https://doi.org/10.3389/fpls.2018.00606

Lu, X., Han, T., Jiang, J., Sun, K., Sun, Y., & Yang, W. (2020). Comprehensive insights into the influences of acid-base properties of chemical pretreatment reagents on biomass pyrolysis behavior and wood vinegar properties. *Journal of Analytical and Applied Pyrolysis*, *151*, 104907.https://doi.org/10.1016/j.jaap.2020.104907

Lu, X., Jiang, J., He, J., Sun, K., & Sun, Y. (2019). Effect of pyrolysis temperature on the characteristics of wood vinegar derived from Chinese fir waste: A comprehensive study on its growth regulation performance and mechanism. *ACS omega*, *4*(21), 19054-19062.https://doi.org/10.1021/acsomega.9b02240

Ma, B., Gao, L., Zhang, H., Cui, J., & Shen, Z. (2012). Aluminum-induced oxidative stress and changes in antioxidant defenses in the roots of rice varieties differing in Al tolerance. *Plant Cell Reports*, *31*(4), 687-696.https://doi.org/10.1007/s00299-011-1187-7

Ma, J., Islam, F., Ayyaz, A., Fang, R., Hannan, F., Farooq, M. A., Ali, B., Huang, Q., Sun, R., & Zhou, W. (2022). Wood vinegar induces salinity tolerance by alleviating oxidative damages and protecting photosystem II in rapeseed cultivars. *Industrial Crops and Products*, *189*, 115763.https://doi.org/10.1016/j.indcrop.2022.115763

Ma, J. F., Hiradate, S., Nomoto, K., Iwashita, T., & Matsumoto, H. (1997). Internal detoxification mechanism of Al in hydrangea (identification of Al form in the leaves). *Plant physiology*, *113*(4), 1033-1039.https://doi.org/10.1104/pp.113.4.1033

Ma, J. F., Ryan, P. R., & Delhaize, E. (2001). Aluminium tolerance in plants and the complexing role of organic acids. *Trends in Plant Science*, *6*(6), 273-278.https://doi.org/10.1016/S1360-1385(01)01961-6

Ma, Q. B., Yi, R., Li, L., Liang, Z. Y., Zeng, T. T., Zhang, Y., Huang, H., Zhang, X., Yin, X. L., Cai, Z. D., Mu, Y. H., Cheng, Y. B., Zeng, Q. Y., Li, X. P., & Nian, H. (2018). GsMATE encoding a multidrug and toxic compound extrusion transporter enhances aluminum tolerance in *Arabidopsis thaliana* [Article]. *BMC Plant Biology*, *18*, 10, Article 212.https://doi.org/10.1186/s12870-018-1397-z

Ma, X. L., Ren, J., Dai, W. R., Yang, W., & Bi, Y. F. (2020a). Effects of aluminium on the root activity, organic acids and free proline accumulation of alfalfa grown in nutrient solution. *New Zealand Journal of Agricultural Research*, *63*(3), 341-352.https://doi.org/10.1080/00288233.2018.1540436

Ma, X. W., An, F., Wang, L. F., Guo, D., Xie, G. S., & Liu, Z. F. (2020b). Genome-Wide Identification of Aluminum-Activated Malate Transporter (ALMT) Gene Family in Rubber Trees (Hevea brasiliensis) Highlights Their Involvement in Aluminum Detoxification [Article]. *Forests*, *11*(2), 15, Article 142.https://doi.org/10.3390/f11020142

Ma, Y.-H., Ma, F.-W., Zhang, J.-K., Li, M.-J., Wang, Y.-H., & Liang, D. (2008). Effects of high temperature on activities and gene expression of enzymes involved in ascorbate–glutathione cycle in apple leaves. *Plant Sci.*, *175*(6), 761-766.https://doi.org/10.1016/j.plantsci.2008.07.010

Maach, M., Boudouasar, K., Akodad, M., Skalli, A., Moumen, A., & Baghour, M. (2021). Application of biostimulants improves yield and fruit quality in tomato. *International Journal of Vegetable Science*, *27*(3), 288-293.https://doi.org/10.1080/19315260.2020.1780536

Maejima, E., Osaki, M., Wagatsuma, T., & Watanabe, T. (2017). Contribution of constitutive characteristics of lipids and phenolics in roots of tree species in Myrtales to aluminum tolerance. *Physiologia plantarum*, *160*(1), 11-20.https://doi.org/10.1111/ppl.12527

Magalhaes, J. V., Liu, J., Guimaraes, C. T., Lana, U. G. P., Alves, V., Wang, Y.-H., Schaffert, R. E., Hoekenga, O. A., Pineros, M. A., & Shaff, J. E. (2007). A gene in the multidrug and toxic compound extrusion (MATE) family confers aluminum tolerance in sorghum. *Nature Genetics*, *39*(9), 1156-1161.https://doi.org/10.1038/ng2074

Magalhaes, J. V., Pineros, M. A., Maciel, L. S., & Kochian, L. V. (2018). Emerging Pleiotropic Mechanisms Underlying Aluminum Resistance and Phosphorus Acquisition on Acidic Soils [Review]. *Frontiers in plant science*, *9*, 12, Article 1420.https://doi.org/10.3389/fpls.2018.01420

Malangisha, G. K., Yang, Y. B., Moustafa-Farag, M., Fu, Q., Shao, W. Q., Wang, J. K., Shen, L., Huai, Y., Lv, X. L., Shi, P. B., Ali, A., Lin, Y., Khan, J., Ren, Y. Y., Yang, J. H., Hu, Z. Y., & Zhang, M. F. (2020). Subcellular distribution of aluminum associated with differential cell ultra-structure, mineral uptake, and antioxidant enzymes in root of two different Al+3-resistance watermelon cultivars [Article]. *Plant Physiology and Biochemistry*, *155*, 613-625.https://doi.org/10.1016/j.plaphy.2020.06.045

Mantovanini, L. J., Gonçalves da Silva, R., de Oliveira Leite Silva, J., Mateus Rosa dos Santos, T., Maria Mathias dos Santos, D., & Marli Zingaretti, S. (2019). Root system development and proline accumulation in sugarcane leaves under aluminum (Al 3+) stress. *Australian Journal of Crop Science*, *13*(02), 1835-2707.https://doi.org/10.21475/ajcs.19.13.02.p1198

Manzoor, Z., Hassan, Z., Ul-Allah, S., Khan, A. A., Sattar, A., Shahzad, U., Amin, H., & Hussain, M. (2022). Transcription factors involved in plant responses to heavy metal stress adaptation. In *Plant Perspectives to Global Climate Changes* (pp. 221-231). Elsevier. https://doi.org/https://doi.org/10.1016/B978-0-323-85665-2.00021-2.

Mariano, E. D., Pinheiro, A. S., Garcia, E. E., Keltjens, W. G., Jorge, R. A., & Menossi, M. (2015). Differential aluminium-impaired nutrient uptake along the root axis of two maize genotypes contrasting in resistance to aluminium. *Plant and Soil*, *388*(1), 323-335.https://doi.org/10.1007/s11104-014-2334-z

Maron, L. G., Guimarães, C. T., Kirst, M., Albert, P. S., Birchler, J. A., Bradbury, P. J., Buckler, E. S., Coluccio, A. E., Danilova, T. V., & Kudrna, D. (2013). Aluminum tolerance in maize is associated with higher MATE1 gene copy number. *Proceedings of the National Academy of Sciences*, *110*(13), 5241-5246.https://doi.org/10.1073/pnas.122076611

Maron, L. G., Kirst, M., Mao, C., Milner, M. J., Menossi, M., & Kochian, L. V. (2008). Transcriptional profiling of aluminum toxicity and tolerance responses in maize roots. *New Phytologist*, *179*(1), 116-128.https://doi.org/10.1111/j.1469-8137.2008.02440.x

Marumoto, S., Yamamoto, S. P., Nishimura, H., Onomoto, K., Yatagai, M., Yazaki, K., Fujita, T., & Watanabe, T. (2012). Identification of a germicidal compound against picornavirus in bamboo pyroligneous acid. *Journal of agricultural and food chemistry*, *60*(36), 9106-9111.https://doi.org/10.1021/jf3021317

Masterson, C., & Wood, C. (2000). Carnitine palmitoyltransferases in pea leaf chloroplasts: partial purification, location, and properties. *Canadian Journal of Botany*, *78*(3), 328-335.https://doi.org/10.1139/b00-008

Masterson, C., & Wood, C. (2009). Influence of mitochondrial beta-oxidation on early pea seedling development. *New Phytologist*, *181*(4), 832-842.https://doi.org/10.1111/j.1469-8137.2008.02717.x

Masum, S. M., Malek, M., Mandal, M. S. H., Haque, M. N., & Akther, Z. (2013). Influence of plant extracted pyroligneous acid on transplanted aman rice. *Journal of Experimental Bioscience*, *4*(3), 31-34.

Mathew, S., & Zakaria, Z. A. (2015). Pyroligneous acid—the smoky acidic liquid from plant biomass. *Applied Microbiology and Biotechnology*, *99*(2), 611-622.https://doi.org/10.1007/s00253-014-6242-1

Mathew, S., Zakaria, Z. A., & Musa, N. F. (2015). Antioxidant property and chemical profile of pyroligneous acid from pineapple plant waste biomass. *Process Biochemistry*, *50*(11), 1985-1992.https://doi.org/10.1016/j.procbio.2015.07.007

Maxwell, K., & Johnson, G. N. (2000). Chlorophyll fluorescence—a practical guide. *Journal of Experimental Botany*, *51*(345), 659-668.https://doi.org/10.1093/jexbot/51.345.659

Melo, J. O., Martins, L. G. C., Barros, B. A., Pimenta, M. R., Lana, U. G. P., Duarte, C. E. M., Pastina, M. M., Guimaraes, C. T., Schaffert, R. E., Kochian, L. V., Fontes, E. P. B., & Magalhaes, J. V. (2019). Repeat variants for the SbMATE transporter protect sorghum roots from aluminum toxicity by transcriptional interplay in cis and trans [Article]. *Proceedings of the National Academy of Sciences of the United States of America*, *116*(1), 313-318.https://doi.org/10.1073/pnas.1808400115

Meyer, J. R., Shew, H. D., & Harrison, U. J. (1994). Inhibition of germination and growth of Thielaviopsis basicola by aluminum. *Phytopathology*, *84*(6), 598-602.

Meyer, S., Cerovic, Z. G., Goulas, Y., Montpied, P., Demotes-Mainard, S., Bidel, L. P. R., Moya, I., & Dreyer, E. (2006). Relationships between optically assessed polyphenols and chlorophyll contents, and leaf mass per area ratio in woody plants: a signature of the carbon–nitrogen balance within leaves? *Plant, Cell & Environment*, *29*(7), 1338-1348.https://doi.org/10.1111/j.1365-3040.2006.01514.x

Michelet, L., Zaffagnini, M., Morisse, S., Sparla, F., Pérez-Pérez, M. E., Francia, F., Danon, A., Marchand, C. H., Fermani, S., & Trost, P. (2013). Redox regulation of the Calvin–Benson cycle: something old, something new. *Frontiers in plant science*, *4*, 470.https://doi.org/10.3389/fpls.2013.00470.

Mishra, P., & Dubey, R. S. (2008). Effect of aluminium on metabolism of starch and sugars in growing rice seedlings. *Acta Physiologiae Plantarum*, *30*(3), 265-275.https://doi.org/10.1007/s11738-007-0115-5.

Mittler, R., Vanderauwera, S., Suzuki, N., Miller, G. A. D., Tognetti, V. B., Vandepoele, K., Gollery, M., Shulaev, V., & Van Breusegem, F. (2011). ROS signaling: the new wave? *Trends in Plant Science*, *16*(6), 300-309.

Miyoshi, K., & Sato, T. (1997). The Effects of Ethanol on the Germination of Seeds of Japonica and Indica Rice (Oryza sativaL.) under Anaerobic and Aerobic Conditions. *Annals of botany*, *79*(4), 391-395.https://doi.org/10.1006/anbo.1996.0364

Mmojieje, J. (2016). Pyroligneous Acid: A Farmer's Flexible Friend? *Journal of Crop Improvement*, *30*(3), 341-351.https://doi.org/10.1080/15427528.2016.1160462

Mmojieje, J., & Hornung, A. (2015). The potential application of pyroligneous acid in the UK agricultural industry. *Journal of Crop Improvement*, *29*(2), 228-246.https://doi.org/10.1080/15427528.2014.995328

Mockaitis, K., & Estelle, M. (2008). Auxin receptors and plant development: a new signaling paradigm. *Annual Review of Cell and Developmental Biology*, *24*.https://doi.org/10.1146/annurev.cellbio.23.090506.123214

Mohan, D., Pittman, C. U., Jr., & Steele, P. H. (2006). Pyrolysis of Wood/Biomass for Bio-oil: A Critical Review. *Energy & Fuels*, *20*(3), 848-889.https://doi.org/10.1021/ef0502397

Mohd Amnan, M. A., Teo, W. F., Aizat, W. M., Khaidizar, F. D., & Tan, B. C. (2023). Foliar Application of Oil Palm Wood Vinegar Enhances Pandanus amaryllifolius Tolerance under Drought Stress. *Plants*, *12*(4).

Moreno-Alvarado, M., García-Morales, S., Trejo-Téllez, L. I., Hidalgo-Contreras, J. V., & Gómez-Merino, F. C. (2017). Aluminum Enhances Growth and Sugar Concentration, Alters Macronutrient Status and Regulates the Expression of NAC Transcription Factors in Rice [Original Research]. *Frontiers in Plant Science*, *8*.https://doi.org/10.3389/fpls.2017.00073

Morgan, S. H., Lindberg, S., & Muhling, K. H. (2013). Calcium supply effects on wheat cultivars differing in salt resistance with special reference to leaf cytosol ion homeostasis. *Physiologia plantarum*, *149*(3), 321-328.https://doi.org/10.1111/ppl.12036

Morita, A., Yanagisawa, O., Maeda, S., Takatsu, S., & Ikka, T. (2011). Tea plant (Camellia sinensis L.) roots secrete oxalic acid and caffeine into medium containing aluminum. *Soil Science and Plant Nutrition*, *57*(6), 796-802.https://doi.org/10.1080/00380768.2011.629176

Moriyama, U., Tomioka, R., Kojima, M., Sakakibara, H., & Takenaka, C. (2016). Aluminum effect on starch, soluble sugar, and phytohormone in roots of Quercus serrata Thunb. seedlings. *Trees*, *30*(2), 405-413.https://doi.org/10.1007/s00468-015-1252-x

Mourant, D., Yang, D.-Q., Lu, X., & Roy, C. (2007). Anti-fungal properties of the pyroligneous liquors from the pyrolysis of softwood bark. *Wood and Fiber Science*, *37*(3), 542-548.

Moustaka, J., Ouzounidou, G., Bayçu, G., & Moustakas, M. (2016). Aluminum resistance in wheat involves maintenance of leaf Ca2+ and Mg2+ content, decreased lipid peroxidation and Al accumulation, and low photosystem II excitation pressure. *Biometals*, *29*(4), 611-623.https://doi.org/10.1007/s10534-016-9938-0

Mu, J., Uehara, T., & Furuno, T. (2003). Effect of bamboo vinegar on regulation of germination and radicle growth of seed plants. *Journal of wood science*, *49*(3), 262-270.https://doi.org/10.1007/s10086-002-0472-z

Mu, J., Uehara, T., & Furuno, T. (2004). Effect of bamboo vinegar on regulation of germination and radicle growth of seed plants II: composition of moso bamboo vinegar at different collection temperature and its effects. *Journal of wood science*, *50*(5), 470-476.https://doi.org/10.1007/s10086-003-0586-y

Mu, J., Yu, Z.-m., Wu, W.-q., & Wu, Q.-l. (2006). Preliminary study of application effect of bamboo vinegar on vegetable growth. *Forestry Studies in China*, *8*(3), 43-47.https://doi.org/10.1007/s11632-006-0023-6

Muhammad, N., Cai, S., Shah, J. M., & Zhang, G. (2016). The combined treatment of Mn and Al alleviates the toxicity of Al or Mn stress alone in barley. *Acta Physiologiae Plantarum*, *38*(12), 1-7.https://doi.org/10.1007/s11738-016-2296-2

Muhammad, N., Zvobgo, G., & Zhang, G.-p. (2019). A review: The beneficial effects and possible mechanisms of aluminum on plant growth in acidic soil. *Journal of Integrative Agriculture*, *18*(7), 1518-1528.https://doi.org/10.1016/S2095-3119(18)61991-4.

Mun, S.-P., Ku, C.-S., & Park, S.-B. (2007). Physicochemical Characterization of pyrolyzates produced from carbonization of lignocellulosic biomass in a batch-type mechanical kiln. *Journal of Industrial and Engineering Chemistry*, *13*(1), 127-132.

Mungkunkamchao, T., Kesmala, T., Pimratch, S., Toomsan, B., & Jothityangkoon, D. (2013). Wood vinegar and fermented bioextracts: Natural products to enhance growth and yield of tomato (Solanum lycopersicum L.). *Scientia Horticulturae*, *154*, 66-72.https://doi.org/10.1016/j.scienta.2013.02.020

Nagayama, T., Nakamura, A., Yamaji, N., Satoh, S., Furukawa, J., & Iwai, H. (2019). Changes in the distribution of pectin in root border cells under aluminum stress. *Frontiers in plant science*, *10*, 1216.https://doi.org/10.3389/fpls.2019.01216

Najafi-Ghiri, M., Mirsoleimani, A., Boostani, H. R., & Amin, H. (2022). Influence of wood vinegar and potassium application on soil properties and Ca/K ratio in citrus rootstocks. *Journal of Soil Science and Plant Nutrition*, *22*, 1-11.https://doi.org/10.1007/s42729-021-00653-3

Nakano, Y., & Asada, K. (1981). Hydrogen peroxide is scavenged by ascorbate-specific peroxidase in spinach chloroplasts. *Plant and Cell Physiology*, *22*(5), 867-880.https://doi.org/10.1093/oxfordjournals.pcp.a076232

Negishi, T., Oshima, K., Hattori, M., Kanai, M., Mano, S., Nishimura, M., & Yoshida, K. (2012). Tonoplast- and Plasma Membrane-Localized Aquaporin-Family Transporters in Blue Hydrangea Sepals of Aluminum Hyperaccumulating Plant. *PloS One*, *7*(8), e43189.https://doi.org/10.1371/journal.pone.0043189

Nelson, D. C., Flematti, G. R., Ghisalberti, E. L., Dixon, K. W., & Smith, S. M. (2012). Regulation of seed germination and seedling growth by chemical signals from burning vegetation. *Annu. Rev. Plant Biol.*, *63*, 107-130.https://doi.org/10.1146/annurev-arplant-042811-105545

Nezames, C. D., Sjogren, C. A., Barajas, J. F., & Larsen, P. B. (2012). The *Arabidopsis* cell cycle checkpoint regulators TANMEI/ALT2 and ATR mediate the active process of aluminum-dependent root growth inhibition. *The Plant Cell*, *24*(2), 608-621.https://doi.org/10.1105/tpc.112.095596

Nhan, P. P., & Hai, N. T. (2013). Amelioration of aluminum toxicity on OM4900 rice seedlings by sodium silicate. *African Journal of Plant Science*, *7*(6), 208-212.https://doi.org/10.5897/AJPS11.306

Niedziela, A., Domżalska, L., Dynkowska, W. M., Pernisová, M., & Rybka, K. (2022). Aluminum Stress Induces Irreversible Proteomic Changes in the Roots of the Sensitive but Not the Tolerant Genotype of Triticale Seedlings. *Plants (Basel)*, *11*(2).https://doi.org/10.3390/plants11020165.

Njobvu, J., Hamabwe, S. M., Munyinda, K., Kelly, J. D., & Kamfwa, K. (2020). Quantitative trait loci mapping of resistance to aluminum toxicity in common bean. *Crop Science*, *60*(3), 1294-1302.https://doi.org/10.1002/csc2.20043

Nowak, D., Gośliński, M., Wojtowicz, E., & Przygoński, K. (2018). Antioxidant properties and phenolic compounds of vitamin C-rich juices. *Journal of Food Science*, *83*(8), 2237-2246.https://doi.org/10.1111/1750-3841.14284

OECD. (2017). Tomato (Solanum lycopersicum). In *Safety Assessment of Transgenic Organisms in the Environment* (Vol. 7). OECD Publishing.

Ofoe, R., Gunupuru, L. R., & Abbey, L. (2022a). Metabolites, elemental profile and chemical activities of Pinus strobus high temperature-derived pyroligneous acid. *Chemical and Biological Technologies in Agriculture*, *9*(1), 1-13.https://doi.org/10.1186/s40538-022-00357-5.

Ofoe, R., Gunupuru, L. R., Wang-Pruski, G., Fofana, B., Thomas, R. H., & Abbey, L. (2022b). Seed priming with pyroligneous acid mitigates aluminum stress, and promotes tomato seed germination and seedling growth. *Plant Stress*, *4*, 100083.https://doi.org/10.1016/j.stress.2022.100083.

Ofoe, R., Qin, D., Gunupuru, L. R., Thomas, R. H., & Abbey, L. (2022c). Effect of Pyroligneous Acid on the Productivity and Nutritional Quality of Greenhouse Tomato. *Plants*, *11*(13), 1650.https://doi.org/10.3390/plants11131650.

Ofoe, R., Thomas, R. H., Asiedu, S. K., Wang-Pruski, G., Fofana, B., & Abbey, L. (2023). Aluminum in plant: Benefits, toxicity and tolerance mechanisms [Review]. *Frontiers in plant science*, *13*.https://doi.org/10.3389/fpls.2022.1085998.

Okamoto, K., & Yano, K. (2017). Al resistance and mechanical impedance to roots in Zea mays: Reduced Al toxicity via enhanced mucilage production. *Rhizosphere*, *3*, 60-66.https://doi.org/10.1016/j.rhisph.2016.12.005

Onoda, A., Asanoma, M., & Nukaya, H. (2016). Identification of methylglyoxal as a major mutagen in wood and bamboo pyroligneous acids. *Bioscience, biotechnology, and biochemistry*, *80*(5), 833-839.https://doi.org/10.1080/09168451.2015.1136880

Oramahi, H. A., & Yoshimura, T. (2013). Antifungal and antitermitic activities of wood vinegar from Vitex pubescens Vahl. *Journal of wood science*, *59*(4), 344-350.https://doi.org/10.1007/s10086-013-1340-8

Pan, G., Li, L., Liu, X., Cheng, K., Bian, R., Ji, C., Zheng, J., Zhang, X., & Zheng, J. (2015). Industrialization of biochar from biomass pyrolysis: a new option for straw burning ban and green agriculture of China. *Sci. Technol. Rev.*, *33*(13), 92-101.https://www.doi.org/10.3981/j.issn.1000-7857.2015.13.015

Pandey, P., Srivastava, R. K., Rajpoot, R., Rani, A., Pandey, A. K., & Dubey, R. S. (2016). Water deficit and aluminum interactive effects on generation of reactive oxygen species and responses of antioxidative enzymes in the seedlings of two rice cultivars differing in stress tolerance. *Environmental Science and Pollution Research*, *23*(2), 1516-1528.https://doi.org/10.1007/S11356-015-5392-8.

Panter, R. A., & Mudd, J. B. (1969). Carnitine levels in some higherplants. *Febs letters*, *5*, 169-170.https://doi.org/10.1016/0014-5793(69)80322-4

Pareek, A., Dhankher, O. P., & Foyer, C. H. (2020). Mitigating the impact of climate change on plant productivity and ecosystem sustainability. *Journal of Experimental Botany*, *71*(2), 451-456.https://doi.org/10.1093/jxb/erz518.

Park, W., Kim, H.-S., Park, T.-W., Lee, Y.-H., & Ahn, S.-J. (2017). Functional characterization of plasma membrane-localized organic acid transporter (CsALMT1) involved in aluminum tolerance in Camelina sativa L. *Plant Biotechnology Reports*, *11*(3), 181-192.https://doi.org/10.1007/s11816-017-0441-z

Parth, V., Murthy, N. N., & Saxena, P. R. (2011). Assessment of heavy metal contamination in soil around hazardous waste disposal sites in Hyderabad city (India): natural and anthropogenic implications. *Journal of Environmental Research and Management*, *2*(2), 027-034.

Paul, S., & Roychoudhury, A. (2017). Seed priming with spermine and spermidine regulates the expression of diverse groups of abiotic stress-responsive genes during salinity stress in the seedlings of indica rice varieties. *Plant Gene*, *11*, 124-132.https://doi.org/10.1016/j.plgene.2017.04.004

Pavlů, L., Borůvka, L., Drábek, O., & Nikodem, A. (2021). Effect of natural and anthropogenic acidification on aluminium distribution in forest soils of two regions in the Czech Republic. *Journal of Forestry Research*, *32*(1), 363-370.https://doi.org/10.1007/s11676-019-01061-1

Pecha, M. B., & Garcia-Perez, M. (2020). Pyrolysis of lignocellulosic biomass: oil, char, and gas. In A. Dahiya (Ed.), *Bioenergy (Second Edition)* (pp. 581-619). Academic Press. https://doi.org/https://doi.org/10.1016/B978-0-12-815497-7.00029-4

Pedrero, F., Allende, A., Gil, M. I., & Alarcón, J. J. (2012). Soil chemical properties, leaf mineral status and crop production in a lemon tree orchard irrigated with two types of wastewater. *Agricultural Water Management*, *109*, 54-60.https://doi.org/10.1016/j.agwat.2012.02.006

Peixoto, H. P., Da Matta, F. M., & Da Matta, J. C. (2002). Responses of the photosynthetic apparatus to aluminum stress in two sorghum cultivars. *Journal of Plant Nutrition*(4), 821-832.https://doi.org/10.1081/PLN-120002962.

Peralta, I. E., Knapp, S., & Spooner, D. M. (2005). New species of wild tomatoes (Solanum section Lycopersicon: Solanaceae) from Northern Peru. *Systematic Botany*, *30*(2), 424-434.https://doi.org/10.1600/0363644054223657

Pereira, E. G., Fauller, H., Magalhaes, M., Guirardi, B., & Martins, M. A. (2022). Potential use of wood pyrolysis coproducts: A review. *Environmental Progress & Sustainable Energy*, *41*(1), e13705.https://doi.org/10.1002/ep.13705

Pereira, E. G., Martins, M. A., Pecenka, R., & Angélica de Cássia, O. C. (2017). Pyrolysis gases burners: Sustainability for integrated production of charcoal, heat and electricity. *Renewable and Sustainable Energy Reviews*, *75*, 592-600.https://doi.org/10.1016/j.rser.2016.11.028

Pereira, W. E., de Siqueira, D. L., Martínez, C. A., & Puiatti, M. (2000). Gas exchange and chlorophyll fluorescence in four citrus rootstocks under aluminium stress. *Journal of Plant Physiology*, *157*(5), 513-520.https://doi.org/10.1016/S0176-1617(00)80106-6.

Pérez-Díaz, R., Ryngajllo, M., Pérez-Díaz, J., Peña-Cortés, H., Casaretto, J. A., González-Villanueva, E., & Ruiz-Lara, S. (2014). VvMATE1 and VvMATE2 encode putative proanthocyanidin transporters expressed during berry development in Vitis vinifera L. *Plant Cell Reports*, *33*(7), 1147-1159.https://doi.org/10.1007/s00299-014-1604-9

Phukunkamkaew, S., Tisarum, R., Pipatsitee, P., Samphumphuang, T., Maksup, S., & Cha-um, S. (2021). Morpho-physiological responses of indica rice (Oryza sativa sub. indica) to aluminum toxicity at seedling stage. *Environmental Science and Pollution Research*, *28*(23), 29321-29331.https://doi.org/10.1007/s11356-021-12804-1

Piispanen, R., & Saranpaa, P. (2002). Neutral lipids and phospholipids in Scots pine (Pinus sylvestris) sapwood and heartwood. *Tree Physiology*, *22*(9), 661-666.https://doi.org/10.1093/treephys/22.9.661

Pimenta, A. S., Fasciotti, M., Monteiro, T. V., & Lima, K. M. (2018). Chemical composition of pyroligneous acid obtained from Eucalyptus GG100 clone. *Molecules*, *23*(2), 426.https://doi.org/10.3390/molecules23020426

Pinto, V. B., Almeida, V. C., Pereira-Lima, Í. A., Vale, E. M., Araújo, W. L., Silveira, V., & Viana, J. M. S. (2021). Deciphering the major metabolic pathways associated with aluminum tolerance in popcorn roots using label-free quantitative proteomics. *Planta*, *254*, 1-14.https://doi.org/10.1007/s00425-021-03786-y.

Pirzadah, T. B., Malik, B., Tahir, I., Ul Rehman, R., Hakeem, K. R., & Alharby, H. F. (2019). Aluminium stress modulates the osmolytes and enzyme defense system in Fagopyrum species [Article]. *Plant Physiology and Biochemistry*, *144*, 178-186.https://doi.org/10.1016/j.plaphy.2019.09.033

Pollard, A. J., Reeves, R. D., & Baker, A. J. M. (2014). Facultative hyperaccumulation of heavy metals and metalloids. *Plant Science*, *217*, 8-17.https://doi.org/10.1016/j.plantsci.2013.11.011

Polthanee, A., Kumla, N., & Simma, B. (2015). Effect of Pistia stratiotes, cattle manure and wood vinegar (pyroligneous acid) application on growth and yield of organic rainfed rice. *Paddy Water Environment*, *13*(4), 337-342.https://doi.org/10.1007/s10333-014-0453-z

Poschenrieder, C., Tolra, R., Hajiboland, R., Arroyave, C., & Barceló, J. (2015). Mechanisms of hyper-resistance and hyper-tolerance to aluminum in plants. In S. Panda, Baluška, F. (Ed.), *Aluminum stress adaptation in plants* (Vol. 24, pp. 81-98). Springer, Cham. https://doi.org/https://doi.org/10.1007/978-3-319-19968-9_5

Potter, D. A., Powell, A. J., Spicer, P. G., & Williams, D. W. (1996). Cultural Practices Affect Root-Feeding White Grubs (Coleoptera: Scarabaeidae) in Turfgrass. *Journal of Economic Entomology*, *89*(1), 156-164.https://doi.org/10.1093/jee/89.1.156

Pretty, J., & Bharucha, Z. P. (2014). Sustainable intensification in agricultural systems. *Annals of botany*, *114*(8), 1571-1596.https://doi.org/10.1093/aob/mcu205

Pütün, A. E., Özbay, N., Önal, E. P., & Pütün, E. (2005). Fixed-bed pyrolysis of cotton stalk for liquid and solid products. *Fuel Processing Technology*, *86*(11), 1207-1219.https://doi.org/10.1016/j.fuproc.2004.12.006

Quezada, E.-H., Arthikala, M.-K., & Nanjareddy, K. (2022). Cytoskeleton in abiotic stress signaling. In G. Santoyo, A. Kumar, M. Aamir, & S. Uthandi (Eds.), *Mitigation of Plant Abiotic Stress by Microorganisms* (pp. 347-371). Academic Press. https://doi.org/https://doi.org/10.1016/B978-0-323-90568-8.00016-X

Quinet, M., Angosto, T., Yuste-Lisbona, F. J., Blanchard-Gros, R., Bigot, S., Martinez, J.-P., & Lutts, S. (2019). Tomato fruit development and metabolism. *Frontiers in plant science*, *10*, 1554.https://doi.org/10.3389/fpls.2019.01554

Ranal, M. A., Santana, D. G. d., Ferreira, W. R., & Mendes-Rodrigues, C. (2009). Calculating germination measurements and organizing spreadsheets. *Brazilian Journal of Botany*, *32*(4), 849-855.https://doi.org/10.1590/S0100-84042009000400022

Rehmus, A., Bigalke, M., Valarezo, C., Castillo, J. M., & Wilcke, W. (2014). Aluminum toxicity to tropical montane forest tree seedlings in southern Ecuador: response of biomass and plant morphology to elevated Al concentrations. *Plant and Soil*, *382*(1), 301-315.https://doi.org/10.1007/s11104-014-2110-0

Ren, Z., Liu, R., Gu, W., & Dong, X. (2017). The Solanum lycopersicum auxin response factor SlARF2 participates in regulating lateral root formation and flower organ senescence. *Plant Science*, *256*, 103-111.https://doi.org/10.1016/j.plantsci.2016.12.008

Reyna-Llorens, I., Corrales, I., Poschenrieder, C., Barcelo, J., & Cruz-Ortega, R. (2015). Both aluminum and ABA induce the expression of an ABC-like transporter gene (FeALS3) in the Al-tolerant species Fagopyrum esculentum. *Environmental and Experimental Botany*, *111*, 74-82.https://doi.org/10.1016/j.envexpbot.2014.11.005

Riaz, M., Yan, L., Wu, X. W., Hussain, S., Aziz, O., El-Desouki, Z., & Jiang, C. C. (2019). Excess boron inhibited the trifoliate orange growth by inducing oxidative stress, alterations in cell wall structure, and accumulation of free boron [Article]. *Plant Physiology and Biochemistry*, *141*, 105-113.https://doi.org/10.1016/j.plaphy.2019.05.021

Ribeiro, C., de Marcos Lapaz, A., de Freitas-Silva, L., Ribeiro, K. V. G., Yoshida, C. H. P., Dal-Bianco, M., & Cambraia, J. (2022). Aluminum promotes changes in rice root structure and ascorbate and glutathione metabolism. *Physiology and Molecular Biology of Plants*.https://doi.org/10.1007/s12298-022-01262-9

Ribeiro, M. A. Q., Almeida, A.-A. F. d., Mielke, M. S., Gomes, F. P., Pires, M. V., & Baligar, V. C. (2013). Aluminum effects on Growth, Photosynthesis, and Mineral Nutrition of Cacao Genotypes. *Journal of Plant Nutrition*, *36*(8), 1161-1179.https://doi.org/10.1080/01904167.2013.766889

Rodrigues, M., Baptistella, J. L. C., Horz, D. C., Bortolato, L. M., & Mazzafera, P. (2020). Organic plant biostimulants and fruit quality—A review. *Agronomy*, *10*(7), 988.https://doi.org/10.3390/agronomy10070988

Rouina, B., Sensoy, S., & Boukhriss, M. (2009). Saline water irrigation effects on fruit development, quality, and phenolic composition of virgin olive oils, cv. Chemlali. *Journal of agricultural and food chemistry*, *57*(7), 2803-2811.https://doi.org/10.1021/jf8034379

Rui, Z., Wei, D., Zhibin, Y., Chao, Z., & Xiaojuan, A. (2014). Effects of wood vinegar on the soil microbial characteristics. *Journal of Chemical and Pharmaceutical Research*, *6*(3), 1254-1260.

Sade, H., Meriga, B., Surapu, V., Gadi, J., Sunita, M. S. L., Suravajhala, P., & Kavi Kishor, P. B. (2016). Toxicity and tolerance of aluminum in plants: tailoring plants to suit to acid soils. *BioMetals 2016 29:2*, *29*(2), 187-210.https://doi.org/10.1007/S10534-016-9910-Z

Salazar-Chavarria, V., Sanchez-Nieto, S., & Cruz-Ortega, R. (2020). Fagopyrum esculentum at early stages copes with aluminum toxicity by increasing ABA levels and antioxidant system [Article]. *Plant Physiology and Biochemistry*, *152*, 170-176.https://doi.org/10.1016/j.plaphy.2020.04.024

Salehi, M. R., Ashiri, F., & Salehi, H. (2008). Effect of different ethanol concentrations on seed germination of three turfgrass genera. *Advances in Natural and Applied Sciences*, *2*(1), 6-9.

Sami, A., Shah, F. A., Abdullah, M., Zhou, X., Yan, Y., Zhu, Z., & Zhou, K. (2020). Melatonin mitigates cadmium and aluminium toxicity through modulation of antioxidant potential in Brassica napus L [https://doi.org/10.1111/plb.13093]. *Plant Biology*, *22*(4), 679-690.https://doi.org/10.1111/plb.13093

Santos, E., Benito, C., Silva-Navas, J., Gallego, F. J., Figueiras, A. M., Pinto-Carnide, O., & Matos, M. (2018). Characterization, genetic diversity, phylogenetic relationships, and expression of the aluminum tolerance MATE1 gene in Secale species [Article]. *Biologia Plantarum*, *62*(1), 109-120.https://doi.org/10.1007/s10535-017-0749-0

Sasaki, T., Tsuchiya, Y., Ariyoshi, M., Nakano, R., Ushijima, K., Kubo, Y., Mori, I. C., Higashiizumi, E., Galis, I., & Yamamoto, Y. (2016). Two Members of the Aluminum-Activated Malate Transporter Family, SlALMT4 and SlALMT5, are Expressed during Fruit Development, and the Overexpression of SlALMT5 Alters Organic Acid Contents in Seeds in Tomato (*Solanum lycopersicum*). *Plant and Cell Physiology*, *57*(11), 2367-2379.https://doi.org/10.1093/pcp/pcw157

Sasaki, T., Yamamoto, Y., Ezaki, B., Katsuhara, M., Ahn, S. J., Ryan, P. R., Delhaize, E., & Matsumoto, H. (2004). A wheat gene encoding an aluminum-activated malate transporter. *The Plant Journal*, *37*(5), 645-653.https://doi.org/10.1111/j.1365-313x.2003.01991.x.

Sato, S., Tabata, S., Hirakawa, H., Asamizu, E., Shirasawa, K., Isobe, S., Kaneko, T., Nakamura, Y., Shibata, D., & Aoki, K. (2012). The tomato genome sequence provides insights into fleshy fruit evolution. *Nature*, *485*(7400), 635-641.https://doi.org/10.1038/nature11119

Sawaki, Y., Iuchi, S., Kobayashi, Y., Kobayashi, Y., Ikka, T., Sakurai, N., Fujita, M., Shinozaki, K., Shibata, D., & Kobayashi, M. (2009). STOP1 regulates multiple genes that protect *Arabidopsis* from proton and aluminum toxicities. *Plant physiology*, *150*(1), 281-294.https://doi.org/10.1104/pp.108.134700

Sawaki, Y., Kihara-Doi, T., Kobayashi, Y., Nishikubo, N., Kawazu, T., Kobayashi, Y., Koyama, H., & Sato, S. (2013). Characterization of Al-responsive citrate excretion and citrate-transporting MATEs in Eucalyptus camaldulensis. *Planta*, *237*(4), 979-989.https://doi.org/10.1007/s00425-012-1810-z

Schmitt, M., Watanabe, T., & Jansen, S. (2016). The effects of aluminium on plant growth in a temperate and deciduous aluminium accumulating species. *AoB Plants*, *8*.https://doi.org/10.1093/AOBPLA/PLW065

Schroeder, J. I., Delhaize, E., Frommer, W. B., Guerinot, M. L., Harrison, M. J., Herrera-Estrella, L., Horie, T., Kochian, L. V., Munns, R., & Nishizawa, N. K. (2013). Using membrane transporters to improve crops for sustainable food production. *Nature*, *497*(7447), 60-66.https://doi.org/10.1038/nature11909

Setiawati, E., Annisa, W., Soedarmanto, H., & Iskandar, T. (2019). Characterization of neutralized wood vinegar derived from durian wood (Durio zibethinus) and its prospect as pesticide in acidic soil.*IOP Conference Series:* Earth and Environmental Science,

Shan, X., Liu, X., & Zhang, Q. (2018, 2018). Impacts of adding different components of wood vinegar on rape (*Brassica napus L.*) seed germiantion.*IOP Conference Series* IOP Conference Series: Earth and Environmental Science,

Sharma, A., Kapoor, D., Gautam, S., Landi, M., Kandhol, N., Araniti, F., Ramakrishnan, M., Satish, L., Singh, V. P., & Sharma, P. (2022). Heavy metal induced regulation of plant biology: Recent insights. *Physiologia plantarum*, *174*(3), e13688.https://doi.org/10.1111/ppl.13688.

Sharma, P., Jha, A. B., Dubey, R. S., & Pessarakli, M. (2012). Reactive Oxygen Species, Oxidative Damage, and Antioxidative Defense Mechanism in Plants under Stressful Conditions. *Journal of botany*, *2012*, 217037.https://doi.org/10.1155/2012/217037

Sharma, S., Joshi, J., Kataria, S., Verma, S. K., Chatterjee, S., Jain, M., Pathak, K., Rastogi, A., & Brestic, M. (2020). Regulation of the Calvin cycle under abiotic stresses: An overview. *Plant life under changing environment*, 681-717.https://doi.org/10.1016/B978-0-12-818204-8.00030-8.

Sharma, T., Dreyer, I., Kochian, L., & Piñeros, M. A. (2016). The ALMT family of organic acid transporters in plants and their involvement in detoxification and nutrient security. *Frontiers in plant science*, *7*, 1488.https://doi.org/10.3389/fpls.2016.01488

Shavrukov, Y., & Hirai, Y. (2016). Good and bad protons: genetic aspects of acidity stress responses in plants. *Journal of Experimental Botany*, *67*(1), 15-30.https://doi.org/10.1093/jxb/erv437

Shen, R., Zhao, L., Yao, Z., Feng, J., Jing, Y., & Watson, J. (2020). Efficient treatment of wood vinegar via microbial electrolysis cell with the anode of different pyrolysis biochars. *Frontiers in Energy Research*, *8*, 216.https://doi.org/10.3389/fenrg.2020.00216

Shen, X., Xiao, X., Dong, Z., & Chen, Y. (2014). Silicon effects on antioxidative enzymes and lipid peroxidation in leaves and roots of peanut under aluminum stress. *Acta Physiologiae Plantarum*, *36*(11), 3063-3069.https://doi.org/10.1007/s11738-014-1676-8

Shuang, S. U. N., Zi-Ting, G. A. O., Zhan-Chao, L. I., Yue, L. I., Jun-Li, G. A. O., Yuan-Jun, C., Hao, L. I., Xing-Yu, L. I. U., & Zi-Ming, W. (2020). Effect of wood vinegar on adsorption and desorption of four kinds of heavy (loid) metals adsorbents. *Chinese Journal of Analytical Chemistry*, *48*(2), e20013-e20020.https://doi.org/10.1016/S1872-2040(19)61217-X

Silva-Navas, J., Salvador, N., del Pozo, J. C., Benito, C., & Gallego, F. J. (2021). The rye transcription factor ScSTOP1 regulates the tolerance to aluminum by activating the ALMT1 transporter [Article]. *Plant Science*, *310*, 10, Article 110951.https://doi.org/10.1016/j.plantsci.2021.110951

Silva, C. M. S., Zhang, C. Y., Habermann, G., Delhaize, E., & Ryan, P. R. (2018). Does the major aluminium-resistance gene in wheat, TaALMT1, also confer tolerance to alkaline soils? [Article]. *Plant and Soil*, *424*(1-2), 451-462.https://doi.org/10.1007/s11104-017-3549-6

Silva, P., & Matos, M. (2016). Assessment of the impact of Aluminum on germination, early growth and free proline content in Lactuca sativa L. *Ecotoxicology and Environmental Safety*, *131*, 151-156.https://doi.org/10.1016/j.ecoenv.2016.05.014

Silva, S., Pinto, G., Correia, B., Pinto-Carnide, O., & Santos, C. (2013). Rye oxidative stress under long term Al exposure. *Journal of Plant Physiology*, *170*(10), 879-889.https://doi.org/10.1016/j.jplph.2013.01.015

Silva, S., Pinto, G., Dias, M. C., Correia, C. M., Moutinho-Pereira, J., Pinto-Carnide, O., & Santos, C. (2012). Aluminium long-term stress differently affects photosynthesis in rye genotypes. *Plant Physiology and Biochemistry*, *54*, 105-112.https://doi.org/10.1016/j.plaphy.2012.02.004

Silva, T. F., Ferreira, B. G., Isaias, R. M. D., Alexandre, S. S., & Franca, M. G. C. (2020). Immunocytochemistry and Density Functional Theory evidence the competition of aluminum and calcium for pectin binding in Urochloa decumbens roots [Article]. *Plant Physiology and Biochemistry*, *153*, 64-71.https://doi.org/10.1016/j.plaphy.2020.05.015

Simon, L., Kieger, M., Sung, S. S., & Smalley, T. J. (1994). Aluminum toxicity in tomato. Part 2. Leaf gas exchange, chlorophyll content, and invertase activity. *Journal of Plant Nutrition*, *17*(2-3), 307-317.https://doi.org/10.1080/01904169409364729.

Sims, W. L. (1980). History of tomato production for industry around the world. *Acta Horticulturae*, *100*, 25-26.https://doi.org/10.17660/ActaHortic.1980.100.1

Singh, S., Tripathi, D. K., Singh, S., Sharma, S., Dubey, N. K., Chauhan, D. K., & Vaculik, M. (2017). Toxicity of aluminium on various levels of plant cells and organism: a review. *Environmental and Experimental Botany*, *137*, 177-193.https://doi.org/10.1016/j.envexpbot.2017.01.005

Siqueira, J. A., Barros, J. A. S., Dal-Bianco, M., Martins, S. C. V., Magalhães, P. C., Ribeiro, D. M., DaMatta, F. M., Araújo, W. L., & Ribeiro, C. (2020). Metabolic and physiological adjustments of maize leaves in response to aluminum stress. *Theoretical and Experimental Plant Physiology*, *32*(2), 133-145.https://doi.org/10.1007/s40626-020-00175-w.

Sivaguru, M., Liu, J., & Kochian, L. V. (2013). Targeted expression of Sb MATE in the root distal transition zone is responsible for sorghum aluminum resistance. *The Plant Journal*, *76*(2), 297-307.https://doi.org/10.1111/tpj.12290

Sjogren, C. A., Bolaris, S. C., & Larsen, P. B. (2015). Aluminum-dependent terminal differentiation of the *Arabidopsis* root tip is mediated through an ATR-, ALT2-, and SOG1-regulated transcriptional response. *The Plant Cell*, *27*(9), 2501.https://doi.org/10.1111/tpj.12290

Sjogren, C. A., & Larsen, P. B. (2017). SUV2, which encodes an ATR-related cell cycle checkpoint and putative plant ATRIP, is required for aluminium-dependent root growth inhibition in *Arabidopsis*. *Plant, Cell & Environment*, *40*(9), 1849-1860.https://doi.org/10.1111/pce.12992

Slessarev, E. W., Lin, Y., Bingham, N. L., Johnson, J. E., Dai, Y., Schimel, J. P., & Chadwick, O. A. (2016). Water balance creates a threshold in soil pH at the global scale. *Nature*, *540*(7634), 567-569.https://doi.org/10.1038/nature20139.

Sparg, S. G., Kulkarni, M. G., & Van Staden, J. (2006). Aerosol smoke and smoke-water stimulation of seedling vigor of a commercial maize cultivar. *Crop Science*, *46*(3), 1336-1340.https://doi.org/10.2135/cropsci2005.07-0324

Spivak, S. G., Kisel, M. A., & Yakovleva, G. A. (2003). Boosting the immune system of solanaceous plants by lysophosphatidylcholine. *Russian journal of plant physiology*, *50*(3), 293-296.https://doi.org/10.1023/A:1023801732305

Stefanidis, S. D., Kalogiannis, K. G., Iliopoulou, E. F., Michailof, C. M., Pilavachi, P. A., & Lappas, A. A. (2014). A study of lignocellulosic biomass pyrolysis via the pyrolysis of cellulose, hemicellulose and lignin. *Journal of Analytical and Applied Pyrolysis*, *105*, 143-150.https://doi.org/10.1016/j.jaap.2013.10.013

Steiner, C., Das, K. C., Garcia, M., Förster, B., & Zech, W. (2008). Charcoal and smoke extract stimulate the soil microbial community in a highly weathered xanthic Ferralsol. *Pedobiologia*, *51*(5-6), 359-366.https://doi.org/10.1016/j.pedobi.2007.08.002

Straits Research. (2023). *Wood vinegar market*. Retrieved 16/03 from https://straitsresearch.com/report/wood-vinegar-market

Su, C., Jiang, Y., Yang, Y., Zhang, W., & Xu, Q. (2019). Responses of duckweed (Lemna minor L.) to aluminum stress: Physiological and proteomics analyses. *Ecotoxicology and Environmental Safety*, *170*, 127-140.https://doi.org/10.1016/j.ecoenv.2018.11.113.

Sun, C. L., Lv, T., Huang, L., Liu, X. X., Jin, C. W., & Lin, X. Y. (2020a). Melatonin ameliorates aluminum toxicity through enhancing aluminum exclusion and reestablishing redox homeostasis in roots of wheat [Article]. *Journal of Pineal Research*, *68*(4), 11, Article e12642.https://doi.org/10.1111/jpi.12642

Sun, L. L., Zhang, M. S., Liu, X. M., Mao, Q. Z., Shi, C., Kochian, L. V., & Liao, H. (2020b). Aluminium is essential for root growth and development of tea plants (Camellia sinensis) [Article]. *Journal of Integrative Plant Biology*, *62*(7), 984-997.https://doi.org/10.1111/jipb.12942

Sun, M., Peng, F., Xiao, Y., Yu, W., Zhang, Y., & Gao, H. (2020c). Exogenous phosphatidylcholine treatment alleviates drought stress and maintains the integrity of root cell membranes in peach. *Scientia Horticulturae*, *259*, 108821.https://doi.org/10.1016/j.scienta.2019.108821

Surapu, V., Ediga, A., & Meriga, B. (2014). Salicylic acid alleviates aluminum toxicity in tomato seedlings (Lycopersicum esculentum Mill.) through activation of antioxidant defense system and proline biosynthesis. *Advances in Bioscience and Biotechnology*, *5*(9), 777-789.https://doi.org/10.4236/abb.2014.59091

Suresh, B. V., Roy, R., Sahu, K., Misra, G., & Chattopadhyay, D. (2014). Tomato genomic resources database: an integrated repository of useful tomato genomic information for basic and applied research. *PloS One*, *9*(1), e86387.https://doi.org/10.1371/journal.pone.0086387

Sweetlove, L. J., Beard, K. F. M., Nunes-Nesi, A., Fernie, A. R., & Ratcliffe, R. G. (2010). Not just a circle: flux modes in the plant TCA cycle. *Trends in Plant Science*, *15*(8), 462-470.https://doi.org/10.1016/j.tplants.2010.05.006.

Szurman-Zubrzycka, M., Nawrot, M., Jelonek, J., Dziekanowski, M., Kwasniewska, J., & Szarejko, I. (2019). ATR, a DNA Damage Signaling Kinase, Is Involved in Aluminum Response in Barley [Article]. *Frontiers in plant science*, *10*, 14, Article 1299.https://doi.org/10.3389/fpls.2019.01299

Tahara, K., Hashida, K., Otsuka, Y., Ohara, S., Kojima, K., & Shinohara, K. (2014). Identification of a hydrolyzable tannin, oenothein B, as an aluminum-detoxifying ligand in a highly aluminum-resistant tree, Eucalyptus camaldulensis. *Plant physiology*, *164*(2), 683-693.https://doi.org/10.1104/pp.113.222885

Takanashi, K., Sasaki, T., Kan, T., Saida, Y., Sugiyama, A., Yamamoto, Y., & Yazaki, K. (2016). A dicarboxylate transporter, LjALMT4, mainly expressed in nodules of Lotus japonicus. *Molecular Plant-Microbe Interactions*, *29*(7), 584-592.https://doi.org/10.1094/MPMI-04-16-0071-R

Tan, H., Lee, C. T., Ong, P. Y., Wong, K. Y., Bong, C. P. C., Li, C., & Gao, Y. (2021, 2021). A review on the comparison between slow pyrolysis and fast pyrolysis on the quality of lignocellulosic and lignin-based biochar.

Teng, W., Kang, Y., Hou, W., Hu, H., Luo, W., Wei, J., Wang, L., & Zhang, B. (2018). Phosphorus application reduces aluminum toxicity in two Eucalyptus clones by increasing its accumulation in roots and decreasing its content in leaves. *PloS One*, *13*(1), e0190900-e0190900.https://doi.org/10.1371/journal.pone.0190900

Theapparat, Y., Chandumpai, A., & Faroongsarng, D. (2018). Physicochemistry and utilization of wood vinegar from carbonization of tropical biomass waste. *Tropical Forests*, 163-183.https://doi.org/10.5772/intechopen.77380

Theapparat, Y., Chandumpai, A., Leelasuphakul, W., Laemsak, N., & Ponglimanont, C. (2014). Physicochemical characteristics of wood vinegars from carbonization of Leucaena leucocephala, Azadirachta indica, Eucalyptus camaldulensis, Hevea brasiliensis and Dendrocalamus asper. *Agriculture and Natural Resources*, *48*(6), 916-928.

Theerakulpisut, P., Kanawapee, N., & Panwong, B. (2016). Seed priming alleviated salt stress effects on rice seedlings by improving Na+/K+ and maintaining membrane integrity. *International Journal of Plant Biology*, *7*(1).https://doi.org/10.4081/pb.2016.6402

Tian, Q., Zhang, X., Ramesh, S., Gilliham, M., Tyerman, S. D., & Zhang, W.-H. (2014). Ethylene negatively regulates aluminium-induced malate efflux from wheat roots and tobacco cells transformed with TaALMT1. *Journal of Experimental Botany*, *65*(9), 2415-2426.https://doi.org/10.1093/jxb/eru123

Timm, S., & Arrivault, S. (2021). Regulation of Central Carbon and Amino Acid Metabolism in Plants. *Plants*, *10*, 430.https://doi.org/10.3390/plants10030430.

Tokizawa, M., Kobayashi, Y., Saito, T., Kobayashi, M., Iuchi, S., Nomoto, M., Tada, Y., Yamamoto, Y. Y., & Koyama, H. (2015). Sensitive to proton rhizotoxicity1, calmodulin binding transcription activator2, and other transcription factors are involved in aluminum-activated malate transporter1 expression. *Plant physiology*, *167*(3), 991-1003.https://doi.org/10.1104/pp.114.256552

Tolrà, R. P., Poschenrieder, C., Luppi, B., & Barceló, J. (2005). Aluminium-induced changes in the profiles of both organic acids and phenolic substances underlie Al tolerance in Rumex acetosa L. *Environmental and Experimental Botany*, *54*(3), 231-238.https://doi.org/10.1016/j.envexpbot.2004.07.006

Travero, J. T., & Mihara, M. (2016). Effects of Pyroligneous Acid to Growth and Yield of Soybeans (Glycine max). *International Journal of Environmental and Rural Development*, *7*(1), 50-54.https://doi.org/10.32115/ijerd.7.1_50

Tripathi, A. D., Mishra, R., Maurya, K. K., Singh, R. B., & Wilson, D. W. (2019). Estimates for world population and global food availability for global health. In *The role of functional food security in global health* (pp. 3-24). Elsevier. https://doi.org/https://doi.org/10.1016/B978-0-12-813148-0.00001-3

Tripathi, D. K., Singh, V. P., Chauhan, D. K., Prasad, S. M., & Dubey, N. K. (2014). Role of macronutrients in plant growth and acclimation: recent advances and future prospective. In P. Ahmad, Wani, M., Azooz, M., Phan Tran, LS (Ed.), *Improvement of crops in the era of climatic changes* (pp. 197-216). Springer. https://doi.org/https://doi.org/10.1007/978-1-4614-8824-8_8

Turk, H., Erdal, S., & Dumlupinar, R. (2020). Carnitine-induced physio-biochemical and molecular alterations in maize seedlings in response to cold stress. *Archives of Agronomy and Soil Science*, *66*(7), 925-941.https://doi.org/10.1080/03650340.2019.1647336

Turkan, I. (2018). ROS and RNS: key signalling molecules in plants. *Journal of Experimental Botany*, *69*(14), 3313-3315.https://doi.org/10.1093/jxb/ery198

Tuzet, A., Perrier, A., & Leuning, R. (2003). A coupled model of stomatal conductance, photosynthesis and transpiration. *Plant, Cell and Environment*, *26*(7), 1097-1116.https://doi.org/10.1046/j.1365-3040.2003.01035.x

Umehara, M., Hanada, A., Yoshida, S., Akiyama, K., Arite, T., Takeda-Kamiya, N., Magome, H., Kamiya, Y., Shirasu, K., & Yoneyama, K. (2008). Inhibition of shoot branching by new terpenoid plant hormones. *Nature*, *455*(7210), 195-200.https://doi.org/10.1038/nature07272

United Nations. (2019). World population projected to reach 9.8 billion in 2050, and 11.2 billion in 2100, United Nations Department of Economic and Social Affairs: New York. In.

Upadhyay, N., Kar, D., Mahajan, B. D., Nanda, S., Rahiman, R., Panchakshari, N., Bhagavatula, L., & Datta, S. (2019). The multitasking abilities of MATE transporters in plants [Review]. *Journal of Experimental Botany*, *70*(18), 4643-4656.https://doi.org/10.1093/jxb/erz246

Urban, J., Ingwers, M., McGuire, M. A., & Teskey, R. O. (2017). Stomatal conductance increases with rising temperature. *Plant Signal. Behav.*, *12*(8), e1356534.https://www.doi.org/10.1080/15592324.2017.1356534

Valadez-González, N., Colli-Mull, J. G., Brito-Argáez, L., Muñoz-Sánchez, J. A., Aguilar, J. J. Z., Castano, E., & Hernández-Sotomayor, S. M. T. (2007). Differential effect of aluminum on DNA synthesis and CDKA activity in two Coffea arabica cell lines. *Journal of Plant Growth Regulation*, *26*(1), 69-77.https://doi.org/10.1007/s00344-006-0039-0

Van Staden, J., Jäger, A., & Strydom, A. J. P. G. R. (1995). Interaction between a plant-derived smoke extract, light and phytohormones on the germination of light-sensitive lettuce seeds. *Plant Growth Regulation*, *17*(3), 213-218.https://doi.org/10.1007/BF00024728

Van Staden, J., Jager, A. K., Light, M. E., & Burger, B. V. (2004). Isolation of the major germination cue from plant-derived smoke. *South African Journal of Botany*, *70*(4), 654-659.https://doi.org/10.1016/S0254-6299(15)30206-4.

Van Staden, J., Sparg, S. G., Kulkarni, M. G., & Light, M. E. (2006). Post-germination effects of the smoke-derived compound 3-methyl-2H-furo [2, 3-c] pyran-2-one, and its potential as a preconditioning agent. *Field Crops Research*, *98*(2-3), 98-105.https://doi.org/10.1016/j.fcr.2005.12.007

Vannini, A., Moratelli, F., Monaci, F., & Loppi, S. (2021). Effects of wood distillate and soy lecithin on the photosynthetic performance and growth of lettuce (Lactuca sativa L.). *SN Applied Sciences*, *3*(1), 113.https://doi.org/10.1007/s42452-020-04028-8

Vardar, F., Çabuk, E., Aytürk, Ö., & Aydın, Y. (2016). Determination of aluminum induced programmed cell death characterized by DNA fragmentation in Gramineae species. *Caryologia*, *69*(2), 111-115.https://doi.org/10.1080/00087114.2015.1109954

Vehniwal, S. S., Ofoe, R., & Abbey, L. (2020). Concentration, Temperature and Storage duration Influence Chemical Stability of Compost Tea. *Sustainable Agriculture Research*, *9*(526-2021-483), 87-97.https://doi.org/10.5539/sar.v9n3p87

Velmurugan, N., Han, S. S., & Lee, Y. S. (2009). Antifungal activity of neutralized wood vinegar with water extracts of Pinus densiflora and Quercus serrata saw dusts. *International Journal of Environmental Research*, *3*(2), 167-176.https://doi.org/10.22059/IJER.2009.45

Verslues, P. E., & Sharma, S. (2010). Proline metabolism and its implications for plant-environment interaction. *The Arabidopsis Book/American Society of Plant Biologists*, *8*, e0140.https://doi.org/10.1199/tab.0140

Viehweger, K., Dordschbal, B., & Roos, W. (2002). Elicitor-activated phospholipase A2 generates lysophosphatidylcholines that mobilize the vacuolar H+ pool for pH signaling via the activation of Na+-dependent proton fluxes. *The Plant Cell*, *14*(7), 1509-1525.https://doi.org/10.1105/tpc.002329

Wang, H., Chen, L., Ma, X., Liu, X., Zhang, Y., Quan, X., Shan, J., & Zhao, W. (2019a). Effects of wood vinegar on cold resistance of rice seedlings under low-temperature stress. *Journal of Northeast Agricultural University*, *50*, 1-8.

Wang, H., Chen, R. F., Iwashita, T., Shen, R. F., & Ma, J. F. (2015a). Physiological characterization of aluminum tolerance and accumulation in tartary and wild buckwheat. *New Phytologist*, *205*(1), 273-279.https://doi.org/10.1111/nph.13011.

Wang, J., Potoroko, I., & Tsirulnichenko, L. (2021). Wood vinegar and chitosan compound preservative affects on fish balls stability. *Food Bioscience*, *42*, 101102.https://doi.org/10.1016/j.fbio.2021.101102

Wang, J., Yu, X., Ding, Z. J., Zhang, X., Luo, Y., Xu, X., Xie, Y., Li, X., Yuan, T., & Zheng, S. J. (2022). Structural basis of ALMT1-mediated aluminum resistance in *Arabidopsis*. *Cell Research*, *32*(1), 89-98.https://doi.org/10.1038/s41422-021-00587-6

Wang, L., Fan, X.-W., Pan, J.-L., Huang, Z.-B., & Li, Y.-Z. (2015b). Physiological characterization of maize tolerance to low dose of aluminum, highlighted by promoted leaf growth. *Planta*, *242*(6), 1391-1403.https://doi.org/10.1007/s00425-015-2376-3.

Wang, S., Ren, X., Huang, B., Wang, G., Zhou, P., & An, Y. (2016). Aluminium-induced reduction of plant growth in alfalfa (Medicago sativa) is mediated by interrupting auxin transport and accumulation in roots. *Scientific Reports*, *6*.https://doi.org/10.1038/srep30079

Wang, W., Zhao, X. Q., Chen, R. F., Dong, X. Y., Lan, P., Ma, J. F., & Shen, R. F. (2015c). Altered cell wall properties are responsible for ammonium-reduced aluminium accumulation in rice roots. *Plant, Cell and Environment*, *38*(7), 1382-1390.https://doi.org/10.1111/pce.12490

Wang, W., Zhao, X. Q., Hu, Z. M., Shao, J. F., Che, J., Chen, R. F., Dong, X. Y., & Shen, R. F. (2015d). Aluminium alleviates manganese toxicity to rice by decreasing root symplastic Mn uptake and reducing availability to shoots of Mn stored in roots. *Annals of botany*, *116*(2), 237-246.https://doi.org/10.1093/aob/mcv090

Wang, Y., Li, R., Li, D., Jia, X., Zhou, D., Li, J., Lyi, S. M., Hou, S., Huang, Y., Kochian, L. V., & Liu, J. (2017). NIP1;2 is a plasma membrane-localized transporter mediating aluminum uptake, translocation, and tolerance in *Arabidopsis*. *Proceedings of the National Academy of Sciences of the United States of America*, *114*(19), 5047-5052.https://doi.org/10.1073/pnas.1618557114

Wang, Y., Qiu, L., Song, Q., Wang, S., Wang, Y., & Ge, Y. (2019b). Root proteomics reveals the effects of wood vinegar on wheat growth and subsequent tolerance to drought stress. *International Journal of Molecular Sciences*, *20*(4), 943.https://doi.org/10.3390/ijms20040943.

Wang, Y. Q., Yu, W. C., Cao, Y., Cai, Y. F., Lyi, S. M., Wu, W. W., Kang, Y., Liang, C. Y., & Liu, J. P. (2020a). An exclusion mechanism is epistatic to an internal detoxification mechanism in aluminum resistance in *Arabidopsis* [Article]. *BMC Plant Biology*, *20*(1), 12, Article 122.https://doi.org/10.1186/s12870-020-02338-y

Wang, Z., Liu, L., Su, H., Guo, L., Zhang, J., Li, Y., Xu, J., Zhang, X., Guo, Y. D., & Zhang, N. (2020b). Jasmonate and aluminum crosstalk in tomato: Identification and expression analysis of WRKYs and ALMTs during JA/Al-regulated root growth. *Plant Physiology and Biochemistry*, *154*, 409-418.https://doi.org/10.1016/j.plaphy.2020.06.026

Wang, Z. Q., Xu, X. Y., Gong, Q. Q., Xie, C., Fan, W., Yang, J. L., Lin, Q. S., & Zheng, S. J. (2014). Root proteome of rice studied by iTRAQ provides integrated insight into aluminum stress tolerance mechanisms in plants. *Journal of Proteomics*, *98*, 189-205.https://doi.org/10.1016/j.jprot.2013.12.023.

Waszczak, C., Carmody, M., & Kangasjärvi, J. (2018). Reactive oxygen species in plant signaling. *Annual Review of Plant Biology*, *69*, 209-236.https://doi.org/10.1146/annurev-arplant-042817-040322

Watanabe, M., Netzer, F., Tohge, T., Orf, I., Brotman, Y., Dubbert, D., Fernie, A. R., Rennenberg, H., Hoefgen, R., & Herschbach, C. (2018). Metabolome and lipidome profiles of populus× canescens twig tissues during annual growth show phospholipid-linked storage and mobilization of C, N, and S. *Frontiers in plant science*, *9*, 1292.https://doi.org/10.3389/fpls.2018.01292

Watanabe, T., Jansen, S., & Osaki, M. (2005). The beneficial effect of aluminium and the role of citrate in Al accumulation in Melastoma malabathricum. *New Phytologist*, 773-780.https://doi.org/10.1111/j.1469-8137.2004.01261.x

Watanabe, T., Jansen, S., & Osaki, M. (2006). Al–Fe interactions and growth enhancement in Melastoma malabathricum and Miscanthus sinensis dominating acid sulphate soils. *Plant, Cell & Environment*, *29*(12), 2124-2132.https://doi.org/10.1111/j.1365-3040.2006.001586.x

Watanabe, T., Misawa, S., Hiradate, S., & Osaki, M. (2008a). Characterization of root mucilage from Melastoma malabathricum, with emphasis on its roles in aluminum accumulation. *New Phytologist*, *178*(3), 581-589.https://doi.org/10.1111/j.1469-8137.2008.02397.x

Watanabe, T., Misawa, S., Hiradate, S., & Osaki, M. (2008b). Root mucilage enhances aluminum accumulation in Melastoma malabathricum, an aluminum accumulator. *Plant Signaling & Behavior*, *3*(8), 603-605.https://doi.org/10.4161/psb.3.8.6356

Wei, P., Demulder, M., David, P., Eekhout, T., Yoshiyama, K. O., Nguyen, L., Vercauteren, I., Eeckhout, D., Galle, M., De Jaeger, G., Larsen, P., Audenaert, D., Desnos, T., Nussaume, L., Loris, R., & De Veylder, L. (2021a). *Arabidopsis* casein kinase 2 triggers stem cell exhaustion under Al toxicity and phosphate deficiency through activating the DNA damage response pathway [Article]. *Plant Cell*, *33*(4), 1361-1380.https://doi.org/10.1093/plcell/koab005

Wei, Q., Ma, X., Zhao, Z., Zhang, S., & Liu, S. (2010). Antioxidant activities and chemical profiles of pyroligneous acids from walnut shell. *Journal of Analytical and Applied Pyrolysis*, *88*(2), 149-154.https://doi.org/10.1016/j.jaap.2010.03.008.

Wei, Y., Han, R., Xie, Y., Jiang, C., & Yu, Y. (2021b). Recent advances in understanding mechanisms of plant tolerance and response to aluminum toxicity. *Sustainability*, *13*(4), 1782.https://doi.org/10.3390/su13041782

Wiszniewska, A. (2021). Priming Strategies for Benefiting Plant Performance under Toxic Trace Metal Exposure. *Plants*, *10*(4), 623.https://doi.org/10.3390/plants10040623

Wititsiri, S. (2011). Production of wood vinegars from coconut shells and additional materials for control of termite workers, Odontotermes sp. and striped mealy bugs, Ferrisia virgata. *Songklanakarin Journal of Science & Technology*, *33*(3).

Wood, C., Noh Hj Jalil, M., Ariffin, A., Yong, B. C., & Thomas, D. R. (1983). Carnitine short-chain acyltransferase in pea mitochondria. *Planta*, *158*(2), 175-178.https://doi.org/10.1007/BF00397711

Wu, L., Guo, Y., Cai, S., Kuang, L., Shen, Q., Wu, D., & Zhang, G. (2020). The zinc finger transcription factor ATF1 regulates aluminum tolerance in barley. *Journal of Experimental Botany*, *71*(20), 6512-6523.https://doi.org/10.1093/JXB/ERAA349

Wu, Q., Tao, Y., Huang, J., Liu, Y. S., Yang, X. Z., Jing, H. K., Shen, R. F., & Zhu, X. F. (2022). The MYB transcription factor MYB103 acts upstream of TRICHOME BIREFRINGENCE-LIKE27 in regulating aluminum sensitivity by modulating the O-acetylation level of cell wall xyloglucan in *Arabidopsis thaliana*. *Plant Journal*, *111*(2).https://doi.org/10.1111/tpj.15837

Wu, W. W., Lin, Y., Chen, Q. Q., Peng, W. T., Peng, J. C., Tian, J., Liang, C. Y., & Liao, H. (2018). Functional Conservation and Divergence of Soybean GmSTOP1 Members in Proton and Aluminum Tolerance [Article]. *Frontiers in plant science*, *9*, 13, Article 570.https://doi.org/10.3389/fpls.2018.00570

Xia, J., Yamaji, N., Kasai, T., & Ma, J. F. (2010). Plasma membrane-localized transporter for aluminum in rice. *Proceedings of the National Academy of Sciences*, *107*(43), 18381-18385.https://doi.org/10.1073/pnas.1004949107

Xia, J., Yamaji, N., & Ma, J. F. (2013). A plasma membrane-localized small peptide is involved in rice aluminum tolerance. *The Plant Journal*, *76*(2), 345-355.https://doi.org/10.1111/tpj.12296

Xu, J. M., Lou, H. Q., Jin, J. F., Chen, W. W., Wan, J. X., Fan, W., & Yang, J. L. (2018). A half-type ABC transporter FeSTAR1 regulates Al resistance possibly via UDP-glucose-based hemicellulose metabolism and Al binding [Article]. *Plant and Soil*, *432*(1-2), 303-314.https://doi.org/10.1007/s11104-018-3805-4

Xu, J. M., Wang, Z. Q., Jin, J. F., Chen, W. W., Fan, W., Zheng, S. J., & Yang, J. L. (2019). FeSTAR2 interacted by FeSTAR1 alters its subcellular location and regulates Al tolerance in buckwheat [Article]. *Plant and Soil*, *436*(1-2), 489-501.https://doi.org/10.1007/s11104-019-03943-z

Xu, M., Gruber, B. D., Delhaize, E., White, R. G., James, R. A., You, J., Yang, Z., & Ryan, P. R. (2015). The barley anion channel, HvALMT1, has multiple roles in guard cell physiology and grain metabolism. *Physiologia plantarum*, *153*(1), 183-193.https://doi.org/10.1111/ppl.12234

Xu, Q., Wang, Y., Ding, Z., Song, L., Li, Y., Ma, D., Wang, Y., Shen, J., Jia, S., & Sun, H. (2016a). Aluminum induced metabolic responses in two tea cultivars. *Plant Physiology and Biochemistry*, *101*, 162-172.https://doi.org/10.1016/j.plaphy.2016.02.001

Xu, T., Liu, X., Wang, R., Dong, X., Guan, X., Wang, Y., Jiang, Y., Shi, Z., Qi, M., & Li, T. (2016b). SlARF2a plays a negative role in mediating axillary shoot formation. *Scientific Reports*, *6*(1), 1-13.https://doi.org/10.1038/srep33728

Xu, Y., & Fu, X. (2022). Reprogramming of plant central metabolism in response to abiotic stresses: a metabolomics view. *International Journal of Molecular Sciences*, *23*(10), 5716.https://doi.org/10.3390/ijms23105716.

Yamaji, N., Huang, C. F., Nagao, S., Yano, M., Sato, Y., Nagamura, Y., & Ma, J. F. (2009). A zinc finger transcription factor ART1 regulates multiple genes implicated in aluminum tolerance in rice. *The Plant Cell*, *21*(10), 3339-3349.https://doi.org/10.1105/tpc.109.070771

Yamamoto, Y. (2019). Aluminum toxicity in plant cells: Mechanisms of cell death and inhibition of cell elongation. *Soil Science and Plant Nutrition*, *65*(1), 41-55.https://doi.org/10.1080/00380768.2018.1553484

Yamamoto, Y., Kobayashi, Y., Devi, S. R., Rikiishi, S., & Matsumoto, H. (2002). Aluminum toxicity is associated with mitochondrial dysfunction and the production of reactive oxygen species in plant cells. *Plant physiology*, *128*(1), 63-72.https://doi.org/10.1104/pp.010417

Yan, L., Riaz, M., Liu, Y., Zeng, Y., & Jiang, C. (2019). Aluminum toxicity could be mitigated with boron by altering the metabolic patterns of amino acids and carbohydrates rather than organic acids in trifoliate orange. *Tree Physiology*, *39*(9), 1572-1582.https://doi.org/10.1093/treephys/tpz047

Yan, L., Riaz, M., Wu, X., Du, C., Liu, Y., & Jiang, C. (2018). Ameliorative effects of boron on aluminum induced variations of cell wall cellulose and pectin components in trifoliate orange (Poncirus trifoliate (L.) Raf.) rootstock. *Environmental Pollution*, *240*, 764-774.https://doi.org/10.1016/j.envpol.2018.05.022

Yang, J., Qu, M., Fang, J., Shen, R. F., Feng, Y. M., Liu, J. Y., Bian, J. F., Wu, L. S., He, Y. M., & Yu, M. (2016a). Alkali-soluble pectin is the primary target of aluminum immobilization in root border cells of pea (Pisum sativum). *Frontiers in plant science*, *7*, 1297.https://doi.org/10.3389/fpls.2016.01297

Yang, J. F., Yang, C. H., Liang, M. T., Gao, Z. J., Wu, Y. W., & Chuang, L. Y. (2016b). Chemical Composition, Antioxidant, and Antibacterial Activity of Wood Vinegar from Litchi chinensis. *Molecules*, *21*(9), 1150.https://doi.org/10.3390/molecules21091150

Yang, J. L., Zhu, X. F., Peng, Y. X., Zheng, C., Li, G. X., Liu, Y., Shi, Y. Z., & Zheng, S. J. (2011a). Cell wall hemicellulose contributes significantly to aluminum adsorption and root growth in *Arabidopsis*. *Plant physiology*, *155*(4), 1885-1892.https://doi.org/10.1104/pp.111.172221

Yang, J. L., Zhu, X. F., Peng, Y. X., Zheng, C., Ming, F., & Zheng, S. J. (2011b). Aluminum regulates oxalate secretion and plasma membrane H+-ATPase activity independently in tomato roots. *Planta*, *234*(2), 281-291.https://doi.org/10.1007/s00425-011-1402-3

Yang, J. L., Zhu, X. F., Zheng, C., Zhang, Y. J., & Zheng, S. J. (2011c). Genotypic differences in Al resistance and the role of cell-wall pectin in Al exclusion from the root apex in Fagopyrum tataricum. *Annals of botany*, *107*(3), 371-378.https://doi.org/10.1093/aob/mcq254

Yang, L.-T., Jiang, H.-X., Qi, Y.-P., & Chen, L.-S. (2012). Differential expression of genes involved in alternative glycolytic pathways, phosphorus scavenging and recycling in response to aluminum and phosphorus interactions in Citrus roots. *Molecular Biology Reports*, *39*(5), 6353-6366.https://doi.org/10.1007/s11033-012-1457-7

Yang, M., Tan, L., Xu, Y., Zhao, Y., Cheng, F., Ye, S., & Jiang, W. (2015). Effect of Low pH and Aluminum Toxicity on the Photosynthetic Characteristics of Different Fast-Growing Eucalyptus Vegetatively Propagated Clones. *PloS One*, *10*(6), e0130963.https://doi.org/10.1371/journal.pone.0130963

Yang, T., Peng, H., Whitaker, B. D., & Jurick, W. M. (2013a). Differential expression of calcium/calmodulin-regulated SlSRs in response to abiotic and biotic stresses in tomato fruit. *Physiologia plantarum*, *148*(3), 445-455.https://doi.org/10.1111/ppl.12027

Yang, X. Y., Zeng, Z. H., Yan, J. Y., Fan, W., Bian, H. W., Zhu, M. Y., Yang, J. L., & Zheng, S. J. (2013b). Association of specific pectin methylesterases with Al-induced root elongation inhibition in rice. *Physiologia plantarum*, *148*(4), 502-511.https://doi.org/10.1111/ppl.12005

Yang, Y., Liu, Y., Huang, C.-F., de Silva, J., & Zhao, F.-J. (2016c). Aluminium alleviates fluoride toxicity in tea (Camellia sinensis). *Plant and Soil*, *402*(1), 179-190.https://doi.org/10.1007/s11104-015-2787-8

Yang, Y., Wang, Q. L., Geng, M. J., Guo, Z. H., & Zhao, Z. (2011d). Rhizosphere pH difference regulated by plasma membrane H+-ATPase is related to differential Al tolerance of two wheat cultivars. *Plant, Soil and Environment*, *57*(5), 201-206.https://doi.org/10.17221/419/2010-PSE

Yang, Z.-B., Geng, X., He, C., Zhang, F., Wang, R., Horst, W. J., & Ding, Z. (2014). TAA1-regulated local auxin biosynthesis in the root-apex transition zone mediates the aluminum-induced inhibition of root growth in *Arabidopsis*. *The Plant Cell*, *26*(7), 2889-2904.https://doi.org/10.1105/tpc.114.127993

Yang, Z.-B., He, C., Ma, Y., Herde, M., & Ding, Z. (2017a). Jasmonic Acid Enhances Al-Induced Root Growth Inhibition. *Plant physiology*, *173*(2), 1420-1433.https://doi.org/10.1104/PP.16.01756

Yang, Z.-B., & Horst, W. J. (2015). Aluminum-induced inhibition of root growth: roles of cell wall assembly, structure, and function. In *Aluminum stress adaptation in plants* (pp. 253-274). Springer. https://doi.org/https://doi.org/10.1007/978-3-319-19968-9_13

Yang, Z. B., Liu, G., Liu, J., Zhang, B., Meng, W., Müller, B., Hayashi, K. i., Zhang, X., Zhao, Z., De Smet, I., & Ding, Z. (2017b). Synergistic action of auxin and cytokinin mediates aluminum-induced root growth inhibition in *Arabidopsis*. *EMBO Reports*, *18*(7), 1213-1230.https://doi.org/10.15252/EMBR.201643806

Yanık, F., & Vardar, F. (2015). Toxic Effects of Aluminum Oxide (Al2O3) Nanoparticles on Root Growth and Development in Triticum aestivum. *Water, Air, & Soil Pollution*, *226*(9), 296.https://doi.org/10.1007/s11270-015-2566-4

Ye, J., Wang, X., Hu, T., Zhang, F., Wang, B., Li, C., Yang, T., Li, H., Lu, Y., Giovannoni, J. J., Zhang, Y., & Ye, Z. (2017). An InDel in the promoter of AI-ACTIVATED MALATE TRANSPORTER9 selected during tomato domestication determines fruit malate contents and aluminum tolerance. *Plant Cell*, *29*(9), 2249-2268.https://doi.org/10.1105/tpc.17.00211.

Ye, L., Zhao, X., Bao, E., Li, J., Zou, Z., & Cao, K. (2020). Bio-organic fertilizer with reduced rates of chemical fertilization improves soil fertility and enhances tomato yield and quality. *Scientific Reports*, *10*(1), 1-11.https://doi.org/10.1038/s41598-019-56954-2

Ye, Y., Hongwei, S., Yue, W., Zisong, X., Shixin, H., Guoqiang, H., Kuide, Y., & Zhang, H. (2022). Wood vinegar alleviates photosynthetic inhibition and oxidative damage caused by Pseudomonas syringae pv. tabaci (Pst) infection in tobacco leaves. *Journal of Plant Interactions*, *17*(1), 801-811.https://doi.org/10.1080/17429145.2022.2106385

Yi, M., Yi, H., Li, H., & Wu, L. (2010). Aluminum induces chromosome aberrations, micronuclei, and cell cycle dysfunction in root cells of Vicia faba. *Environmental Toxicology*, *25*(2), 124-129. https://doi.org/10.1002/tox.20482

Yin, Y.-G., Kobayashi, Y., Sanuki, A., Kondo, S., Fukuda, N., Ezura, H., Sugaya, S., & Matsukura, C. (2010). Salinity induces carbohydrate accumulation and sugar-regulated starch biosynthetic genes in tomato (Solanum lycopersicum L. cv. 'Micro-Tom') fruits in an ABA- and osmotic stress-independent manner. *Journal of Experimental Botany*, *61*(2), 563-574.https://www.doi.org/10.1093/jxb/erp333

Yokosho, K., Yamaji, N., Fujii-Kashino, M., & Ma, J. F. (2016a). Functional analysis of a MATE gene OsFRDL2 revealed its involvement in Al-induced secretion of citrate, but a lower contribution to Al tolerance in rice. *Plant and Cell Physiology*, *57*(5), 976-985.https://doi.org/10.1093/pcp/pcw026

Yokosho, K., Yamaji, N., Mitani-Ueno, N., Shen, R. F., & Ma, J. F. (2016b). An Aluminum-Inducible IREG Gene is Required for Internal Detoxification of Aluminum in Buckwheat. *Plant and Cell Physiology*, *57*(6), 1169-1178.https://doi.org/10.1093/PCP/PCW065

Yoshiyama, K. O., Kobayashi, J., Ogita, N., Ueda, M., Kimura, S., Maki, H., & Umeda, M. (2013). ATM-mediated phosphorylation of SOG1 is essential for the DNA damage response in *Arabidopsis*. *EMBO Reports*, *14*(9), 817-822.https://doi.org/10.1038/embor.2013.112

Young, A. J., & Lowe, G. L. (2018). Carotenoids—antioxidant properties. *Antioxidants*, *7*(2), 28.https://doi.org/10.1016/S0098-2997(03)00030-X

Yousuf, P. Y., Hakeem, K. U. R., Chandna, R., & Ahmad, P. (2012). Role of glutathione reductase in plant abiotic stress. In P. Ahmad, Prasad, M. (Ed.), *Abiotic stress responses in plants* (pp. 149-158). Springer. https://doi.org/https://doi.org/10.1007/978-1-4614-0634-1_8

Yu, Y., Jin, C., Sun, C., Wang, J., Ye, Y., Zhou, W., Lu, L., & Lin, X. (2016). Inhibition of ethylene production by putrescine alleviates aluminium-induced root inhibition in wheat plants. *Scientific Reports*, *6*(1), 1-10.https://doi.org/10.1038/srep18888

Yusuf, M., Khan, T. A., & Fariduddin, Q. (2016). Responses of photosynthesis, stress markers and antioxidants under aluminium, salt and combined stresses in wheat cultivars. *Cogent Food & Agriculture*, *2*(1).https://doi.org/10.1080/23311932.2016.1216246

Zahra, N., Hafeez, M. B., Shaukat, K., Wahid, A., & Hasanuzzaman, M. (2021). Fe toxicity in plants: Impacts and remediation. *Physiologia plantarum*, *173*(1), 201-222.https://doi.org/10.1111/ppl.13361

Zeng, Q. L., Jiang, Y. Q., Dong, G. Q., Wei, J. G., Jiang, J. F., Tian, L. L., & Yu, H. (2020). Effect of Al on the growth and nutrients uptake of blueberries (Vaccinium spp.) [Article]. *Notulae Botanicae Horti Agrobotanici Cluj-Napoca*, *48*(2), 656-665.https://doi.org/10.15835/nbha48211643

Zhai, M., Shi, G., Wang, Y., Mao, G., Wang, D., & Wang, Z. (2015). Chemical compositions and biological activities of pyroligneous acids from walnut shell. *BioResources*, *10*(1), 1715-1729.https://doi.org/10.15376/biores.10.1.1715-1729

Zhang, F., Yan, X. Y., Han, X. B., Tang, R. J., Chu, M. L., Yang, Y., Yang, Y. H., Zhao, F. G., Fu, A. G., Luan, S., & Lan, W. Z. (2019a). A Defective Vacuolar Proton Pump Enhances Aluminum Tolerance by Reducing Vacuole Sequestration of Organic Acids [Article]. *Plant physiology*, *181*(2), 743-761.https://doi.org/10.1104/pp.19.00626

Zhang, H., Jiang, Z., Qin, R., Zhang, H., Zou, J., Jiang, W., & Liu, D. (2014a). Accumulation and cellular toxicity of aluminum in seedling of Pinus massoniana. *BMC Plant Biology*, *14*(1), 1-16.https://doi.org/10.1186/s12870-014-0264-9

Zhang, J., Wei, J., Li, D., Kong, X., Rengel, Z., Chen, L., Yang, Y., Cui, X., & Chen, Q. (2017a). The role of the plasma membrane H+-ATPase in plant responses to aluminum toxicity. *Frontiers in plant science*, *8*, 1757-1757.https://doi.org/10.3389/fpls.2017.01757

Zhang, J., Zeng, B., Mao, Y., Kong, X., Wang, X., Yang, Y., Zhang, J., Xu, J., Rengel, Z., & Chen, Q. (2017b). Melatonin alleviates aluminium toxicity through modulating antioxidative enzymes and enhancing organic acid anion exudation in soybean. *Functional Plant Biology*, *44*(10), 961-968.https://doi.org/10.1071/FP17003

Zhang, J. R., Li, D. X., Wei, J., Ma, W. N., Kong, X. Y., Rengel, Z., & Chen, Q. (2019b). Melatonin alleviates aluminum-induced root growth inhibition by interfering with nitric oxide production in *Arabidopsis* [Article]. *Environmental and Experimental Botany*, *161*, 157-165.https://doi.org/10.1016/j.envexpbot.2018.08.014

Zhang, L., Dong, D., Wang, J., Wang, Z., Zhang, J., Bai, R. Y., Wang, X., Rubio Wilhelmi, M. D. M., Blumwald, E., & Zhang, N. (2022). A zinc finger protein SlSZP1 protects SlSTOP1 from SlRAE1-mediated degradation to modulate aluminum resistance. *New Phytologist*, *236*(1), 165-181.https://doi.org/10.1111/nph.18336

Zhang, L., Wu, X. X., Wang, J. F., Qi, C. D., Wang, X. Y., Wang, G. L., Li, M. Y., Li, X. S., & Guo, Y. D. (2018). BoALMT1, an Al-Induced Malate Transporter in Cabbage, Enhances Aluminum Tolerance in *Arabidopsis thaliana* [Article]. *Frontiers in plant science*, *8*, 9, Article 2156.https://doi.org/10.3389/fpls.2017.02156.

Zhang, M., Ma, Y., Horst, W. J., & Yang, Z.-B. (2016). Spatial–temporal analysis of polyethylene glycol-reduced aluminium accumulation and xyloglucan endotransglucosylase action in root tips of common bean (Phaseolus vulgaris). *Annals of botany*, *118*(1), 1-9.https://doi.org/10.1093/aob/mcw062

Zhang, Y., Chen, B., Xu, Z., Shi, Z., Chen, S., Huang, X., Chen, J., & Wang, X. (2014b). Involvement of reactive oxygen species in endosperm cap weakening and embryo elongation growth during lettuce seed germination. *Journal of Experimental Botany*, *65*(12), 3189-3200.https://doi.org/10.1093/jxb/eru167

Zhang, Y., Zhang, J., Guo, J. L., Zhou, F. L., Singh, S., Xu, X., Xie, Q., Yang, Z. B., & Huang, C. F. (2019c). F-box protein RAE1 regulates the stability of the aluminum-resistance transcription factor STOP1 in *Arabidopsis* [Article]. *Proceedings of the National Academy of Sciences of the United States of America*, *116*(1), 319-327.https://doi.org/10.1073/pnas.1814426116

Zhao, H., Huang, W., Zhang, Y. E., Zhang, Z. W., Li, Y., Tang, C., Huang, J., & Ni, D. J. (2018). Natural variation of CsSTOP1 in tea plant (Camellia sinensis) related to aluminum tolerance [Article]. *Plant and Soil*, *431*(1-2), 71-87.https://doi.org/10.1007/s11104-018-3746-y

Zhao, X., Chen, Q., Wang, Y., Shen, Z., Shen, W., & Xu, X. (2017). Hydrogen-rich water induces aluminum tolerance in maize seedlings by enhancing antioxidant capacities and nutrient homeostasis. *Ecotoxicology and Environmental Safety*, *144*, 369-379.https://doi.org/10.1016/j.ecoenv.2017.06.045

Zhao, Z., Hu, L., Hu, T., & Fu, J. (2015). Differential metabolic responses of two tall fescue genotypes to heat stress. *Acta Prataculturae Sinica*, *24*(3), 58-69.https://doi.org/10.11686/cyxb20150306

Zhao, Z. K., Gao, X. F., Ke, Y., Chang, M. M., Xie, L., Li, X. F., Gu, M. H., Liu, J. P., & Tang, X. L. (2019). A unique aluminum resistance mechanism conferred by aluminum and salicylic-acid-activated root efflux of benzoxazinoids in maize [Article]. *Plant and Soil*, *437*(1-2), 273-289.https://doi.org/10.1007/s11104-019-03971-9

Zheng, H., Sun, C., Hou, X., Wu, M., Yao, Y., & Li, F. (2018). Pyrolysis of Arundo donax L. to produce pyrolytic vinegar and its effect on the growth of dinoflagellate Karenia brevis. *Bioresource technology*, *247*, 273-281.https://doi.org/10.1016/j.biortech.2017.09.049

Zheng, J., Johnson, M., Mandal, R., & Wishart, D. S. (2021). A Comprehensive Targeted Metabolomics Assay for Crop Plant Sample Analysis. *Metabolites*, *11*(5), 303.https://doi.org/10.3390/metabo11050303

Zheng, S. J., Yang, J. L., He, Y. F., Yu, X. H., Zhang, L., You, J. F., Shen, R. F., & Matsumoto, H. (2005). Immobilization of aluminum with phosphorus in roots is associated with high aluminum resistance in buckwheat. *Plant physiology*, *138*(1), 297-303.https://doi.org/10.1104/pp.105.059667

Zhou, D., Yang, Y., Zhang, J., Jiang, F., Craft, E., Thannhauser, T. W., Kochian, L. V., & Liu, J. (2017). Quantitative iTRAQ proteomics revealed possible roles for antioxidant proteins in sorghum aluminum tolerance. *Frontiers in plant science*, *7*, 2043-2043.https://doi.org/10.3389/fpls.2016.02043

Zhou, G., Delhaize, E., Zhou, M., & Ryan, P. R. (2011). Biotechnological solutions for enhancing the aluminium resistance of crop plants. In A. S. a. B. Venkaseswarlu (Ed.), *Abiotic stress in plants—mechanisms and adaptations. Brisbane: InTech* (Vol. 6, pp. 119 - 142). https://doi.org/https://doi.org/10.5772/25187

Zhou, S., Sauve, R., & Thannhauser, T. W. (2009). Aluminum induced proteome changes in tomato cotyledons. *Plant Signaling & Behavior*, *4*(8), 769-772.https://doi.org/10.4161/psb.4.8.9182

Zhou, X., Shi, A., Rensing, C., Yang, J., Ni, W., Xing, S., & Yang, W. (2022). Wood vinegar facilitated growth and Cd/Zn phytoextraction of Sedum alfredii Hance by improving rhizosphere chemical properties and regulating bacterial community. *Environmental Pollution*, *305*, 119266.https://doi.org/10.1016/j.envpol.2022.119266

Zhou, Y., Yang, Z., Gong, L., Liu, R. K., Sun, H. R., & You, J. F. (2018). Molecular characterization of GmSTOP1 homologs in soybean under Al and proton stress [Article]. *Plant and Soil*, *427*(1-2), 213-230.https://doi.org/10.1007/s11104-018-3645-2

Zhou, Y. P., Neuhauser, B., Neumann, G., & Ludewig, U. (2020). LaALMT1 mediates malate release from phosphorus-deficient white lupin root tips and metal root to shoot translocation [Article]. *Plant, Cell and Environment*, *43*(7), 1691-1706.https://doi.org/10.1111/pce.13762

Zhu, C. Q., Cao, X. C., Zhu, L. F., Hu, W. J., Hu, A. Y., Abliz, B., Bai, Z. G., Huang, J., Liang, Q. D., & Sajid, H. (2019). Boron reduces cell wall aluminum content in rice (Oryza sativa) roots by decreasing H2O2 accumulation. *Plant Physiology and Biochemistry*, *138*, 80-90.https://doi.org/10.1016/j.plaphy.2019.02.022

Zhu, J., Gao, W., Zhao, W., Ge, L., Zhu, T., Zhang, G., & Niu, Y. (2021a). Wood vinegar enhances humic acid-based remediation material to solidify Pb (II) for metal-contaminated soil. *Environmental Science and Pollution Research*, *28*(10), 12648-12658.https://doi.org/10.1007/s11356-020-11202-3

Zhu, K., Gu, S., Liu, J., Luo, T., Khan, Z., Zhang, K., & Hu, L. (2021b). Wood Vinegar as a Complex Growth Regulator Promotes the Growth, Yield, and Quality of Rapeseed. *Agronomy*, *11*(3), 510.https://doi.org/10.3390/agronomy11030510

Zhu, K., Liu, J., Luo, T., Zhang, K., Khan, Z., Zhou, Y., Cheng, T., Yuan, B., Peng, X., & Hu, L. (2022). Wood Vinegar Impact on the Growth and Low-Temperature Tolerance of Rapeseed Seedlings. *Agronomy*, *12*(10).

Zhu, X. F., Shi, Y. Z., Lei, G. J., Fry, S. C., Zhang, B. C., Zhou, Y. H., Braam, J., Jiang, T., Xu, X. Y., & Mao, C. Z. (2012). XTH31, encoding an in vitro XEH/XET-active enzyme, regulates aluminum sensitivity by modulating in vivo XET action, cell wall xyloglucan content, and aluminum binding capacity in *Arabidopsis*. *The Plant Cell*, *24*(11), 4731-4747.https://doi.org/10.1105/tpc.112.106039

Zhu, X. F., Wan, J. X., Sun, Y., Shi, Y. Z., Braam, J., Li, G. X., & Zheng, S. J. (2014). Xyloglucan endotransglucosylase-hydrolase17 interacts with xyloglucan endotransglucosylase-hydrolase31 to confer xyloglucan endotransglucosylase action and affect aluminum sensitivity in *Arabidopsis*. *Plant physiology*, *165*(4), 1566-1574.https://doi.org/10.1104/pp.114.243790

Zhu, X. F., Wan, J. X., Wu, Q., Zhao, X. S., Zheng, S. J., & Shen, R. F. (2017). PARVUS affects aluminium sensitivity by modulating the structure of glucuronoxylan in *Arabidopsis thaliana*. *Plant, Cell & Environment*, *40*(9), 1916-1925.https://doi.org/10.1111/pce.12999

Zouine, M., Fu, Y., Chateigner-Boutin, A.-L., Mila, I., Frasse, P., Wang, H., Audran, C., Roustan, J.-P., & Bouzayen, M. (2014). Characterization of the tomato ARF gene family uncovers a multi-levels post-transcriptional regulation including alternative splicing. *PloS One*, *9*(1), e84203.https://doi.org/10.1371/journal.pone.0084203

Zulkarami, B., Ashrafuzzaman, M., Husni, M. O., & Ismail, M. R. (2011). Effect of pyroligneous acid on growth, yield and quality improvement of rockmelon in soilless culture. *Australian Journal of Crop Science*, *5*(12), 1508-1514.

APPENDIX

Table S4.1. Primers used for gene expression analysis

Gene	Sequence (5'-3')	Locus	Product size
SlPOD - F	ACTGGCACTGAGAGAACAGC	Solyc01g105070	209
SlPOD - R	GCGCTTGAAACTCGTCCATC		
SIGR - F	GTCGCCTCAGGCTATTGTCA	Solyc09g065900	179
SIPGR - R	CGTCAACCTCTATGGCTCCG		
SlSOD - F	TCTTCACCACAACCAGCACT	Solyc11g066390	167
SlSOD - R	CAGTAAGGGGTTTAGGGGTAGT		
SICAT - F	TCCTTGTCGTCCTGCTGAG	Solyc12g094620	150
SICAT - R	TTGATGTATCTGTCTTGCCTGTC		
SIAPX1 F	TACAGTTGCCGTCAGACAAG	Solyc06g005160	130
SIAPX1 R	CCCAATTCAGAAAGCTTCAAG		
SIARF2A - F	TAGGAGTAGTTCCGGTGTCGG	Solyc03g118290	181
SIARF2A - R	AAGTGGCTGACCAGCAGATG		
SlEF1α - F	TGGAAACGGATATGCCCCTG	Solyc06g005060	170
SlEF1α - R	TGGGCTTGGTGGGAATCATC		

Table S4.2. Interaction effect of pyroligneous acid (PA) and priming time on the growth characteristics of tomato seedlings.

PA*Priming time	Germination velocity		Mean germination rate		Germination Index		Germination Rate Index		Mean Germination Time (days)		Final Germination Percentage (%)	
Control * 1	19.65	fg	0.197	fg	46.00	bcd	30.88	efg	5.09	ab	96.75	a
Control * 12	19.72	efg	0.197	efg	46.00	bcd	31.32	defg	5.07	abc	94.593	a
Control * 2	20.28	cdefg	0.203	cdefg	47.33	bcd	33.05	cdefg	4.93	abcde	94.593	a
Control * 24	20.00	defg	0.200	defg	48.33	bcd	33.08	cdefg	5.00	abcd	97.667	a
Control * 4	20.00	defg	0.200	defg	48.33	bcd	33.08	cdefg	5.00	abcd	97.667	a
Control * 6	20.00	defg	0.200	defg	50.00	bcd	34.29	bcdefg	5.00	abcd	100	a
0.5:100 * 1	20.17	cdefg	0.202	cdefg	49.00	bcd	34.30	bcdefg	4.96	abcde	97.667	a
0.5:100* 12	19.96	efg	0.200	efg	50.00	bcd	35.01	bcdefg	5.01	abcd	100	a
0.5:100* 2	20.17	cdefg	0.202	cdefg	49.00	bcd	34.30	bcdefg	4.96	abcde	97.667	a
0.5:100* 24	20.17	cdefg	0.202	cdefg	47.33	bcd	33.99	bcdefg	4.96	abcde	96.75	a
0.5:100* 4	20.17	cdefg	0.202	cdefg	50.67	bcd	36.07	bcdefg	4.96	abcde	100	a
0.5:100* 6	19.37	g	0.194	g	42.00	d	28.25	g	5.16	a	87.76	a
1:100 * 1	20.60	cdefg	0.206	cdefg	46.33	bcd	32.86	cdefg	4.86	abcdef	93.304	a
1:100 * 12	20.00	defg	0.200	defg	50.00	bcd	34.29	bcdefg	5.00	abcd	100	a
1:100 * 2	20.28	cdefg	0.203	cdefg	47.33	bcd	33.05	cdefg	4.93	abcde	94.593	a
1:100 * 24	21.01	bcdefg	0.210	bcdefg	52.67	abcd	38.40	abcdefg	4.76	abcdefg	100	a
1:100 * 4	20.79	bcdefg	0.208	bcdefg	52.00	abcd	37.47	bcdefg	4.81	abcdefg	100	a
1:100 * 6	20.00	defg	0.200	defg	46.67	bcd	31.94	cdefg	5.00	abcd	94.593	a
1:1200 * 1	24.21	abc	0.242	abc	55.33	abcd	46.16	abc	4.15	efg	96.75	a
1:1200 * 12	19.96	efg	0.200	efg	48.33	bcd	33.90	cdefg	5.01	abcd	97.667	a
1:1200 * 2	21.84	abcdefg	0.218	abcdefg	50.67	bcd	38.62	abcdefg	4.58	abcdefg	94.593	a
1:1200 * 24	22.99	abcde	0.230	abcde	51.00	abcd	40.79	abcdef	4.35	cdefg	93.304	a
1:1200 * 4	20.00	defg	0.200	defg	41.67	d	28.51	fg	5.00	abcd	84.743	a
1:1200 * 6	21.11	abcdefg	0.211	abcdefg	52.67	abcd	38.68	abcdefg	4.74	abcdefg	100	a
1:300 * 1	19.72	efg	0.197	efg	49.33	bcd	33.60	cdefg	5.07	abc	100	a
1:300 * 12	19.40	g	0.194	g	45.33	bcd	30.29	efg	5.16	a	96.75	a
1:300 * 2	20.32	cdefg	0.203	cdefg	45.67	bcd	31.91	cdefg	4.92	abcde	93.304	a
1:300 * 24	20.49	cdefg	0.205	cdefg	48.00	bcd	33.97	bcdefg	4.88	abcde	96.75	a
1:300 * 4	19.69	fg	0.197	fg	46.00	bcd	31.22	efg	5.08	ab	94.593	a

1:300 * 6	20.00	defg	0.200	defg	45.00	bcd	30.86	efg	5.00	abcd	90	a
1:600 * 1	19.72	efg	0.197	efg	46.00	bcd	31.32	defg	5.07	abc	94.593	a
1:600 * 12	22.51	abcdef	0.225	abcdef	48.67	bcd	38.28	abcdefg	4.46	bcdefg	87.76	a
1:600 * 2	19.44	g	0.194	g	47.00	bcd	31.69	cdefg	5.15	a	97.667	a
1:600 * 24	20.28	cdefg	0.203	cdefg	47.33	bcd	33.05	cdefg	4.93	abcde	94.593	a
1:600 * 4	20.18	cdefg	0.202	cdefg	44.00	cd	30.68	efg	4.96	abcde	91.809	a
1:600 * 6	21.08	abcdefg	0.211	abcdefg	51.00	abcd	37.44	bcdefg	4.75	abcdefg	97.667	a
1:900 * 1	19.72	efg	0.197	efg	49.33	bcd	33.60	cdefg	5.07	abc	100	a
1:900 * 12	22.74	abcdef	0.227	abcdef	55.00	abcd	43.09	abcde	4.41	bcdefg	97.667	a
1:900 * 2	21.73	abcdefg	0.217	abcdefg	52.33	abcd	39.46	abcdefg	4.61	abcdefg	97.667	a
1:900 * 24	20.83	bcdefg	0.208	bcdefg	52.00	abcd	37.62	bcdefg	4.80	abcdefg	100	a
1:900 * 4	19.98	efg	0.200	efg	48.33	bcd	34.03	bcdefg	5.01	abcd	97.667	a
1:900 * 6	20.28	cdefg	0.203	cdefg	49.00	bcd	34.69	bcdefg	4.93	abcde	97.667	a
2:100 * 1	20.00	defg	0.200	defg	45.00	bcd	30.67	efg	5.00	abcd	93.304	a
2:100 * 12	20.70	cdefg	0.207	cdefg	48.67	bcd	34.33	bcdefg	4.84	abcdef	96.75	a
2:100 * 2	21.58	abcdefg	0.216	abcdefg	54.00	abcd	41.56	abcde	4.64	abcdefg	100	a
2:100 * 24	26.40	ab	0.264	ab	58.00	ab	50.77	ab	3.79	fg	96.75	a
2:100 * 4	27.60	a	0.276	a	64.67	a	58.14	a	3.64	g	100	a
2:100 * 6	23.75	abcd	0.238	abcd	56.33	abc	45.98	abcd	4.22	defg	97.667	a

Table S4.3. Interaction effect of pyroligneous acid (PA) and priming time on the growth characteristics of tomato seedlings.

PA*Priming time	Total root length (cm)		Total root surface area (cm^2)		Root volume (cm^3)		Total hypocotyl length (cm)		Total hypocotyl surface area (cm^2)		Fresh weight (g)	
Control * 1	10.42	hij	7.65	fghijk	0.0069	efghi	3.02	defghi	2.29	cdefghi	0.11	bcde
Control * 12	13.78	cdefgh	7.53	ghijk	0.0082	abcdefg	2.76	efghi	2.26	defghi	0.10	de
Control * 2	11.39	fghij	8.45	bcdefghijk	0.0073	cdefghi	3.06	defghi	2.43	bcdefghi	0.12	abcde
Control * 24	10.75	ghij	5.25	k	0.0092	abcde	4.27	abcd	2.22	efghi	0.13	abcd
Control * 4	13.42	cdefgh	9.44	abcdefgh	0.0082	abcdefg	3.62	abcdef	2.85	abcdef	0.11	abcde
Control * 6	14.30	bcdefgh	9.67	abcdefg	0.0092	abcde	3.35	bcdefgh	2.82	abcdefg	0.11	abcde
0.5:100 * 1	12.52	defgh	9.77	abcdefg	0.0083	abcdefg	3.74	abcdef	2.67	abcdefg	0.12	abcde
0.5:100* 12	12.64	defgh	10.12	abcdefg	0.0079	abcdefgh	4.50	abcd	2.95	abcde	0.13	abcde
0.5:100* 2	13.69	cdefgh	6.27	ijk	0.0106	a	4.06	abcdef	2.24	efghi	0.13	abcde
0.5:100* 24	12.55	defgh	8.63	bcdefghij	0.0062	ghi	4.03	abcdef	2.93	abcde	0.11	abcde
0.5:100* 4	11.67	efghij	7.58	fghijk	0.0069	efghi	2.28	ghi	1.77	hi	0.10	cde
0.5:100* 6	8.18	ij	6.53	hijk	0.0062	ghi	2.18	hi	2.06	ghi	0.09	e
1:100 * 1	16.00	abcdef	10.24	abcdefg	0.0090	abcdef	4.06	abcdef	2.88	abcdef	0.12	abcde
1:100 * 12	16.28	abcdef	10.20	abcdefg	0.0084	abcdefg	4.04	abcdef	3.04	abcd	0.13	abcd
1:100 * 2	15.36	abcdefgh	9.97	abcdefg	0.0084	abcdefg	4.83	ab	3.11	ab	0.13	abcd
1:100 * 24	13.52	cdefgh	8.41	cdefghijk	0.0077	bcdefghi	3.56	abcdefg	2.52	bcdefgh	0.13	abcde
1:100 * 4	14.51	bcdefgh	10.13	abcdefg	0.0094	abcd	3.93	abcdef	2.79	abcdefg	0.12	abcde
1:100 * 6	14.69	bcdefgh	10.49	abcdef	0.0092	abcdef	3.27	cdefgh	2.66	abcdefg	0.12	abcde
1:1200 * 1	15.52	abcdefg	10.27	abcdefg	0.0089	abcdef	4.36	abcd	3.34	a	0.15	a
1:1200 * 12	11.71	efghij	8.39	cdefghijk	0.0071	defghi	3.30	bcdefgh	2.54	bcdefgh	0.11	bcde
1:1200 * 2	12.46	defgh	5.22	k	0.0098	abc	3.73	abcdef	2.26	defghi	0.12	abcde
1:1200 * 24	16.19	abcdef	10.00	abcdefg	0.0079	abcdefgh	4.70	abc	3.05	abc	0.13	abcde
1:1200 * 4	12.91	cdefgh	9.09	abcdefghij	0.0072	defghi	3.93	abcdef	2.89	abcdef	0.12	abcde
1:1200 * 6	18.54	abc	7.53	ghijk	0.0086	abcdef	4.23	abcd	2.61	abcdefg	0.11	abcde
1:300 * 1	7.76	j	6.33	hijk	0.0057	i	2.00	i	1.73	i	0.09	e
1:300 * 12	13.76	cdefgh	9.91	abcdefg	0.0076	bcdefghi	3.95	abcdef	2.78	abcdefg	0.13	abcde
1:300 * 2	12.94	cdefgh	8.70	bcdefghij	0.0074	cdefghi	3.17	cdefghi	2.79	abcdefg	0.11	bcde
1:300 * 24	14.52	bcdefgh	10.74	abcde	0.0090	abcdef	5.05	a	3.21	ab	0.14	ab
1:300 * 4	10.68	ghij	7.89	efghijk	0.0059	hi	2.66	fghi	2.26	defghi	0.10	de

1:300 * 6	15.33	abcdefgh	10.15	abcdefg	0.0086	abcdef	3.24	cdefghi	2.75	abcdefg	0.12	abcde
1:600 * 1	12.63	defgh	10.27	abcdefg	0.0080	abcdefgh	3.72	abcdef	2.68	abcdefg	0.12	abcde
1:600 * 12	12.59	defgh	8.84	bcdefghij	0.0079	abcdefgh	4.26	abcd	3.05	abc	0.12	abcde
1:600 * 2	13.33	cdefgh	8.93	abcdefghij	0.0067	fghi	3.70	abcdef	2.77	abcdefg	0.11	bcde
1:600 * 24	12.63	defgh	7.75	fghijk	0.0072	defghi	4.10	abcde	2.54	bcdefgh	0.12	abcde
1:600 * 4	13.62	cdefgh	9.22	abcdefghij	0.0083	abcdefg	4.33	abcd	2.95	abcde	0.11	abcde
1:600 * 6	12.17	defghi	8.86	bcdefghij	0.0073	cdefghi	3.48	abcdefg	2.76	abcdefg	0.12	abcde
1:900 * 1	11.68	efghij	8.39	cdefghijk	0.0071	defghi	3.75	abcdef	2.81	abcdefg	0.12	abcde
1:900 * 12	14.33	bcdefgh	9.42	abcdefgh	0.0077	bcdefghi	4.03	abcdef	2.81	abcdefg	0.12	abcde
1:900 * 2	12.27	defghi	8.23	defghijk	0.0077	bcdefghi	4.02	abcdef	2.63	abcdefg	0.12	abcde
1:900 * 24	14.03	bcdefgh	9.35	abcdefghi	0.0102	ab	3.66	abcdef	2.52	bcdefgh	0.14	abc
1:900 * 4	13.28	cdefgh	8.69	bcdefghij	0.0068	efghi	3.84	abcdef	2.82	abcdefg	0.11	abcde
1:900 * 6	17.50	abcd	10.95	abcd	0.0093	abcde	4.06	abcdef	2.92	abcde	0.13	abcde
2:100 * 1	12.19	defghi	8.92	abcdefghij	0.0077	bcdefghi	4.02	abcdef	2.73	abcdefg	0.12	abcde
2:100 * 12	11.23	fghij	6.09	jk	0.0096	abcd	3.60	abcdefg	2.11	fghi	0.12	abcde
2:100 * 2	20.25	ab	11.67	a	0.0092	abcde	3.65	abcdef	2.89	abcdef	0.13	abcde
2:100 * 24	14.60	bcdefgh	10.04	abcdefg	0.0079	abcdefgh	4.70	abc	2.97	abcde	0.14	ab
2:100 * 4	21.66	a	11.27	ab	0.0098	abc	4.18	abcde	2.63	abcdefg	0.13	abcd
2:100 * 6	17.06	abcde	11.17	abc	0.0092	abcde	3.96	abcdef	2.75	abcdefg	0.13	abcde

Table S5.1. Chemical composition of pyroligneous acid (PA) obtained from white pine.

Mineral element	Unit	RL	Content
Nitrate & Nitrite	mg/L	50	100
Aluminum	mg/L	1	2
Antimony	mg/L	0.1	< 0.10
Arsenic	mg/L	1	< 1.00
Barium	mg/L	1	< 1.00
Beryllium	mg/L	0.1	< 0.10
Bismuth	mg/L	1	< 1.00
Boron	mg/L	1	< 1.00
Cadmium	mg/L	0.01	0.2
Calcium	mg/L	50	100
Chromium	mg/L	1	< 1.00
Cobalt	mg/L	0.1	< 0.10
Copper	mg/L	1	< 1.00
Iron	mg/L	20	< 20.00
Lead	mg/L	0.1	0.6
Lithium	mg/L	0.1	< 0.10
Magnesium	mg/L	10	< 10.00
Manganese	mg/L	1	1
Molybdenum	mg/L	0.1	< 0.10
Nickel	mg/L	1	< 1.00
Potassium	mg/L	20	180
Rubidium	mg/L	0.1	0.1
Selenium	mg/L	1	< 1.00
Silver	mg/L	0.1	< 0.10
Sodium	mg/L	50	< 50.00
Strontium	mg/L	1	< 1.00
Tellurium	mg/L	0.1	< 0.1.00
Thallium	mg/L	0.1	< 0.10
Tin	mg/L	1	< 1.00
Uranium	mg/L	0.1	< 0.10
Vanadium	mg/L	1	< 1.00
Zinc	mg/L	1	10
Salicylic acid	μM	0.06	8.33
Oxalic acid	μM	0.1	47.8
Propionic acid	μM	0.03	4120
Malic acid	μM	0.06	70.3
Shikimic acid	μM	0.32	1.87
Hydroxytetradecenoylcarnitine	μM	0.06	0.25

Tetradecadienylcarnitine	μM	0.05	0.37
Hydroxytetradecadienylcarnitine	μM	0.05	0.6
Hexadecanoylcarnitine	μM	0.03	0.3

RL; reporting limit

Table S5.2. Pearson's correlation between the morpho-physiological, yield and quality of tomato plants in response to PA application.

Variables	Flower number	Number of suckers	Plant height	SPAD	Ci	Intracellular CO_2	E	A	gs	Total Fruit weight	Fruit number	Salinity	EC	TDS	Juice pH	Brix	TA	Carotenoid	Total sugar	Total phenolics	Flavonoid	Total ascorbate	Total protein
Number of suckers	**0.903**																						
Plant height	0.076	0.165																					
SPAD	-0.71	-0.588	-0.363																				
Ci	-0.32	0.011	0.547	-0.123																			
Intracellular CO2	-0.834	-0.667	-0.023	**0.927**	0.157																		
E	0.065	0.313	0.485	-0.531	**0.888**	-0.31																	
A	0.828	0.865	0.307	**-0.891**	0.222	-0.87	0.608																
gs	-0.008	0.238	0.519	-0.495	**0.914**	-0.251	**0.996**	0.548															
Total Fruit weight	0.292	0.36	**0.943**	-0.639	0.565	-0.33	0.651	0.584	0.664														
Fruit number	0.305	0.229	**0.915**	-0.501	0.188	-0.232	0.229	0.36	0.252	**0.887**													
Salinity	0.677	0.58	-0.666	-0.315	-0.516	-0.64	-0.167	0.461	-0.248	-0.434	-0.477												
EC	0.669	0.577	-0.681	-0.263	-0.543	-0.598	-0.213	0.426	-0.294	-0.465	-0.491	**0.998**											
TDS	0.652	0.568	-0.69	-0.271	-0.513	-0.603	-0.179	0.432	-0.26	-0.467	-0.512	**0.999**	**0.999**										
pH	-0.319	-0.135	0.832	0.212	0.518	0.521	0.213	-0.181	0.266	0.613	0.651	-0.864	-0.848	-0.862									
Brix	0.688	0.564	-0.667	-0.217	-0.65	-0.562	-0.338	0.369	-0.417	-0.482	-0.439	**0.979**	**0.988**	**0.98**	-0.809								
TA	0.045	0.171	-0.754	0.558	-0.371	0.248	-0.432	-0.234	-0.478	-0.786	-0.779	0.567	0.612	0.607	-0.428	0.623							
Carotenoid	0.492	0.14	-0.028	-0.169	-0.848	-0.294	-0.71	0.008	-0.725	-0.053	0.36	0.253	0.271	0.231	-0.151	0.399	-0.059						
Total sugar	0.365	0.576	-0.447	-0.212	0.204	-0.392	0.423	0.519	0.355	-0.223	-0.569	0.703	0.692	0.717	-0.553	0.589	0.547	-0.48					
Total phenolics	-0.296	-0.192	-0.83	0.744	-0.324	0.466	-0.481	-0.521	-0.501	**-0.915**	**-0.897**	0.371	0.413	0.416	-0.412	0.416	**0.93**	-0.177	0.393				
Flavonoid	-0.185	-0.144	**-0.903**	0.652	-0.454	0.334	-0.545	-0.459	-0.573	**-0.953**	**-0.906**	0.5	0.538	0.539	-0.546	0.546	**0.933**	-0.056	0.411	**0.984**			
Total ascorbate	-0.224	-0.17	-0.43	0.841	-0.478	0.649	-0.752	-0.639	-0.753	-0.659	-0.414	0.053	0.118	0.092	0.061	0.209	0.76	0.225	-0.105	0.768	0.734		
Total protein	0.597	0.416	0.441	**-0.972**	0.092	-0.856	0.461	0.769	0.442	0.678	0.604	0.157	0.103	0.108	-0.126	0.072	-0.711	0.249	-0.008	-0.842	-0.751	-0.869	
Peroxidase activity	0.742	0.772	-0.03	-0.815	0.158	**-0.885**	0.577	**0.928**	0.508	0.293	0.011	0.665	0.625	0.643	-0.489	0.539	-0.035	-0.12	0.736	-0.268	-0.188	-0.613	0.663

A, photosynthetic rate; E, transpiration rate; gs, stomatal conductance; Ci, Sub-stomatal CO2; EC, electrical conductivity; TDS, total dissolved solids; TA; titratable acidity. Values in bold indicate significance at $p < 0.05$. The different colors and intensity indicate the degree of correlation: dark green is highly positive correlation, light green is medium to low positive correlation, dark red indicates highly negative correlation and light red indicates medium to low negative correlation.

Table S6.1. Direct effect of foliar pyroligneous acid (PA) application on physiology, yield and quality of tomato.

Treatment	Chlorophyll a (mg/g FW)	Chlorophyll b (mg/g FW)	Total chlorophyll content (mg/g FW)	Fruit number	Total fruit weight (g)	°Brix	pH	TDS (ppt)	EC (mS)	Salinity (ppt)	Leaf Carotenoid Content (mg/g FW)	Leaf Total Flavonoid (mg quercetin/g FW)	Leaf Total sugar (mg glucose/g FW)	Leaf Total Phenolics (mg GAE/g FW)	Leaf DPPH (%)	Fruit DPPH (%)	Fruit Carotenoid Content (mg/g FW)	Fruit Total flavonoid Content (mg quercetin/g FW)	fruit Total Phenolic Content (mg GAE/g FW)	Fruit Total sugar (mg glucose/g FW)	Fruit total Protein (mg/g FW)	Leaf protein (mg/g FW)
0.25% PA	219.07 bc	103.90 cd	319.68 cd	24 b	1263.21 a	4.99 c	4.58 a	3.45 d	3.9 d	2.05 d	79.00 bc	0.92 c	7.24 d	647.23 a	52.08 e	24.79 d	2.70 c	58.60 d	118.32 d	16.68 d	1.19 ab	2.23 c
0.5% PA	247.90 a	130.27 b	365.9 b	23 b	1050.14 b	5.33 b	4.55 ab	3.83 ab	4.35 a	2.28 ab	85.16 a	0.99 a	7.63 c	605.62 c	58.64 cd	30.08 c	2.93 b	62.36 c	185.87 a	17.13 d	1.14 b	2.25 c
1% PA	226.95 b	107.33 c	330.26 c	24 b	992.97 bc	5.32 b	4.52 bc	3.71 bc	4.18 bc	2.19 bc	78.78 bc	0.84 d	7.14 d	555.2 e	74.02 a	33.04 a	2.74 bc	50.35 e	89.84 e	16.69 d	1.16 b	2.48 a
2% PA	255.37 a	149.98 a	388.18 a	28 a	1359.82 a	5.49 a	4.51 c	3.86 a	4.32 ab	2.33 a	81.33 b	1.00 a	8.23 b	572.63 d	69.34 b	33.04 a	3.19 a	94.44 a	144.15 b	24.66 a	1.24 a	2.49 a
Water	222.83 b	99.64 de	317.72 cd	19 c	846.40 c	5.41 ab	4.53 bc	3.57 cd	4.06 cd	2.14 cd	77.67 c	0.95 b	9.06 a	633.28 b	61.26 c	29.99 c	2.90 bc	47.38 f	140.22 b	21.17 b	0.80 d	2.41 ab
No spray	207.90 c	93.85 e	300.85 d	19 c	830.98 c	4.82 d	4.50 c	3.71 bc	4.09 cd	2.23 bc	72.78 d	0.95 b	7.87 c	625.49 b	57.09 d	30.96 b	2.74 bc	68.12 b	129.41 c	19.59 c	0.87 c	2.32 bc
p-value	<0.001	<0.001	<0.001	<0.001	<0.001	<0.001	0.001	<0.001	<0.001	<0.001	<0.001	<0.001	<0.001	<0.001	<0.001	<0.001	<0.001	<0.001	<0.001	<0.001	<0.001	<0.001

Table S6.2. Fruit grading category of harvested tomato fruits

Treatment	Canada Commercial (≥ 63 mm)	Canada No.2 (63 mm < x ≥ 38 mm)	Non-marketable (< 38 mm)	Total number
0.25% PA + Full	0	93	12	105
0.25% PA + Half	0	67	17	84
0.5% PA + Full	2	80	30	112
0.5% PA + Half	0	54	12	66
1% PA + Full	0	60	16	76
1% PA + Half	0	61	48	109
2% PA + Full	0	101	10	111
2% PA + Half	0	65	47	112
No spray + Full	2	47	23	72
No spray + Half	0	46	35	81
Water + Full	1	62	18	81
Water +Half	0	46	24	70
Total number	5	782	292	1079
Percentage	0.46	72.47	27.06	

Table S6.3. T-test results of phytochemical properties of fruit and leaf tissues in response to the interactive effect of pyroligneous acid (PA) and NPK application

Tissue	Carotenoid (mg/g FW)	Total protein (mg/mL)	Total sugar (mg glucose/g FW)	Total phenolic content (mg GAE/ g FW)	Total flavonoid Content (µg quecertin/ g FW)	DPPH (%)
Fruit	2.82 ± 0.34	1.07 ± 0.23	19.60 ± 4.39	141.2 ± 47.6	67.8 ± 26.6	30.29 ± 2.94
Leaf	77.04 ± 8.57	2.34 ± 0.19	7.90 ± 1.05	608 ± 65.6	947 ± 107	61.6 ± 10.9

p-value	<0.001	<0.001	<0.001	<0.001	<0.001	<0.001

Table S6.4. Pearson correlation coefficients (r) and their significance at $p \leq 0.05$ amongst response variables of tomato plants treated with pyroligneous acid (PA) and NPK combination.

Variables	Fv/Fm	Fv/Fo	FN	TFW	AFW	ADW	Brix	pH	TDS	EC	Salt	LSC	LFC	Chl a	Chl b	LCC	LPC	LPhC	LDPPH	FSC	FPhC	FFC	FCC	FPC
Fv/Fo	**r = 0.996 p = 0.000**																							
FN	r = 0.238 p = 0.104	r = 0.252 p = 0.084																						
TFW	**r = 0.385 p = 0.007**	**r = 0.386 p = 0.007**	**r = 0.691 p = 0.000**																					
AFW	r = 0.157 p = 0.286	r = 0.151 p = 0.305	r = 0.224 p = 0.125	r = 0.039 p = 0.790																				
ADW	r = 0.167 p = 0.255	r = 0.164 p = 0.266	r = 0.162 p = 0.270	r = 0.055 p = 0.711	**r = 0.855 p = 0.000**																			
Brix	r = -0.181 p = 0.218	r = -0.195 p = 0.184	r = -0.050 p = 0.735	r = -0.139 p = 0.348	r = 0.104 p = 0.482	r = 0.042 p = 0.775																		
pH	**r = 0.473 p = 0.001**	**r = 0.470 p = 0.001**	**r = 0.327 p = 0.023**	r = 0.252 p = 0.084	r = 0.069 p = 0.642	r = 0.107 p = 0.471	r = -0.203 p = 0.166																	
TDS	r = -0.026 p = 0.859	r = -0.027 p = 0.853	r = -0.001 p = 0.996	r = -0.077 p = 0.604	r = -0.030 p = 0.839	r = -0.232 p = 0.112	**r = 0.465 p = 0.001**	r = -0.196 p = 0.181																
EC	r = 0.075 p = 0.612	r = 0.082 p = 0.580	r = 0.042 p = 0.777	r = 0.012 p = 0.933	r = -0.010 p = 0.947	r = -0.183 p = 0.214	**r = 0.542 p = 0.000**	r = -0.133 p = 0.368	**r = 0.900 p = 0.000**															
Salt	r = -0.052 p = 0.726	r = -0.058 p = 0.697	r = -0.012 p = 0.933	r = -0.119 p = 0.422	r = -0.041 p = 0.780	r = -0.238 p = 0.103	**r = 0.477 p = 0.001**	r = -0.224 p = 0.126	**r = 0.963 p = 0.000**	**r = 0.866 p = 0.000**														
LSC	r = -0.15 p = 0.310	r = -0.189 p = 0.199	**r = -0.454 p = 0.001**	r = -0.283 p = 0.051	r = 0.154 p = 0.295	r = 0.104 p = 0.483	**r = 0.473 p = 0.001**	**r = -0.300 p = 0.038**	r = 0.239 p = 0.102	r = 0.202 p = 0.168	**r = 0.288 p = 0.048**													
LFC	r = -0.037 p = 0.804	r = -0.061 p = 0.680	**r = -0.352 p = 0.014**	r = 0.006 p = 0.970	**r = -0.442 p = 0.002**	**r = -0.335 p = 0.020**	r = 0.138 p = 0.351	r = -0.18 p = 0.222	r = 0.088 p = 0.552	r = 0.123 p = 0.405	r = 0.103 p = 0.485	**r = 0.390 p = 0.006**												

Chl a	r = 0.265 p = 0.069	r = 0.251 p = 0.085	**r = 0.489 p = 0.000**	**r = 0.329 p = 0.022**	r = 0.113 p = 0.443	r = 0.035 p = 0.811	r = -0.045 p = 0.762	r = 0.235 p = 0.108	r = 0.037 p = 0.805	r = 0.056 p = 0.703	r = 0.009 p = 0.953	r = -0.153 p = 0.300	r = 0.111 p = 0.454											
Chl b	r = 0.246 p = 0.092	r = 0.235 p = 0.108	**r = 0.479 p = 0.001**	**r = 0.369 p = 0.010**	r = 0.092 p = 0.532	r = 0.041 p = 0.784	r = 0.002 p = 0.987	r = 0.168 p = 0.253	r = 0.113 p = 0.446	r = 0.131 p = 0.374	r = 0.077 p = 0.602	r = -0.109 p = 0.462	r = 0.159 p = 0.280	**r = 0.934 p = 0.000**										
LCC	r = 0.237 p = 0.106	r = 0.228 p = 0.118	**r = 0.290 p = 0.046**	r = 0.065 p = 0.663	r = 0.033 p = 0.822	r = -0.001 p = 0.994	r = 0.087 p = 0.555	r = 0.136 p = 0.357	r = 0.005 p = 0.971	r = 0.026 p = 0.859	r = -0.005 p = 0.974	r = -0.114 p = 0.442	r = 0.137 p = 0.352	**r = 0.905 p = 0.000**	**r = 0.809 p = 0.000**									
LPC	**r = -0.542 p = 0.000**	**r = -0.544 p = 0.000**	r = 0.024 p = 0.870	**r = -0.384 p = 0.007**	r = 0.016 p = 0.916	r = -0.086 p = 0.561	**r = 0.396 p = 0.005**	r = -0.267 p = 0.067	r = 0.201 p = 0.170	r = 0.201 p = 0.170	r = 0.276 p = 0.057	r = 0.071 p = 0.631	r = -0.120 p = 0.417	r = 0.125 p = 0.398	r = 0.109 p = 0.462	r = 0.216 p = 0.140								
LPhC	**r = -0.473 p = 0.001**	**r = -0.455 p = 0.001**	**r = -0.350 p = 0.015**	**r = -0.433 p = 0.002**	r = -0.267 p = 0.067	r = -0.190 p = 0.197	r = 0.083 p = 0.576	r = -0.136 p = 0.357	r = -0.183 p = 0.214	r = -0.145 p = 0.325	r = -0.161 p = 0.274	r = -0.100 p = 0.501	r = -0.091 p = 0.537	**r = -0.687 p = 0.000**	**r = -0.710 p = 0.000**	**r = -0.542 p = 0.000**	**r = 0.310 p = 0.032**							
LDPPH	**r = -0.510 p = 0.000**	**r = -0.515 p = 0.000**	r = -0.182 p = 0.215	r = -0.101 p = 0.493	r = -0.177 p = 0.228	r = -0.131 p = 0.376	**r = 0.521 p = 0.000**	**r = -0.513 p = 0.000**	r = 0.179 p = 0.223	r = 0.195 p = 0.185	r = 0.207 p = 0.159	r = 0.262 p = 0.072	r = 0.119 p = 0.420	**r = -0.445 p = 0.002**	**r = -0.385 p = 0.007**	**r = -0.382 p = 0.007**	r = 0.236 p = 0.107	**r = 0.354 p = 0.014**						
FSC	r = -0.239 p = 0.102	r = -0.237 p = 0.104	r = 0.248 p = 0.089	**r = 0.364 p = 0.011**	r = 0.053 p = 0.720	r = -0.124 p = 0.401	r = 0.231 p = 0.114	**r = -0.292 p = 0.044**	**r = 0.450 p = 0.001**	**r = 0.382 p = 0.007**	**r = 0.483 p = 0.001**	r = 0.133 p = 0.368	r = 0.094 p = 0.524	r = 0.045 p = 0.759	r = 0.146 p = 0.323	r = -0.162 p = 0.272	r = 0.087 p = 0.558	r = -0.153 p = 0.300	r = 0.156 p = 0.289					
FPhC	r = 0.034 p = 0.819	r = 0.043 p = 0.772	r = -0.125 p = 0.395	r = -0.063 p = 0.672	r = -0.031 p = 0.834	r = -0.072 p = 0.626	**r = 0.344 p = 0.017**	r = -0.099 p = 0.503	**r = 0.612 p = 0.000**	**r = 0.546 p = 0.000**	**r = 0.591 p = 0.000**	r = 0.043 p = 0.770	r = 0.175 p = 0.234	r = -0.082 p = 0.578	r = 0.004 p = 0.979	r = -0.034 p = 0.821	r = -0.028 p = 0.848	r = 0.002 p = 0.992	r = -0.001 p = 0.996	**r = 0.461 p = 0.001**				
FFC	r = -0.233 p = 0.110	r = -0.234 p = 0.110	r = -0.097 p = 0.512	r = -0.069 p = 0.640	r = 0.019 p = 0.899	r = -0.067 p = 0.650	**r = 0.559 p = 0.000**	**r = -0.455 p = 0.001**	**r = 0.670 p = 0.000**	**r = 0.58 p = 0.000**	**r = 0.708 p = 0.000**	**r = 0.361 p = 0.012**	r = 0.115 p = 0.435	r = -0.271 p = 0.063	r = -0.159 p = 0.281	r = -0.216 p = 0.140	r = 0.202 p = 0.169	r = 0.048 p = 0.744	**r = 0.398 p = 0.005**	**r = 0.592 p = 0.000**	**r = 0.491 p = 0.000**			
FCC	r = -0.187 p = 0.203	r = -0.212 p = 0.149	r = -0.025 p = 0.867	r = 0.003 p = 0.986	r = -0.040 p = 0.788	r = 0.005 p = 0.971	**r = 0.342 p = 0.017**	r = -0.210 p = 0.151	r = -0.015 p = 0.921	r = -0.019 p = 0.896	r = 0.053 p = 0.719	r = 0.217 p = 0.139	**r = 0.348 p = 0.015**	r = -0.030 p = 0.838	r = 0.009 p = 0.953	r = 0.011 p = 0.941	r = 0.069 p = 0.639	r = 0.087 p = 0.554	**r = 0.392 p = 0.006**	r = 0.187 p = 0.203	r = 0.133 p = 0.367	r = 0.276 p = 0.057		
FPC	**r = 0.322 p = 0.026**	**r = 0.322 p = 0.026**	**r = 0.536 p = 0.000**	**r = 0.475 p = 0.001**	r = 0.100 p = 0.499	r = 0.183 p = 0.213	r = 0.116 p = 0.433	r = 0.231 p = 0.115	r = 0.132 p = 0.369	r = 0.282 p = 0.052	r = 0.098 p = 0.508	r = -0.169 p = 0.252	r = 0.045 p = 0.763	**r = 0.429 p = 0.002**	**r = 0.473 p = 0.001**	**r = 0.314 p = 0.030**	r = -0.026 p = 0.863	**r = -0.477 p = 0.001**	r = 0.043 p = 0.774	r = -0.115 p = 0.437	r = -0.129 p = 0.382	r = -0.022 p = 0.880	r = 0.088 p = 0.550	
FDPPH	**r = -0.491 p = 0.000**	**r = -0.503 p = 0.000**	r = 0.064 p = 0.665	r = -0.075 p = 0.611	r = -0.238 p = 0.104	r = -0.282 p = 0.052	r = 0.261 p = 0.073	**r = -0.444 p = 0.002**	r = 0.271 p = 0.063	r = 0.192 p = 0.191	**r = 0.289 p = 0.046**	r = 0.098 p = 0.506	r = 0.191 p = 0.194	r = 0.249 p = 0.088	r = 0.249 p = 0.088	r = 0.221 p = 0.131	**r = 0.448 p = 0.001**	r = -0.017 p = 0.906	**r = 0.573 p = 0.000**	r = 0.236 p = 0.107	r = -0.020 p = 0.891	r = 0.089 p = 0.549	r = 0.259 p = 0.075	r = 0.040 p = 0.786

FN, fruit number; TFW, total fruit weight; AFW, aboveground fresh weight; ADW, aboveground dry weight; TDS, total dissolved solids; EC, electrical conductivity; Salt, salinity; LSC, leaf sugar content; LFC, leaf flavonoid content; Chl a, chlorophyll a; Chl b, chlorophyll b; LCC, leaf carotenoid content; LPC, leaf protein content; LPhC, leaf phenolic content; LDPPH, leaf DPPH activity; FSC, fruit sugar content; FPhC, fruit phenolic content; FFC, fruit flavonoid content; FCC, fruit carotenoid content; FPC, fruit protein content; FDPPH, fruit DPPH activity.

Table S8.1. Metabolite content from tomato leaf tissues analyzed by LC-MRM-MS.

Table S8.2. Pearson correlation and *p*-values between individual metabolites of the central carbon metabolic routes in leaves of tomato 'Scotia' seedlings treated with pyroligneous acid (PA) under aluminum (Al) stress. This file is attached to this document.

Figure S8.1. Chromatograms for all identified metabolites of CCM routes. The sections (1-3) show detection of CCM metabolites. The compound names and the ion transition of each compound are shown on the extracted ion chromatograms (XICs)

1. TCA cycle

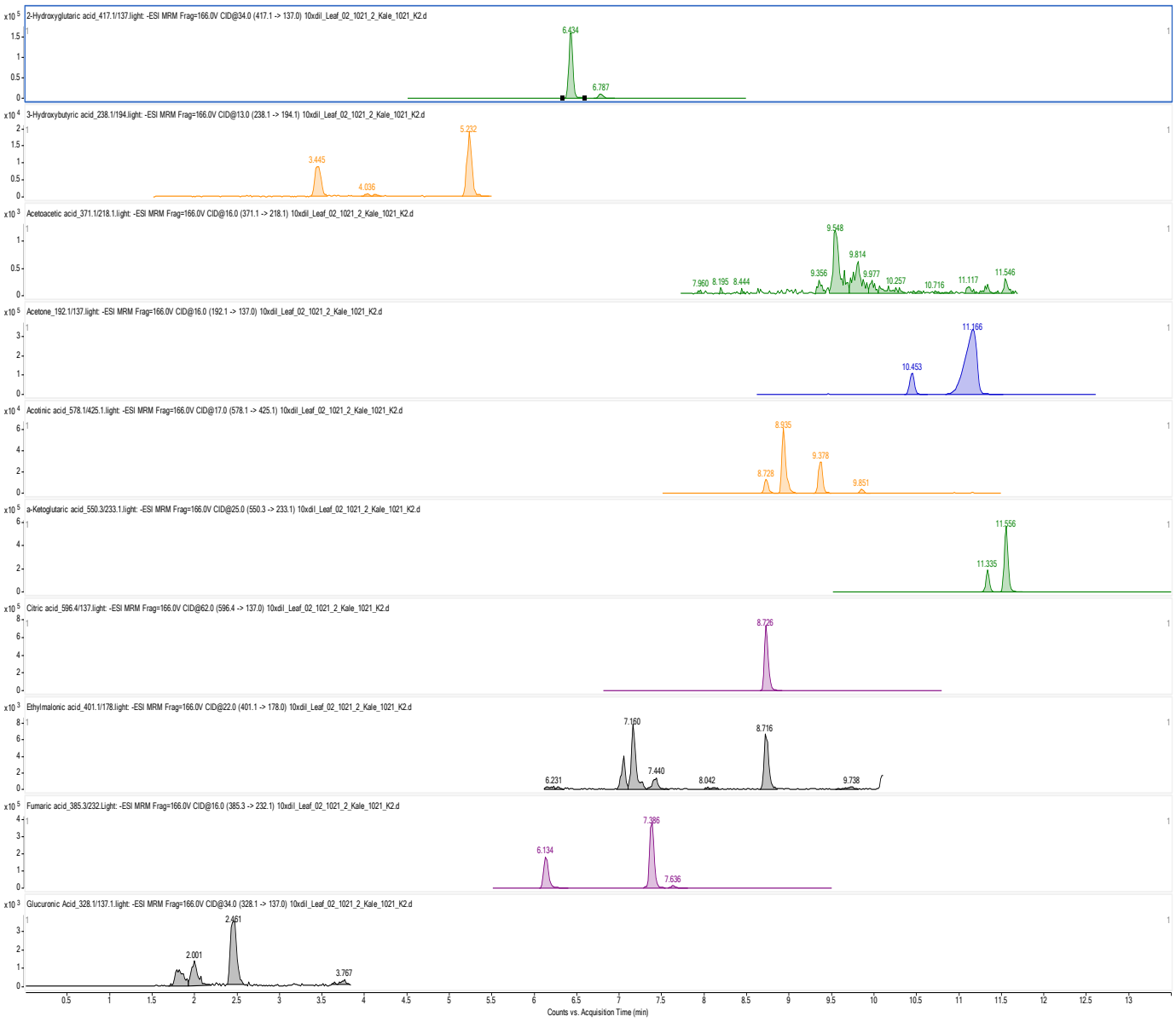

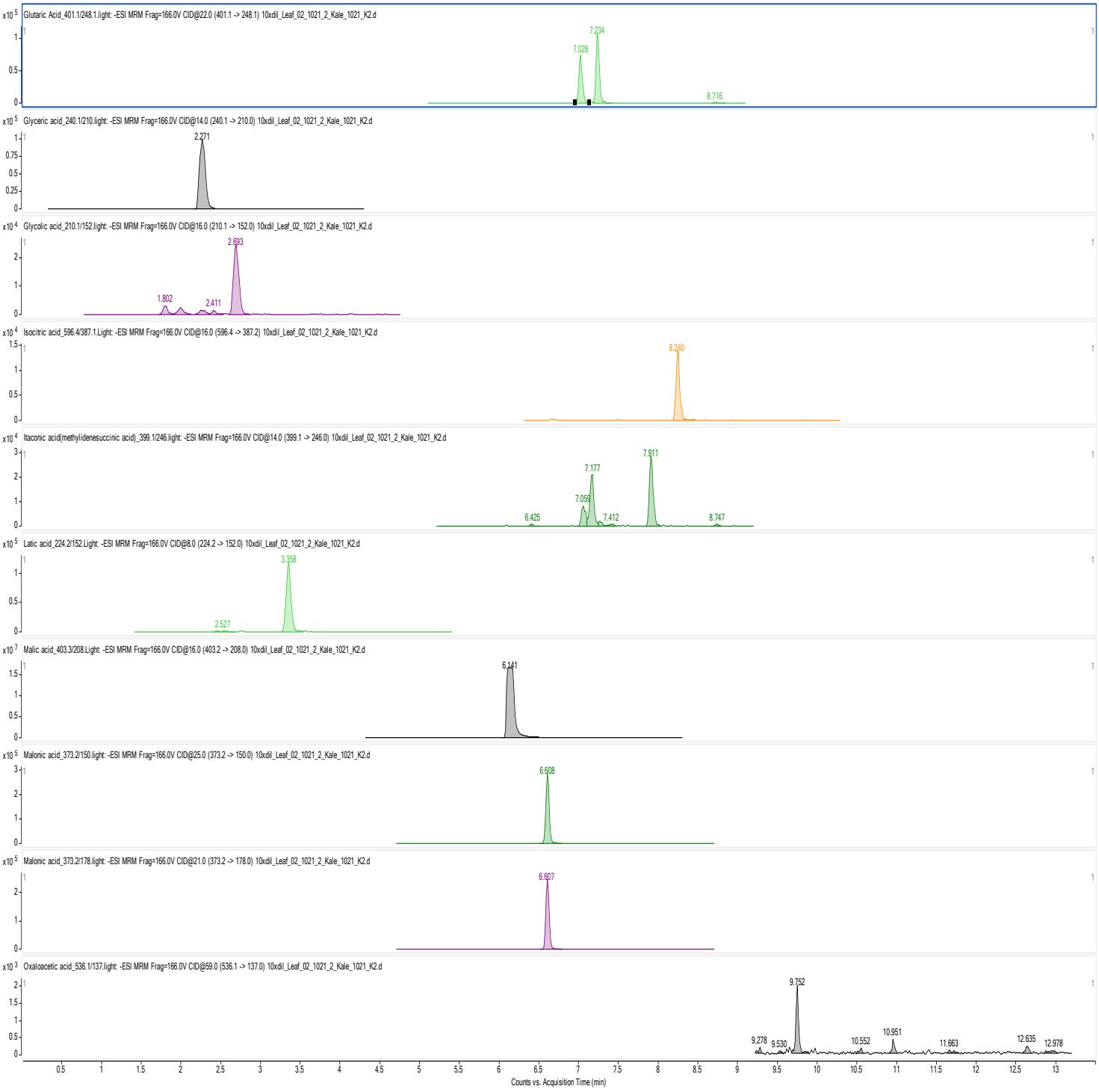
Glutaric Acid_401.1/248.1.light: -ESI MRM Frag=166.0V CID@22.0 (401.1 -> 248.1) 10xdil_Leaf_02_1021_2_Kale_1021_K2.d
7.234
7.028
8.716
Glyceric acid_240.1/210.light: -ESI MRM Frag=166.0V CID@14.0 (240.1 -> 210.0) 10xdil_Leaf_02_1021_2_Kale_1021_K2.d
2.271
Glycolic acid_210.1/152.light: -ESI MRM Frag=166.0V CID@16.0 (210.1 -> 152.0) 10xdil_Leaf_02_1021_2_Kale_1021_K2.d
2.693
1.802
2.411
Isocitric acid_596.4/387.1.Light: -ESI MRM Frag=166.0V CID@16.0 (596.4 -> 387.2) 10xdil_Leaf_02_1021_2_Kale_1021_K2.d
8.240
Itaconic acid(methylidenesuccinic acid)_399.1/246.light: -ESI MRM Frag=166.0V CID@14.0 (399.1 -> 246.0) 10xdil_Leaf_02_1021_2_Kale_1021_K2.d
7.911
7.177
7.059
6.425
7.412
8.747
Latic acid_224.2/152.Light: -ESI MRM Frag=166.0V CID@8.0 (224.2 -> 152.0) 10xdil_Leaf_02_1021_2_Kale_1021_K2.d
3.358
2.527
Malic acid_403.3/208.Light: -ESI MRM Frag=166.0V CID@16.0 (403.2 -> 208.0) 10xdil_Leaf_02_1021_2_Kale_1021_K2.d
6.141
Malonic acid_373.2/150.light: -ESI MRM Frag=166.0V CID@25.0 (373.2 -> 150.0) 10xdil_Leaf_02_1021_2_Kale_1021_K2.d
6.608
Malonic acid_373.2/178.light: -ESI MRM Frag=166.0V CID@21.0 (373.2 -> 178.0) 10xdil_Leaf_02_1021_2_Kale_1021_K2.d
6.607
Oxaloacetic acid_536.1/137.light: -ESI MRM Frag=166.0V CID@59.0 (536.1 -> 137.0) 10xdil_Leaf_02_1021_2_Kale_1021_K2.d
9.752
9.278
9.530
10.552
10.951
11.663
12.635
12.978
Counts vs. Acquisition Time (min)

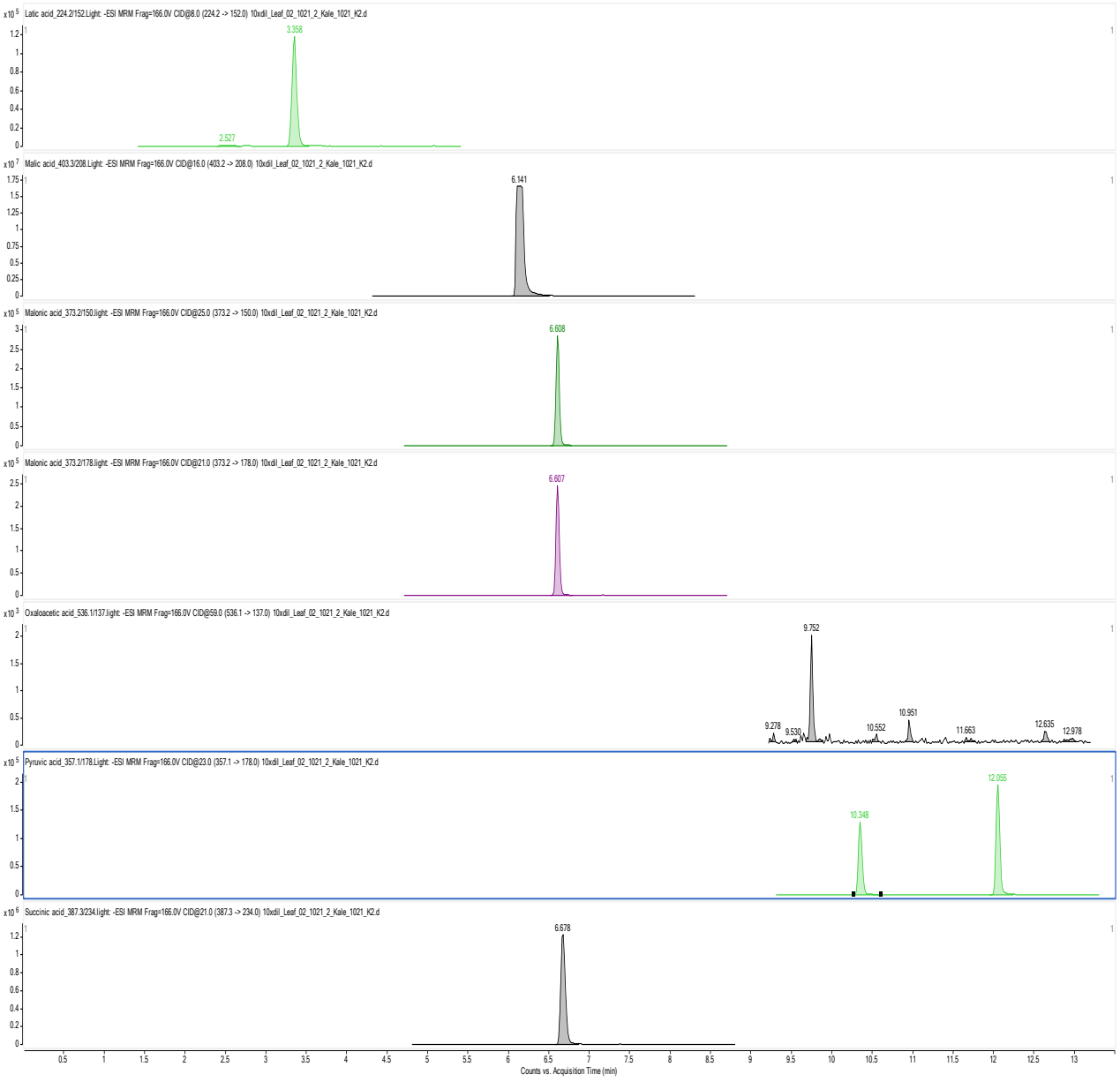
Latic acid_224.2/152.Light: -ESI MRM Frag=166.0V CID@8.0 (224.2 -> 152.0) 10xdil_Leaf_02_1021_2_Kale_1021_K2.d
3.358
2.527
Malic acid_403.3/208.Light: -ESI MRM Frag=166.0V CID@16.0 (403.2 -> 208.0) 10xdil_Leaf_02_1021_2_Kale_1021_K2.d
6.141
Malonic acid_373.2/150.light: -ESI MRM Frag=166.0V CID@25.0 (373.2 -> 150.0) 10xdil_Leaf_02_1021_2_Kale_1021_K2.d
6.608
Malonic acid_373.2/178.light: -ESI MRM Frag=166.0V CID@21.0 (373.2 -> 178.0) 10xdil_Leaf_02_1021_2_Kale_1021_K2.d
6.607
Oxaloacetic acid_536.1/137.light: -ESI MRM Frag=166.0V CID@59.0 (536.1 -> 137.0) 10xdil_Leaf_02_1021_2_Kale_1021_K2.d
9.752
9.278
9.530
10.552
10.951
11.663
12.635
12.978
Pyruvic acid_357.1/178.Light: -ESI MRM Frag=166.0V CID@23.0 (357.1 -> 178.0) 10xdil_Leaf_02_1021_2_Kale_1021_K2.d
12.055
10.348
Succinic acid_387.3/234.light: -ESI MRM Frag=166.0V CID@21.0 (387.3 -> 234.0) 10xdil_Leaf_02_1021_2_Kale_1021_K2.d
6.678
Counts vs. Acquisition Time (min)

2. Sugars and selected sugar phosphates

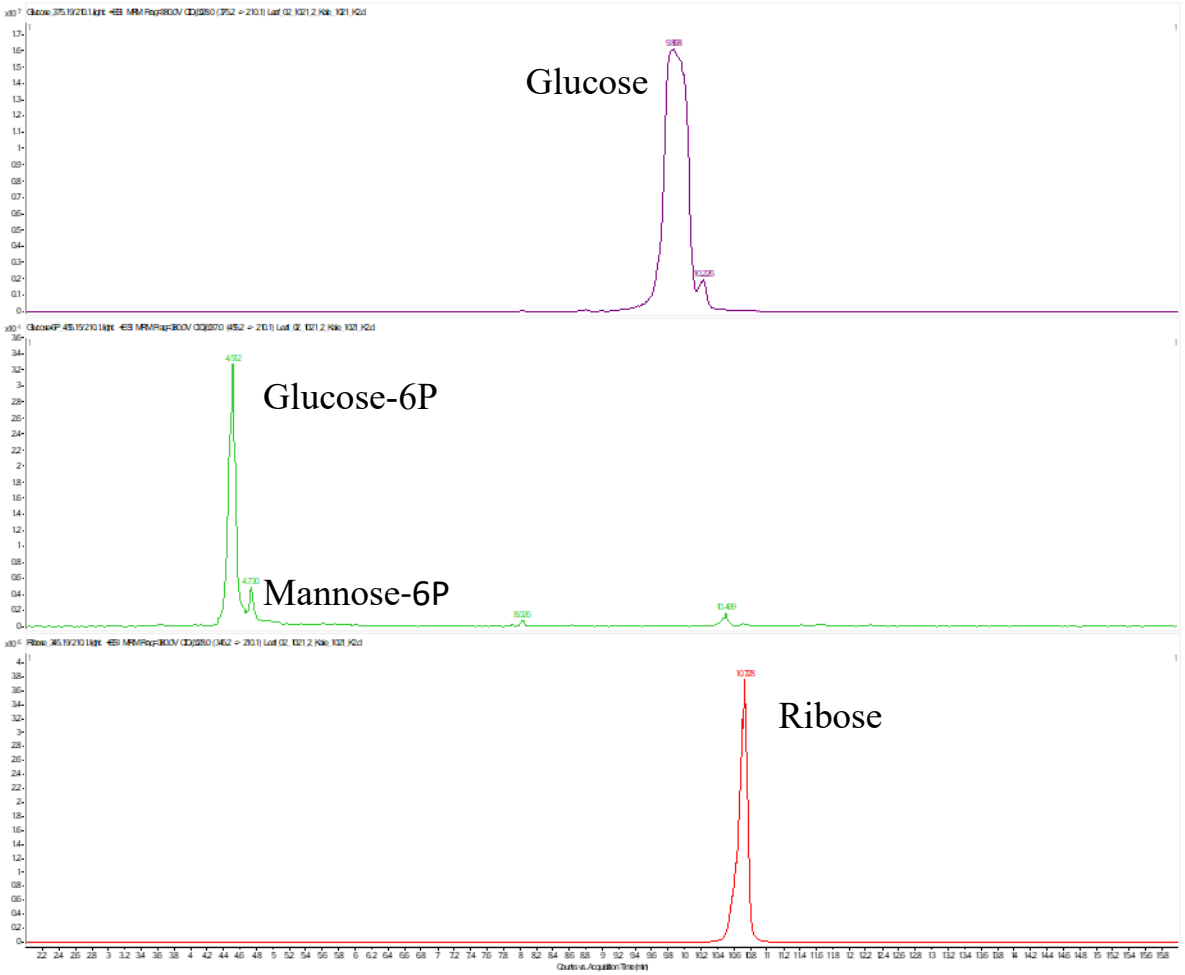

3. Phosphometabolites

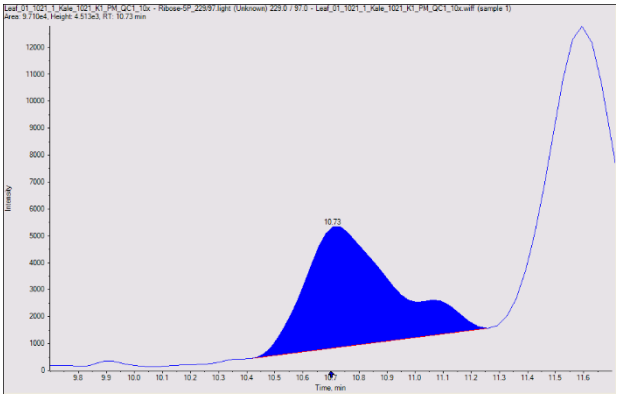

Ribose-5P

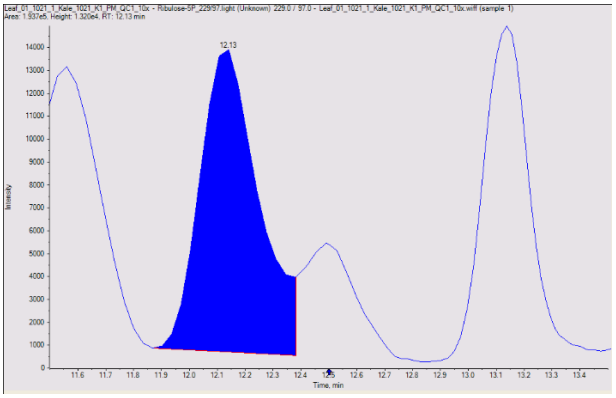

Ribulose-5P

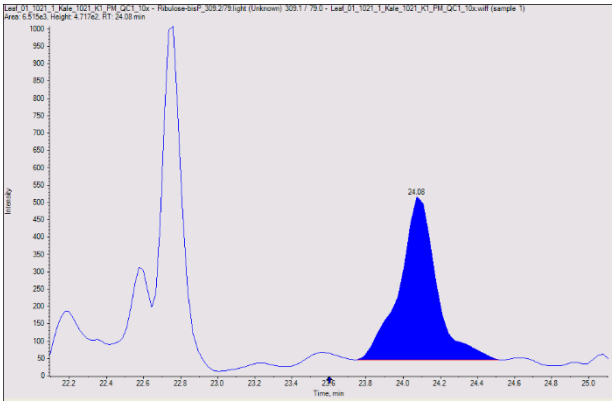

Ribulose-bisP

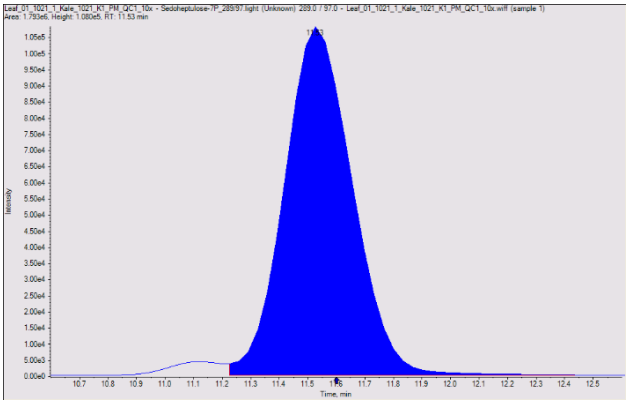

Sedoheptulose-7P

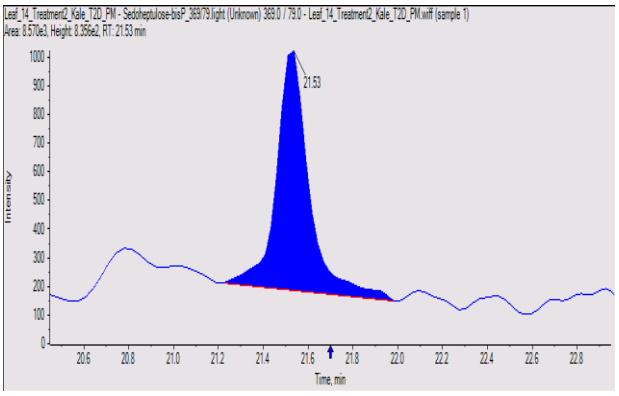

Sedoheptulose-1,7-bisP

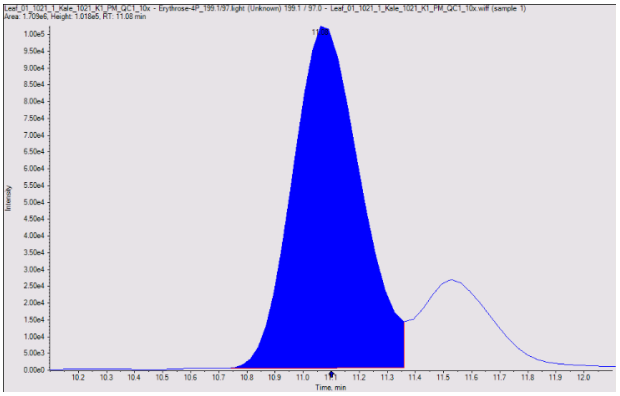

Erythrose-4P

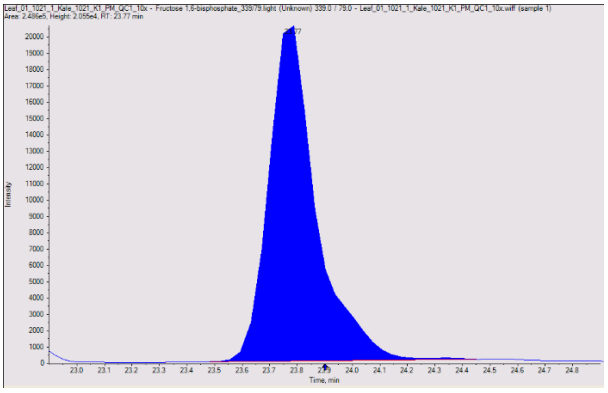

Fructose-1,6-bisP

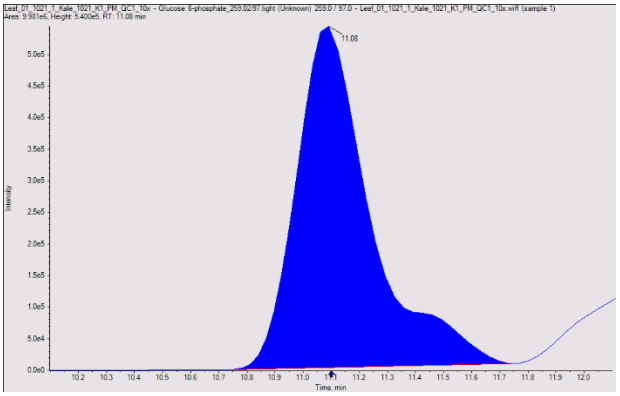

Fructose-6P

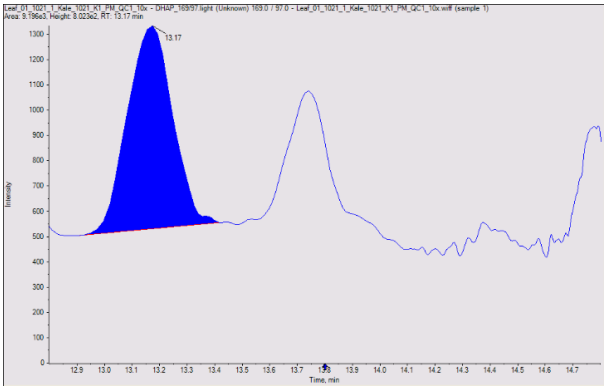

DHAP

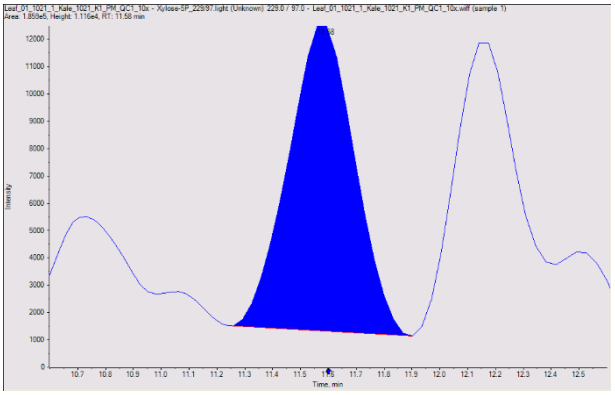

Xylose-5P

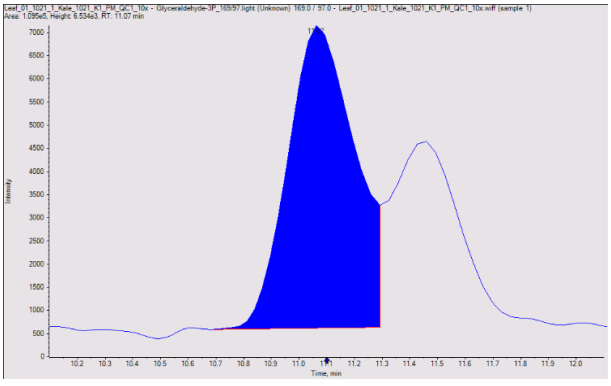

Glyceraldehyde-3P

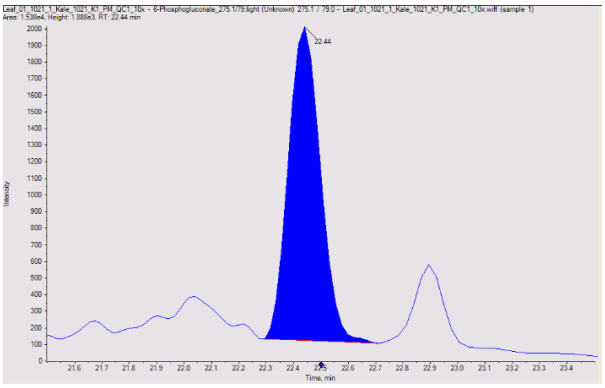

6-Phosphogluconate

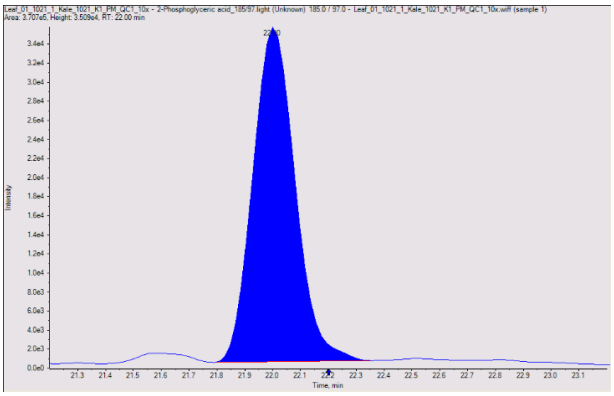

3-Phosphoglyceric acid

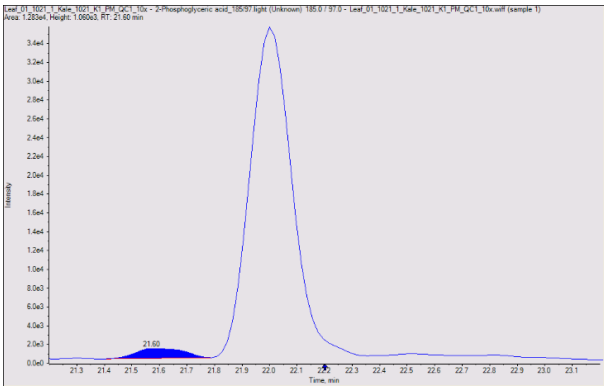

2-Phosphoglyceric acid

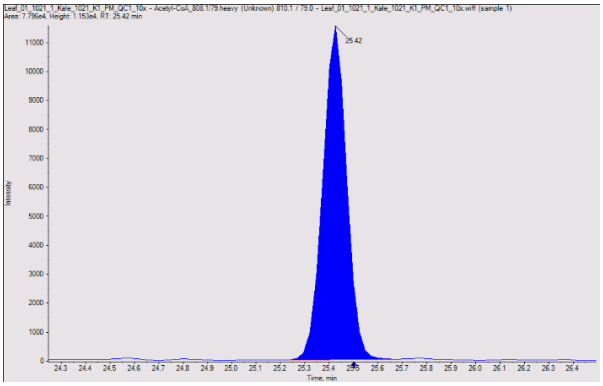

Acetyl-CoA

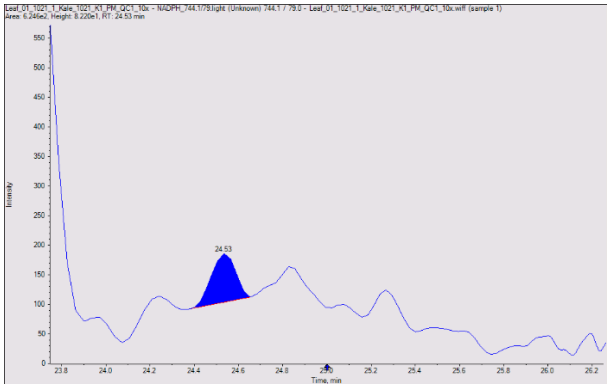

NADPH

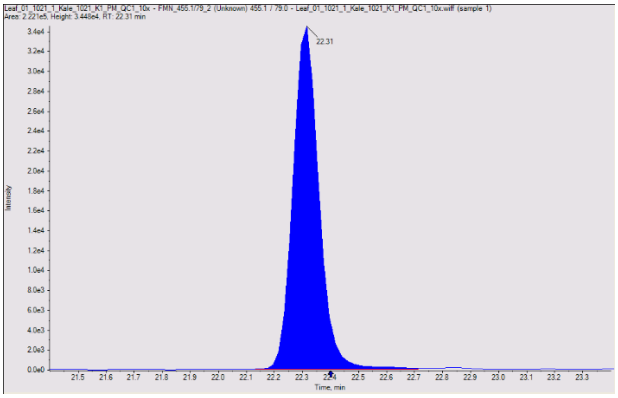

FMN

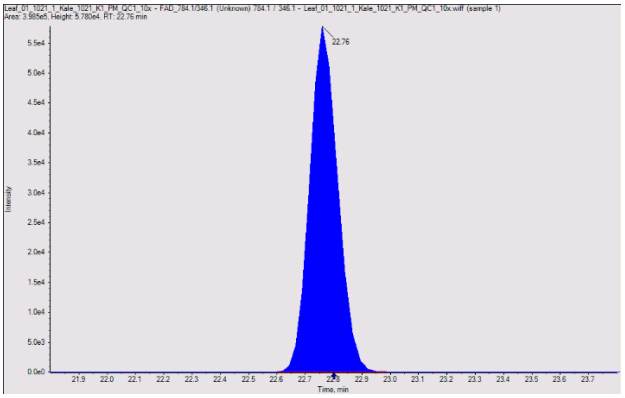

FAD

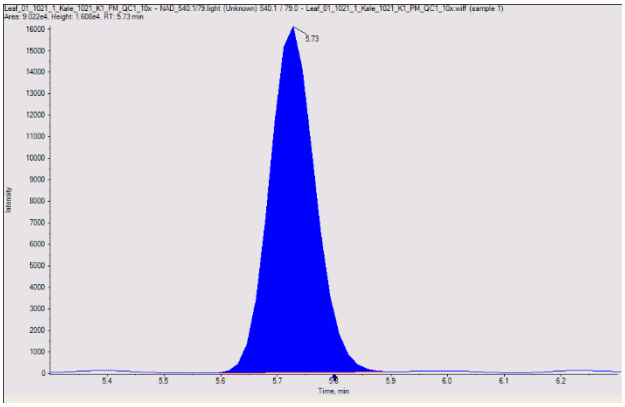

NAD

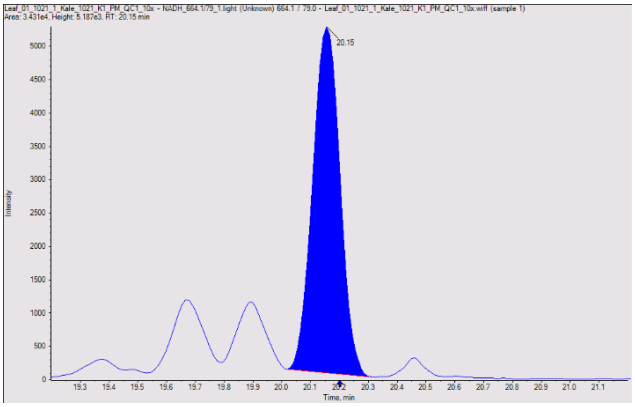

NADH

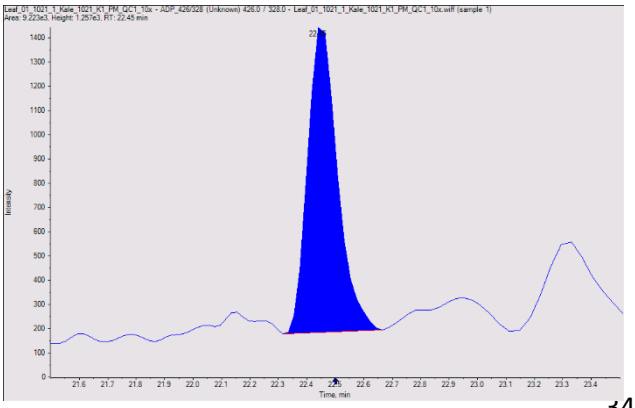

ADP

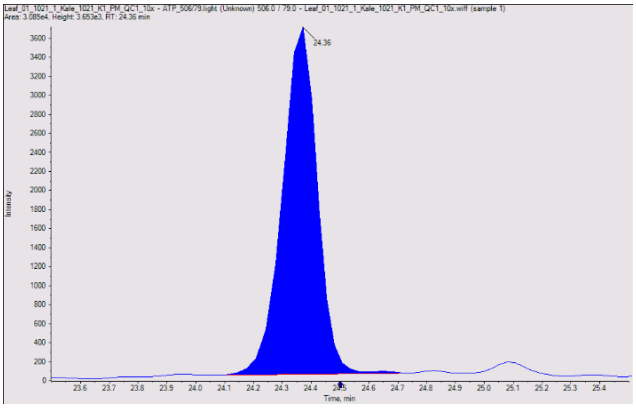

ATP

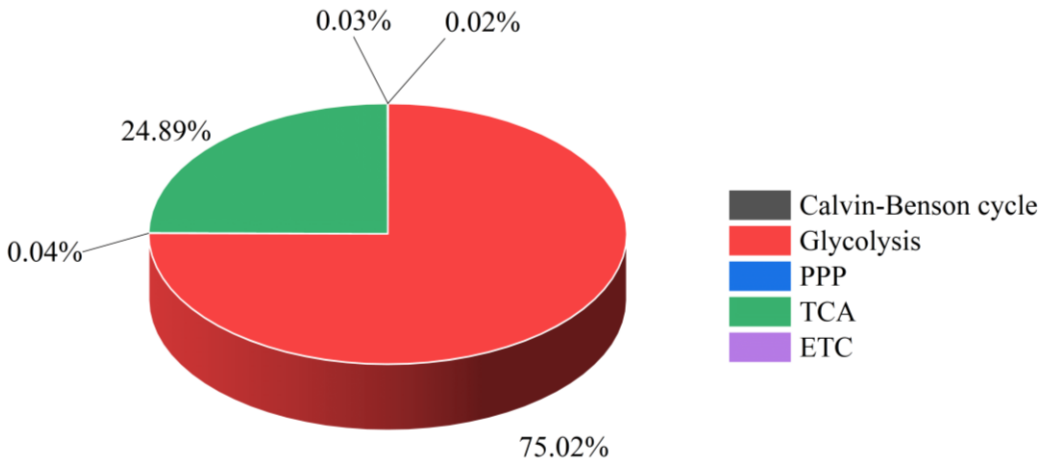

Figure S8.2. Classification of metabolites involved in CCM route in leaves of tomato 'Scotia' seedlings treated with pyroligneous acid (PA).